Green Chemistry

Cutting-edge research for a greener sustainable future

www.rsc.org/greenchem

Volume 9 | Number 12 | December 2007 | Pages 1261–1384

ISSN 1463-9262

RSC Publishing

1463-9262(2007)9:12;1-R

The must-have primary research journal for environmental issues

Comprehensive and high quality coverage of multidisciplinary, international research relating to the measurement, pathways, impact and management of contaminants in all environments.

- Highly visible and cited in MEDLINE
- Accelerated publication rates, typically around 80 days
- Dedicated to the measurement of natural and anthropogenic sources of pollution with a view to assessing environmental and human health effects

Submit your work to JEM today

13080760

RSC Publishing

www.rsc.org/jem

Registered Charity Number 207890

Green Chemistry

Cutting-edge research for a greener sustainable future

www.rsc.org/greenchem

RSC Publishing is a not-for-profit publisher and a division of the Royal Society of Chemistry. Any surplus made is used to support charitable activities aimed at advancing the chemical sciences. Full details are available from www.rsc.org

IN THIS ISSUE

ISSN 1463-9262 CODEN GRCHFJ 9(12) 1261–1384 (2007)

Cover
See Sheldon, pp. 1273–1283. Bioconversion of renewable raw materials to specialty chemicals in a cell factory. Image reproduced by permission of Petr Vlk.

CHEMICAL TECHNOLOGY

Chemical Technology highlights the latest applications and technological aspects of research across the chemical sciences.

Chemical Technology
December 2007/Volume 4/Issue 12
www.rsc.org/chemicaltechnology

PERSPECTIVE

The E Factor: fifteen years on

Roger A. Sheldon

This perspective reviews the effect that the E Factor concept has had over the last fifteen years on developments in the (fine) chemical industry and pharmaceutical industry with regard to waste minimisation and to assess its current status in the broader context of green chemistry and sustainability.

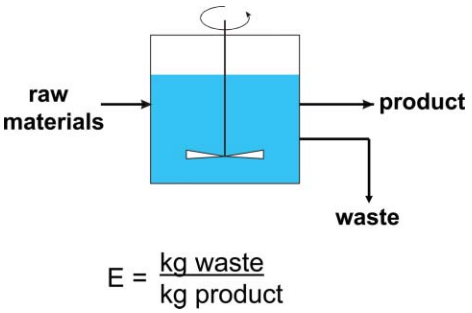

Green Chemistry

Cutting-edge research for a greener sustainable future

www.rsc.org/greenchem

Green Chemistry focuses on cutting-edge research that attempts to reduce the environmental impact of the chemical enterprise by developing a technology base that is inherently non-toxic to living things and the environment.

Green Chemistry (print: ISSN 1463-9262; electronic: ISSN 1463-9270) is published 12 times a year by the Royal Society of Chemistry, Thomas Graham House, Science Park, Milton Road, Cambridge, UK CB4 0WF.

All orders, with cheques made payable to the Royal Society of Chemistry, should be sent to RSC Distribution Services, c/o Portland Customer Services, Commerce Way, Colchester, Essex, UK CO2 8HP. Tel +44 (0) 1206 226050; E-mail sales@rscdistribution.org

2007 Annual (print + electronic) subscription price: £902; US$1705. 2007 Annual (electronic) subscription price: £812; US$1534. Customers in Canada will be subject to a surcharge to cover GST. Customers in the EU subscribing to the electronic version only will be charged VAT.

If you take an institutional subscription to any RSC journal you are entitled to free, site-wide web access to that journal. You can arrange access via Internet Protocol (IP) address at www.rsc.org/ip. Customers should make payments by cheque in sterling payable on a UK clearing bank or in US dollars payable on a US clearing bank. Periodicals postage paid at Rahway, NJ, USA and at additional mailing offices. Airfreight and mailing in the USA by Mercury Airfreight International Ltd., 365 Blair Road, Avenel, NJ 07001, USA.

US Postmaster: send address changes to Green Chemistry, c/o Mercury Airfreight International Ltd., 365 Blair Road, Avenel, NJ 07001. All despatches outside the UK by Consolidated Airfreight.

PRINTED IN THE UK

Advertisement sales: Tel +44 (0) 1223 432246; Fax +44 (0) 1223 426017; E-mail advertising@rsc.org

INFORMATION FOR AUTHORS

Full details of how to submit material for publication in Green Chemistry are given in the Instructions for Authors (available from http://www.rsc.org/authors). Submissions should be sent *via* ReSourCe: http://www.rsc.org/resource.

Authors may reproduce/republish portions of their published contribution without seeking permission from the RSC, provided that any such republication is accompanied by an acknowledgement in the form: (Original citation) – Reproduced by permission of the Royal Society of Chemistry.

♾ The paper used in this publication meets the requirements of ANSI/NISO Z39.48-1992 (Permanence of Paper).

Royal Society of Chemistry: Registered Charity No. 207890

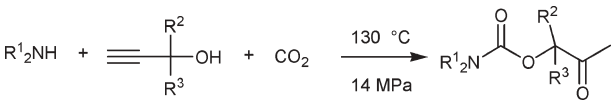

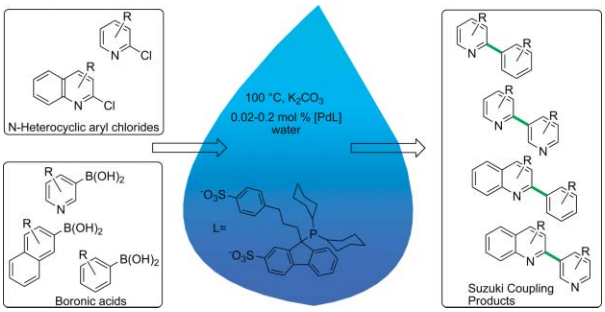

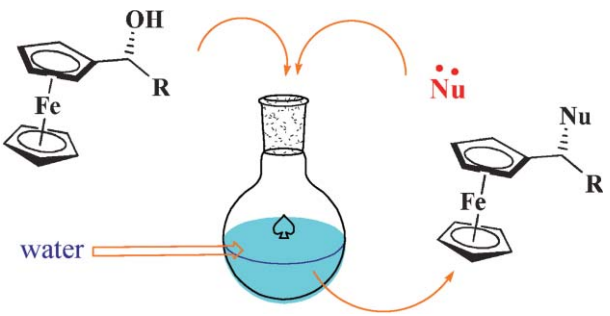

1299

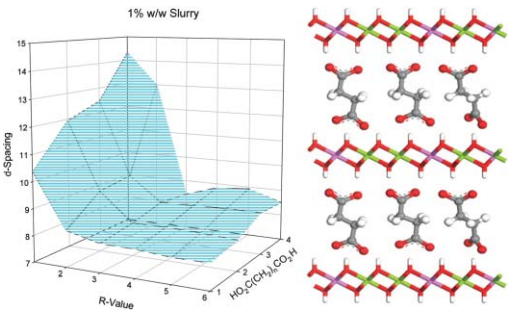

Synthesis of organo-layered double hydroxides by an environmentally friendly co-hydration route

H. C. Greenwell,* C. C. Marsden and W. Jones

We describe a method for the efficient preparation of layered double hydroxides using a method whereby two oxides are co-hydrated in aqueous solution and in the presence of organic anions at low temperatures. An inert atmosphere was not required and the product was determined to be free of carbonate contamination.

1308

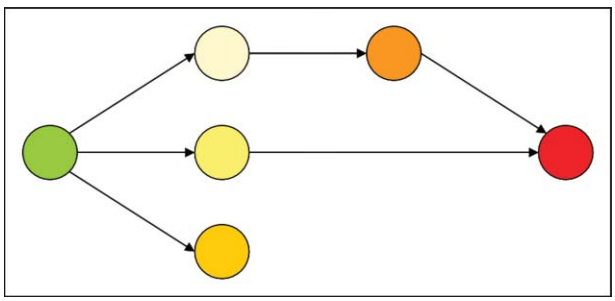

Implementing objectives of sustainability into ionic liquids research and development

Dana Kralisch,* Denise Reinhardt* and Günter Kreisel

Methodology for ecological and economic optimisation during the R&D stage, presented on the example of ionic liquids synthesis and work-up.

1319

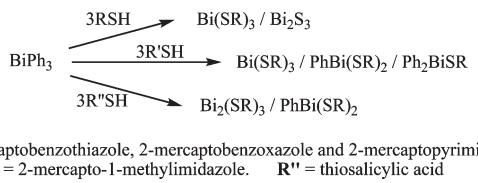

R' = 2-mercaptobenzothiazole, 2-mercaptobenzoxazole and 2-mercaptopyrimidine.
R' = 2-mercapto-1-methylimidazole. **R''** = thiosalicylic acid

Exploration of solvent free and/or microwave assisted syntheses of bismuth(III) thiolates

Philip C. Andrews,* Glen B. Deacon, Peter C. Junk and Nadia F. Spiccia

The formation of bismuth(III) thiolates under standard reflux conditions and under microwave irradiation in toluene or mesitylene, and solvent free reactions using conventional and microwave heating, have been studied and compared.

1328

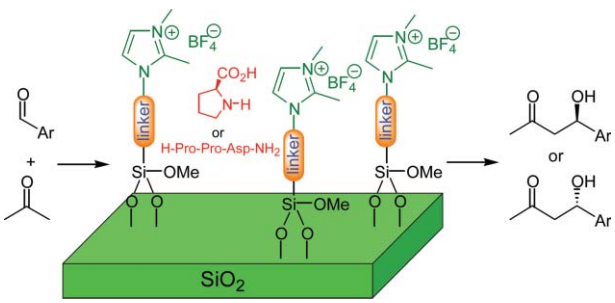

New ionic liquid-modified silica gels as recyclable materials for L-proline- or H–Pro–Pro–Asp–NH_2-catalyzed aldol reaction

Carmela Aprile, Francesco Giacalone, Michelangelo Gruttadauria,* Adriana Mossuto Marculescu, Renato Noto, Jefferson D. Revell and Helma Wennemers

High levels of recyclability (up to nine cycles) and/or selectivity in the aldol reaction have been reached by adsorption of L-proline or tripeptide H–Pro–Pro–Asp–NH_2 onto the surface of ionic liquid modified silica gels.

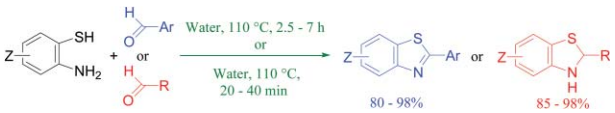

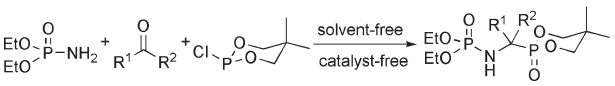

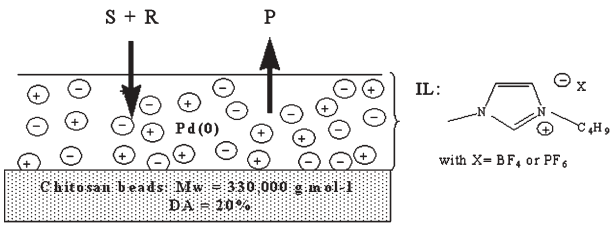

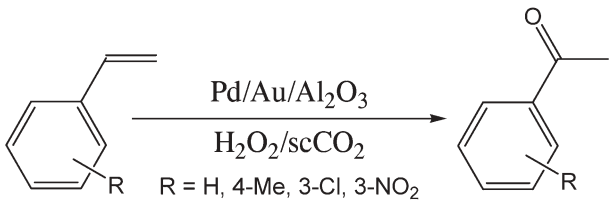

AUTHOR INDEX

FREE E-MAIL ALERTS AND RSS FEEDS

Contents lists in advance of publication are available on the web *via* www.rsc.org/greenchem - or take advantage of our free e-mail alerting service (www.rsc.org/ej_alert) to receive notification each time a new list becomes available.

Try our RSS feeds for up-to-the-minute news of the latest research. By setting up RSS feeds, preferably using feed reader software, you can be alerted to the latest Advance Articles published on the RSC web site. Visit www.rsc.org/publishing/technology/rss.asp for details.

ADVANCE ARTICLES AND ELECTRONIC JOURNAL

Free site-wide access to Advance Articles and the electronic form of this journal is provided with a full-rate institutional subscription. See www.rsc.org/ejs for more information.

* Indicates the author for correspondence: see article for details.

Electronic supplementary information (ESI) is available *via* the online article (see http://www.rsc.org/esi for general information about ESI).

Analytical Abstracts...

NEW & IMPROVED

Analytical Abstracts covers all areas of analytical and bioanalytical science, including the latest applications and cutting edge techniques. The database is updated weekly and spans 25 years of research sourced from over 100 international journals.

...the first stop for analytical scientists

New and improved features include:

Improved search features with a basic search and optional advanced searches by index term and bibliographic data. You can also browse by subject area.

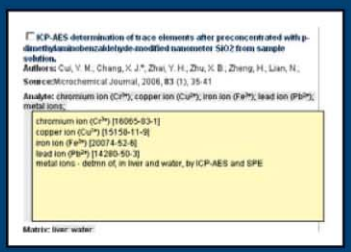

Results can be sorted and displayed in different formats and have additional information embedded in the text accessed via pop up boxes.

Results can be exported to reference management software and to email.

06020716

RSC Publishing

www.rsc.org/aa
Registered Charity Number 207890

December 2007 / Volume 4 / Issue 12 / ISSN 1744-1560 / CTHEC2 / www.rsc.org/chemicaltechnology

Chemical Technology

Only one light source required to swap isomers thanks to ferrocene

Mastering molecular memory

A molecule that switches shape when triggered by light could lead to nanoscale memory devices, say chemists in Japan.

Hiroshi Nishihara and colleagues from the University of Tokyo have combined photochemistry and electrochemistry to make a molecule that can be switched from one form to another, and then back again, using a single source of light. Previous such photochromic molecules have needed a second light source of a different wavelength to be flipped back to their original state.

'Focussing dual light sources on the same small spot can be a problem from the perspective of both technical difficulty and cost performance,' said Nishihara. 'Our system is the first monolayer film of photochromic molecules which can be reversibly switched by a single light source.'

The Tokyo team used a photochromic molecule that incorporates an iron-containing ferrocene group, which they deposited in a single layer onto a transparent electrode surface. When the molecule's iron core is in the 2+ oxidation state, green light isomerises a double bond in the structure from *trans* to *cis*, changing the shape. When the iron is electrochemically converted to Fe(III), the same green light will convert *cis* form back to the *trans* isomer.

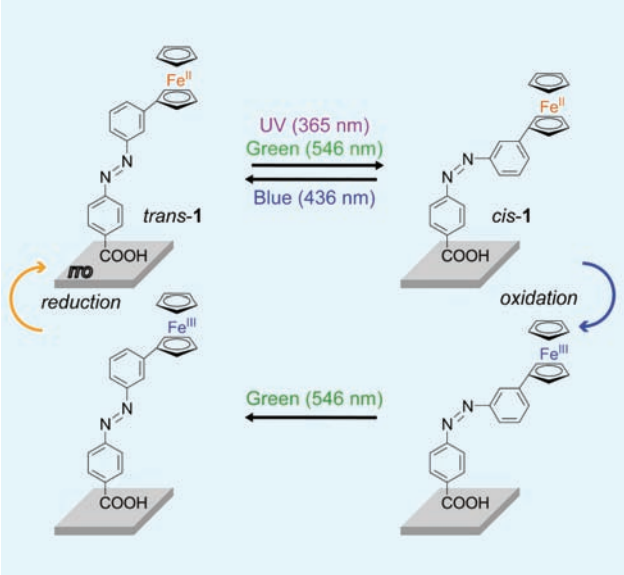

The molecule flips between states using only green light

'This work takes one of the most challenging leaps for chemists: to interface small molecule materials with developing infrastructure from microtechnology,' said Amar Flood, who researches molecular switches at Indiana University, Bloomington, US. 'It is critical to take this step – chemists mustn't lose sight of engineering, because otherwise our engineering colleagues will lose sight of us.'

Nishihara is now working to fine-tune the chemical structure of the molecule, to increase the proportion of molecules in the sample that isomerise in response to the light. 'The other [project] is to immobilise the molecules onto submicron-sized electron arrays, to demonstrate high density memory device fabrication,' he said.

James Mitchell Crow

Reference
K Namiki *et al.*, *Chem. Commun.*, 2007, 4650 (DOI: 10.1039/b713107k)

In this issue

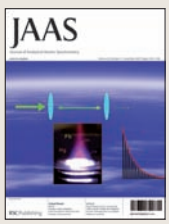

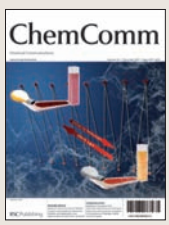

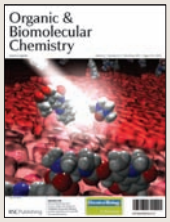

The latest applications and technological aspects of research across the chemical sciences

Application highlights

Hydrogen and oxygen are evolved in separate streams

Water splitting

A team of Italian scientists has created a sunlight-powered cell that produces pure hydrogen from water.

The team from the University of Milan and the University of Pavia are studying environmentally friendly ways to generate hydrogen, which could in future replace fossil fuels as a major energy source.

The new cell has two compartments filled with water and separated by an electrode made of platinum and titanium dioxide. When it is illuminated, by sunlight or an ordinary lamp, the electrode catalyses the splitting of the water into hydrogen and oxygen gas.

Elena Selli, who led the research, pointed out 'Almost all the photocatalytic water splitting systems described so far imply the evolution of a mixture of hydrogen and oxygen in only one reactor; of course, a separation step would be required prior to any use of hydrogen.' The new design of cell keeps the production of the two gases separate, resulting in streams of hydrogen and oxygen that do not need any purification to be useful.

'Our results demonstrate that hydrogen production from water photocatalytic splitting should be regarded as a practically viable, extremely promising way for clean, low cost and environmentally friendly conversion of solar energy into chemical energy,' said Selli. The team is working on improving the efficiency of the cell by making the titanium dioxide layer of the electrode more sensitive to visible light.

Clare Boothby

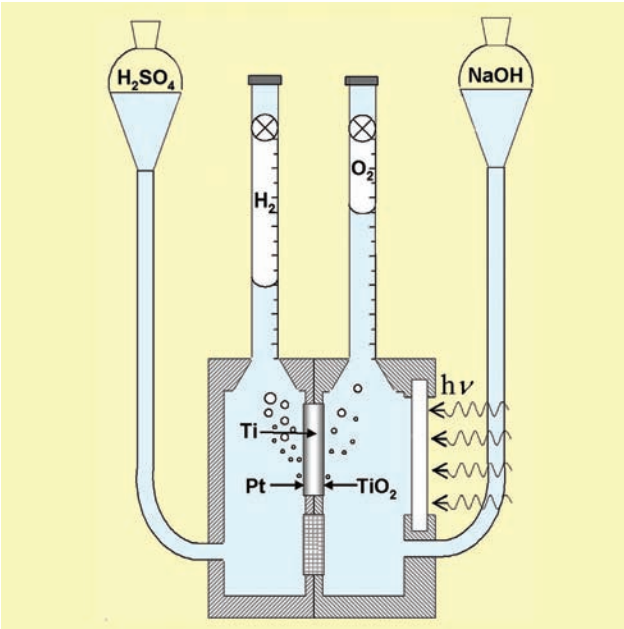

The two gases are produced from different sides of the membrane

Reference
E Selli *et al*, *Chem. Commun.*, 2007, DOI: 10.1039/b711747g

Nickel ions used for simulataneous purification and immobilisation

Ready-to-use enzyme reactors within minutes

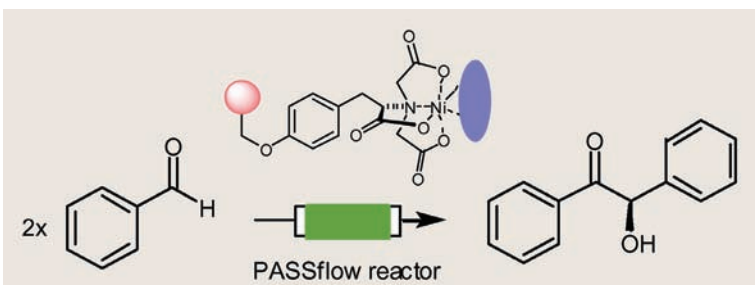

The enzymes (blue) are linked to the polymers (pink) by Ni-NTA

A fast multi-step microreactor for enzymatic synthesis has been developed by scientists in Germany.

The system has influences from both chemical synthesis and molecule biology according to its developers, Gerald Dräger and colleagues from University of Hannover in Leibniz. The new system enables both the immobilisation and purification of enzymes in the same reactor, which can then be used for a variety of enzymatic syntheses. Using this technique it is possible to obtain ready-to-use enzyme reactors from crude protein mixtures within minutes.

The system uses immobilised Ni-NTA (nitrilotriacetic acid) with a new tyrosine linker, attached to polymeric materials inside the reactor chamber. The reactor itself is integrated into an HPLC set-up. The NTA component is used in metal ion affinity chromatography, which in turn can be used to purify His6-tagged proteins from crude cell extracts. The polymeric materials in the reactor have also been altered to be more polar, ideal for biological molecules.

'The NTA linker is used to chelate with the Ni ion. The bound Ni ions themselves catch enzymes or proteins in the solution,' explained Dräger. This means that crude cell extracts can be both purified and immobilised simultaneously using this system, speeding up the whole process as normal reactors miss the purification step.

'The new tyrosine-based linker as compared to the standard lysine linker gives us higher loadings, increased efficiency and less purity problems,' added Dräger. The reactor system is flexible, meaning that different enzymes can be used. It also has the added advantages that it is licence-free and the reactor can be re-used a number of times.

Michele Zgraggen

Reference
G Dräger *et al*, *Org. Biomol. Chem.*, 2007, **5**, 3657 (DOI: 10.1039/b712804e)

Spectroscopy measures atomic ratios to find explosives

Detection at a distance

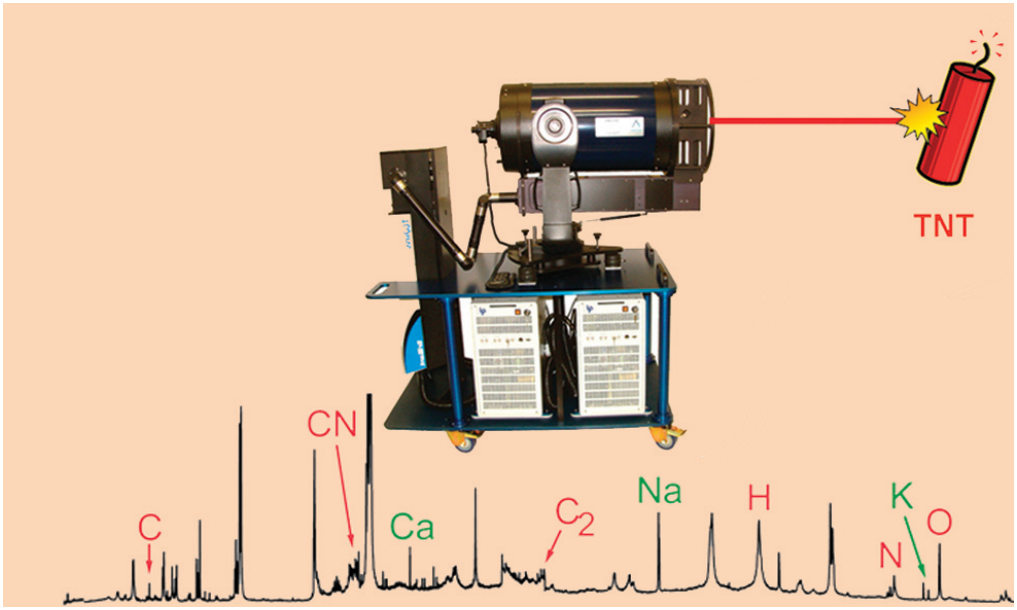

Laser-induced breakdown spectroscopy looks at how much oxygen and nitrogen are present

Chemistry is helping scientists in the US to detect explosives from a safer distance.

Detecting trace amounts of explosives from a distance quickly and accurately is a key aim for both the military and security sectors. Jennifer Gottfried and her team at the US Army Research Laboratory in Maryland have developed a detection system sensitive and selective enough to detect explosive residues at 20 m. Their system uses laser induced breakdown spectroscopy (LIBS) to identify molecules.

LIBS uses a laser pulse to turn a small part of a sample into a plasma of excited atoms and ions. As the plasma cools the characteristic atomic spectra of its constituents can be detected. The idea is that energetic molecules (potential explosives) contain higher ratios of oxygen and nitrogen to carbon and so can be identified by looking at the ratios of these atoms in a sample. This is far from straightforward, however, not least because nitrogen and oxygen are the main components of air.

Gottfried and her colleagues think they have overcome the problems. Using an argon flow to displace air reduced the interference from air sufficiently, but is impractical for detecting explosives at a distance. For this, they discovered that using a second laser pulse instead of only a single pulse enabled sufficient separation of the N and O peaks due to air from those of the sample compounds.

The team then developed suitable chemometric methods to enable interpretation of the data so that detection of energetic molecules was possible, even in the presence of interferences, such as dust.

Gottfried hopes these developments will fill an important gap in security systems. 'Currently there are no proven technologies that can accomplish residue explosives detection at a distance in a real-world scenario,' said Gottfried. She is optimistic that it will develop into a usable device, saying 'We expect that this technology will be available commercially very soon.'

Further development is still needed though, as Gottfried makes clear: 'This technology still needs to be verified and validated in real-world applications. We are moving in that direction.'

Edward Morgan

Reference
J L Gottfried *et al*, *J. Anal. At. Spectrom.*, 2008, DOI: 10.1039/b703891g

News in brief

Finding the right blend
Non-invasive infra-red spectrometry can provide scientists with improved quality checks for pharmaceutical production.

Cell culture and lysis on a chip is BASIC
US researchers have come up with a general strategy to integrate several biological steps in one microchip reactor.

See **www.rsc.org/chemicaltechnology** *for full versions of these articles*

This month in *Chemical Science*

Water – not just a solvent
Scientists in Germany have used water to improve the catalytic activity of coupling reactions making them greener and faster.

Pesticide persists in German rivers
Levels of the pesticide terbutryn in German rivers have not fallen, despite having been banned in 2003, say environmental researchers.

The changing colour of gold
DNA and gold nanoparticles provide a more sensitive way to detect copper ions in nature.

See **www.rsc.org/chemicalscience** *for full versions of these articles*

This month in *Chemical Biology*

Bringing warhead efficiency to light
US scientists can now compare molecular warheads that inactivate proteins.

Emotional enzymes
Chemists in the US have created fluorescent probes that can detect enzymes affecting our emotions.

Cells surface in semisynthesis
Scientists in Japan are using cells as protein factories

See **www.rsc.org/chembiology** *for full versions of these articles*

Selective ligand loves carbon monoxide, hates hydrogen

I capture the catalyst

The largest transition metal-catalysed process in the chemical industry could soon get an efficiency boost, thanks to the isolation of a key catalytic intermediate.

UK chemists have made a new series of catalysts in an effort to up the efficiency of one of the most widely used, and energy-intensive, catalytic processes in the chemical industry – the conversion of carbon monoxide (CO) and methanol into acetic acid. Matthew Clarke and colleagues at St Andrews University, UK, have examined a series of diphosphine ligands in the rhodium-catalysed carbonylation of methanol. 'This is one of the simplest organic reactions there is, but because of the scale, it must be done so incredibly efficiently,' said Clarke.

The industrial process used currently, BP's Cativa process, requires the starting CO to be purified, and the final product to be distilled – both of which are energy-expensive processes. Now BP is funding a project to look for the next generation of catalyst to get around either, or both, of these drawbacks.

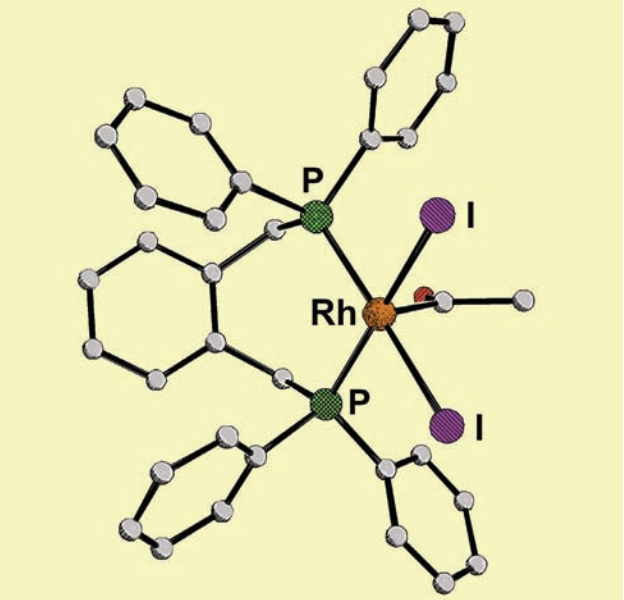

The rhodium complex could cut out the purification step

Cheaper, lower grade CO includes large amounts of hydrogen, so to use it you need a catalyst that reacts with the CO but not the hydrogen, said Clarke. 'We identified a ligand, dppx [tetrakis(diphenylphosphino)-*p*-xylene], that was very selective,' he said. 'We isolated the catalytic intermediate, and showed it doesn't react with hydrogen, where the others do, so this is likely to be the origin of the selectivity.

'We're already making new catalysts based on this work, trying to gain a rational understanding of the selectivity,' Clarke added. 'We haven't cracked it yet, but I have an inkling there is a ligand out there that is active, selective, stable and commercially viable.'

Andreas Danopoulos, who studies catalysis at the University of Southampton, UK, said the work was a good approach to understanding the catalyst. 'But I'm not sure that rational design is the best way to solve this problem – I think a combinatorial approach [to screen a large number of possible ligands] would be better,' he said.

James Mitchell Crow

Reference
G Lamb *et al.*, *Dalton Trans.*, 2007 (DOI: 10.1039/b712974b)

Microbes fuel the way to better water treatment

Bacteria act as miner's canary for toxins

Microbial fuel cells for detecting pollutant levels in wastewater have been developed by Korean scientists.

Hyung Joo Kim from Konkuk University, Seoul, and collaborators have developed fuel cells powered by bacteria for monitoring levels of toxins in water entering wastewater treatment plants.

Biological wastewater treatment plants rely on maintaining a carefully balanced mixture of bacteria and other organisms, said William Draper, an expert in environmental health from the Department of Health, California, US. He explained that effective methods are needed to monitor excessive levels of toxins in the water entering the plants so the organism balance can be maintained.

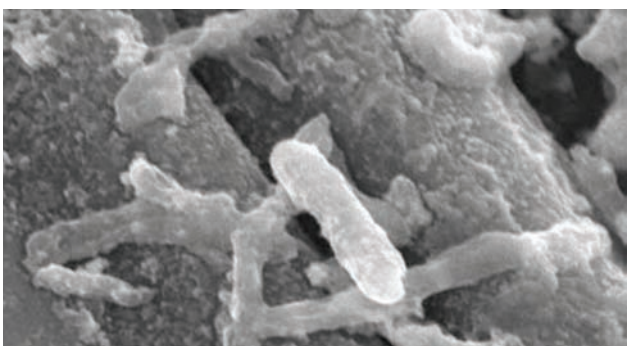

The fuel cell's output dips as toxins increase

The bacteria in Kim's fuel cells convert biochemical energy into electrical energy by oxidizing organic matter in the water. The electric current is then detected by a potentiometer, explained Kim.

The bacteria generate a constant electric current under standard water pollutant levels. When the toxin levels in the water increase, however, the microbes become less efficient and electricity generation is inhibited. Draper likened this monitoring concept to 'the miner's canary'.

Further work is needed before these fuel cells can replace existing methods, explained Kim. He said that detection limits and specificity to various toxins need to be found, as well as ensuring the microbe community won't adapt to changes in pollutant levels.

Nina Athey-Pollard

Reference
M Kim *et al*, *J. Environ. Monit.*, 2007, DOI: 10.1039/b713114c

Interview

The fascination of catalysis

Ferdi Schüth talks to Madelaine Chapman about rockets, catalysis and law

Ferdi Schüth

Ferdi Schüth is a professor at the Max-Planck-Institut für Kohlenforschung in Mülheim an der Ruhr, Germany. His research focuses on the synthesis and characterisation of inorganic materials which have a use in catalysis. He is a member of the *Physical Chemistry Chemical Physics* advisory editorial board.

Who or what inspired you to become a scientist?
There was a fellow student in high school when I was 11 years old who went out after New Year, when we have rockets and fireworks in Germany, and collected the empty shells. We filled them with black powder and then tried to make them go again. We never got them to fly. They just exploded, but that was fun. Ever since then, I wanted to be a chemist.

How did you become interested in catalysis?
I wasn't interested in a particular topic so I selected an advisor to work with, who happened to do catalysis. For my habilitation, I worked with Professor Klaus Unger in Mainz, who is an inorganic chemist. I find this combination of inorganic/materials chemistry with catalysis really enjoyable. My career path involved many chance decisions which, in hindsight, turned out to be wonderful. Now I tell my students: 'don't plan too much.' My grandmother always said the one who plans early has to plan twice. There is a lot of wisdom in that.

What part of your research are you most proud of?
In 1992, I had an idea to stick a molecule into a zeolite channel. I proposed that if I had a single crystal of a zeolite, I should be able to analyse the orientation of the molecule in the zeolite with polarised infrared radiation using an infrared microscope. Infrared microscopes had just been introduced one year before. I wrote a proposal for this microscope which was granted. The very first day of experiments provided the spectra for a good paper. The fact that the idea immediately and directly worked made me very proud. Normally that never happens. Normally you have an idea but it fails and takes three times as long as you think.

I am also proud of a field we have developed over the last few years - the analysis of silicate species and the development of different species with mass spectrometry. This was much more complex and it certainly did not work straight away.

You are involved in the application of high-throughput experimentation to catalysis. How is this field progressing?
The field, which allows us to quickly screen a large number of catalysts, is pretty mature although it's only about 10 years old. The development of cutting-edge technology has moved into companies and is less of an academic topic nowadays. But there are still aspects of it where there are big challenges. In biotechnology, scientists do computational screening of molecule libraries. We would benefit greatly if we applied similar technology to materials science, especially catalysis. Even with the most powerful high-throughput techniques, it's not possible to explore all possible new catalysts experimentally. Developing computational methods to narrow down the search is one of the biggest challenges we have.

Can these techniques be used to gain physical insight into what's actually happening in a catalytic reaction?
Absolutely. Normally if we want to get insight, we measure the performance of different catalysts, we analyse catalyst composition, structure and so on and then we build models and try to derive structure-activity relationships. Thanks to high-throughput experimentation, we have more catalysts and more characterisation data and so the database from which we are establishing these relationships is a much wider one. Consequently, we can either get insight into these structure-activity relationships more quickly or we can get deeper insight because we see more.

What is the secret to running a successful research group?
My belief is that people working with me should have freedom. They have to think for themselves. I also strongly believe that people have to have fun at work. They have to like what they are doing. When I hire new people I am always looking for a fire burning in them. They need to be fascinated by the chemistry. I also think you need material resources. You can only go so far with just ideas - at some point you need steel and glass.

If you weren't a scientist, what would you do?
I would probably be a judge. I have both a law degree and a chemistry PhD. I had several different career possibilities - industrial chemist, patent lawyer, academic or judge - and I weighed up all their pros and cons. The ones that scored highest were an academic chemist and a judge in administration law.

ACS and RSC:
Building the Future,
one molecule at a time.

The American Chemical Society and Royal Society of Chemistry are not-for-profit society publishers. We support excellence in research and education by investing in our future generations of chemists.

ACS PUBLICATIONS
HIGH QUALITY. HIGH IMPACT.

RSC Publishing

Instant insight

Holographic data storage

Avtar Matharu and colleagues from the University of York, UK, explain how, when it comes to data, size matters

Modern-day society lives in an information-obsessed world. The volume of information produced and stored annually is exponential in growth. The information age has arrived in all its glory with on-line access to vast resources of electronic information never imagined less than one decade ago. On a daily basis we are bombarded with high resolution digitised images utilising mega- and giga-bytes of information. In the area of home entertainment we can now purchase the latest state-of-the-art BluRay DVD player capable of storing a staggering 27 GB, surpassing its counterparts, the CD (750 MB or 75 minutes of music) and DVD (4.7 GB or a 2 hour movie). However, this is still not enough as the societal needs of the 21st century for increased information content with even faster processing speeds continue to grow at breakneck speed.

There's one big problem – storage space. Although magnetic disk is still the best medium for storage of large amounts of information, it has severe limitations. Magnetic disk, and conventional magneto-optical data storage technology, use the surface of the medium to store and retrieve bits of data. The available area on a magnetic disk cannot be compressed indefinitely to record even smaller bits of information due to the superparamagnetic effect. The diameter of the magnetic domains is limited to around 10 nm: smaller than this and thermal self-erasure occurs. The magnetised bit flips randomly, finding it difficult to attain a stable state.

New, alternative technologies need to be considered. Holography, an optical 3-D volumetric approach, may be the answer to meet the societal needs of the 21st century rather than the current 2-D surface approach. The concept of holography was first introduced by Gabor in 1948 but remained dormant for many years due to a lack of technological advances in complementary optics and image processing instrumentation. Holographic storage provides the potential to store in excess of one terabyte of information with transfer rates exceeding 1 GB/s and data access time of less than 100 µs.

The world's information could be stored and retrieved within a liquid crystal holographic box

In holographic storage, a whole page of information in the form of a bit-map is recorded at once, instead of storing single bits as in digital storage. Typically, two laser beams derived from a single laser source are overlapped on a photosensitive material. One of the beams, called the object beam, passes through the object (bit-map) of interest, and the other beam is a plane wave providing a phase reference. In conventional holography, the two beams have the same polarization. They create a complicated interference pattern in the film that is characteristic of the object. The recorded information is read out with a conjugate of the reference wave. By the process of angular multiplexing several holograms can be recorded in the same volume.

Significant advances have been made in holography, as exemplified by InPhase Technologies' tapestry™ holographic media, capable of storing and retrieving 200 GB on a standard 120 mm CD format at high speed, equivalent to a near ten-fold improvement on optical BluRay DVD technology. There are still drawbacks, however, as the ideal material is still to be found. Any material suitable for holographic storage should possess fast optical switching between two states, high thermal stability over a wide temperature range and non-destructive read-out. As the search for holographic materials continues, liquid crystals may play an important role. Liquid crystals constitute the fourth state of matter intermediate between the solid and the liquid states. The intermediate ordering of molecules between order and disorder may enhance storage properties. Although liquid crystals are not a pre-requisite for holographic storage, their anisotropic shape is important.

Imagine one day we may all be carrying a credit card with a 1 × 1 cm square hologram capable of storing all our personal details including medical records with X-ray scans. In the event of sudden serious illness the hologram may be read immediately to display your full medical history rather than having to wait for information to be sent by email or post. The time saved may ultimately save your life.

Reference
A S Matharu, S Jeeva and P S Ramanujam, *Chem. Soc. Rev.*, 2007, DOI: 10.1039/b706242g

Read the full Tutorial Review 'Liquid crystals for holographic optical data storage' in Issue 12 of Chemical Society Reviews.

Essential elements

New RSC Books website

The RSC Books website has recently undergone a substantial revamp, and we are pleased to present our new and improved site. New features include improved functionality that allows users to browse RSC books by series, subject area, publication copyright year and by A–Z title searching. Alternatively, keyword or author searches can now be carried out using the built-in Google search. Forty years of RSC books are included on the new website, from early titles in 1968 to the books RSC will be publishing next year in 2008.

The new RSC Books website site is closely linked to our online shop with direct links to the RSC eBook Collection. This enhanced visibility enables you to view the table of contents and first chapter of any book in the collection free of charge. The new RSC Books website provides all the browser requirements, such as a shopping cart facility with selected special discounts function, needed for simple website navigation and ease of use. All the latest information can be found in the new RSC Books website: how to publish your book with RSC Publishing, titles in our RSC eBook Collection and regular website updates on our new releases, most popular titles and books for students.

For more information visit www.rsc.org/books

Tokeshi wins Pioneers in Miniaturisation prize

Manabu Tokeshi has been named as the 2007 winner of the Pioneers in Miniaturisation prize.

The prize, first awarded in 2006, was established by two of the major players in the miniaturisation sector, *Lab on a Chip* and Corning Incorporated.

Joydeep Lahiri, research director at Corning Inc., commented 'Tokeshi's multi-disciplinary research exemplifies the essential outreach that is necessary – particularly to the molecular biology or medical areas – in order to find "the next big thing" that will succeed, for example, Corning's μPlate technology.'

The prize aims to promote miniaturisation through micro and nanotechnologies to the wider scientific community and encourage both young and new scientists into the field.

From left: Harp Minhas, editor, *Lab on a Chip*; Manabu Tokeshi (2007 Award Winner); Joydeep Lahiri, research director, Corning Inc.; and Andreas Manz, chair of the *Lab on a Chip* editorial board.

Yoshinobu Baba of the Plasma Nanotechnology Research Center Nagoya University, Japan, said 'Tokeshi has been the powerhouse behind many interdisciplinary publications as his record shows.'

The presentation of this prestigious award was made at the μTAS 2007 conference held in Paris, France, in October.

For more information see www.rsc.org/loc

And finally...

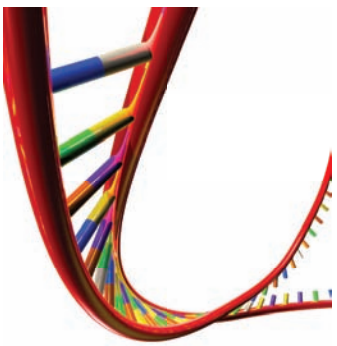

***Molecular BioSystems* unzips ...**

From January 2008 *Molecular BioSystems* will form its very own strand of science as a stand alone monthly journal, becoming solely available to readers and subscribers independently of its host journal. Read more on how the journal is serving the community and why it is ready to unzip at *www.molecularbiosystems.org*

Speaking volumes...

Times flies when you're publishing high impact science. In 2008, four RSC journals celebrate their tenth year of publication: *Physical Chemistry Chemical Physics*, *CrystEngComm*, *Green Chemistry* and the *Journal of Environmental Monitoring*. These diverse journals are all now firmly established as market leaders in their subject areas, with each continuing to go from strength to strength. Watch out for special 10th anniversary events and celebrations throughout 2008!

Chemical Technology (ISSN: 1744-1560) is published monthly by the Royal Society of Chemistry, Thomas Graham House, Science Park, Milton Road, Cambridge UK CB4 0WF. It is distributed free with *Chemical Communications*, *Journal of Materials Chemistry*, *The Analyst*, *Lab on a Chip*, *Journal of Environmental Monitoring*, *Green Chemistry*, *CrystEngComm*, *Physical Chemistry Chemical Physics* and *Analytical Abstracts*. *Chemical Technology* can also be purchased separately. 2007 annual subscription rate: £199; US $376. All orders accompanied by payment should be sent to Sales and Customer Services, RSC (address above). Tel +44 (0) 1223 432360, Fax +44 (0) 1223 426017 Email: sales@rsc.org

Editor: Neil Withers

Associate editors: Nicola Nugent, Celia Clarke

Interviews editor: Joanne Thomson

Essential Elements: Daniel Bradnam, Rebecca Jeeves, and Kathryn Lees

Publishing assistant: Ruth Bircham

Publisher: Graham McCann

RSC Publishing

Green Chemistry

Cutting-edge research for a greener sustainable future

www.rsc.org/greenchem

Volume 9 | Number 12 | December 2007 | Pages 1261–1384

ISSN 1463-9262

RSC Publishing

1463-9262(2007)9:12;1-R

The E Factor: fifteen years on

Roger A. Sheldon

Received 6th September 2007, Accepted 2nd October 2007
First published as an Advance Article on the web 19th October 2007
DOI: 10.1039/b713736m

The purpose of this perspective is to review the effect that the E Factor concept has had over the last fifteen years on developments in the (fine) chemical industry and pharmaceutical industry with regard to waste minimisation and to assess its current status in the broader context of green chemistry and sustainability. We conclude that the E Factor concept has played a major role in focusing the attention of the chemical industry world-wide, and particularly the pharmaceutical industry, on the problem of waste generation in chemicals manufacture. It provided, and continues to provide, the impetus for developing cleaner, more sustainable processes.

1. Introduction: origins of the E Factor concept

The fifteenth anniversary of the publication of the E Factor concept[1] seemed like a good moment in time to reflect on the effect it has had on process chemistry and process chemists and the role it may have played in promoting change. In the early 1980s our attention was drawn to the problem of waste in the (fine) chemicals industry by the closure of a phloroglucinol plant at Océ Andeno (later to become part of DSM Fine Chemicals). The plant was shut down because the cost of disposing of the waste was rapidly approaching the selling price of the product. As is shown in Fig. 1, the process involved vintage 19th century organic chemistry: oxidation of 2,4,6-trinitrotoluene (TNT) with potassium dichromate in fuming sulfuric acid (oleum), followed by Béchamp reduction with iron and hydrochloric acid to give, after *in situ* decarboxylation, 1,3,5-triaminobenzene.[2] Subsequent heating of the acidic solution of the latter afforded phloroglucinol.

This process generated *ca.* 40 kg of solid waste containing $Cr_2(SO_4)_3$, NH_4Cl, $FeCl_2$ and $KHSO_4$ for every kg of phloroglucinol. Based on this edifying experience we began

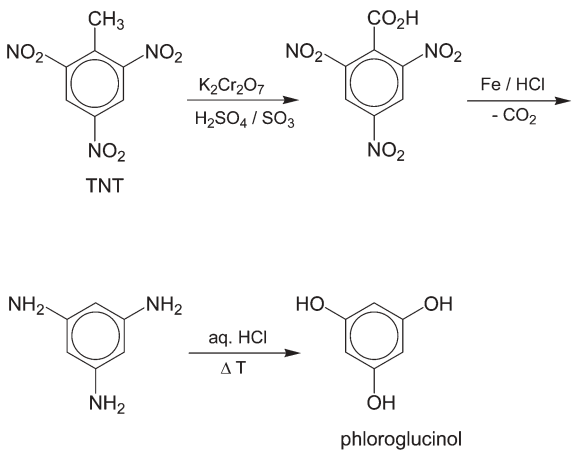

Fig. 1 Phloroglucinol manufacture from TNT.

Biocatalysis & Organic Chemistry, Delft University of Technology, 2628 BL Delft, Netherlands. E-mail: R.A.Sheldon@.tudelft.nl

an inventory of the amount of waste formed in processes for the manufacture of other fine chemicals and pharmaceutical intermediates and some bulk chemicals. It soon became clear that tens of kg of waste per kg product was no exception in the fine chemicals industry. This led us, in the late 1980s, to propose what we called the E(nvironmental) Factor (kg waste/kg product) for assessing the environmental impact of manufacturing processes and the now well-known Table of E Factors was used to illustrate the problem of waste in different segments of the chemical industry (see later).

At about the same time we also began using what we called the *atom utilisation* concept for quickly assessing the environmental acceptability of processes at an early stage, by analogy with the use of '*syn gas utilisation*'. We developed the latter in the late 1970s to roughly assess the commercial viability of various processes for the production of commodity chemicals from syn gas.[3] The idea was simple: the more atoms of the syn gas that ended up in the product the better. Methanol synthesis, for example, involves 100% syn gas utilisation, while ethylene utilises only 44%. Extension of this concept afforded the idea of using *atom utilisation* to assess the (potential) environmental acceptability of processes. An example, which we used to illustrate this concept, was a comparison of the traditional chlorohydrin route to ethylene oxide with the commercial process *via* oxidation of ethylene with molecular oxygen (see Fig. 2). The concept was reported in an interview published in 1991.[4] At about the same time Trost published his elegant paper[5] on the *atom economy* which became the widely accepted terminology, although it is also referred to as *atom efficiency*. We presented our concepts at the International Symposium on Catalytic Chemistry for Global Environment in Sapporo, Japan, in July, 1991, and they were subsequently published in 1992.[1]

2. Enter green chemistry and sustainability

Interestingly, at about the same time the concept of green chemistry was being formulated, by Anastas[6–10] at the US Environmental Protection Agency (EPA), to address the environmental issues of both chemical products and the processes by which they are produced. The guiding principle is the *design* of environmentally benign products and processes

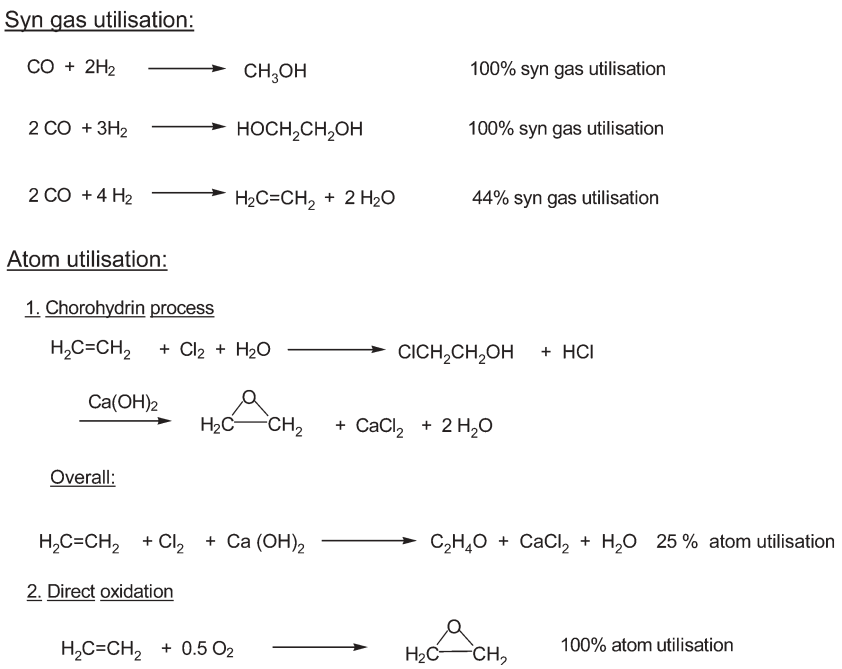

Fig. 2 Syn gas utilisation and atom utilisation.

(*benign by design*) which is embodied in the 12 Principles of Green Chemistry,[6] the essence of which can be reduced to the following working definition.

Green chemistry efficiently utilises (preferably renewable) raw materials, eliminates waste and avoids the use of toxic and/or hazardous reagents and solvents in the manufacture and application of chemical products.

According to this definition 'raw materials' includes the source of energy. Green chemistry eliminates waste at source, *i.e.*, it is primary pollution prevention rather than waste remediation (end-of-pipe solutions). Prevention is better than cure (the first of the twelve principles of green chemistry). In the last fifteen years the concept of green chemistry has become firmly entrenched in both industrial and academic circles and several books have been devoted to the subject.[6,7,9–14] Subsequently, Anastas and Zimmerman[15] proposed the twelve principles of green engineering which embody the same underlying features—conserve energy and resources and avoid waste and hazardous materials—as those of green chemistry, but from an engineering viewpoint. More recently, a mnemonic, PRODUCTIVELY, has been proposed by Poliakoff *et al.*[16] which captures the spirit of the twelve principles of green chemistry and can be presented as a single slide.

An alternative term, often more favoured by the chemical industry, is sustainable development, a concept which dates back to the late 1980s and can be defined as:[17] *Meeting the needs of the present generation without compromising the ability of future generations to meet their own needs*. One could say that sustainability is our ultimate common goal and green chemistry is the means of achieving it.

3. E Factors and atom efficiency as green metrics

It is now generally accepted that two useful measures of the (potential) environmental acceptability of chemical processes are the E factor,[1,18–21] defined as the mass ratio of waste to desired product, and the atom efficiency, calculated by dividing the molecular weight of the desired product by the sum of the molecular weights of all substances produced in the stoichiometric equation. The enormity of the waste problem in chemicals manufacture is readily apparent from a consideration of typical E factors in various segments of the chemical industry (Table 1).

The E factor is the actual amount of waste produced in the process, defined as everything but the desired product. It takes the chemical yield into account and includes reagents, solvent losses, all process aids and, in principle, even fuel (although this is often difficult to quantify). There is one exception: we generally excluded water from the calculation of the E factor. For example, when considering an aqueous waste stream only the inorganic salts and organic compounds contained in the water are counted, the water itself is excluded. Inclusion of water used in the process can lead to exceptionally high E factors in many cases and can make meaningful comparisons of processes difficult.[13]

A higher E factor means more waste and, consequently, greater negative environmental impact. The ideal E factor is zero. Put quite simply, it is kilograms (of raw materials) in, minus kilograms of desired product, divided by kilograms of product out. It can be easily calculated from a knowledge of the number of tons of raw materials purchased and the number

Table 1 E factors in the chemical industry

Industry segment	Product tonnage	E Factor (kg waste/kg product)
Oil refining	10^6–10^8	<0.1
Bulk chemicals	10^4–10^6	<1–5
Fine chemicals	10^2–10^4	5–50
Pharmaceuticals	10–10^3	25–100

of tons of product sold, for a particular product or a production site or even a whole company. It is perhaps surprising, therefore, that many companies are not aware of the E factors of their processes. We hasten to point out, however, that this situation is rapidly changing and the E factor is being widely adopted by the fine chemicals, pharmaceutical and even the bulk chemical industries. We also note that this method of calculation will automatically exclude water used in the process but not water formed.

Other metrics have been proposed for measuring the environmental acceptability of processes. Hudlicky and co-workers,[22] for example, proposed the effective mass yield (EMY), which is defined as the percentage of product of all the materials used in its preparation. As proposed, it does not include so-called environmentally benign compounds, such as sodium chloride, acetic acid, *etc*. This is questionable as the environmental impact of such substances is very volume-dependent. Constable and co-workers of GlaxoSmithKline[23] proposed the use of mass intensity (MI), defined as the total mass used in a process divided by the mass of product, *i.e.*, MI = E factor + 1, and the ideal MI is 1 compared with zero for the E factor. These authors also suggest the use of so-called mass productivity, which is the reciprocal of the MI and, hence, is effectively the same as EMY. Attempts have also been made to unify the different green metrics.[24] More recently, the Green Chemistry Institute Pharmaceutical Round Table has used the Process Mass Intensity (PMI), which is the same as Mass Intensity, to benchmark the environmental acceptability of processes used by its members (see the Green Chemistry Institute website). The latter include several leading pharmaceutical companies (Eli Lilly, GlaxoSmithKline, Pfizer, Merck, AstraZeneca, Schering-Plough and Johnson & Johnson). The aim was to use this data to drive the greening of the pharmaceutical industry.

In our opinion none of these alternative metrics offers any particular advantage over the E factor for giving a mental picture of how wasteful a process is. As noted above, the ideal (P)MI is 1 whereas the ideal E Factor is 0, which more clearly reflects the ultimate goal of zero waste.

As is clear from Table 1, enormous amounts of waste, comprising primarily inorganic salts, such as sodium chloride, sodium sulfate and ammonium sulfate, are formed in the reaction or in subsequent neutralisation and other work-up steps. One of the reasons that the E factor increases dramatically on going downstream from bulk to fine chemicals and pharmaceuticals is that the latter involve multi-step syntheses and pharmaceutical companies have emphasised that the *absolute* amount of waste is lower than in bulk chemicals because of the much lower production volumes involved. However, the larger E Factors in the fine chemical and pharmaceutical industries are also due to the widespread use of classical stoichiometric reagents rather than catalysts (see later). Hence, we felt that the lower absolute amounts, compared with bulk chemicals, should not be used as an excuse for not doing anything to reduce the E Factor of processes in the fine chemicals and pharmaceuticals segments. It was abundantly clear, 15 years ago, that a paradigm shift was necessary to change from the traditional concepts of process efficiency and optimisation that exclusively focus on chemical yield of the desired product to one that assigns economic value to eliminating waste and avoiding the use of toxic and/or hazardous chemicals. It was necessary that enviro-economics become a major driving force in technological innovation.

4. Atom for atom

The atom utilisation, atom efficiency or atom economy concept, elegantly promulgated by Trost,[25] is an extremely useful tool for rapid evaluation of the amounts of waste that will be generated by alternative processes. It is calculated by dividing the molecular weight of the product by the sum total of the molecular weights of all substances formed in the stoichiometric equation for the reaction involved. For example, the atom efficiencies of stoichiometric (CrO_3) *versus* catalytic (O_2) oxidation of a secondary alcohol to the corresponding ketone are compared in Fig. 3.

In contrast to the E factor, it is a theoretical number, *i.e.*, it assumes a chemical yield of 100% and exactly stoichiometric amounts and disregards substances which do not appear in the stoichiometric equation. A theoretical E factor can be derived from the atom efficiency, *e.g.*, an atom efficiency of 40% corresponds to an E factor of 1.5 (60/40). In practice, however, the E factor will generally be much higher since the yield is not 100%, an excess of reagent(s) is used and solvent losses and salt generation during work-up have to be taken into account.

It is interesting to calculate the atom efficiency of the phloroglucinol process discussed above. The stoichiometric equation for that process is shown in Fig. 4. This affords an atom efficiency of *ca*. 5% which translates to a theoretical E Factor of *ca*. 20, whereas in reality it is 40.

5. The nature of the waste

All of the metrics discussed above take only the mass of waste generated into account. However, what is important is the environmental impact of this waste, not just its amount, *i.e.*, the nature of the waste must be considered. One kg of sodium chloride is obviously not equivalent to one kg of a chromium salt. Hence, we introduced[18] the term 'environmental quotient', EQ, obtained by multiplying the E factor with an arbitrarily assigned unfriendliness quotient, Q. For example,

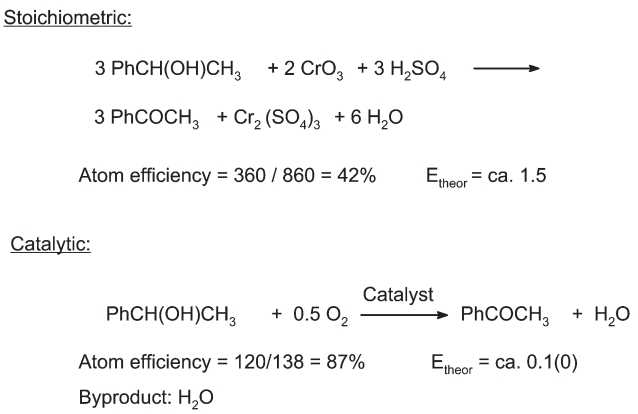

Fig. 3 Atom efficiency of stoichiometric *versus* catalytic oxidation of an alcohol.

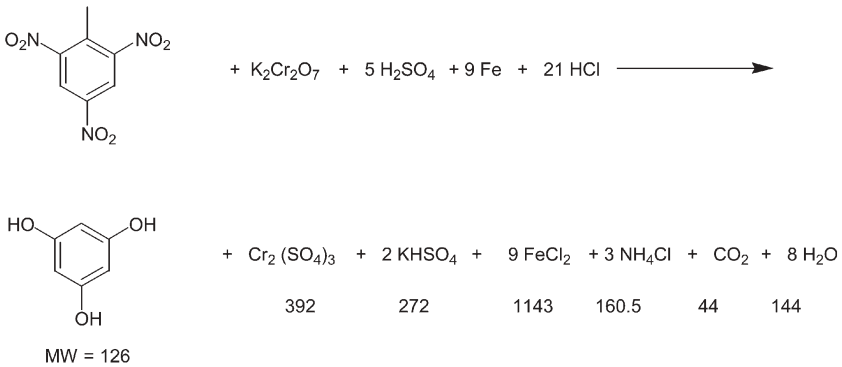

Fig. 4 Stoichiometric equation of the TNT to phloroglucinol process.

one could arbitrarily assign a Q value of 1 to NaCl and, say, 100–1000 to a heavy metal salt, such as chromium, depending on its toxicity, ease of recycling, *etc*. The magnitude of Q is obviously debatable and difficult to quantify but, importantly, 'quantitative assessment' of the environmental impact of chemical processes is, in principle, possible. It is also worth noting that Q for a particular substance can be both volume-dependent and influenced by the location of the production facilities. For example, the generation of 100–1000 tons per annum of sodium chloride is unlikely to present a waste problem, and could be given a Q of zero. The generation of 10 000 tons per annum, on the other hand, may already present a disposal problem and would warrant assignation of a Q value greater than zero. Ironically, when very large quantities of sodium chloride are generated the Q value could decrease again as recycling by electrolysis becomes a viable proposition, *e.g.*, in propylene oxide manufacture *via* the chlorohydrin route. Thus, generally speaking the Q value of a particular waste will be determined by its ease of disposal or recycling. We also mention that, in our experience, organic waste is, generally speaking, more easy to dispose of than inorganic waste. This is important when considering biocatalytic processes (see later).

6. The role of catalysis

As noted above, the waste generated in the manufacture of organic compounds consists primarily of inorganic salts. This is a direct consequence of the use of stoichiometric inorganic reagents in organic synthesis, particularly in fine chemicals and pharmaceuticals manufacture. Examples which readily come to mind are stoichiometric reductions with metals (Na, Mg, Zn, Fe) and metal hydride reagents ($LiAlH_4$, $NaBH_4$), oxidations with permanganate, manganese dioxide and chromium(VI) reagents. A classic example is the phloroglucinol process discussed above, which combines an oxidation with stoichiometric amounts of chromium(VI) with a stoichiometric reduction with Fe/HCl. Similarly, a multitude of reactions, *e.g.*, sulfonations, nitrations, halogenations, diazotisations and Friedel–Crafts acylations, employing stoichiometric amounts of mineral acids (H_2SO_4, HF, H_3PO_4) and Lewis acids ($AlCl_3$, $ZnCl_2$, BF_3) are major sources of waste. The solution is evident: substitution of antiquated stoichiometric methodologies with cleaner catalytic alternatives. Indeed, a major challenge in chemicals manufacture in general is to develop processes based on H_2, O_2, H_2O_2, CO, CO_2 and NH_3 as the direct sources of H, O, C and N. Catalytic hydrogenation, oxidation and carbonylation (Fig. 5) are good examples of highly atom efficient, low-salt processes.

The generation of copious amounts of inorganic salts can similarly be largely circumvented by replacing stoichiometric mineral acids, such as H_2SO_4, and Lewis acids and stoichiometric bases, such as NaOH, KOH, with recyclable solid acids and bases, preferably in catalytic amounts.[26]

7. Bulk chemicals: propylene oxide and caprolactam

The waste problem is not limited to fine chemicals. Although catalytic processes have, for economic reasons, been widely applied in the manufacture of bulk chemicals, there are still some processes which use stoichiometric inorganic reagents

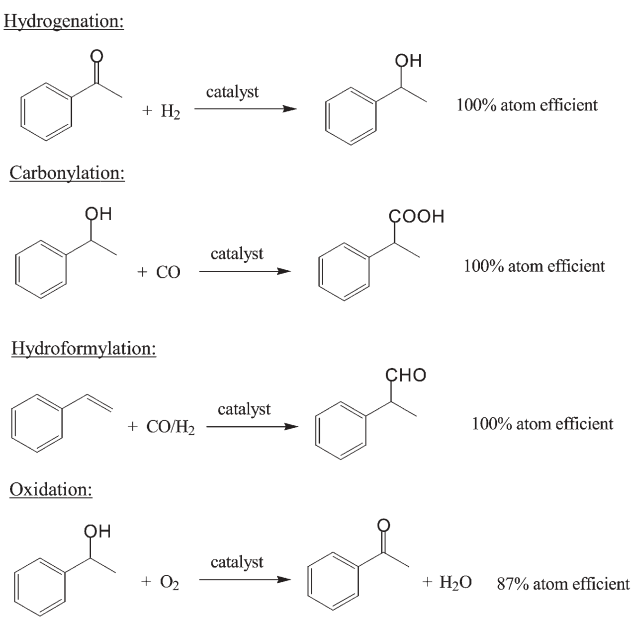

Fig. 5 Atom efficient catalytic processes.

and generate several kg of waste per kg of product (hence the range of <1–5 in Table 1). Although catalytic oxidation is widely applied in the bulk chemicals industry[27] there are still a few processes which use stoichiometric inorganic oxidants. A case in point is propylene oxide manufacture. The chlorohydrin route, which generates *ca.* 2 kg of $CaCl_2$, accounts for more than half of the *ca.* 4 million tons of propylene oxide produced annually. The rest is produced by so-called co-product processes which use oxygen as the primary oxidant but generate *tert*-butanol or styrene as the co-product. It has been known since the mid-eighties that titanium silicalite, developed by Enichem,[28] is able to catalyse the epoxidation of propylene with the green oxidant hydrogen peroxide, but the latter was too expensive for this application. However, Headwaters Technology Innovation (HTI) received a 2007 Presidential Green Chemistry Challenge Award for the development of a palladium–platinum nanocatalyst, which enables the direct synthesis of hydrogen peroxide from hydrogen and oxygen in high selectivity below the flammability limit of hydrogen.[29] Combination of this with the Enichem technology enables the direct synthesis of propylene oxide from propylene, hydrogen and oxygen, with water as the sole by-product (Fig. 6). This process is now being commercialised in partnership with Degussa (now Evonik). BASF, in partnership with Dow Chemical, have similarly commercialized the Enichem epoxidation technology but without the added benefit of direct formation of hydrogen peroxide from hydrogen and oxygen.[30]

Similarly, Sumitomo has commercialised a process for caprolactam, the raw material for nylon 6, which involves combining the Enichem technology[31] for ammoximation of cyclohexanone with NH_3–H_2O_2 over the titanium silicalite catalyst (TS-1) with a novel vapour phase Beckmann rearrangement over a high-silica MFI zeolite,[32] affording caprolactam in >98% yield based on cyclohexanone and 93%

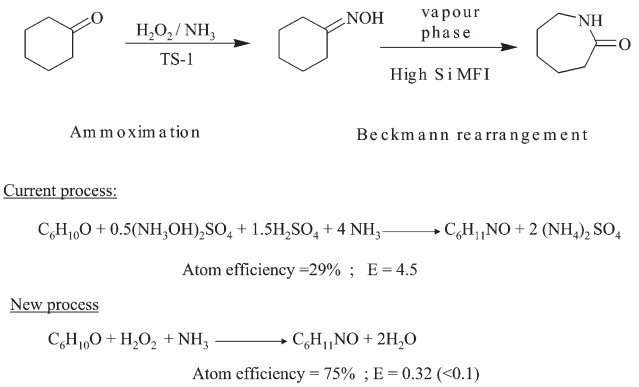

Fig. 7 Sumitomo caprolactam process.

based on H_2O_2 (Fig. 7). The conventional process involves the reaction of cyclohexanone with hydroxylamine sulfate (or another salt), producing cyclohexanone oxime, which is subjected to the Beckmann rearrangement in the presence of stoichiometric amounts of sulfuric acid or oleum. The overall process generates *ca.* 4.5 kg of ammonium sulfate per kg of caprolactam (Fig. 7). In contrast, the Sumitomo process generates two molecules of water as the sole co-product, *i.e.*, it is essentially salt-free. It was gratifying, therefore, that the Sumitomo scientist, Ichihashi, used the E Factor to illustrate the difference between the classical and the new, catalytic process (see Fig. 7).

8. Catalytic C–C bond formation

C–C bond formation is a key transformation in organic synthesis and an important catalytic methodology for generating C–C bonds is carbonylation. In the bulk chemicals arena it is used, for example, for the production of acetic acid by rhodium-catalysed carbonylation of methanol. Since such

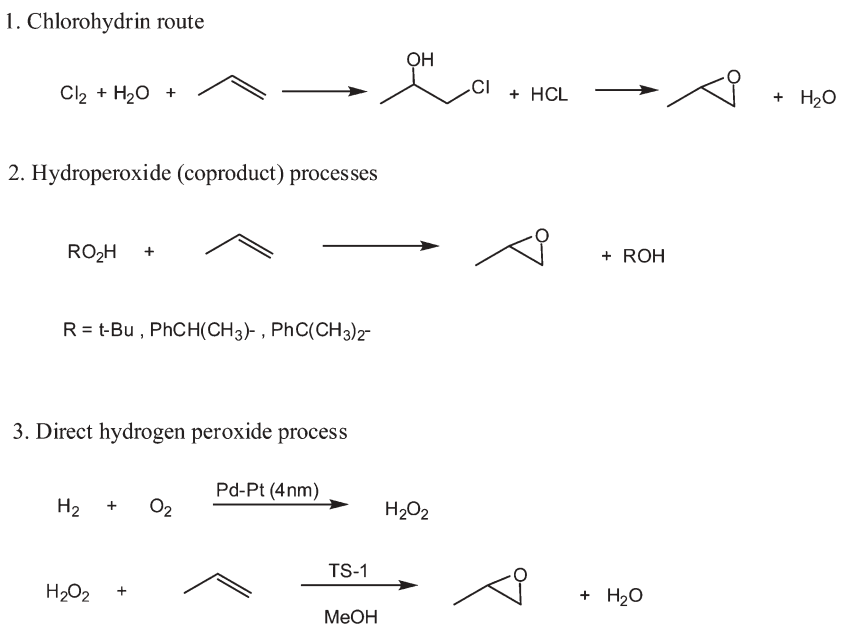

Fig. 6 Different processes to propylene oxide.

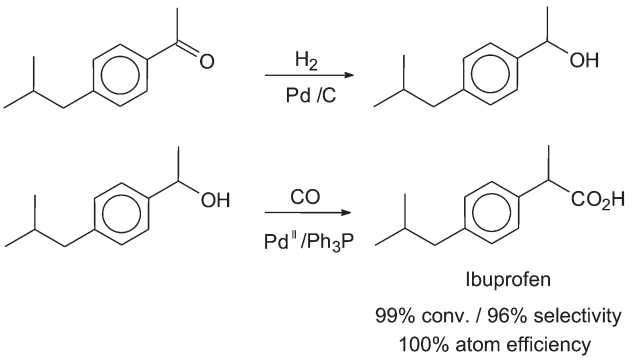

Fig. 8 Hoechst–Celanese process for ibuprofen.

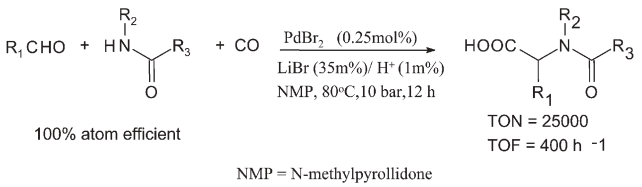

Fig. 9 Palladium-catalysed amidocarbonylation.

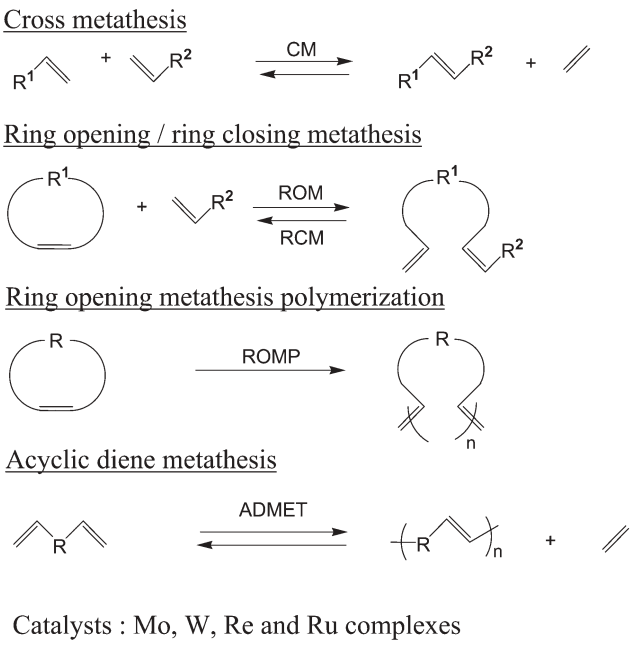

Fig. 10 Olefin metathesis reactions.

reactions are 100% atom efficient they are increasingly being applied to fine chemicals manufacture. An elegant example of this is the Hoechst–Celanese process for the manufacture of the analgesic, ibuprofen, with an annual production of several thousands tons. In this process ibuprofen is produced in two catalytic steps (hydrogenation and carbonylation) from *p*-isobutylacetophenone (Fig. 8) with 100% atom efficiency.[33] This process replaced a more classical route which involved more steps and a much higher E factor.

Another elegant example is the palladium-catalysed, one-step, 100% atom efficient synthesis of α-amino acid derivatives from an aldehyde, CO and an amide (Fig. 9).[34]

No discussion of catalytic C–C bond formation would be complete without a mention of olefin metathesis in its many forms: cross metathesis (CM), ring closing metathesis (RCM), ring opening metathesis (ROM), ring opening metathesis polymerization (ROMP) and acyclic diene metathesis (ADMET) (Fig. 10).[35] It should be noted, however, that olefin metatheses, in contrast to carbonylations, are often not 100% atom efficient in that they produce an olefin co-product.

Following its discovery in the 1960s olefin metathesis was applied to bulk chemicals manufacture, a prominent example being the Shell Higher Olefins Process (SHOP).[36] In the succeeding decades the development of catalysts, in particular the ruthenium-based ones developed by Grubbs, that function in the presence of most functional groups, paved the way for widespread application of olefin metathesis in the synthesis of complex organic molecules. The importance of olefin metathesis as a pre-eminent, green methodology for the formation of C–C bonds under mild conditions was underpinned by the award of the 2005 Nobel Prize in Chemistry to Chauvin, Grubbs and Schrock for the development of the olefin metathesis reaction. According to the Swedish academy olefin metathesis is "a great step forward for green chemistry".

9. Chirotechnology and asymmetric catalysis

At roughly the same time that waste minimization was becoming an important issue enantiomeric purity of biologically active agents, *e.g.*, pharmaceuticals and pesticides, was becoming the focus of regulatory attention. We noted in 1993 that "the current climate of 'environmentality' is precipitating a dramatic move towards enantiomeric purity in bioactive agents".[37] When a chiral molecule exhibits biological activity the desired activity almost always resides in one of the enantiomers and the other enantiomer is at best isomeric ballast that does not contribute to the desired effect. In the worst case scenario it may exhibit toxic side-effects, the most well-known example being the thalidomide tragedy in the 1960s. Pregnant women who received this drug in racemic form gave birth to deformed babies as a result of the mutagenicity of the "wrong" enantiomer. However, although this effect of chirality on biological activity was already known in the 1960s, it took about thirty years before sufficient regulatory pressure stimulated the shift towards marketing drugs in enantiomerically pure form. Consequently, in the last two decades there has been a marked trend towards marketing chiral pharmaceuticals and pesticides as pure enantiomers. This, in turn, generated a need for economically viable methods for their synthesis.

Here again, for economic and environmental viability, processes need to be atom efficient and have low E factors, *i.e.*, they should employ catalytic methodologies. This has manifested itself in the last 15 years in increasing attention for enantioselective catalysis, using enzymes (see later), chiral metal complexes or, more recently, chiral organocatalysts.[38] Its importance was underpinned by the award of the 2001 Nobel Prize in Chemistry to Knowles, Noyori and Sharpless for their contributions to enantioselective catalysis. Indeed, as Noyori has recently noted,[39] asymmetric hydrogenation is ideal green chemistry.

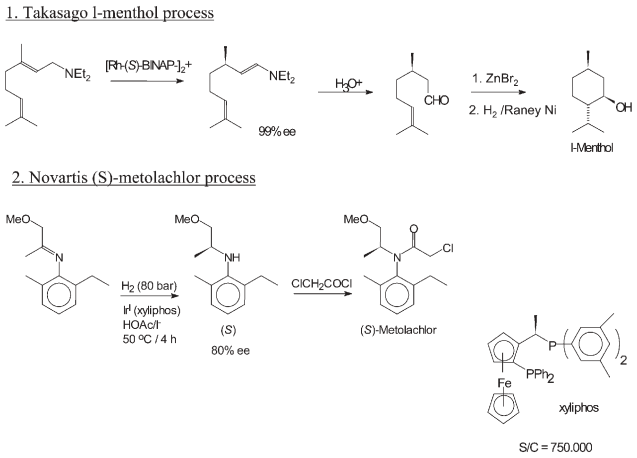

Fig. 11 Enantioselective catalysis in (*S*)-metolachlor and l-menthol manufacture.

Two elegant examples of highly efficient asymmetric catalysis on a multi-thousand tons per annum scale, which we have discussed in detail elsewhere,[14] are the Takasago l-menthol process and the Syngenta (*S*)-metalochlor process, in which an enantioselective isomerisation and an enantioselective hydrogenation are the key steps, respectively (Fig. 11).

10. The question of solvents: non-conventional reaction media

Another important issue in green chemistry is the use of organic solvents. So many of the solvents that are favoured by organic chemists, such as chlorinated hydrocarbons, have been blacklisted that the whole question of solvent use requires rethinking and has become a primary focus, especially in the fine chemicals industry.[40,41] In our original studies of E factors of various processes we assumed, if details were not known, that solvents would be recycled by distillation and that this would involve a 10% loss. However, the organic chemist's penchant for using different solvents for the various steps in multi-step syntheses makes recycling difficult owing to cross contamination. The benchmarking exercise performed by the GCI Pharmaceutical Round Table (see above) revealed that solvents were a major contributor to the E Factors of pharmaceutical manufacturing processes. Indeed, it has been estimated by GSK workers[42] that *ca.* 85% of the total mass of chemicals involved in pharmaceutical manufacture comprises solvents. It is also worth noting that in the redesign of the sertraline manufacturing process,[43] for which Pfizer received a Presidential Green Chemistry Challenge Award in 2002, among other improvements a three-step sequence was streamlined by employing ethanol as the sole solvent. This eliminated the need to use, distil and recover four solvents (methylene chloride, tetrahydrofuran, toluene and hexane). Similarly, Pfizer workers also reported[44] impressive improvements in solvent usage in the process for sildenafil (Viagra) manufacture reducing the solvent usage from 1700 l kg^{-1} of product used in the medicinal chemistry route to 7 l kg^{-1} in the current commercial process, with a target for the future of 4 l kg^{-1}. The E Factor for the current process is 6, placing it more in the lower end of fine chemicals rather than with typical pharmaceutical manufacturing processes.

These issues surrounding a wide range of volatile and non-volatile, polar aprotic solvents have stimulated the fine chemical and pharmaceutical industries to seek more benign alternatives. There is a marked trend away from hydrocarbons and chlorinated hydrocarbons towards lower alcohols, esters and, in some cases, ethers. Inexpensive natural products such as ethanol have the added advantage of being readily biodegradable and ethyl lactate, produced by combining two innocuous natural products, is currently being touted as an environmentally attractive solvent for chemical reactions.

The problem with solvents is not so much their use but the seemingly inherent inefficiencies associated with their containment, recovery and re-use. Alternative solvents should, therefore, provide for their efficient removal from the product and re-use. The subject of alternative reaction media also touches on another issue that is important from both an environmental and an economic viewpoint: recovery and re-use of the catalyst. An insoluble solid, *i.e.*, a heterogeneous catalyst, is easily separated by centrifugation or filtration. A homogeneous catalyst, in contrast, presents more of a problem and a serious shortcoming of homogeneous catalysis is the cumbersome separation of the catalyst from reaction products and the quantitative recovery of the catalyst in an active form. In pharmaceuticals manufacture quantitative separation of the catalyst is also important in order to avoid contamination of the product. Attempts to heterogenise homogeneous catalysts by attachment to organic or inorganic supports have, generally speaking, not resulted in commercially viable processes, for a number of reasons, such as leaching of the metal, poor catalyst productivities, irreproducible activities and selectivities and degradation of the support.

The conclusion is evident: we need to maintain the advantages of homogeneous catalysts while providing for facile separation of product and catalyst. This can be achieved by employing liquid–liquid biphasic catalysis, whereby the catalyst is dissolved in one phase and the reactants and product(s) in the second liquid phase. The catalyst is recovered and recycled by simple phase separation. Preferably, the catalyst solution remains in the reactor and is re-used with a fresh batch of reactants without further treatment or, ideally, it is adapted to continuous operation. Obviously, both solvents are subject to the same restrictions as discussed above for monophasic systems. Several different combinations have been intensely studied in recent years, including *water (aqueous biphasic), supercritical CO_2, fluorous biphasic, and ionic liquids* and *multiphase homogeneous catalysis* has become an important area of research.[45] We also note that the use of water and supercritical carbon dioxide as reaction media is consistent with the current trend towards the use of renewable, biomass-based raw materials, which are ultimately derived from carbon dioxide and water.

The best solvent is no solvent and if a solvent (diluent) is needed then water has much to offer: it is non-toxic, non-inflammable, abundantly available and inexpensive. Furthermore, performing the reaction in an aqueous biphasic system,[46] whereby the catalyst resides in the water phase and the product is dissolved in the organic phase, allows for

recovery and recycling of the catalyst by simple phase separation. An example of a large scale application of this concept is the Ruhrchemie/Rhône Poulenc process for the hydroformylation of propylene to n-butanal, which employs a water-soluble rhodium(I) complex of trisulfonated triphenylphosphine (tppts) as the catalyst and has an E Factor of 0.1 compared with 0.6–0.9 for conventional monophasic hydroformylation processes.[47] Similarly, we have reported examples of aqueous biphasic carbonylations and oxidations.[48]

An aqueous biphasic system is not the answer in all cases, however, and other alternative reaction media, such as fluorous biphasic systems,[49] supercritical carbon dioxide,[50] and ionic liquids,[51,52] have also been extensively studied, as well as biphasic mixtures of these alternative media,[42] *e.g.*, an ionic liquid with $scCO_2$. In a recent variation on this theme,[53] the so-called 'miscibility switch' was used to perform a catalytic reaction smoothly in a monophasic ionic liquid–$scCO_2$ mixture. Subsequent lowering of the pressure afforded a biphasic system whereby the catalyst was contained in the ionic liquid phase and the product in the $scCO_2$ phase, enabling their facile separation. Another approach worthy of mention is the use of amidine/alcohol or guanidine/alcohol mixtures as "switchable solvents", whereby a switch from a low-polarity form to a high-polarity form is achieved upon treatment with carbon dioxide at atmospheric pressure.[54]

11. Biocatalysis

Biocatalysis has many attractive features in the context of green chemistry: mild reaction conditions (physiological pH and temperature), an environmentally compatible, biodegradable catalyst (an enzyme) and solvent (water) combined with high activities and chemo-, regio- and stereoselectivities in reactions of multifunctional molecules. Furthermore, the use of enzymes generally circumvents the need for functional group activation and avoids the protection and deprotection steps required in traditional organic syntheses. This affords processes which are shorter, generate less waste and are, therefore, both environmentally and economically more attractive than conventional routes.

Biocatalytic processes can be performed with isolated enzymes or as whole cell biotransformations. Isolated enzymes have the advantage of not being contaminated with other enzymes present in the cell while the use of whole cells is less expensive as it avoids separation and purification of the enzyme. In the case of dead cells, the E Factors of the two methods are essentially the same: the waste cell debris is separated before or after the biotransformation. In contrast, when growing microbial cells are used, *i.e.*, in fermentation processes, substantial amounts of biomass can be generated as waste but little attention has been paid to this aspect. To our knowledge there are no reported E Factors for fermentation processes. This would seem to be a hiatus which needs to be filled. We note, however, that the waste biomass is generally easy to dispose of, *e.g.*, as animal feed, or can, in principle, be used as a source of energy for the process.

The time is ripe for the widespread application of biocatalysis in industrial organic synthesis. Advances in recombinant DNA techniques have made it, in principle,

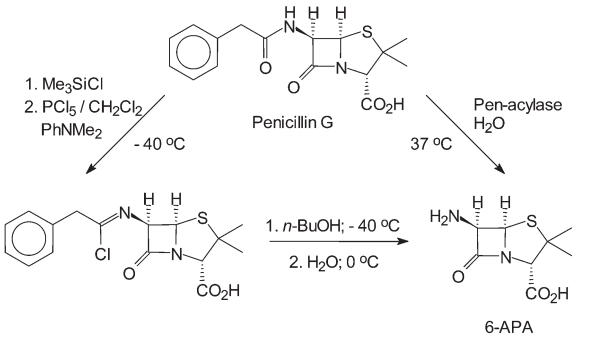

Fig. 12 Enzymatic *versus* chemical deacylation of penicillin G.

possible to produce virtually any enzyme for a commercially acceptable price and protein engineering has made it possible, using techniques such as site directed mutagenesis and *in vitro* evolution, to manipulate enzymes such that they exhibit the desired substrate specificity, activity, stability, pH profile, *etc.*.[55] Furthermore, the development of effective immobilisation techniques has paved the way for optimising the performance and recovery and recycling of enzymes.[56]

An illustrative example of the benefits to be gained by replacing conventional organic chemistry by biocatalysis is provided by the manufacture of 6-aminopenicillanic acid (6-APA), a key raw material for semi-synthetic penicillin and cephalosporin antibiotics, by hydrolysis of penicillin G.[57] Up until the mid-1980s a chemical procedure was used for this hydrolysis (Fig. 12). It involved the use of environmentally unattractive reagents, a chlorinated hydrocarbon solvent (CH_2Cl_2) and a reaction temperature of −40 °C. Thus, 0.6 kg Me_3SiCl, 1.2 kg PCl_5, 1.6 kg $PhNMe_2$, 0.2 kg NH_3, 8.4 l of n-BuOH and 8.4 l of CH_2Cl_2 were required to produce 1 kg of 6-APA.[58]

In contrast, enzymatic cleavage of penicillin G (Fig. 12) is performed in water at 37 °C and the only reagent used is NH_3 (0.09 kg per kg of 6-APA), to adjust the pH. The enzymatic process currently accounts for the majority of the several thousand tons of 6-APA produced annually on a world-wide basis.

Similarly, subsequent enzymatic coupling of the side-chain to the 6-APA nucleus or the related 7-amino desacetoxycephalosporanic acid (7-ADCA) has replaced chemical coupling in the synthesis of certain semi-synthetic penicillins and cephalosporins.[57] An example of what can be achieved by applying modern biotechnology to biocatalysis is provided by the process developed by Codexis for the production of an intermediate for Pfizer's blockbuster drug Atorvastatin (Lipitor). The process, for which Codexis received a 2006 Presidential Green Chemistry Challenge Award, involved three enzymatic steps (Fig. 13), all of which were optimised by *in vitro* evolution of the individual enzymes using gene shuffling.[59]

12. Chemicals from renewable raw materials: biomass utilisation

Another important goal of green chemistry is the utilisation of renewable raw materials, *i.e.*, production of chemicals

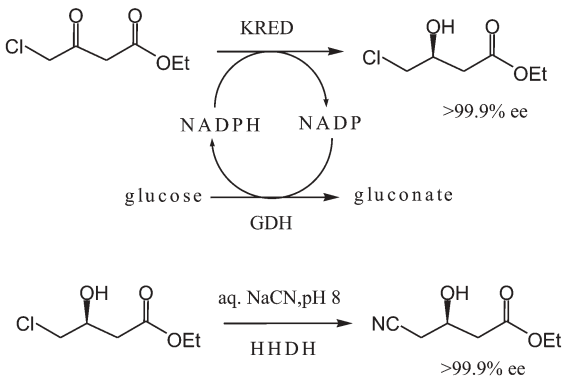

Fig. 13 Codexis process for atorvastatin intermediate.

from biomass rather than fossil resources such as oil, coal and natural gas. Here again, the processes used for the conversion of renewable feedstocks—mainly carbohydrates but also triglycerides and terpenes—should produce minimal waste, *i.e.*, they should be preferably catalytic in order to be sustainable.

In the short term maize is being used as a renewable raw material to produce bioethanol and chemicals such as lactic acid and 1,3-propanediol but it is clear that lignocellulosic materials, available as agricultural waste, *e.g.*, corn stover, or dedicated energy crops will be the feedstocks for second generation biofuels and biobased commodity chemicals. This will be necessary to avoid the food *versus* fuel dilemma. A so-called biobased economy is envisaged in which commodity chemicals (including biofuels), specialty chemicals such as vitamins, flavours and fragrances and industrial monomers will be produced in biorefineries.

Conversion of lignocellulosic biomass in biorefineries could involve thermochemical and/or biotechnological processes.[60,61] In the former, pyrolysis or gasification of lignocellulose affords pyrolysis oil or syn gas, respectively. In the case of syn gas, the technologies developed in the 1970s, based on coal gasification, can be used to convert the syn gas to liquid fuels or chemicals.[3] In the biotechnological approach, the lignocellulose is hydrolysed to liberate the lignin, which can be used as an energy source, and polysaccharides, which are depolymerised to fermentable sugars. This is currently the focus of considerable attention and is perceived as the key to developing a sustainable source of liquid fuels and chemicals.[62] Metabolic pathway engineering[63] is used to optimise the production of the required product based on the amount of substrate (glucose) consumed, *i.e.*, the atom efficiency. Alternatively, the monosaccharides can be converted to valuable chemicals by chemical catalysis, *e.g.*, dehydration and/or hydrogenation.[64] Whichever approach is used, here again optimum biomass utilisation and minimisation/elimination of waste, that is low E Factors, is the key to sustainability. There is a clear need for a meaningful metric for comparing different methodologies for biomass conversion.

The (partial) shift from oil to biomass as a raw material will have far reaching consequences for the structure of the chemical and allied industries. Different value chains will be formed. For example, a direct consequence of the recent enormous increase in biodiesel production is that the co-product, glycerol, has become a low-priced commodity chemical which could, in turn, form the raw material for other bulk chemicals such as 1,2- and 1,3-propane diol and acrylic acid.[65] These processes will also have to be efficient in raw material utilisation and generate minimum waste.

13. Conclusions and future outlook

As Lord Kelvin said: "To measure is to know". Fine chemical and pharmaceutical companies always knew that their manufacturing processes were generating substantial quantities of waste but putting a number to it *via* the conception of the E factor really brought the message home. By publishing the table of E Factors we challenged the fine chemical and pharmaceutical industries to make the paradigm shift from a concept of process efficiency which was exclusively focused on chemical yield to one that is motivated by elimination of waste and maximisation of raw materials utilisation. The fact that the absolute amounts of waste generated in these sectors are lower than those in the bulk chemicals industry should not be used as an excuse not to address this issue. The E Factor provided a very simple means of measuring one's performance and has been adopted by the chemical industry world-wide for this purpose. The pharmaceutical industry in particular has made substantial progress in the last few years and has adopted the E Factor, or its direct equivalent, as its measuring staff. This was underscored by the recent statement: "Another aspect of process development mentioned by all pharmaceutical company process chemists who spoke with C&EN is the need for determining an E Factor".[66] Similarly, a recent publication from members of the ACS GCI Pharmaceutical Round Table identified a list of key areas where further improvement is most needed.[67]

The impact of the E Factor has not been restricted to the fine chemicals industry but has also played a broader role as a "measure of the efficiency of the chemical industry"[68] and, hopefully, will continue to do so as the chemical industry progresses towards being a sustainable enterprise. Looking to the future, the displacement of archaic "stoichiometric" technologies by greener catalytic alternatives and the replacement of toxic and/or hazardous solvents and reagents with cleaner alternatives will continue to be important drivers. In addition, two other more recent trends will gain in importance. First, the change from fossil fuels to renewable resources as feedstocks for existing products, and second the development of new products that are biocompatible and biodegradable and are also produced from renewable resources by green catalytic processes with low E Factors.

References

1 R. A. Sheldon, *Chem. Ind. (London)*, 1992, 903–906.
2 See T. Iwata, H. Miki and Y. Fujita, in *Ullmann's Encyclopedia of Industrial Chemistry*, 1991, vol. A19, p. 347.
3 R. A. Sheldon, *Chemicals from Synthesis Gas*, Reidel, Dordrecht, 1983, p. 15.
4 C. M. Caruana, *Chem. Eng. Progr.*, 1991, **87**(12), 11–13.
5 B. M. Trost, *Science*, 1991, **254**, 1471–1477.

6 *Green Chemistry: Theory and Practice*, eds. P. Anastas and J. C. Warner, Oxford University Press, Oxford, 1998.
7 *Green Chemistry: Frontiers in Chemical Synthesis and Processes*, eds. P. T. Anastas and T. C. Williamson, Oxford University Press, Oxford, 1998.
8 P. T. Anastas and M. M. Kirchhoff, *Acc. Chem. Res.*, 2002, **35**, 686–693.
9 *Green Chemical Syntheses and Processes*, eds. P. T. Anastas, L. G. Heine and T. C. Williamson, American Chemical Society, Washington DC, 2000.
10 *Benign by Design: Alternative Synthetic Design for Pollution Prevention*, ACS Symp. Ser. nr. 577, eds. P. T. Anastas and C. A. Farris, American Chemical Society, Washington DC, 1994.
11 J. H. Clark and D. J. Macquarrie, *Handbook of Green Chemistry and Technology*, Blackwell, Abingdon, 2002.
12 A. S. Matlack, *Introduction to Green Chemistry*, Marcel Dekker, New York, 2001.
13 M. Lancaster, *Green Chemistry: An Introductory Text*, Royal Society of Chemistry, Cambridge, 2002.
14 R. A. Sheldon, I. W. C. E. Arends and U. Hanefeld, *Green Chemistry and Catalysis*, Wiley-VCH, Weinheim, 2007.
15 P. T. Anastas and J. B. Zimmerman, in *Sustainability Science and Engineering Defining Principles*, ed. M. A. Abrahams, Elsevier, 2006, pp. 11–32.
16 S. L. Y. Tang, R. L. Smith and M. Poliakoff, *Green Chem.*, 2005, **7**, 761.
17 C. G. Brundtland, *Our Common Future*, The World Commission on Environmental Development, Oxford University Press, Oxford, 1987.
18 R. A. Sheldon, *Chemtech*, 1994, 38–47.
19 R. A. Sheldon, *Chem. Ind. (London)*, 1997, 12–15.
20 R. A. Sheldon, *J. Chem. Technol. Biotechnol.*, 1997, **68**, 381–388.
21 R. A. Sheldon, *Pure Appl. Chem.*, 2000, **72**, 1233–1246.
22 T. Hudlicky, D. A. Frey, L. Koroniak, C. D. Claeboe and L. E. Brammer, *Green Chem.*, 1999, **1**, 57–59.
23 D. J. C. Constable, A. D. Curzons and V. L. Cunningham, *Green Chem.*, 2002, **4**, 521–527, see also: A. D. Curzons, D. J. C. Constable, D. N. Mortimer and V. L. Cunningham, *Green Chem.*, 2001, **3**, 1–6; D. J. C. Constable, A. D. Curzons, L. M. Freitas dos Santos, G. R. Green, R. E. Hannah, J. D. Hayler, J. Kitteringham, M. A. McGuire, J. E. Richardson, P. Smith, R. L. Webb and M. Yu, *Green Chem.*, 2001, **3**, 7–9.
24 J. Andraos, *Org. Process Res. Dev.*, 2005, **9**, 149–163.
25 B. M. Trost, *Angew. Chem., Int. Ed.*, 1995, **34**, 259–281.
26 *Fine Chemicals Through Heterogeneous Catalysis*, eds. R. A. Sheldon and H. van Bekkum, Wiley-VCH, Weinheim, 2001, ch. 3–7.
27 R. A. Sheldon and J. K. Kochi, *Metal Catalyzed Oxidations of organic Compounds*, Academic Press, 1981.
28 B. Notari, *Stud. Surf. Sci. Catal.*, 1998, **37**, 413–425.
29 See www.epa.gov/greenchemistry/pubs/pgcc/past.html.
30 A. Tulle, *Chem. Eng. News*, Sept. 6, 2004, 15.
31 P. Roffia, G. Leofanti, A. Cesana, M. Mantegazza, M. Padovan, G. Petrini, S. Tonti and P. Gervasutti, *Stud. Surf. Sci. Catal.*, 1990, **55**, 43–50; G. Bellussi and C. Perego, *CATTECH*, 2000, **4**, 4–16.
32 H. Ichihashi and M. Kitamura, *Catal. Today*, 2002, **73**, 23–28; H. Ichihashi and H. Sato, *Appl. Catal., A*, 2001, **221**, 359–366.
33 V. Elango, M. A. Murphy, B. L. Smith, K. G. Davenport, G. N. Mott and G. L. Moss, US Pat. 4981995 (1991) to Hoechst–Celanese Corp.
34 D. Gördes, H. Neumann, A. Jacobi van Wangelin, C. Fischer, K. Drauz, H. P. Krimmer and M. Beller, *Adv. Synth. Catal.*, 2003, **345**, 510–516.
35 *Adv. Synth. Catal.*, Olefin Metathesis Issue, eds. A. Fürstner, R. H. Grubbs and R. R. Schrock, 2002, **344**(6+7), 567–793; Ed. R. H. Grubbs, *Handbook of Metathesis*, Wiley-VCH, Weinheim, 2003.
36 B. Reuben and H. Wittcoff, *J. Chem. Educ.*, 1988, **65**, 605–607.
37 R. A. Sheldon, *Chirotechnology: the Industrial Synthesis of Optically Active Compounds*, Marcel Dekker, New York, 1993.
38 A. Berkessel and H. Groerger, *Asymmetric Organocatalysis*, Wiley-VCH, Weinheim, 2005; J. Seayad and B. List, *Org. Biomol. Chem.*, 2005, **3**, 719.
39 R. Noyori, *Proc. Ind. Nat. Sci. Acad.*, 2006, **72**(4), 267–273.
40 R. A. Sheldon, *Green Chem.*, 2005, **7**, 267–278.
41 *Green Chem.*, Special Issue on Green Solvents for Catalysis, eds. W. Leitner, K. R. Seddon and P. Wasserscheid, 2003, **5**, 99–284.
42 C. Jiminez-Gonzales, A. D. Curzons, D. J. C. Constable and V. L. Cunningham, *Int. J. Life Cycle Assess.*, 2004, **9**, 115–121.
43 G. P. Taber, D. M. Pfistere and J. C. Colberg, *Org. Proc. Res. Dev.*, 2004, **8**, 385–388.
44 P. J. Dunn, S. Galvin and K. Hettenbach, *Green Chem.*, 2004, **6**, 43.
45 *Multiphase Homogeneous Catalysis*, eds. B. Cornils, W. Herrmann, I. T. Horvath, W. Leitner, S. Mecking, H. Olivier-Bourbigou and D. Vogt, Wiley, Weinheim, 2005.
46 U. M. Lindström, *Organic Reactions in Water*, Blackwell, Oxford, 2007.
47 B. Cornils in *Organic Reactions in Water*, Blackwell, Oxford, 2007.
48 G. Papadogianakis and R. A. Sheldon, in *Catalysis*, Specialist Periodical Report, *Royal Society of Chemistry*, Cambridge, 1997, vol. 13, pp. 114–193; G. Verspui, G. Papadogianakis and R. A. Sheldon, *Catal. Today*, 1998, **42**, 449–458; G. J. ten Brink, I. W. C. E. Arends and R. A. Sheldon, *Science*, 2000, **287**, 1636–1639.
49 I. T. Horvath and J. Rabai, *Science*, 1994, **266**, 72; I. T. Horvath, *Acc. Chem. Res.*, 1998, **31**, 641; J. A. Gladysz, D. P. Curran and I. T. Horvath, *Handbook of Fluorous Chemistry*, Wiley, Weinheim, 2004.
50 *Chemical Synthesis using Supercritical Fluids*, eds. P. G. Jessop and W. Leitner, Wiley_VCH, Weinheim, 1999; W. Leitner, *Top. Curr. Chem.*, 1999, **206**, 107; W. Leitner, *Acc. Chem. Res.*, 2002, **35**, 746; E. J. Beckman, *J. Supercrit. Fluids*, 2004, **28**, 121; P. Licence, J. Ke, M. Sokolova, S. K. Ross and M. Poliakoff, *Green Chem.*, 2003, **5**, 99.
51 R. A. Sheldon, *Chem. Commun.*, 2001, 2399; J. Dupont, R. F. de Souza and P. A. Z. Suarez, *Chem. Rev.*, 2002, **102**, 3667; C. E. Song, *Chem. Commun.*, 2004, 1033–1043; D. Zhao, M. Wu, Y. Kou and E. Min, *Catal. Today*, 2002, **74**, 157; V. I. Parvulescu and C. Hardacre, *Chem. Rev.*, 2007, **107**, 2615–2665; *Ionic Liquids as Green Solvents; Progress and Prospects*, ACS Symposium Series 856, eds. R. D. Rogers and K. R. Seddon, American Chemical Society, Washington DC, 2003.
52 For a recent review of biocatalysis in ionic liquids see: F. van Rantwijk and R. A. Sheldon, *Chem. Rev.*, 2007, **107**, 2757–2785.
53 M. C. Kroon, J. van Spronsen, C. J. Peters, R. A. Sheldon and G.-J. Witkamp, *Green Chem.*, 2006, **8**, 246–249.
54 P. G. Jessop, D. J. Heldebrant, X. Li, C. A. Eckert and C. L. Liotta, *Nature*, 2005, **436**, 1102.
55 K. A. Powell, S. W. Ramer, S. B. del Cardayré, W. P. C. Stemmer, M. B. Tobin, P. F. Longchamp and G. W. Huisman, *Angew. Chem. Int. Ed.*, 2001, **40**, 3948–3959.
56 R. A. Sheldon, *Adv. Synth. Catal.*, 2007, **349**, 1289–1307.
57 M. A. Wegman, M. H. A. Janssen, F. van Rantwijk and R. A. Sheldon, *Adv. Synth. Catal.*, 2001, **343**, 559–576; A. Bruggink, E. C. Roos and E. de Vroom, *Org. Proc. Res. Dev.*, 1998, **2**, 128–133.
58 *Ullmann's Encyclopedia of Industrial Chemistry*, VCH, Weinheim, 5th edn., 1995, vol. B8, pp. 302–304.
59 R. J. Fox, C. S. Davis, E. C. Mundorff, L. M. Newman, V. Gavrilovic, S. K. Ma, L. M. Chung, C. Ching, S. Tam, S. Muley, J. Grate, J. Gruber, J. C. Whitman, R. A. Sheldon and G. W. Huisman, *Nature Biotechnol.*, 2007, **25**, 338–344.
60 J. H. Clark, *J. Chem. Technol. Biotechnol.*, 2007, **82**, 603–609.
61 J. P. Lange, *Biofuels Bioprod. Bioref.*, 2007, **1**, 39–48.
62 B. E. Dale, *Biofuels Bioprod. Bioref.*, 2007, **1**, 24–38; B. E. Dale, *J. Chem. Technol. Biotechnol.*, 2003, **78**, 1093–1103.
63 C. E. Nakamura and G. M. Whited, *Curr. Opin. Biotechnol.*, 2003, **14**, 454–459.
64 See for example Y. Roman-Leshkov, C. J. Barrett, Z. Y. Liu and J. A. Dumesic, *Nature*, 2007, **447**, 982–985; J. N. Chheda, J. A. Dumesic and A. James, *Catal. Today*, 2007, **123**(1–2), 59–70; J. N. Chheda, Y. Roman-Leshkov and J. A. Dumesic, *Green Chem.*, 2007, **9**, 342–350; R. R. Soares, D. A. Simonetti and J. A. Dumesic, *Angew. Chem., Int. Ed.*, 2006, **45**, 3982–3985.
65 See for example M. A. Dasari, P.-P. Kiatsimkul, W. R. Sutterlin and G. J. Suppes, *Appl. Catal., A*, 2005, **281**(1–2), 225–231; S. Carrettin, P. McMorn, P. Johnston, K. Griffin, C. J. Kiely, G. A. Atard and C. J. Hutchings, *Top. Catal.*, 2004, **27**, 137–142.
66 A. N. Thayer, *Chem. Eng. News*, August 6, 2007, pp.11–19.

67 D. J. Constable, P. J. Dunn, J. D. Hayler, G. R. Humphrey, J. L. Leazer, R. J. Linderman, K. Lorenz, J. Manley, B. A. Pearlman, A. Wells, A. Zaks and T. Y. Zhang, *Green Chem.*, 2007, **9**, 411–420; see also J. S. Carey, D. Laffan, C. Thomson and M. T. Williams, *Org. Biomol. Chem.*, 2006, **4**, 2337–2347; R. W. Dugger, J. A. Ragan and D. H. Brown Ripin, *Org. Proc. Res. Dev.*, 2005, **9**, 253–258.
68 See in *Sustainability in the Chemical Industry: Grand Challenges and Research Needs*, National Research Council of the National Academies, National Academies Press, Washington, DC, 2006, p. 22.

Efficient synthesis of β-oxopropylcarbamates in compressed CO_2 without any additional catalyst and solvent†

Chao-Rong Qi and Huan-Feng Jiang*

Received 24th May 2007, Accepted 19th September 2007
First published as an Advance Article on the web 26th September 2007
DOI: 10.1039/b707893e

The efficient synthesis of β-oxopropylcarbamates *via* a three-component coupling of CO_2, secondary amines and propargyl alcohols was achieved in compressed carbon dioxide in the absence of any additional catalyst and solvent.

Organic carbamates are compounds of great interest because of their growing application in agriculture (pesticides, fungicides, herbicides), pharmacology (medical drugs) and as useful intermediates in organic synthesis.[1] In addition, carbamates have played an important role in peptide chemistry as protective groups of an amine function.[2] The classical method for the synthesis of carbamates involves the use of highly toxic phosgene as starting material which may cause serious environmental pollution and safety problems.[1a]

Recently, carbon dioxide has emerged as an attractive substitute for phosgene in carbamate synthesis because it is a cheap, nontoxic, nonflammable and typically renewable feedstock.[3] In 1987, Dixneuf and Sasaki reported the synthesis of β-oxopropylcarbamates *via* the ruthenium(II)-catalyzed reaction of propargyl alcohols, secondary amines and CO_2 in organic solvents.[4] Subsequently, Kim and co-workers described that iron complexes based on 1,1′-bis(diphenylphosphino)-ferrocene were good catalysts for this reaction.[5] Other catalysts such as lanthanide chlorides[6] and copper(I) complexes[7] have also been developed. However, in those reaction systems, although expensive metal catalysts and large amount of solvent were used, the yield of the desired products still remained low.

In the present work, we report that the titled compounds could be synthesized efficiently from propargyl alcohols, secondary amines in the absence of any additional catalyst and organic solvent in compressed carbon dioxide (Scheme 1).

We first examined the reaction of diethylamine (**1a**, 20 mmol), 2-methyl-3-butyn-2-ol (**2a**, 10 mmol) and CO_2 under different reaction conditions, and the results are summarized in Table 1.‡§ When the reaction was carried out at 80 °C and 14 MPa for 48 h, 1,1-dimethyl-2-oxopropyl-*N*,*N*-diethylcarbamate (**3a**) was obtained in only 18% isolated yield (entry 1). The results in Table 1 showed that both reaction temperature and CO_2 pressure have strong impacts on the reaction. When raising the temperature from 80 to 130 °C, the obtained product raised from 18% to 82% isolated yields (entries 1, 2, 7). However, the changes of CO_2 pressure gave interesting results. When the CO_2 pressure was increased from 3 to 14 MPa, the obtained yields were increased from 25% to 82% at 130 °C (entries 3–7), but a further increase in the pressure above 14 MPa resulted in a slight decrease in the yield of the carbamate product (entry 8). In addition, compared to 1 equiv. of Et_2NH, 2 equiv. of the amine gave better results (entries 7, 9). This may be ascribed to the fact that the excess amine could act as a solvent during the reaction. Therefore the best reaction conditions were as follows: diethylamine (20 mmol), 2-methyl-3-butyn-2-ol (10 mmol); CO_2 pressure: 14 MPa; reaction temperature: 130 °C; time: 48 h.

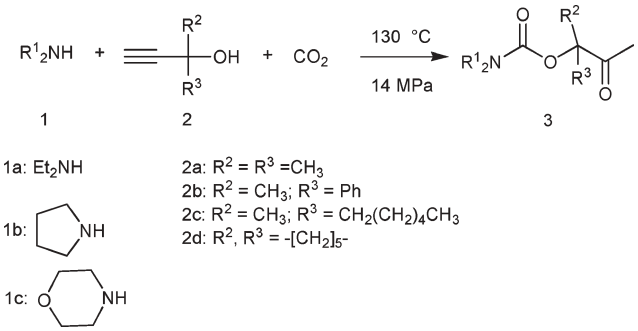

Scheme 1 β-Oxopropylcarbamates synthesis from secondary amines, propargyl alcohols and CO_2.

As seen in Table 2, a series of secondary amines (**1a**–**c**), such as diethyl amine, pyrrolidine and morpholine, were employed to undergo the three-component assembly with various propargyl

Table 1 Synthesis of 1,1-dimethyl-2-oxopropyl-*N*,*N*-diethylcarbamate from the reaction of diethylamine, 2-methyl-3-butyn-2-ol and CO_2[a]

Entry	Temp./°C	Pressure/MPa	Yield[b] (%)
1	80	14	18
2	110	14	57
3	130	3	25
4	130	5	55
5	130	8	71
6	130	12	74
7	130	14	82
8	130	17	69
9[c]	130	14	54
10[d]	130	8	8[e]
11[f]	130	8	85

[a] Reaction conditions: Diethylamine (20 mmol), 2-methyl-3-butyn-2-ol (10 mmol), 48 h. [b] Isolated yield. [c] Diethylamine (10 mmol). [d] Diethylamine (1 mmol). [e] α-Methylene cyclic carbonate with 10% isolated yield was also obtained. [f] 0.5 mmol of $P(n\text{-}C_4H_9)_3$ was added.

Center of Green Chemistry, College of Chemistry, South China University of Technology, Guangzhou, 510640, P. R. China. E-mail: jianghf@scut.edu.cn.; Fax: +86 20 87112906; Tel: +86 20 87112906

† Electronic supplementary information (ESI) available: Experimental section and analytical details of the products. See DOI: 10.1039/b707893e

Table 2 Reaction of CO_2, secondary amines and propargyl alcohols[a]

Amine	Alcohol	Conv. (%)	Product	Yield (%)
1a	**2a**	93	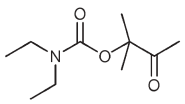 **3a**	82
1a	**2b**	99	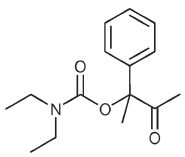 **3b**	57
1a	**2c**	76	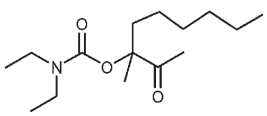 **3c**	35
1a	**2d**	88	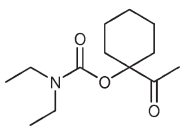 **3d**	76
1b	**2a**	100	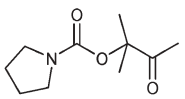 **3e**	88
1b	**2b**	100	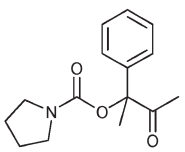 **3f**	65
1b	**2c**	100	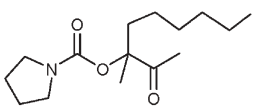 **3g**	73
1b	**2d**	100	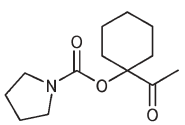 **3h**	83
1c	**2a**	89	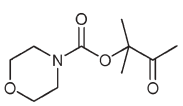 **3i**	78

[a] Reaction conditions: Secondary amine (20 mmol), propargyl alcohol (10 mmol), CO_2 pressure 14 MPa, 130 °C, 48 h. [b] Isolated yield.

alcohols (**2a**–**d**) under the optimized conditions, and the corresponding β-oxopropylcarbamates (**3a**–**i**) were afforded in moderate to high yields. It is noteworthy that morpholine (**1c**), which was reported to show poor reactivity toward the reaction even in the presence of metal catalysts due to its low basicity,[4a,5] could smoothly react with **2a** to generate carbamate **3i** in 78% isolated yield. When the alcohols were investigated under the same reaction conditions, the sterically more bulky **2b** and **2c** afforded the desired products in lower yields along with the occurrence of the retro-Favorsky reaction as a side reaction (eqn (1)). The major by-products, ketones, derived from the elimination of acetylene from alcohols were isolated and determined by GC-MS. Additionally, no polymeric products were observed in our protocol.

In order to clarify the reaction mechanism, we compared the reactions of **2a** in the presence of different amounts of Et_2NH under different conditions. Interestingly, we found that treatment of **2a** with 0.1 equiv. of Et_2NH at 130 °C under 8 MPa of CO_2 pressure for 48 h gave a mixture of α-methylene cyclic carbonate and 1,1-dimethyl-2-oxopropyl-*N*,*N*-diethylcarbamate (Table 1, entry 10). In the presence of a catalytic amount of Et_2NH (1 mol%) under 14 MPa of CO_2 pressure at 130 °C for 24 h, α-methylene cyclic carbonate was obtained in 8% yield. Without Et_2NH, no reaction occurred. These results confirmed that Et_2NH could promote the formation of α-methylene cyclic carbonate, and an excess amount of Et_2NH could convert α-methylene cyclic carbonate to carbamate. In fact, α-methylene cyclic carbonate could be quantitatively transformed to **3a** in the presence of 2 equiv. of Et_2NH at 130 °C and 14 MPa of CO_2 pressure for 20 h.

Another experiment showed that addition of 0.5 mmol $P(n\text{-}C_4H_9)_3$ could raise the carbamate yield to 85% (Table 1, entries 5, 11). Previous reports have already disclosed that $P(n\text{-}C_4H_9)_3$ is an efficient catalyst for the synthesis of α-methylene cyclic carbonates from the coupling reaction of CO_2 with propargyl alcohols.[8] All of these results seem to suggest that α-methylene cyclic carbonate was most likely the intermediate species.[4a,b,6c]

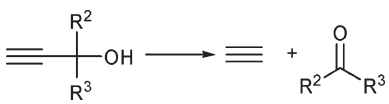

(1)

Based on the above results, a plausible mechanism for the reaction is postulated in Scheme 2. Firstly, ammonium carbonate **4** is formed by the reaction of **2a**, **1a** and CO_2,[9] which may undergoes cyclization under the assistance of a proton to yield the

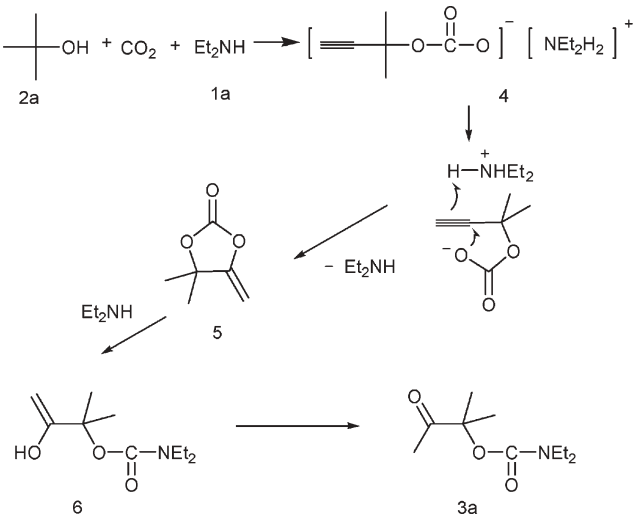

Scheme 2 Proposed mechanism for the formation of the β-oxopropylcarbamates.

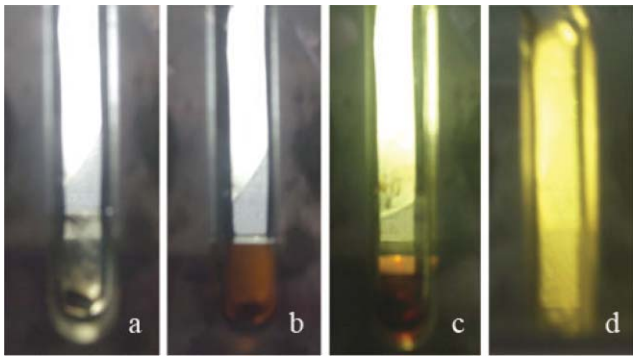

Fig. 1 Photographs of the reaction mixture. The black object at the bottom of the reactor is a magnetic stirring bar. Conditions: (a) 20 °C, 6 MPa (before heating); (b) 130 °C, 14 MPa; (c) 130 °C, 17 MPa; (d) 130 °C, 20 MPa.

α-methylene cyclic carbonate **5**;[10] then **1a** attacks the carbonyl group of the α-methylene cyclic carbonate formed to give the intermediate **6** which could tautomerize to afford the corresponding β-oxopropylcarbamate **3a**. In this mechanism, the secondary amine was used not only as a reaction reagent but also as an active catalyst. The positive effect of CO_2 pressure may be explained by promotion of the formation of **4**.

Visual inspection of the reaction mixture using a high-pressure view cell revealed a complex phase behavior. At 20 °C and 6 MPa (before heating), three phases were present, that is, a liquid **2a**–diethylamine phase saturated in CO_2 at the reactor base, a liquid CO_2 phase in the middle and an upper gas CO_2 phase (Fig. 1a). With increasing reaction temperature, the liquid–gas interface of CO_2 disappeared gradually. At 130 °C, where the pressure reached 14 MPa, the reaction mixture formed two phases, including a liquid phase saturated in CO_2 at the bottom of the reactor and an upper dense CO_2-rich phase (Fig. 1b). When the temperature was kept at 130 °C and the pressure was increased to 17 MPa, the volume of the liquid phase was reduced obviously due to the enhancement of the solubility of reaction component in dense CO_2 (Fig. 1c). The lower reaction rate at 17 MPa in comparison with that of 14 MPa is possibly ascribed to the reduction of the liquid reaction phase considering the proposed mechanism for the reaction may be favourable in a polar liquid phase. The investigation of the phase behavior also showed that the reaction mixture formed a homogeneous phase at 20 MPa (Fig. 1d).

In conclusion, we have showed that β-oxopropylcarbamates could be synthesized in moderate to high yield *via* the one-pot three-component coupling reaction of CO_2, propargyl alcohols and secondary amines in the absence of any catalyst and organic solvent. The catayst-free methodology described herein is simple, efficient and environmentally benign. Efforts are underway to elucidate the mechanistic details of this reaction and to disclose its scope and limitations.

This work was financially supported by the National Natural Science Foundation of China (Nos. 20625205, 20572027 and 20332030) and Guangdong Natural Science Foundation (No. 07118070). We also thank Professor Buxing Han and Dr Tao Jiang (Institute of Chemistry, Chinese Academy of Sciences) for providing the high-pressure view cell and their helpful discussions.

Notes and references

‡ CAUTION: Highly compressed CO_2 must be used under appropriate safety conditions to minimize the risk of personal injury.

§ Reaction procedures: In a typical experiment, diethylamine (**1a**, 20 mmol), 2-methyl-3-butyn-2-ol (**2a**, 10 mmol) were added into a 15 mL stainless autoclave with a magnetic stirrer. The reactor was pressurized with CO_2 at approximately 8 MPa by using a high-pressure liquid pump. The initial pressure was generally adjusted to 14 MPa at 130 °C. The autoclave was heated at that temperature for 48 h, and the pressure was kept constant during the reaction. After the reaction, the reactor was cooled to 0 °C, and CO_2 was slowly vented. The resulting mixture was extracted with diethyl ether. The residue obtained by evaporation of the ethereal solution was purified by column chromatography on silica gel (eluent: petroleum–ethyl acetate = 9 : 1) to give the desired 1,1-dimethyl-2-oxopropyl-*N*,*N*-diethylcarbamate (**3a**, yield: 82%). The carbamate was identified by IR, GC/MS and 400 MHz NMR spectroscopy.

1 (*a*) P. Adams and F. A. Baron, *Chem. Rev.*, 1965, **65**, 567–602; (*b*) T. T. Wu, J. Huang, N. D. Arrington and G. M. DillName, *J. Agric. Food Chem.*, 1987, **35**, 817–823; (*c*) I. Vauthey, F. Valot, C. Gozzi, F. Fache and M. Lemaire, *Tetrahedron Lett.*, 2000, **41**, 6347–6350; (*d*) J. Barthelemy, *Lyon. Pharm.*, 1986, **37**, 249–263.

2 T. W. Greene and P. G. M. Wuts, in *Protective Groups in Organic Synthesis*, John Wiley and Sons, New York, 2nd edn, 1999, pp. 315–348.

3 (*a*) M. Yoshida, N. Hara and S. Okuyama, *Chem. Commun.*, 2000, 151–152; (*b*) D. Chaturvedi, N. Mishra and V. Mishra, *Monatsh. Chem.*, 2007, **138**, 57–60; (*c*) M. Rohr, C. Geyer, R. Wandeler, M. S. Schneider, E. F. Murphy and A. Baiker, *Green Chem.*, 2001, **3**, 123–125; (*d*) R. N. Salvatore, V. L. Flanders, D. Ha and K. W. Jung, *Org. Lett.*, 2000, **2**, 2797–2800; (*e*) R. N. Salvatore, S. I. Shin, A. S. Nagle and K. W. Jung, *J. Org. Chem.*, 2001, **66**, 1035–1037; (*f*) M. Abla, J.-C. Choi and T. Sakakura, *Chem. Commun.*, 2001, 2238–2239; (*g*) R. Srivastava, D. Srinivas and P. Ratnasamy, *Appl. Catal. A: Gen.*, 2005, **289**, 128–134; (*h*) M. Feroci, M. A. Casadei, M. Orsini, L. Palombi and A. Inesi, *J. Org. Chem.*, 2003, **68**, 1548–1551; (*i*) D. Chaturvedi and S. Ray, *Monatsh. Chem.*, 2006, **137**, 127–145.

4 (*a*) Y. Sasaki and P. H. Dixneuf, *J. Org. Chem.*, 1987, **52**, 4389–4391; (*b*) C. Burncau and P. H. Dixneuf, *Tetrahedron Lett.*, 1987, **28**, 2005–2008; (*c*) Y. Sasaki, *JP. Pat. 62 61 961*, 1987.

5 T. J. Kim, K. H. Kwon, S. C. Kwon, J. O. Baeg, S. C. Shim and D. H. Lee, *J. Organomet. Chem.*, 1990, **389**, 205–217.

6 S.-C. Shim, J.-O. Baeq, C.-H. Doh, Y.-Z. Youn and T.-J. Kim, *Bull. Korean Chem. Soc.*, 1990, **11**, 467–468.

7 (*a*) H.-S. Kim, J.-W. Kim, S.-C. Kwon, S.-C. Shim and T.-J. Kim, *J. Organomet. Chem.*, 1997, **545–546**, 337–344; (*b*) S.-C. Kwon, C.-S. Cho, S.-C. Shim and T.-J. Kim, *Bull. Korean Chem. Soc.*, 1999, **20**, 103–105.

8 (*a*) J. Fournler, C. Bruneau and P. H. Dixeuf, *Tetrahedron Lett.*, 1989, **30**, 3981–3982; (*b*) J. M. Joumier, J. Fournier, C. Bruneau and P. H. Dixneuf, *J. Chem. Soc., Perkin Trans. 1*, 1991, 3271–3274; (*c*) C. Bruneau and P. H. Dixneuf, *J. Mol. Catal.*, 1992, **74**, 97–107; (*d*) Y. Kayaki, M. Yamamoto and T. Ikariya, *J. Org. Chem.*, 2007, **72**, 647–649.

9 Y. Inoue, J. Ishikawa, M. Taniguchi and H. Hashimoto, *Bull. Chem. Soc. Jpn.*, 1987, **60**, 1204–1206.

10 (*a*) S. Fujiwara, Y. Shikano, T. Shin-ike, N. Kambe and N. Sonoda, *J. Org. Chem.*, 2002, **67**, 6275–6278; (*b*) Y. Kayaki, M. Yamamoto, T. Suzuki and T. Ikariya, *Green Chem.*, 2006, **8**, 1019–1021.

Aqueous cross-coupling: highly efficient Suzuki–Miyaura coupling of *N*-heteroaryl halides and *N*-heteroarylboronic acids†

Christoph A. Fleckenstein and Herbert Plenio*

Received 9th August 2007, Accepted 26th September 2007
First published as an Advance Article on the web 5th October 2007
DOI: 10.1039/b711965h

The palladium complex of the new disulfonated 9-(3-phenylpropyl)-9′-PCy$_2$-fluorene ligand is a highly active catalyst for aqueous Suzuki coupling reactions of *N*-heterocyclic chlorides and *N*-heterocyclic boronic acids; catalyst loadings of 0.02–0.1 mol% of Pd and two equiv. of phosphine result in the near quantitative formation of the respective coupling products at 100 °C.

During the last decade the Suzuki–Miyaura coupling reaction has become a powerful tool in synthetic chemistry.[1] However, most of the catalysts used for such reactions were developed to perform best in organic solvents. The use of water is primarily discussed in the context of green solvents[2] but less so as a solvent leading to the superior performance of the catalyst.[3,4] According to a recent MDL Drug Data Report, pyridines are the most common heterocycles in pharmaceutically active compounds.[5] Unfortunately, nitrogen-containing heterocycles are difficult substrates for Suzuki coupling reactions.[6–9] Especially, electron-rich pyridines with amino-substituents *ortho*- or *para*- to the pyridine nitrogen atom display high basicities which go along with an increasing propensity for the coordination (inhibition) of the catalytically active palladium complexes. Improvements in the coupling of such substrates were recently reported by Guram *et al.*,[10] Buchwald and co-workers[11] and Fu's group.[12] Interestingly, coupling reactions involving such substrates were performed in water or water containing solvent mixtures (with toluene, dioxane, CH_3CN or butanol). We reasoned that, in the presence of water, the nitrogen atoms prefer to engage in hydrogen bonding with water rather than to coordinate to the soft Pd, leading to much higher catalytic activities. However, all of the catalysts previously employed were not optimized for use in water with respect to solubility.

Consequently, we attempted the synthesis of highly water-soluble ligands to enable Pd-catalyzed coupling reactions in pure water as the solvent at low catalyst loading.

We recently reported the synthesis of fluorenyldialkylphosphines whose Pd complexes are excellent catalysts for various cross-coupling reactions.[13,14] The facile introduction of functional groups was demonstrated with the monosulfonation of a 9-ethyl-fluoren-9-yl-dicyclohexylphosphine, but the solubility of the respective Pd complexes in water is modest. Consequently, we wish to describe here the synthesis of a disulfonated fluorenyl-dicyclohexylphosphine and the preliminary screening of the catalytic activity of the respective Pd complexes in the Suzuki cross-coupling of various *N*-heterocyclic substrates. Furthermore, the use of the solvent water leads to catalysts which are superior to the best ones used in conventional organic solvents. In this manner, optimum catalytic performance and benign properties are combined.

In order to obtain a disulfonated fluorenylphosphine the use of more reactive sulfonating reagents (oleum, $ClSO_3H$) on 9-ethyl-fluoren-9-yl-dicyclohexylphosphine was tested, but led to the oxidation of the P(III) centre during aqueous workup. Less forcing reaction conditions gave the monosulfonated product. Consequently, we decided to introduce another phenyl ring in the periphery of the ligand to serve as an anchor for the second sulfonato group. First the 9-fluorenyl anion was reacted with 1-bromo-3-phenylpropane to result in the 9-alkylfluorene **1** (Scheme 1); deprotonation of **1** with *n*BuLi and reaction with Cy_2PCl led to the formation of the fluorenylphosphine **2**, whose treatment with sulfuric acid leads to the double sulfonation. Starting from fluorene, the disulfonated fluorenylphosphine **3** is easily available in three steps in a 49% overall yield, making use of simple, commercially available starting materials.

We have tested a number of different 2-chloropyridines and 2-chloroquinolines in Suzuki reactions of various boronic acids (mainly tolyl-, naphthyl-boronic acids, Table 1, entries 1–20). The catalyst is formed *in situ* from Na_2PdCl_4, and two equivalents of the triply protonated ligand **3** in the presence of five equivalents of base. Under these reaction conditions all substrates are converted in quantitative yields into the respective products. No conversion at all was observed in the absence of the phosphine ligand. Typical coupling reactions were carried out at 100 °C in pure water during 12 h with K_2CO_3 as the base utilizing between 0.02 and 0.05 mol% of Pd catalyst. Notably, even difficult substrate combinations, such as the highly basic 2-chloro-4-aminopyridine with tolylboronic

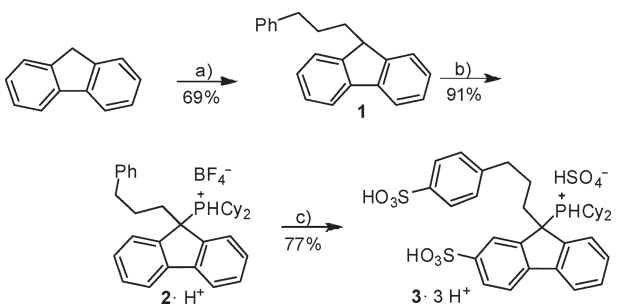

Scheme 1 Synthesis of double sulfonated fluorenyldicyclohexyl-phosphine. *Reagents and conditions*: a) *n*BuLi, 1-bromo-3-phenylpropane, THF, −60 °C; b) *n*BuLi, Cy_2PCl, Et_2O, −60 °C, $HBF_4{\cdot}Et_2O$; c) CH_2Cl_2, H_2SO_4, 50 °C.

Anorganische Chemie im Zintl-Institut, TU Darmstadt, Petersenstr. 18, 64287 Darmstadt, Germany. E-mail: plenio@tu-darmstadt.de
† Electronic supplementary information (ESI) available: Spectra of the new coupling products. See DOI: 10.1039/b711965h

Table 1 Suzuki reaction with *N*-heteroaryl chlorides in water[a]

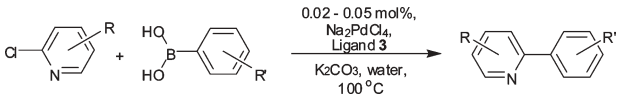

Entry	Aryl chloride	Boronic acid	Product	Yield (%)[b]
1		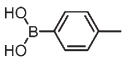	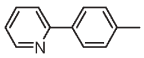	⩾99[c] 95
2	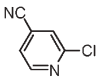	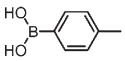	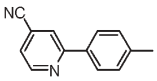	⩾99[c] 93
3	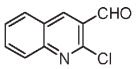	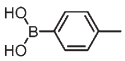	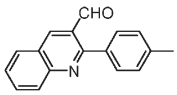	⩾99[c] 97
4	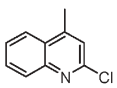	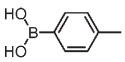	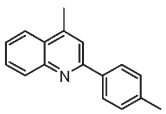	⩾99[d] 95
5		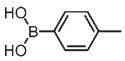	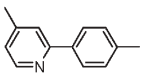	⩾99[d] 92
6	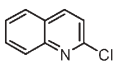	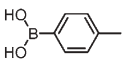	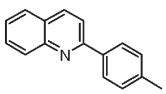	⩾99[c] 95
7	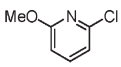	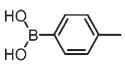	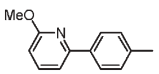	⩾99[d] 94
8		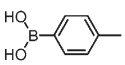	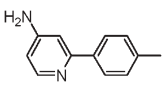	⩾99[d] 92
9	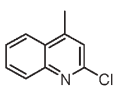	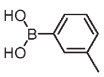	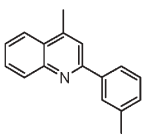	⩾99[d] 96
10	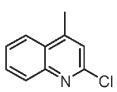	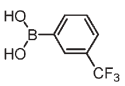	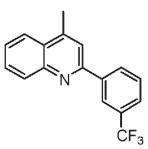	⩾99[d] 95
11	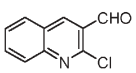	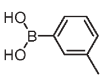	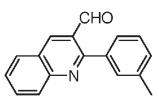	⩾99[c] 93
12	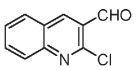	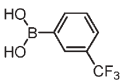	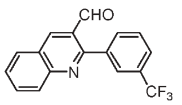	⩾99[c] 92
13	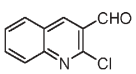	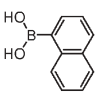	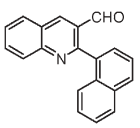	⩾99[d] 96
14				⩾99[d] 94

Table 1 Suzuki reaction with *N*-heteroaryl chlorides in water[a] (*Continued*)

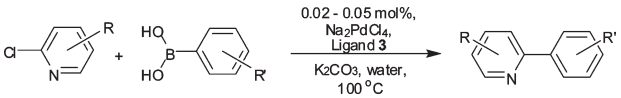

Entry	Aryl chloride	Boronic acid	Product	Yield (%)[b]
15	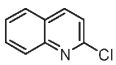		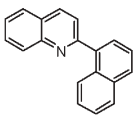	⩾99[d] 95
16			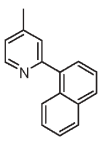	⩾99[d] 93
17			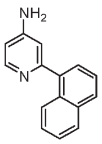	97[d] 90
18	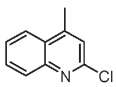		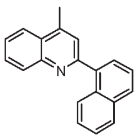	⩾99[d] 95
19	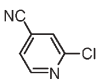		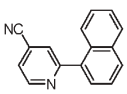	⩾99[d] 94
20	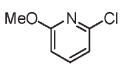		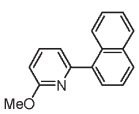	⩾99[d] 98

[a] Reaction conditions: 1.0 equiv. aryl halide, 1.2 equiv. boronic acid, 3.2 equiv. K_2CO_3, degassed water (4 mL $mmol^{-1}$), 100 °C, 12 h, cat. (respective volume of catalyst stock solution, c_{Pd} = 0.01 mol L^{-1}, Na_2PdCl_4/ligand **3**·$3H^+$, L/Pd = 2 : 1). Reaction times not optimized. [b] Average of two runs: the first number indicates the conversion determined *via* GC using an internal heptadecane standard, the second number is the isolated yield (column chromatography). [c] [Pd] = 0.02 mol%. [d] [Pd] = 0.05 mol%.

acid or the sterically hindered naphthylboronic acid (entries 13–20) require only 0.05 mol% of catalyst for quantitative conversion at 100 °C; 3-CF_3-substituted phenylboronic acid, as an example for an electron-deficient metalloid (entries 10 and 12), is quantitatively reacted at 0.02–0.05 mol%.

Even more difficult coupling reactions are those in which both coupling partners contain nitrogen donors. We tested several reactions of 2-chloropyridines and 2-chloroquinolines with 3-pyridineboronic acid (Table 2) using 0.1 mol% catalyst leading to the quantitative formation of the respective coupling products (entries 1–5). Suzuki–Miyaura reactions of the more electron-rich methoxy-substituted 2-chloropyridine (entry 6) gives 93% conversion and 90% isolated yield. The most challenging combination is that of 2-chloro-4-aminopyridine and 3-pyridineboronic acid (entry 7), which gives 94% conversion at 0.2 mol% catalyst. Consequently, the present catalyst is 10–100 times more active than other systems, which typically require 1–2 mol% Pd at slightly higher temperatures (100–120 °C).[10,11,15] To the best of our knowledge, the catalysts reported here are the most efficient for the Suzuki–Miyaura coupling with chloropyridines.[11,12,16–24]

All products from the screening experiments were obtained by ether extraction from the aqueous solution. In order to demonstrate that organic solvents can be completely avoided in the synthesis of the coupling products, we have run one coupling reaction [2-chloro-4-picoline + $PhB(OH)_2$] on a gram-scale. After the coupling reaction, the water-insoluble product deposits as an oil on the water surface, which can be separated easily from the aqueous phase containing base and excess boronic acid. The purity of the crude product is excellent (>98%).

In conclusion, a disulfonated sterically demanding and electron-rich fluorenylphosphine was synthesized in three steps from simple, commercially available starting materials in 49% overall yield. We have demonstrated for numerous substrate combinations that chloropyridines (quinolines) and aryl- or pyridineboronic acids can be Suzuki coupled in quantitative yields in pure water as the solvent, typically using between 0.02 and 0.1 mol% of Pd catalyst at 100 °C. We are currently evaluating the potential of this catalyst system in aqueous Sonogashira and Buchwald–Hartwig cross-coupling reactions also using different substitution patterns.

Table 2 Suzuki reaction with *N*-heteroaryl chlorides and *N*-heteroarylboronic acids in water[a]

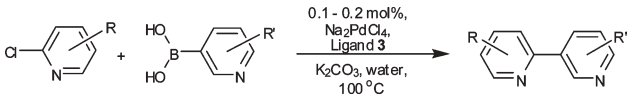

Entry	Aryl chloride	Boronic acid	Product	Yield (%)[b]
1	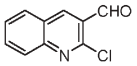	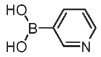	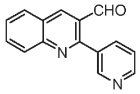	⩾99[c] 95
2		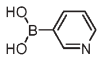	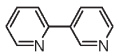	⩾99[c] 96
3	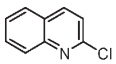	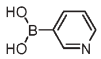	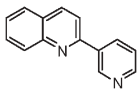	⩾99[c] 93
4		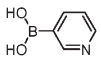	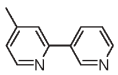	⩾99[c] 92
5	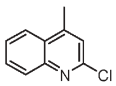	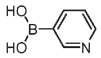	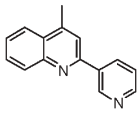	⩾99[c] 95
6	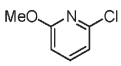	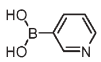	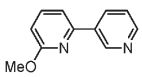	93[c] 90
7		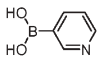	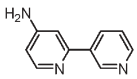	94[d] 90

[a] Reaction conditions: 1.0 equiv. aryl halide, 1.2 equiv. boronic acid, 3.2 equiv. K_2CO_3, degassed water (4 mL mmol^{-1}), 100 °C, 12 h, cat. (respective volume of catalyst stock solution, c_{Pd} = 0.01 mol L^{-1}, Na_2PdCl_4/ligand **3**·3H$^+$, L/Pd = 2 : 1). Reaction times not optimized. [b] Average of two runs: the first number indicates the conversion determined *via* GC using an internal heptadecane standard, the second number is the isolated yield (column chromatography). [c] [Pd] = 0.1 mol%. [d] [Pd] = 0.2 mol%.

Experimental. *Catalyst stock solution*: Na_2PdCl_4 (5.9 mg, 0.02 mmol), phosphonium salt (**3**·3 H$^+$) (50 mg) and K_2CO_3 (300 mg) were placed in Schlenk tube. Water (20 mL) was added and the mixture was stirred at 50–55 °C for 2 h until the clear solution turns nearly colourless. This stock solution has a concentration of c_{Pd} = 0.001 mol L^{-1}. *Cross-coupling reaction*: to the aryl chloride (1 mmol), boronic acid (1.5 mmol) and K_2CO_3 (2 mmol), water (4 mL) and the catalyst stock solution were added. The reaction mixture was stirred at 100 °C in an aluminium block during 12 h. After cooling to room temperature the reaction mixture was diluted with diethyl ether (15 mL), washed with water (10 mL), the organic phase dried over $MgSO_4$, filtered and concentrated *in vacuo*. Products were purified by column chromatography. Alternatively the yield was determined *via* gas chromatography with heptadecane or diethylene glycol di-*n*butyl ether as an internal standard.

Procedure for gram-scale cross-coupling reaction. Preparation of the catalyst solution: Na_2PdCl_4 (11.8 mg, 0.04 mmol), phosphonium salt (**3**·3H$^+$) (100 mg) and K_2CO_3 (500 mg) were placed in Schlenk tube. Water (25.0 mL) was added and the mixture was stirred at 55 °C for 2 h until the clear solution turns nearly colourless. *Cross-coupling reaction*: a 30 mL Schlenk tube was charged with phenylboronic acid (3.17 g, 26 mmol) and K_2CO_3 (5.53 g, 40 mmol). The reaction vessel was evacuated and backfilled with argon twice. The catalyst solution and 2-chloro-4-picoline (1.75 mL, 20 mmol) were added. The reaction mixture was stirred vigorously for 12 h at 100 °C and then allowed to cool down to ambient temperature without stirring. A brown organic (upper) oily layer separates and was transferred into a flask. This oil was vacuum stripped at 40 mbar at 80 °C for 1 h to afford 3.05 g (90%) of the crude product as a brown oil. Purity >98% (GC-FID, ^{1}H-NMR).

This work was supported by the DFG and the Degussa AG, Provadis (Partner für Bildung und Beratung) GmbH, C. A. F. by the Fonds der Chemischen Industrie and the Studienstiftung des Deutschen Volkes with a fellowship. Experimental support by Jan Pschierer is acknowledged.

Notes and references

1 J. Hassan, M. Sevignon, C. Gozzi, E. Schulz and M. Lemaire, *Chem. Rev.*, 2002, **102**, 1359–1469.
2 D. J. C. Constable, C. Jimenez-Gonzalez and R. K. Henderson, *Org. Process Res. Dev.*, 2007, **11**, 133–137.
3 K. H. Shaughnessy, *Eur. J. Org. Chem.*, 2006, 1827–1835.
4 C.-J. Li, *Chem. Rev.*, 2005, **105**, 3095–3165.
5 J. A. Lowe, W. Qian, S. E. Drozda, R. A. Volkmann, D. Nason, R. B. Nelson, C. Nolan, D. Liston, K. Ward, S. Faraci, K. Verdries, P. Seymour, M. Majchrzak, A. Villalobos and W. F. White, *J. Med. Chem.*, 2004, **47**, 1575–1586.

6 M. Feuerstein, H. Doucet and M. Santelli, *Tetrahedron Lett.*, 2005, **46**, 1717–1720.
7 M. Moreno-Mañas, R. Pleixats and A. Serra-Muns, *Synlett.*, 2006, 3001–3004.
8 T. Itoh and T. Mase, *Tetrahedron Lett.*, 2005, **46**, 3573–3577.
9 P. Capek, M. Vrábel, Z. Hasník, R. Pohl and M. Hocek, *Synthesis*, 2006, 3515–3526.
10 A. S. Guram, X. Wang, E. E. Bunel, M. M. Faul, R. D. Larsen and M. J. Martinelli, *J. Org. Chem.*, 2007, **72**, 5104–5112.
11 K. L. Billingsley, K. W. Anderson and S. L. Buchwald, *Angew. Chem., Int. Ed.*, 2006, **45**, 3484–3488.
12 N. Kudo, M. Perseghini and G. C. Fu, *Angew. Chem., Int. Ed.*, 2006, **45**, 1282–1284.
13 C. A. Fleckenstein and H. Plenio, *Chem.–Eur. J.*, 2007, **13**, 2701–2716.
14 C. A. Fleckenstein and H. Plenio, *Organometallics*, 2007, **26**, 2758–2767.
15 K. Billingsley and S. L. Buchwald, *J. Am. Chem. Soc.*, 2007, **129**, 3358–3366.
16 A. E. Thompson, G. Hughes, A. S. Batsanov, M. R. Bryce, P. R. Parry and B. Tarbit, *J. Org. Chem.*, 2005, **70**, 388–390.
17 K. W. Anderson and S. L. Buchwald, *Angew. Chem., Int. Ed.*, 2005, **44**, 6173–6177.
18 A. S. Guram, A. O. King, J. G. Allen, X. Wang, L. B. Schenkel, J. Chan, E. E. Bunel, M. M. Faul, R. D. Larsen, M. J. Martinelli and P. J. Reider, *Org. Lett.*, 2006, **8**, 1787–1789.
19 S. Li, Y. Lin, J. Cao and S. Zhang, *J. Org. Chem.*, 2007, **72**, 4067–4072.
20 T. Brendgen, M. Frank and J. Schatz, *Eur. J. Org. Chem.*, 2006, 2378–2383.
21 L. Botella and C. Najera, *Angew. Chem., Int. Ed.*, 2002, **41**, 179–181.
22 M. an der Heiden and H. Plenio, *Chem.–Eur. J.*, 2004, **10**, 1789–1797.
23 A. Datta and H. Plenio, *Chem. Commun.*, 2003, 1504–1505.
24 C. Fleckenstein, S. Roy, S. Leuthäußer and H. Plenio, *Chem. Commun.*, 2007, 2870–2872.

Nucleophilic substitution of ferrocenyl alcohols "on water"†

Pier Giorgio Cozzi* and Luca Zoli

Received 27th July 2007, Accepted 11th September 2007
First published as an Advance Article on the web 18th September 2007
DOI: 10.1039/b711523g

Nucleophilic substitution of ferrocenyl alcohols is effectively promoted "on water", without the presence of Lewis acids, Brønsted acids or surfactants.

The use of water as a reaction medium in organic synthesis has received considerably attention.[1] Water as a reaction medium conveys many important advantages; it is considered cheap, safe and environmentally benign.[2] Moreover, the application of water as a solvent has led to an observed difference in both reactivity and selectivity from that found in common organic solvents.[3] Indeed, it has been found that coupling reactions between benzylic halides and nucleophiles are possible in water[4] despite the fact that carbocations may be generated in the process. These efficient protocols for carbon–carbon bond forming reactions can be further enhanced when alcohols are used as substrates. In fact, in this case the by-product generated is water. The application of alcohols in nucleophilic substitution reaction is limited due to the poor leaving group ability of the hydroxy group;[5] nevertheless, there have been a number of catalytic methods for the promotion of direct nucleophilic substitution in organic solvents reported.[6] There have also been examples of efficient catalytic systems reported in the literature to effect dehydrative nucleophilic substitution in water as solvent; however, this area still remains a challenging research topic. Kobayashi, during his studies of organic reaction in water,[7] has disclosed that dodecylbenzenesulfonic acid (DBSA) efficiently catalyzes the dehydrative esterification of carboxylic acids in water[8] and he has reported that DBSA is also able to promote the catalytic nucleophilic substitution of benzylic alcohols with various carbon nucleophiles in water.[9] We report herein the direct substitution of optically active ferrocenyl alcohols "on water"[10] without the use of any type of Brønsted or Lewis acids.

Recently, we have studied the direct substitution of optically active ferrocenyl alcohols[11] with different nucleophiles in organic solvents in the presence of catalytic amounts of indium salts.[12] While the reaction was generally found to be efficient, there were some examples that proved to be more problematic (for example, in the addition of dimethyl and diethyl malonate) under the reaction conditions applied.[13] In the search for a more efficient nucleophilic substitution of ferrocenyl alcohols, we have examined the Friedel–Crafts type substitution reaction of (*R*)-(1-hydroxyethyl)ferrocene **1** with indole **3a**[14] (Scheme 1) in different solvents and in the presence of various Lewis acids. Water and a combination of Lewis acids ($Yb(OTf)_3$, $Al(OTf)_3$, $In(OTf)_3$, $InBr_3$ and $Bi(OTf)_3$) with amino acids[15] were also examined and we found excellent conversion at 60 °C.

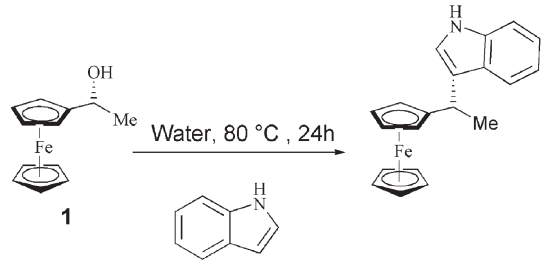

Scheme 1 Direct nucleophilic substitution of ferrocenyl alcohol **1** with indole "on water".

Quite remarkably, the isolated yields were in the range of 90–100% for almost all of the combinations of Lewis acid examined. Finally, the model reaction was performed at 80 °C in pure water, giving complete conversion, and suggesting that the presence of Lewis acid was not necessary in order to perform the reaction. It is worthy to mention that the reaction between benzydrol and 1-methylindole is not promoted in water, and common Brønsted acids, such as AcOH (acetic acid), TFA (trifluoroacetic acid), TfOH (triflic acid) and TsOH (*p*-toluene sulfonic acid), were not effective catalysts for this reaction in water.[9] Nevertheless, the reaction could be effected by the use of DBSA probably due to both the surfactant property and the strong Brønsted acidity.

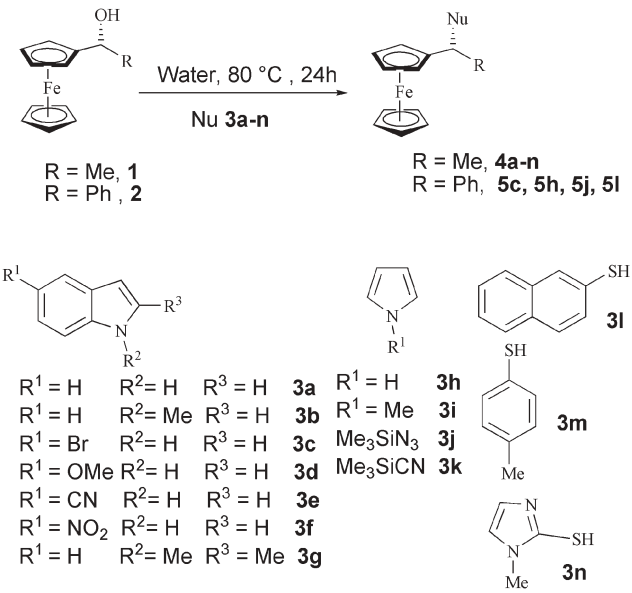

Scheme 2 Nuclephilic substitution of ferrocene alcohols **1** and **2** with the nucleophiles **3a–n** "on water"

Dipartimento di Chimica "G. Ciamician" Via Selmi 2, 40126 Bologna, Italy. E-mail: piergiorgio.cozzi@unibo.it; Fax: +39 051 2099456; Tel: +39 051 2099511

† Electronic supplementary information (ESI) available: Complete characterization for the compounds and HPLC data. See DOI: 10.1039/b711523g

Table 1 Reaction of ferrocenyl alcohols **1** and **2** with the nucleophiles **3a–n** "on water"

Entry	Alcohol[b]	Nu	Product	Yield (%)[c]	ee (%)[d]	Entry	Alcohol[b]	Nu	Product	Yield (%)[c]	ee (%)[d]
1	**1**	**3a**	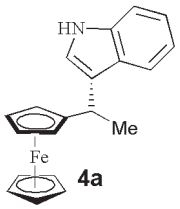 **4a**	85	99	11	**1**	**3j**	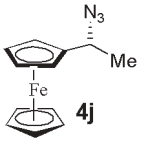 **4j**	83	97
2	**1**	**3b**	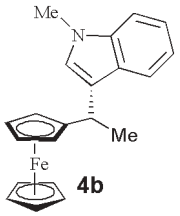 **4b**	68	99	12	**1**	**3k**	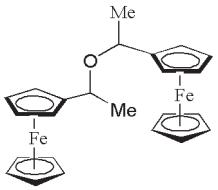	71	[g]
3	**1**	**3c**	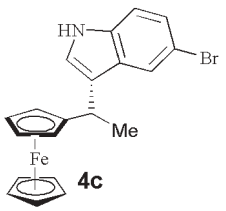 **4c**	45	99	13	**1**	**3l**	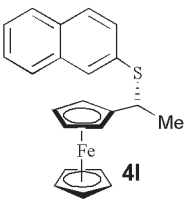 **4l**	63	96
4	**1**	**3d**	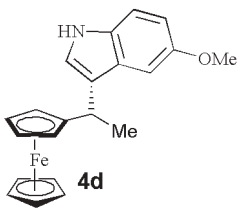 **4d**	81	99	14	**1**	**3m**	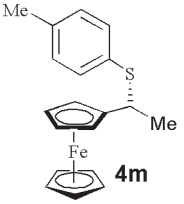 **4m**	46	90
5	**1**	**3e**	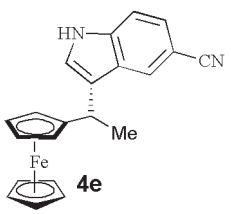 **4e**	43	99	15	**1**	**3n**	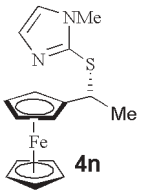 **4n**	63	80
6	**1**	**3f**	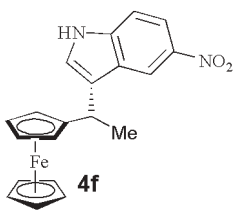 **4f**	0		16	**2**	**3c**	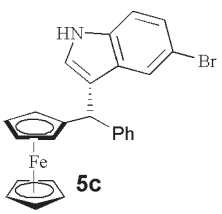 **5c**	0	
7	**1**	**3g**	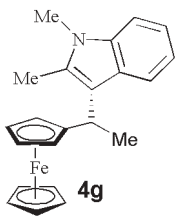 **4g**	82	99	17[h]	**2**	**3h**	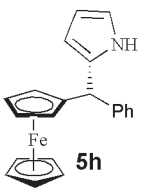 **5h**	60	94
8	**1**	**3h**	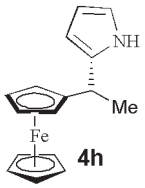 **4h**	58[e]	99	18	**2**	**3j**	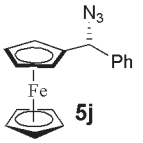 **5j**	95	72

Table 1 Reaction of ferrocenyl alcohols **1** and **2** with the nucleophiles **3a–n** "on water" (*Continued*)

Entry	Alcohol[b]	Nu	Product	Yield (%)[c]	ee (%)[d]	Entry	Alcohol[b]	Nu	Product	Yield (%)[c]	ee (%)[d]
9[f]	**1**	**3h**	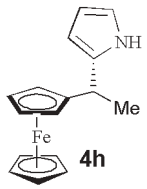 **4h**	68[e]	99	19	**2**	**3l**	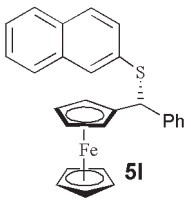 **5l**	47	94
10	**1**	**3i**	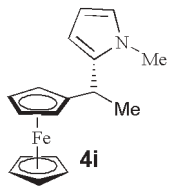 **4i**	81	99						

[a] All the reactions were carried out in air with 0.1 mmol of ferrocene alcohol and 0.2 mmol of nucleophile suspended in 1.0 mL of water at 80 °C for 24–36 h. [b] Alcohol **1** was obtained in 99% ee by enantioselective hydrogenation with Ru–P–Phos.[29] Alcohol **2** was prepared by Corey–Bakshi–Shibata[30] reduction, and was obtained in 94% ee. [c] Yield of purified product. [d] The enantiomeric excesses were evaluated by chiral HPLC (see ESI for details). [e] 2,5-Di(1-ethylferrocene)pyrrole was isolated in 10 mol% (in the small-scale reaction), and in 15 mol% (in the increased-scale reaction) as by-product of the reaction. [f] The reaction was performed with 1.5 mmol of (*R*)-(1-hydroxyethyl)ferrocene **1** with 10 equiv. of pyrrole. [g] The reaction product was obtained as a mixture of two diastereoisomers in ratio 4 : 1, judged by ^{1}H-NMR. The absolute and relative stereochemistry was not assigned. [h] 2,5-Di(phenylmethylferrocene)pyrrole was isolated in 30 mol% as by-product of the reaction.

Many different nucleophiles were tested[16] and it was found that pyrrole, Me_3SiN_3 and thiophenols reacted with ferrocenyl alcohols in water without requirement for Lewis or Brønsted acids (Scheme 2). Electron rich and electron poor indoles could also be employed in the reaction, although the conversions observed with indole substituted by electron withdrawing groups was inferior (Table 1, entry 5). 5-Nitroindole was not reactive in the reactions conditions, even with a prolonged reaction time of 36 h. Whereas in our previous work[12] we were obliged to use neat pyrrole to effect the reaction (at −40 °C!), in this case we can efficiently carry out the reaction with just 5–10 equiv. of pyrrole. The absence of Lewis acids avoids polymerization of pyrrole or pyrrole derivatives. This reaction could be readily scaled up (Table 1, entry 9). The reaction was easily performed in deionised water at 80 °C, and the work up simply consisted of the separation of the products by the addition an organic solvent. Me_3SiN_3 was found to react with both ferrocene derivatives **1** and **2** giving the desired products in good yield. Thiophenols and 1-methyl-*H*-imidazol-2-thiol are also suitable nucleophiles for this reaction (Table 1, entries 13–15) and the corresponding thioethers **4l–n** are produced in moderate yield.[17] For all the examined reactions the use of optically active ferrocene derivatives allows the straightforward preparation of the corresponding enantioenriched ferrocene **4a–j**, **4l–n**, **5h**, **5j** and **5l**.[18] Particularly remarkable is the reaction with Me_3SiN_3 in water that allows the obtainment of an interesting enantioenriched building block (**4j** and **5j**) for "Click Chemistry".[19] As the cycloaddition of alkynes catalyzed by copper(I) ascorbate is performed in water, a consecutive reaction between ferrocene azide derivatives obtained "on water", and alkynes, appears possible.[20] Acidic nucleophiles (*i. e.* 4-nitrophenol) or nucleophiles hydrolyzed in water to weak acids (Me_3SiCN to HCN) promoted the reaction of ferrocenyl alcohol with itself (Table 1, entry 12).

Unfortunately, benzylic and allylic alcohols[21] or benzydrols[9] were not found to react with indole in pure water.

It is possible that the stability of ferrocenyl cations generated and the easy formation of the stabilized cation play an important role in this reaction. Jørgensen and Zhuang have reported a Friedel–Crafts reaction of a reactive ethyl glyoxalate with indole and pyrrole in water, or in basic conditions.[22] Our and Jørgensen's results are based on the reactivity scale of indoles revealed by Mayr *et al.*[23] Many electron-rich π-systems are more nucleophilic than aqueous acetone or aqueous acetonitrile. In slightly basic or neutral conditions the intermediates of the S_N1 reaction could be trapped with electron rich π-systems. Our reaction could be classified, according to Sharpless *et al.*,[2] as reaction "on water". Marcus and Jung have recently explained the origin of the rate increase of reactions carried out "on water". In particular, the structure of water at the oil–water interface of an oil emulsion, in which free ("dangling") OH groups are protruding into the organic phase, is quite important. These groups play a key role in catalyzing reactions *via* the formation of hydrogen bonds. The structural arrangement at the "oil–water" interface is quite different to the structure of water molecules around a small hydrophobic solute in homogeneous solution, where the water molecules are tangentially oriented.[24,25]

In summary, we have described a challenging dehydration reaction "on water" without the use of Lewis acids or surfactants, that allows the direct functionalyzation of ferrocene alcohols in pure water.[26] To the best of our knowledge this is the first example of a direct nucleophilic substitution of an alcohol "on water".[27] The mild reaction conditions and the use of water without the presence of co-solvents, additive, Lewis, or Brønsted acids, can be exploited for introducing the ferrocene moiety into biological molecules through bioconjugation,[28] expanding the scope of ferrocene as sensitive electrochemical probe. These and other options will be pursued by further work in our laboratory.‡

Acknowledgements

This work was supported by PRIN 2005 (Progetto Nazionale: Sintesi e Stereocontrollo di Molecole Organiche per lo Sviluppo di Metodologie Innovative di Interesse Applicativo),

and ST Microelectronics. Antonio Zanotti Gerosa and Johnson Matthey Catalysis are acknowledged for the generous gift of chemicals.

Notes and references

‡ Typical procedure: Ferrocene alcohol (0.023 g, 0.1 mmol) and indole (0.023 g, 0.197 mmol) were introduced in a reaction flask under air, and deionised water (pH = 6.52, 1.0 mL) was added. The flask was sealed and stirred under air at 80 °C for 24 h, then allowed to cool to room temperature. Diethyl ether (5 mL) was added and the organic phase was separated, dried over anhydrous Na_2SO_4, and evaporated to reduced pressure to give a yellow oil purified by chromatography (cyclohexane : diethyl ether 9 : 1). Yield 85%.

1 (*a*) C.-J. Li and T.-H. Chan, *Organic Reaction in Aqueous Media*, Wiley, New York, 1997; (*b*) *Organic Synthesis in Water*, ed. P.A. Grieco, Blackie Academic and Professional, London, 1998; (*c*) C.-J. Li, *Chem. Rev.*, 2005, **105**, 3095; (*d*) C.-J. Li and L. Chen, *Chem. Soc. Rev.*, 2006, **35**, 68; (*e*) *Organic Reaction in Water*, ed. U. M. Lindström, Blackwell Publishing, Oxford, 2007.

2 S. Narayan, J. Muldoon, M. G. Finn, V. V. Fokin, H. C. Kolb and K. B. Sharpless, *Angew. Chem., Int. Ed.*, 2005, **44**, 3275.

3 (*a*) U. M. Lindström and F. Andersson, *Angew. Chem., Int. Ed.*, 2006, **45**, 548; (*b*) M. C. Pirrung, *Chem.–Eur. J.*, 2006, **12**, 1312; (*c*) S. Otto and J. B. F. N. Engberts, *Org. Biomol. Chem.*, 2003, **1**, 2809.

4 (*a*) M. Hofmann, N. Hampel, T. Kanzian and H. Mayr, *Angew. Chem., Int. Ed.*, 2004, **43**, 5402; (*b*) M. Westermaier and H. Mayr, *Org. Lett.*, 2006, **8**, 4791.

5 (*a*) G. C. Gullickson and D. E. Lewis, *Aust. J. Chem.*, 2003, **56**, 385; (*b*) F. Bisaro, G. Prestat, M. Vitale and G. Poli, *Synlett*, 2002, 1823; (*c*) S.J. Coote, S. G. Davies, D. Middlemiss and A. Naylor, *Tetrahedron Lett.*, 1989, **30**, 3581.

6 For recent reports of catalyzed C–C, C–N and C–O bond formation through direct substitution of allylic or propargylic alcohols with nucleophiles, see: (*a*) V. Terrasson, S. Marque, J.-M. Campagne and D. Prim, *Adv. Synth. Catal.*, 2006, **348**, 2063; (*b*) Z. Zhan, W. Wang, R. Yang, J. Yu, J. Li and H. Liu, *Chem. Commun.*, 2006, 3352; (*c*) Y. Nishibayashi, A. Shinoda, Y. Miyake, H. Matsuzawa and M. Sato, *Angew. Chem., Int. Ed.*, 2006, **45**, 4835; (*d*) K. Motokura, N. Fujita, K. Mori, T. Mizugaki, K. Ebitani and K. Kaneda, *Angew. Chem., Int. Ed.*, 2006, **45**, 2605; (*e*) H. Qin, N. Yamagiwa, S. Matsunaga and M. Shibasaki, *Angew. Chem., Int. Ed.*, 2007, **46**, 409; (*f*) R. Sanz, A. Martínez, D. Miguel, J. M. Álvarez-Guitiérrez and F. Rodríguez, *Adv. Synth. Catal.*, 2006, **348**, 1841; (*g*) T. Saito, Y. Nishimoto, M. Yasuda and A. Baba, *J. Org. Chem.*, 2006, **71**, 8516; (*h*) M. Yasuda, T. Somyo and A. Baba, *Angew. Chem., Int. Ed.*, 2006, **45**, 793; (*i*) R. Sanz, D. Miguel, A. Martinez, J. M. Alvarez-Gutiérrez and F. Rodriguez, *Org. Lett.*, 2007, **9**, 2027; (*j*) R. Sanz, D. Miguel, A. Martinez, J. M. Alvarez-Gutiérrez and F. Rodriguez, *Org. Lett.*, 2007, **9**, 727; (*k*) M. Rueping, B. J. Nachtsheim and A. Kuenkel, *Org. Lett.*, 2007, **9**, 825; (*l*) M. Noji, Y. Konno and Keitaro Ishii, *J. Org. Chem.*, 2007, **72**, 5161; (*m*) W. Huang, J. Wang, Q. Shen and X. Zhou, *Tetrahedron Lett.*, 2007, **48**, 3969; (*n*) U. Jana, S. Biswas and S. Maiti, *Tetrahedron Lett.*, 2007, **48**, 4065; (*o*) J. Le Bras and J. Muzart, *Tetrahedron*, 2007, **63**, 7942; (*p*) J. Kischel, K. Mertins, D. Michalik, A. Zapf and M. Beller, *Adv. Synth. Catal.*, 2007, **349**, 865.

7 S. Kobayashi and C. Ogawa, *Chem.–Eur. J.*, 2006, **12**, 5945 and ref. therein.

8 K. Manabe, S. Iimura, X.-M. Sun and S. Kobayashi, *J. Am. Chem. Soc.*, 2002, **124**, 1197.

9 S. Shirakawa and S. Kobayashi, *Org. Lett.*, 2007, **9**, 311.

10 Ferrocene alcohols **1** and **2** are insoluble in water. For a discussion of reactions performed in water, see ref. 2. See also: (*a*) A. P. Brogan, T. J. Dickerson and K. D. Janda, *Angew. Chem., Int. Ed.*, 2006, **45**, 8100; (*b*) Y. Hayashi, *Angew. Chem., Int. Ed.*, 2006, **45**, 8103; (*c*) J. E. Klijn and J. B. F. N. Engberts, *Nature*, 2005, **453**, 746.

11 R. Gòmez Arrayás, J. Adrio and J. C. Carretero, *Angew. Chem., Int. Ed.*, 2006, **45**, 7674.

12 P. Vicennati and P. G. Cozzi, *Eur. J. Org. Chem.*, 2007, 2248.

13 Ferrocene ethanol in the presence of acids gives ethers and alkenes derivatives. Sanz has recently reported the formation of these by-products, in the reaction of alcohols promoted by Brønsted acids; see ref. 6i.

14 For "on water" promoted direct coupling of indole with 1,4 benzoquinones, see: H.-B. Zhang, L. Liu, Y.-J. Chen, D. Wang and C.-J. Li, *Eur. J. Org. Chem.*, 2006, 869.

15 K. Aplander, R. Ding, U. M. Lindström, J. Wennerberg and S. Schultz, *Angew. Chem., Int. Ed.*, 2007, **46**, 4543. A detailed study of the addition of nucleophiles to benzylic or allylic alcohols in water in the presence of Lewis acids is under investigation.

16 2,5-Dimethylthiophene, 1,3-$MeOC_6H_4$, $tBuOCONH_2$, allyltin, allylsilane, 4-$MeOC_6H_4NH_2$, Bu_3SnCN, 4-butyn-1-ol, 3-acetylbutanol, 2,4-di*tert*butylphenol, *p*-toluensufonamide, and NaN_3 were tested as nucleophiles in the model reaction with water at 80 °C for 24 h. In these cases only starting material was recovered. No decomposition of the alcohol, oxidation of ferrocene, or formation of ferrocenyl ether take place.

17 *t*–BOC-(L)-cysteine methylester does not react with the alcohol **1** in water at 80 °C.

18 A review about investigations of structural features of metallocene derivatives in which carbenium ion center is connected adjacent to a cyclopentadienyl ring η-bound to a transition metal was recently published; see: R. Gleiter, C. Bleiholder and F. Rominger, *Organometallics*, 2007, **26**, 4850. Structure proposed and calculations suggested stereoselectivity for the nucleophile substitution of α-ferrocenylalkyl derivatives. This topic, well established in ferrocene chemistry, was dealt with Ugi see: (*a*) G. W. Gokel, P. Hoffmann, H. Klusacek, D. Marquarding, E. Ruch and I. Ugi, *Angew. Chem., Int. Ed. Engl.*, 1970, **9**, 64; (*b*) D. Marquarding, H. Klusacek, G. W. Gokel, P. Hoffmann and I. Ugi, *J. Am. Chem. Soc.*, 1970, **92**, 5389; (*c*) G. W. Gokel, D. Marquarding and I. Ugi, *J. Org. Chem.*, 1972, **37**, 3052. For reaction of ferrocenyl acetates and other derivatives for the synthesis of optically active ferrocenyl phosphines, see ref. 11.

19 H. C. Kolb, M. G. Finn and K. B. Sharpless, *Angew. Chem., Int. Ed.*, 2001, **40**, 2004.

20 For recent reviews, see: (*a*) V. Bock, H. Hiemstra and J. H. van Maarseveen, *Eur. J. Org. Chem.*, 2006, 51; (*b*) J. E. Moses and A. D. Moorhouse, *Chem. Soc. Rev.*, 2007, **36**, 1249; (*c*) A. Dondoni, *Chem.–Asian J.*, 2007, **1**, 700. See also: P. G. Cozzi, R. Hilgraf and N. Zimmermann, *Eur. J. Org. Chem.*, 2004, 4095.

21 We have tested in the standard reaction conditions benzylic alcohol, allylic alcohol and 2-naphthylethanol.

22 W. Zhuang and K. A. Jørgensen, *Chem. Commun.*, 2002, 1336.

23 S. Lakhdar, M. Westermaier, F. Terrier, R. Goumont, T. Boubaker, A. R. Ofial and H. Mayr, *J. Org. Chem.*, 2006, **71**, 9088.

24 Y. Jung and R. A. Marcus, *J. Am. Chem. Soc.*, 2007, **129**, 5492.

25 A referee suggested that the weak Lewis acidity of ferrocenyl derivatives (starting materials and products) could play the role of catalysts. We have performed an experiment carrying out the reaction "on water" at 80 °C of 1-hydroxyethyl)ferrocene **1** with indole in the presence ferrocene (3 equivalent), stopping the reaction after 3 h. Unfortunately, in the reaction conditions ferrocene is partially oxidised to the Lewis acidic ferrocinium, that accelerates the reaction with indole; see also ref. 15.

26 Water is an essential component for the reactions. If indole is milled at 25 °C with (*R*)-(1-hydroxyethyl)ferrocene **1**, a reaction takes place immediately, but only the formation of the ether by-product is detected by TLC. If indole (4.5 mmole) is mixed with racemic (1-hydroxyethyl)-ferrocene **1** (4.5 mmole), immediately the two solids melt. If the resulting mixture is stirred at 25 °C for 24 h, only the reaction of ferrocenyl alcohol with itself (35% yield) occurs.

27 For other interesting reactions "on water", see: (*a*) M. C. Pirrung and K. Das Sarma, *J. Am. Chem. Soc.*, 2004, **126**, 444; (*b*) B. K. Price and J. Tour, *J. Am. Chem. Soc.*, 2006, **128**, 12899; (*c*) D. Gonzàles-Cruz, D. Tejedor, P. de Armas and F. Garcia-Telaldo, *Chem.–Eur. J.*, 2007, **13**, 4823.

28 D. R. van Staveren and N. Metzler-Nolte, *Chem. Rev.*, 2004, **104**, 5931.

29 W.-S. Lam, S. H. L. Kok, T. T.-L. Au-Yeung, J. Wu, H.-Y. Cheung, F.-L. Lam, C.-H. Yeung and A. S. C. Chan, *Adv. Synth. Catal.*, 2006, **348**, 370.

30 (*a*) E. J. Corey, R. K. Bakshi and S. Shibata, *J. Am. Chem. Soc.*, 1987, **109**, 7925. For the application of the CBS method to the reduction of ferrocene derivatives, see: (*b*) K. Tappe and P. Knochel, *Tetrahedron: Asymmetry*, 2004, **15**, 91 and references therein.

Methyltrioxorhenium revisited: improving the synthesis for a versatile catalyst

Evangeline Tosh,[a] Josef K. M. Mitterpleininger,[a] Alexandra M. J. Rost,[a] Draganco Veljanovski,[a] Wolfgang A. Herrmann*[a] and Fritz E. Kühn*[b]

Received 15th June 2007, Accepted 3rd September 2007
First published as an Advance Article on the web 11th September 2007
DOI: 10.1039/b709072b

Previously reported synthetic pathways require the use of highly toxic tin containing methylating agents. A more environmentally sound tin free synthetic route to the versatile catalyst MTO has been developed recently, using the principles of green chemistry.

Introduction

Replacement of stoichiometric reagents with catalytic reagents is one of the founding principles of green chemistry.[1] Though catalysts lower the energy of activation, providing a more efficient energetic pathway to a given chemical target without being consumed in the reaction, they are often transition metal complexes, made using toxic and carcinogenic reagents and can require rigorous energy intensive procedures to prepare.

Methyltrioxorhenium (MTO) has been studied extensively in industry and academia due to the numerous reactions it is capable of catalyzing.[2] Previously reported synthetic routes to MTO require the use of tetramethyltin or related derivatives, which are highly toxic.[3–7] Industrial application of MTO is limited by the expensive and complex safety precautions required for synthesis and purification using tetramethyltin as a reagent. Recently an improved synthesis of MTO has been communicated. We herein report the advantages of this synthetic route to MTO, using the principles of green chemistry as a guide, in more detail and describe its potential impact on the applications of MTO.[8]

Results and discussion

The preparation of alkylrhenium(VII) oxides *via* bis(alkyl) zinc precursors has been reported,[9] however in the presence of dimethylzinc, Re_2O_7 and related Re(VII) precursor compounds are easily reduced.[5,9] By substitution of bis(alkyl) zinc precursors with methyl zinc acetate,[10] we have observed a clean methylation, without any reduction of Re(VII) (Fig. 1).

The common synthesis of $CH_3ZnOC(=O)CH_3$ is described below in Equ. 2, Fig 2. Methylzinc acetate can also be synthesized

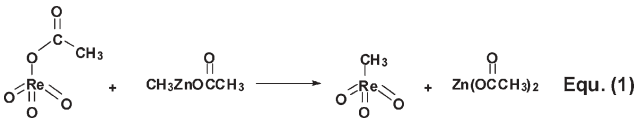

Fig. 1 Synthesis of MTO starting from perrhenylacetate and methylzinc acetate

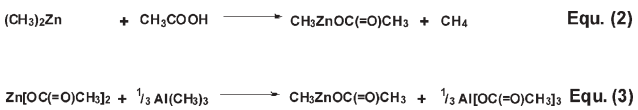

Fig. 2 Synthesis of methylzinc acetate

from inexpensive shelf chemicals (Equ. 3, Fig 2) and zinc acetate, the side product of the MTO synthesis (Equ. 1, Fig. 1).[8] Since the first report on the synthesis of MTO, the total cost of production on a laboratory scale has reduced from *ca.* 834 € g^{-1} for the original synthesis published in 1979 to *ca.* 42 € g^{-1} for the new synthesis of 2007 (Table 1).

The use of $Zn[OC(=O)CH_3]_2$ not only reduces the cost of $CH_3ZnOC(=O)CH_3$ production, but also eliminates the need to employ pyrophoric dimethzlyinc and uses one of the waste products from CH_3ReO_3 as a feed stock, as shown in Fig. 2.

The synthesis, shown below in Scheme 1, proceeds conveniently as follows: Re_2O_7 is dissolved in acetonitrile to form perrhenylacetate upon treatment with acetic anhydride. The methylating reagent is then added slowly at −10 °C. For purification, the resulting solution is separated from the precipitated zinc acetate and the solvent is removed. The product is then extracted with *n*-pentane and sublimated to give pure MTO. This method offers an improved atom economy (*ca.* 46%) compared to the currently

Table 1 Costs for common laboratory scale production of MTO (starting material 10 g Re_2O_7)

Route for MTO synthesis	Price of MTO/€ g^{-1}
$Me_6Re_2O_3$ or Me_3ReO_2 with air[3d]	833.92
Re_2O_7 with Me_4Sn[5]	73.07
$(CF_3CO)_2O$ with Bu_3SnMe[6]	49.69
$Ca(ReO_4)_2$ with Me_4Sn[7]	49.99
$Ag(ReO_4)$ with Me_4Sn[7]	66.90
Using MeZnOAc synthesised from Me_2Zn	46.00
Using MeZnOAc synthesised from $Al(CH_3)_3$	41.75
Using MeZnOAc synthesised from $Al(CH_3)_3$ + recycling of waste $Zn(OAc)_2$	41.71

[a]*Lehrstuhl für Anorganische Chemie, Department für Chemie der Technischen Universität München, Lichtenbergstrasse 4, D-85747, Garching bei München, Germany. E-mail: wolfgang.herrmann@ch.tum.de; Fax: (+49)89-289-13473*
[b]*Molekulare Katalyse, Department für Chemie der Technischen Universität München, Lichtenbergstrasse 4, D-85747, Garching bei München, Germany. E-mail: fritz.kuehn@ch.tum.de; Fax: (+49)89-289-13473*

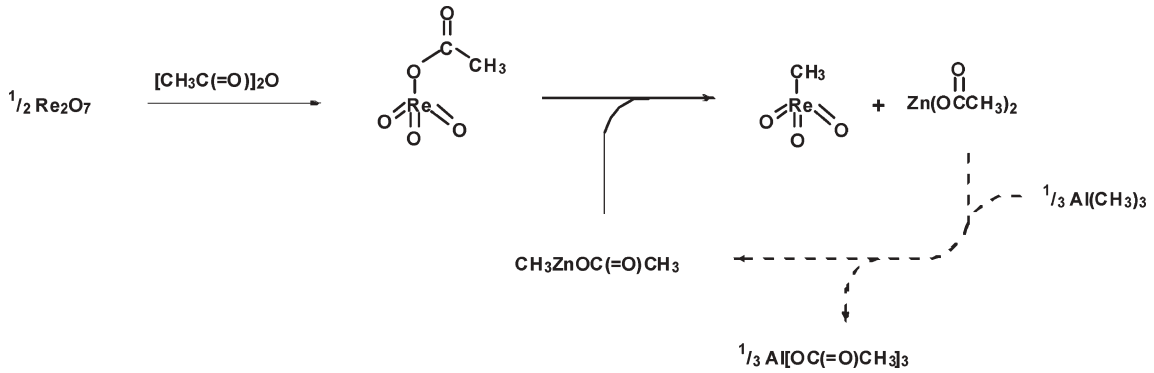

Scheme 1

Table 2 Atom economy by the production of MTO [*M* (MTO)/*M* (waste products) × 100, where *M* is the molecular weight]

Route for MTO synthesis	A.E. (%)
$Me_6Re_2O_3$ or Me_3ReO_2 with air[3d]	49.73
Re_2O_7 with Me_4Sn[5]	37.57
$(CF_3CO)_2O$ with Bu_3SnMe[6]	38.21
$Ca(ReO_4)_2$ with Me_4Sn[7]	43.11
$Ag(ReO_4)$ with Me_4Sn[7]	38.58
Using MeZnOAc synthesised from Me_2Zn	46.09

most widespread lab scale synthesis for the production of MTO (Table 2).

This synthetic method also provides a convenient route to homologues CH_3ReO_3 and $C_2H_5ReO_3$ to give 85% and 60% yields, respectively.

As previously mentioned, the precipitated zinc acetate side product can be recycled. Though direct, *via* $Al(CH_3)_3$, or catalytic, by *in situ* generation of $CH_3ZnOC(=O)CH_3$, alkylation would be ideal as derivatization would be eliminated or reduced, this is not possible due the decomposition of Re oxides in the presence of $Al(CH_3)_3$.

Reaction conditions were optimized to use a minimum amount of solvent and be as close to ambient conditions as possible to reduce the amount of waste generated and energy consumed, respectively. The use of auxillary substances were eliminated entirely in the purification and recovery of CH_3ReO_3, as this complex is isolated by sublimation.

Conclusions

Over the last 20 years significant improvements with respect to efficiency, cost, and environmental friendliness have been made with respect to the synthesis of the extremely versatile catalyst MTO. In particular, the most recent synthesis represents a milestone in the context of the principles of green chemistry. Not only could the use of the hazardous tetramethyltin and related compounds in synthesis be eliminated, but the atom economy of the overall synthesis was also further improved. Nevertheless, many areas for optimization still remain. Further efforts to make the synthesis even more environmentally benign are currently being undertaken in our laboratories, including the substitution of acetonitrile as a reaction solvent and catalyst immobilization to reduce the use of solvents and auxiliary substances in catalyst recovery.

Experimental

Methylzinc acetate, $CH_3ZnOC(=O)CH_3$

Finely ground $Zn[OC(=O)CH_3]_2{\cdot}2H_2O$ (11.1 g, 60.6 mmol) was dried for 3 h at 70 °C. Loss of water was gravimetrically determined and the resultant anhydrous zinc acetate was suspended in 50 mL of dry toluene. The anhydrous zinc acetate toluene solution was cooled to −10 °C, and a solution of 20 mmol $Al(CH_3)_3$ in toluene at −10 °C added dropwise. This resultant solution was kept stirring at −10 °C for 5 h. After filtration and removal of solvent *in vacuo*, methylzinc acetate was obtained as a white solid.

Yield: 80% (6.7 g); ^{1}H-NMR (400 MHz, $CDCl_3$, 25 °C) δ = 2.14 (s, 3H, C–C*H*$_3$), −0.68 (s, 3H, Zn–C*H*$_3$); ^{13}C-NMR (400 MHz, $CDCl_3$, 25 °C) δ = 180.4 (s, *C*=O), −15.2 (s, Zn–*C*H$_3$).

Methyltrioxorhenium(VII), CH_3ReO_3

Re_2O_7 (10 g, 22.0 mmol) was suspended in 50 ml of acetonitrile and one molar equivalent of acetic anhydride was added. The resultant reaction mixture was stirred for 30 min, then two molar equivalents of methylzinc actate were added dropwise. This solution was stirred for an additional 30 min, then, after filtration, the solvent was removed *in vacuo* and the resultant solid was extracted with *n*-pentane and sublimated to give analytically pure CH_3ReO_3. Yield: 85%, NMR values obtained matched previously reported values observed for this complex.[6]

Acknowledgements

The authors are grateful to the Margarethe-Ammon Foundation (Ph.D. Grant for A. R.), the Bayerische Forschungsstiftung (Ph.D. Grant for J. M.), and the NanoCat program of the Elitenetzwerk Bayern (Ph.D. Grant for E. T.). Süd-Chemie AG (Dr R. W. Fischer, Dr. N. Szesni) is acknowledged for helpful discussions and continuous support.

Notes and reference

1 Paul Anastas and John Warner, *Green Chemistry: Theory and Practice*, Oxford University Press, New York, 1998.

2 Pertinent review articles: (*a*) F. E. Kühn, A. M. Santos and M. Abrantes, *Chem. Rev.*, 2006, **106**, 2455; (*b*) C. C. Romão, F. E. Kühn and W. A. Herrmann, *Chem. Rev.*, 1997, **97**, 3197; (*c*) A. M. Santos and F. E. Kühn, in *Homogeneous Multiphase Catalysis*, ed. B. Cornils,

W. A. Herrmann, I. T. Horváth, W. Leitner, S. Mecking, H. Olivier-Bourbigou and D. Vogt, Wiley-VCH, Weinheim, 2005, vol. 2, 807.
3 (*a*) F. E. Kühn, A. Scherbaum and W. A. Herrmann, *J. Organomet. Chem.*, 2004, **689**, 4149; (*b*) F. E. Kühn, A. M. Santos and W. A. Herrmann, *Dalton Trans.*, 2005, 2483; (*c*) W. A. Herrmann and F. E. Kühn, *Acc. Chem. Res.*, 1997, **30**, 169; (*d*) I. R. Beattie and P. J. Jones, *Inorg. Chem.*, 1979, **18**, 2318.
4 (*a*) A. M. J. Rost, W. A. Herrmann and F. E. Kühn, *Tetrahedron Lett.*, 2007, **48**, 1775; (*b*) F. E. Kühn, K. R. Jain and M. Zhou, *Rare Metals*, 2006, **25**, 411.
5 W. A. Herrmann, J. G. Kuchler, J. K. Felixberger, E. Herdtweck and W. Wagner, *Angew. Chem.*, 1988, **100**, 420, (*Angew. Chem., Int. Ed.*, 1988, **27**, 394).
6 W. A. Herrmann, F. E. Kühn, R. W. Fischer, W. R. Thiel and C. C. Romão, *Inorg. Chem.*, 1992, **31**, 4431.
7 W. A. Herrmann, R. M. Kratzer and R. W. Fischer, *Angew. Chem.*, 1997, **109**, 2767, (*Angew. Chem., Int. Ed.*, 1997, **36**, 2652).
8 W. A. Herrmann, A. M. J. Rost, J. K. M. Mitterpleininger, N. Szesni, S. Sturm, R. W. Fischer and F. E. Kühn, *Angew. Chem.*, 2007, DOI: 10.1002/ange.200703017; W. A. Herrmann, A. M. J. Rost, J. K. M. Mitterpleininger, N. Szesni, S. Sturm, R. W. Fischer and F. E. Kühn, *Angew. Chem., Int. Ed.*, 2007, DOI: 10.1002/anie.200703017.
9 (*a*) W. A. Herrmann, C. C. Romão, R. W. Fischer, P. Kiprof and C. Meric de Bellefon, *Angew. Chem.*, 1991, **103**, 183, (*Angew. Chem., Int. Ed.*, 1991, **30**, 185); (*b*) W. A. Herrmann, F. E. Kühn, C. C. Romão, H. Tran Huy, M. Wang, R. W. Fischer, W. Scherer and P. Kiprof, *Chem. Ber.*, 1993, **126**, 45; (*c*) A. M. J. Rost, A. Scherbaum, W. A. Herrmann and F. E. Kühn, *New J. Chem.*, 2006, **30**, 1559.
10 G. E. Coates and D. Ridley, *J. Chem. Soc.*, 1964, 1870.

Synthesis of organo-layered double hydroxides by an environmentally friendly co-hydration route†

H. C. Greenwell,*[a] C. C. Marsden[b] and W. Jones[c]

Received 30th April 2007, Accepted 7th September 2007
First published as an Advance Article on the web 26th September 2007
DOI: 10.1039/b706445d

Environmentally attractive synthetic routes are studied for the synthesis of MgAl-layered double hydroxides (LDHs) incorporating a series of organic dicarboxylate anions. The reaction conditions are systematically explored to ascertain the effect of acid chain length and layer charge (*i.e.* Mg/Al ratio). The materials are characterised by powder X-ray diffraction, scanning electron microscopy, infra-red spectroscopy and thermal methods. The effect of reaction conditions on product purity and the packing arrangement of the intercalated organic molecules is reported, with impurity free organo-LDHs observed at Mg/Al = 2 and increased interlayer packing as Mg/Al approaches 1.

1. Introduction

The increasing use of LDHs as mixed metal oxide catalysts,[1,2] organo-LDH catalysts[3–5] and clay-polymer nano-composites[6–8] has motivated research towards understanding factors that affect the performance and properties of these versatile materials. Structure–property relationships that have been identified as being important include: the morphology of the crystallites, with a high surface area being favourable for catalysts and high aspect ratio favourable for nano-composites, the control of the M^{2+}/M^{3+} ratio and M^{3+} dispersion within the catalysts, and the avoidance of impurity phases during synthesis.[1,2,6] Conceptually, the organization and properties of the anions in the interlayer domain are largely directed by the nature of the inorganic sheets, which has been shown to vary as a function of synthesis method.

The favoured method for the synthesis of LDHs has been the co-precipitation route due, principally, to its simplicity and general application.[9,10] This method, however, has some significant drawbacks. For example, a high excess of the organic anion of interest is required to compensate against inclusion of the counter anion of the metal salts being used. Additionally, in order to prevent contamination by carbonate, which is formed from atmospheric carbon dioxide in the highly basic reaction mixture, an inert atmosphere is frequently required. Furthermore, the reaction mixture must be filtered and washed to remove the water-soluble counter anion salts. As a result supernatants of high basic nature are generated. Anions with high surface/mass to charge ratios, in particular, are not easily intercalated as they do not compete well with the smaller, higher charge density, counter ions of the metal salt used.[11] These factors do not make the method amenable to the large-scale synthesis of organo-LDHs. A further problem, as shown in the work by Traversa *et al.*,[12] is that using the co-precipitation technique and an *R*-value (*i.e.* M^{2+} : M^{3+} ratio) of 0.5 resulted in the formation of gibbsite and a mixed phase. In general it appears to be the case that the co-precipitation method is only effective over a restricted range of *R*-values, between 2 and 4.[1,12] It should be noted, however, that a later paper by Tsuji *et al.* described using a variation of the co-precipitation method to prepare LDH samples with an elevated Al substitution, as high as an *R*-value of 1.1.[13]

Anions of low charge to mass ratio may be taken up into the LDH gallery region using the re-hydration method, which involves re-hydration of a mixed-metal oxide in an aqueous solution of the anion of interest.[14,15] This method however also suffers the disadvantages of the co-precipitation method if it is used to generate the original LDH precursor that is subsequently calcined to generate the intermediate mixed-metal oxide.

In aqueous solution magnesium oxide (MgO) readily re-hydrates to form the corresponding hydroxide, brucite ($Mg(OH)_2$). Similarly, certain polytypes of aluminium oxide undergo alteration in aqueous conditions to form either gibbsite or bayerite ($Al(OH)_3$). In this article the simultaneous co-hydration of the metal oxides in the presence of an organic acid is investigated. It is anticipated that this will provide a synthetic route to organo-LDHs at low temperature, without the need for an inert atmosphere, and without the formation of secondary products.

As long ago as 1980 Mascolo and Marino acknowledged the difficulty of obtaining phase-pure LDHs, and used alumina gel and magnesia as reactants in an attempt to form phase-pure inorganic LDHs.[16] Following on from this work, Pausch *et al.* described the synthesis of Mg/Al LDHs incorporating inorganic anions with a product Mg/Al ratio reportedly approaching 1.[17] The authors observed that the high Al content could not be confirmed by the position of the 110 PXRD reflection as the a_0 parameter reaches a minima at a Mg/Al

[a]*Addison Wheeler Fellow, Department of Chemistry, Durham University, South Road, Durham, UK DH1 3LE. Fax: +44 (0) 1913 844737; Tel: +44 (0) 1913 342100*
[b]*Sidney Sussex College, University of Cambridge, Cambridge, UK CB2 3HU. E-mail: c.c.marsden.02@cantabgold.net; Tel: +45 6084 0554*
[c]*Department of Chemistry, University of Cambridge, Lensfield Road, Cambridge, UK CB2 IEW*

† Electronic supplementary information (ESI) available: Graph to show the effect of *R*-value on the (110) *d*-spacing for 1% w/w slurry. See DOI: 10.1039/b706445d

ratio 2. Further to this Misra and Perrotta used activated magnesia and alumina liquor, formed by the dissolution of aluminium hydroxide in sodium hydroxide (NaOH), to produce LDHs with a Mg/Al ratio reportedly less than 2.[18] Recently, Kelkar and Schutz demonstrated a synthesis based on the reaction of a divalent cation source with peptised pseudo-boehmite.[19] The organic acids, in this case the mono-carboxylates, were used as both the peptising agent and the charge-balancing species. The authors reported significant morphological control using this approach. In summary, variations on the use of oxides to form LDHs have been shown to hold promise with a variety of M^{2+}/M^{3+} ratios and intercalated species reported. In general though, the method has been treated as an extension of, and therefore constrained to conditions of, the co-precipitation method. LDHs with a Mg/Al ratio approaching 1 are of interest as the increased anion exchange capacity (AEC) of these compounds makes them attractive as adsorbents, catalyst precursors and potential nano-composites.[13,20] A high Al atom content is generally not achieved by most methods of LDH synthesis.

In a recent article, Greenwell *et al.* described the synthesis of LDH catalyst presursors where the Al source was an oxide, and the Mg source was the salt of the organic anion—in this particular case acetate. The motivation for the study was to use green chemistry principles to move towards a more environmentally friendly synthesis of LDH solid base catalysts, considering the whole lifecycle of the catalyst and reactions catalysed.[21]

In the work described in this article the question of whether it is possible to make organo-LDH that satisfy the criteria of good purity and homogeneity using the readily available, and economically attractive, oxides of Mg and Al is addressed. A systematic approach is described where the organic molecules used were the di-carboxylic acids of general formula $HO_2C(CH_2)_nCO_2H$, where n was between 1 and 4 inclusive, and initial Mg/Al ratios (R-values) between 1 and 6 were used across a range of slurry concentrations. The reason for this choice of interlayer species is that these acids have been previously reported in the literature as being readily incorporated into LDHs using various methods of synthesis, and are therefore useful for comparison purposes.[22,23]

2. Experimental

The MgO used was from Aldrich, ACS grade of 99% purity. Al_2O_3 was an Alcoa CP3 (grade of 3 microns mean particle size). The purity of the alumina was ascertained to be 5.8% loss on ignition (LOI). The organic acids were obtained from Aldrich (adipic acid and glutaric acid) and from Lancaster (malonic and succinic acid) and were used without further purification.

Slurries of 1.0% weight mixed oxide content were prepared by adding first MgO and then CP3 (total weight of 1.00 g), to give the desired R-value, in 99.00 g of deionised water, which was preheated to 60 °C. The slurry was stirred using a magnetic stirrer whilst maintaining the temperature at 60 °C. After a period of 10 min the pH of the slurry was recorded. The organic dicarboxylic acid was then added to the slurry, in slight excess, to give an Al^{3+} : COO^- molar ratio of 1.2. The reaction vessel was covered to prevent water loss during heating.

After 4 h the slurry was filtered rapidly under vacuum without washing. The product, a white powder, was placed in an oven at 65 °C until no further mass loss was recorded. The pH of the supernatant was recorded. Prior to analysis the products were finely ground manually in an agate pestle and mortar. Powder X-ray diffraction (PXRD) was carried out using a Philips X'pert PW3710 diffractometer with Cu Kα radiation (λ = 1.5418 Å). Patterns were obtained using a 2θ range of 2.00 to 80.00° in 0.02° increments, each held for 20 s. Fourier transform infra-red (FTIR) spectroscopy was carried out on a ThermoNicolet Nexus spectrometer using a smart golden gate single reflection stage attenuated total reflection (ATR), with data recorded as an average of 64 scans between 400 cm^{-1} to 4000 cm^{-1}. CHN elemental analysis was recorded on an Analytical Inc. CE440 instrument. The thermogravimetric analysis (TGA) was performed on a Polymer Laboratories TGA 1500 instrument. The samples were heated from room temperature to 1200 °C at a ramp rate of 30 °C min^{-1} under a nitrogen atmosphere. Scanning electron microscopy (SEM) with coupled energy dispersive spectroscopy (EDS) was carried out on a Jeol 5800 LV instrument using a 15 kV accelerating voltage. The samples were described using the following nomenclature:

MalXRY, SucXRY, GluXRY, AdiXRY

Mal = malonic acid, Suc = succinic acid, Glu = glutaric acid, Adi = adipic acid, X = 1% w/w slurry, RY = R-value (*e.g.*, R2 = reactant Mg/Al ratio of 2)

3. Results and discussion

In this section the results from the experiments are presented and discussed with comparison to previous studies.

3.1 Synthesis of phase pure $Mg_2Al\text{-}^{-}O_2C(CH_2)_nCO_2^{-}$ LDHs

The PXRD patterns for the samples with an R-value of 2 are given in Fig. 1. The patterns are characteristic of organo-LDHs with basal (00l) reflections at low angles of 2θ, due to the layered structure, and "saw-toothed" reflections at higher angles of 2θ, indicating the presence of turbostratic disorder, in the (11l) and (10l) regions. No impurity phase reflections were observed in the PXRD patterns.

The Mg/Al ratio of the product was determined by scanning electron microscopy with coupled energy dispersive spectroscopy (SEM-EDS) analysis (Table 1). It was observed that the product Mg/Al ratio varied from the reactant Mg/Al ratio. The product bulk Mg/Al ratio was in excess of 2, in most cases approximately 70 atom% Mg to 30 atom% Al. This suggests that some Al was not incorporated during synthesis and removed during washing, or that some Al is present as a dispersed amorphous material not observed in the PXRD patterns or areas sampled by the bulk-EDS measurements. Mascolo and Marino, using a similar method, investigated the cation content of the supernatant after filtration and found this to be negligible.[16] Kelkar and Schutz, again using oxides, but with mono-carboxylic acids, used a constant mass approach, where the products were not filtered, but recovered by oven drying.[19] At the Mg/Al R-value of 2 tested the authors

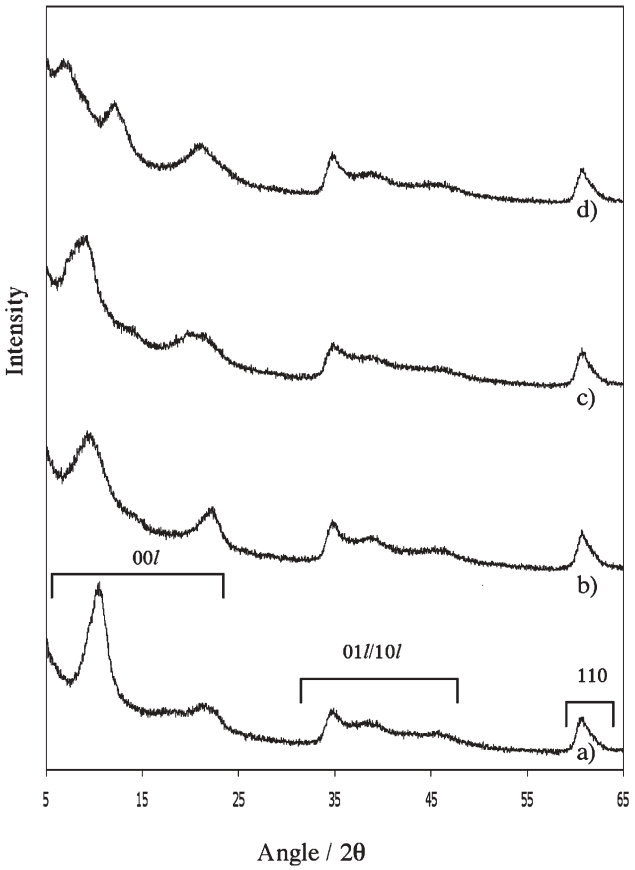

Fig. 1 PXRD patterns for products from 1% w/w slurry at an *R*-value of 2 containing (a) malonate, (b) succinate, (c) glutarate, and (d) adipate anions.

Table 1 Bulk and local (single spot) Mg/Al ratio obtained by SEM-EDS for 1% weight, $R = 2$ samples. Numbers in parenthesis are the deviation about the mean in 3 measurements

Sample	Bulk Mg/Al	Local Mg/Al
Mal1R2	2.27 (0.04)	2.12 (0.45)
Suc1R2	2.16 (0.29)	2.15 (0.12)
Glu1R2	2.03 (0.09)	1.80 (0.26)
Adi1R2	2.21 (0.09)	2.21 (0.11)

did not report any impurity phases, *i.e.* complete conversion to products.

Local EDS analysis of the Glu1R2 sample, Table 1, did reveal some Al rich areas, suggesting Al was present as an amorphous phase.

Sample purity and the intercalation of the acid as the carboxylate anion species was confirmed by FTIR analysis, which showed no adsorption characteristic of brucite (a characteristic OH group stretch at *circa* 3700 cm^{-1}), and did show the expected asymmetric and symmetric R–CO^{2-} group stretches at 1350 to 1400 cm^{-1} and 1550 to 1580 cm^{-1} respectively (Fig. 2). In the case of the longer chain species the C–H stretch adsorption is also observed at approximately 2950 cm^{-1}.

Comparison with the FTIR spectra of the pure acids confirms that the peak position for the carboxylate C=O

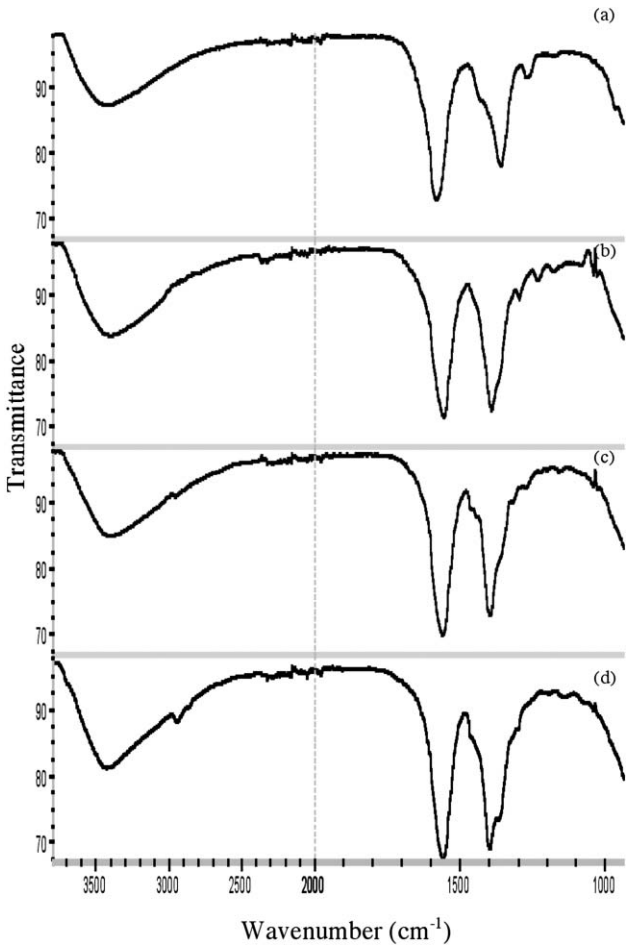

Fig. 2 FTIR spectra for LDH samples with (a) malonate, (b) succinate, (c) glutarate, and (d) adipate. The broad adsorption bands in the spectra at *circa* 3500 cm^{-1} correspond to hydrogen bonding stretching modes between water, interlayer hydroxyls and acid carboxylate groups. Assignments of principal adsorptions are given in Table 2.

stretch has also shifted, indicating a change in the local environment of the acid (Table 2). The shift in position of the carboxylate stretching modes to a lower wave-number, *i.e.* lower energy, can be attributed to an decrease in bond order of the carbonyl group due to dissociation within the interlayer region.

Table 2 Comparison of adsorption bands for the pure carboxylic acid and the carboxylate anion in the LDH gallery

Assignment	Acid	*v* (pure acid)/cm^{-1}	*v* (LDH)/cm^{-1}
C–H stretch	Malonic	2990	—
	Succinic	2931	—
	Glutaric	2953	2960
	Adipic	2950	2947
C=O stretch	Malonic	1694	1580 asym
			1359 sym
	Succinic	1681	1556 asym
			1392 sym
	Glutaric	1682	1561 asym
			1396 sym
	Adipic	1684	1557 asym
			1398 sym

Table 3 Analytical data and possible formulae for $R = 2$ samples

Sample	%H_2O	%C	%H
Mal1R2—analytical data	13.9[a]	5.81[b]	3.46[b]
$[Mg_{2.3}Al(OH)_{6.6}](CO_3)_{0.06}Mal_{0.44}\cdot 2.19H_2O$	13.9	5.85	4.22
$[Mg_{2.3}Al(OH)_{6.6}](OH)_{0.08}Mal_{0.46}\cdot 2.18H_2O$	13.9	5.86	4.27
$[Mg_{2.3}Al(OH)_{6.6}](CO_3)_{0.14}Mal_{0.36}\cdot 0.70H_2O$	5.0	5.79	3.47
$[Mg_{2.3}Al(OH)_{6.6}](OH)_{0.20}Mal_{0.40}\cdot 0.48H_2O$	3.5	5.81	3.48
Suc1R2—analytical data	15.3[a]	7.19[b]	3.68[b]
$[Mg_{2.1}Al(OH)_{6.2}](CO_3)_{0.11}Suc_{0.39}\cdot 2.36H_2O$	15.3	7.21	4.53
$[Mg_{2.1}Al(OH)_{6.2}](OH)_{0.18}Suc_{0.41}\cdot 2.35H_2O$	15.3	5.81	4.28
$[Mg_{2.1}Al(OH)_{6.2}](CO_3)_{0.18}Suc_{0.32}\cdot 0.68H_2O$	5.0	7.20	3.65
$[Mg_{2.1}Al(OH)_{6.2}](OH)_{0.30}Suc_{0.35}\cdot 0.33H_2O$	2.5	7.15	3.67
Glu1R2—analytical data	13.2[a]	8.89[b]	3.87[b]
$[Mg_{2.0}Al(OH)_{6.0}](CO_3)_{0.11}Glu_{0.39}\cdot 2.03H_2O$	13.2	8.92	4.58
$[Mg_{2.0}Al(OH)_{6.0}](OH)_{0.20}Glu_{0.40}\cdot 1.97H_2O$	13.2	8.94	4.70
$[Mg_{2.0}Al(OH)_{6.0}](CO_3)_{0.16}Glu_{0.34}\cdot 0.69H_2O$	5.0	8.94	3.88
$[Mg_{2.0}Al(OH)_{6.0}](OH)_{0.30}Glu_{0.35}\cdot 0.33H_2O$	2.5	8.98	3.90
Adi1R2—analytical data	10.8[a]	10.21[b]	4.08[b]
$[Mg_{2.2}Al(OH)_{6.4}](CO_3)_{0.12}Adi_{0.38}\cdot 1.69H_2O$	10.8	10.23	4.59
$[Mg_{2.2}Al(OH)_{6.4}](OH)_{0.20}Adi_{0.40}\cdot 1.68H_2O$	10.8	10.27	4.73
$[Mg_{2.2}Al(OH)_{6.4}](CO_3)_{0.15}Adi_{0.35}\cdot 0.73H_2O$	5.0	10.32	4.10
$[Mg_{2.2}Al(OH)_{6.4}](OH)_{0.28}Adi_{0.36}\cdot 0.35H_2O$	2.5	10.28	4.09

[a] Analytical data for %H_2O were from TGA. [b] data for %C and %H were from elemental analysis.

Elemental analysis, used in conjunction with TGA, enabled the calculation of possible sample compositions. Table 3 shows the observed sample data and calculated possible compositions for samples. The calculated sample data was determined in two ways: firstly the experimental water content from TGA data was matched; second the observed %H was matched. With these held constant the calculated %C was varied (by inclusion of either carbonate or hydroxide) until the experimental %C was matched. However, using the first method, at the hydration state determined by TGA analysis and with the observed %C matched, the %H in the calculated composition did not agree with the %H determined by elemental analysis. Using the second approach (%H matched), to obtain a calculated composition in agreement with the elemental analysis results hydration states of, or less than, 5% had to be assumed.

A possible reason for the lower calculated water content than determined by TGA arises from the method used for the elemental analysis, where the sample is kept in a stream of pure oxygen gas prior to combustion. It has been observed that, whilst in a stream of dry nitrogen gas at room temperature, samples were observed to adopt a collapsed interlayer phase by PXRD analysis.

The presence of carbonate, though possible due to the high pH of the slurries and the absence of an inert atmosphere, was not confirmed by the PXRD. Had carbonate been present a phase might have been expected with a carbonate interlayer spacing of *circa* 7.7 Å,[24] assuming that a separate phase resulted, rather than inclusion of the carbonate anion within the same gallery as the organic anions. Furthermore, the FTIR spectra did not show the characteristic carbonate C=O stretches at 874 cm^{-1} and 672 cm^{-1},[25] suggesting that the LDHs formed are carbonate free, and if any impurity is present it must be hydroxide, and therefore the calculated compositions for the samples indicate that in addition to the organic anions, some hydroxide is incorporated, or formed, in the interlyaer during co-hydration of the oxides.

In summary, single phase LDHs have been synthesised by the co-hydration of a transition alumina and magnesia, at an *R*-value of 2, in a 1% w/w slurry in the presence of a series of di-carboxylic acids. The reactions were carried out at low temperature, without an inert atmosphere, and resulted in a high degree of anion uptake. Kelkar *et al* also attempted to prepare a malonic acid and glutaric acid intercalated LDH by re-hydration of low reactivity index MgO with pseudo-boehmite at a reactant Mg/Al ratio of 2, but reported only weak LDH reflections with MgO remaining as a by-product.[26]

The results presented here suggest that it is, in fact, possible to produce phase pure organo-LDH at an *R*-value of 2 using this method. The reactivity index (related to the MgO crystallite size) could be an important factor in explaining why the synthesis succeeded using the method described here, as it affects the rate of hydration of MgO.

3.2 Anion arrangement and stability in the intermediate interlayer spacing LDHs

Terephthalic acid can be used as an example of a dicarboxylate–LDH system to describe the possible interlayer arrangements of organo-LDH. In this work we wish to see if similar behaviour is observed for di-carboxylic anions of a less rigid nature than the terephthalate anion.

Fig. 3 illustrates the calculated gallery heights for an expanded interlayer arrangement and the observed gallery heights for the LDH products. The calculated expanded gallery height was obtained by measuring the average inter-carboxylate group O atom to O atom distances from those crystal structures in the Cambridge Crystallographic Data Centre (CCDC) database containing the acid of interest. The observed gallery height was obtained using the (003) reflection of the product and subtracting 4.8 Å to account for the thickness of the inorganic hydroxide layer.

In all cases the observed gallery height is somewhat lower than that calculated for an expanded interlayer arrangement (as shown for succinate in Fig. 4(a)), yet higher than *circa* 3.4 Å expected for a collapsed interlayer arrangement (Fig. 4(b)). No experimental evidence was found to suggest the presence of an interstratified interlayer arrangement. The LDHs were, therefore, observed to have an interlayer arrangement

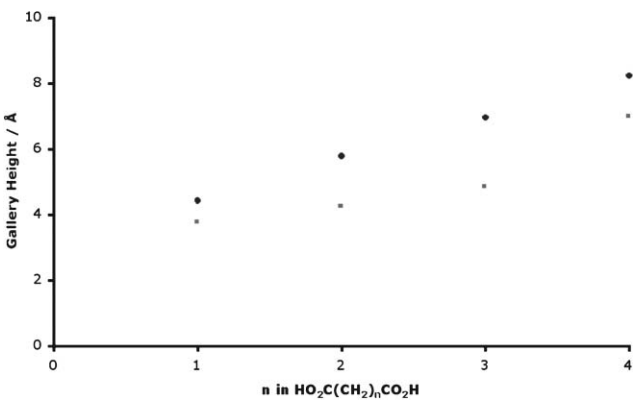

Fig. 3 Graph to illustrate the observed gallery height (■) for 1% weight slurries and *R*-value of 2, compared to the expected gallery height for an expanded interlayer arrangement (●).

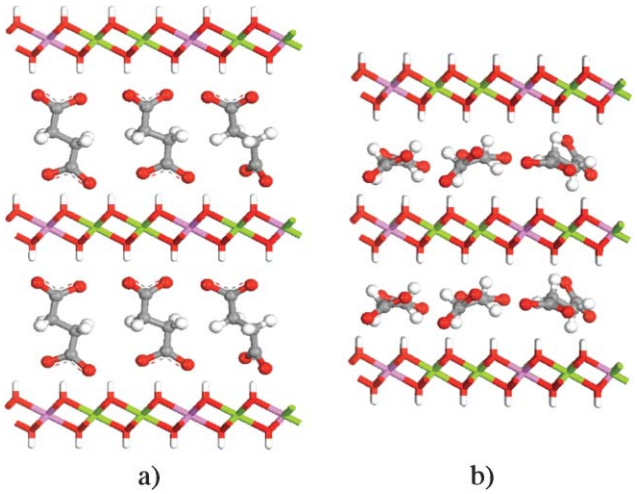

Fig. 4 Schematic to show the interlayer arrangement of, for example, succinate–LDH showing (a) expanded, and (b) collapsed phase. Interlayer water (not shown) and carboxylate groups are arranged adjacent to the hydrophilic LDH sheets, whilst a hydrophobic domain exists in the mid-plane of the interlayer due to the organic chains of the intercalated succinate. The colour scheme is: grey = carbon, white = hydrogen, red = oxygen, green = magnesium, purple = aluminium.

intermediate between that of an expanded and collapsed configuration, due to a particularly stable hydration state, which results in the organic molecules retaining the conformation adopted from the expanded interlayer, but tilted with respect to the plane of the inorganic clay sheets.

The Adi1R2 sample was examined under varying hydration states using a relative humidity cell on a powder X-ray diffractometer. As the humidity was altered a change in interlayer spacing would be expected. This methodology allowed the examination of the influence of humidity, without the influence of temperature and *vice versa*.

The effect upon the initial Adi1R2 sample, at a constant temperature of 25 °C (Fig. 5(a)), of altering the humidity to 0% was an observed reduction in interlayer spacing from 10.98 Å to 7.8 Å (Fig. 5(b)) corresponding to a collapsed interlayer arrangement of the adipate anions. Whilst maintaining the humidity at as close to 0% as possible, the temperature was progressively increased to completely dehydrate the sample.

Upon heating there was little further change in interlayer spacing. The basal LDH reflections showed an increase in relative intensity with increasing temperature (Fig. 5(c) to (g)). This suggested an increase in order within the sample as the sample was heated, possibly due to the loss of further interlayer water, or interlayer molecules adopting a more ordered configuration resulting from thermal motion. The fact that the intermediate-spacing phase collapsed under a dry nitrogen gas flow suggested that the intermediate-spacing phases were principally a result of meta-stable hydration states. The interlayer water in the Adi1R2 sample seemed to be loosely bound, as heating was not required to generate the collapsed state, only a reduction in relative humidity.

3.3 The influence of *R*-value on the formation and structure of the organo-LDHs

The effect of altering the *R*-value in unit increments between 1 and 6, inclusive, upon the position of the (003) reflections and the (110) reflections of the LDH phase products formed are shown in Fig. 6 and Fig. S1†, respectively. Representative PXRD patterns are shown in Fig. 7. From Fig. 6 the intermediate nature of the interlayer spacing in the samples discussed in the previous sections, with an *R*-value of 2, is clearly evident when seen alongside the more obviously

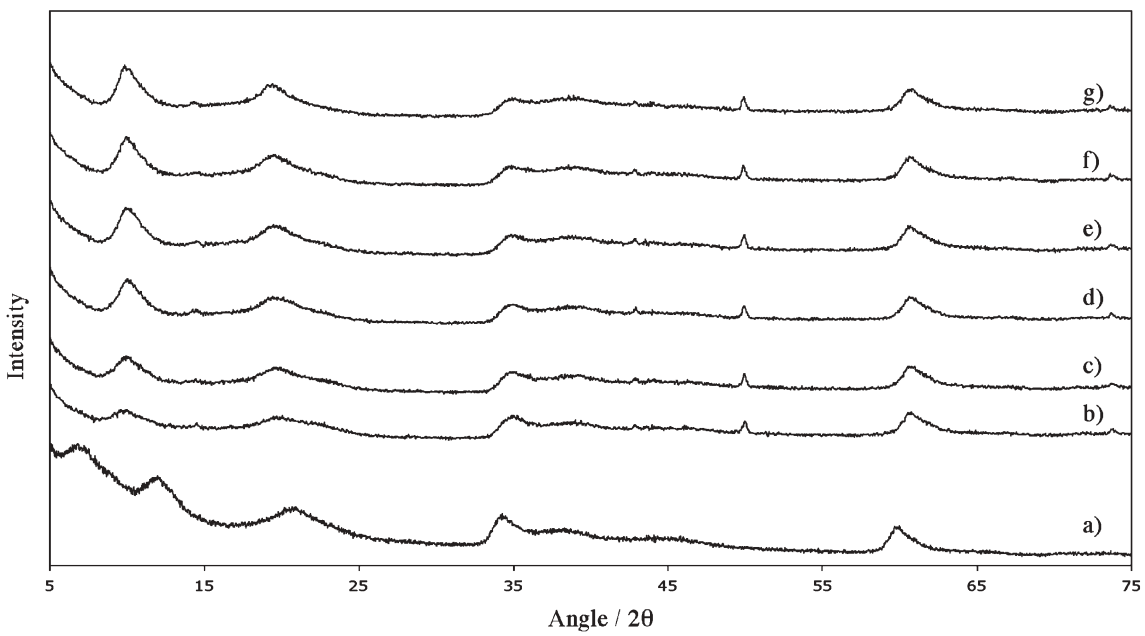

Fig. 5 *In-situ* PXRD patterns for Adi1R2 under atmospheric conditions (a), and at close to 0% humidity (dry N_2) and 25 °C (b), 40 °C (c), 60 °C (d), 80 °C (e), 100 °C (f), and 120 °C (g). The humidity level was set to 0% and each sample equilibrated for 45 min prior to recording the PXRD pattern. * = MgO.

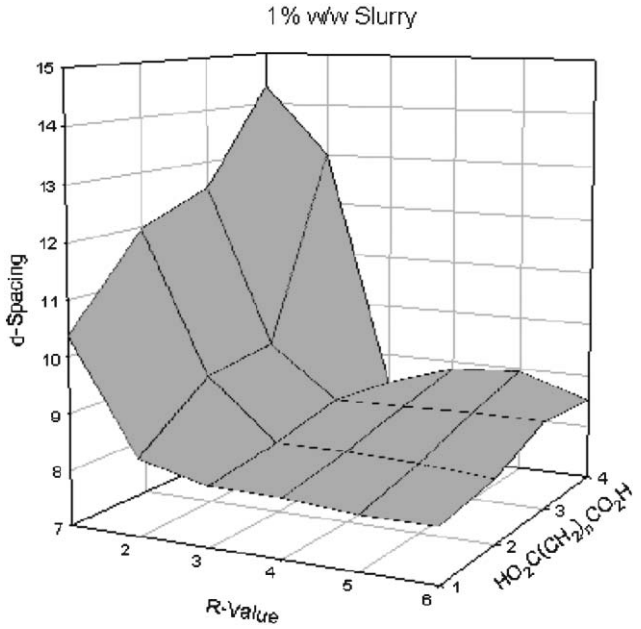

Fig. 6 Graph to show the effect of *R*-value on the position of the (003) reflection for the LDH products with varying acid chain length.

expanded arrangement in the samples with an *R*-value of 1, and the collapsed interlayer spacing in those samples with *R*-values between 3 and 6.

Analysis of the (110) reflections was difficult since the reflections were, in the main, broad and quite possibly comprised of overlapping broad (110) and (113) reflections (Fig. S1, see ESI†). Despite this, it can be seen that in general the average inter-cation distance was at a minimum for the samples with an *R*-value of 1, rising to those samples with an *R*-value of 3, where upon the position of the reflection remained constant. This levelling off at *R*-values greater than 3 will be discussed further in the following sections, and will be shown to be commensurate with the formation of a Mg containing secondary product.

3.4 Homogeneity and interlayer arrangement in $Mg_{1.0}Al$–LDH

MgAl–LDH minerals occur in nature with Mg/Al values of 2 and 3, with MgFe–LDHs sometimes having Mg/Fe values of 4 and 5, but no related mineral exists with M^{2+}/M^{3+} of 1.[27] An Mg/Al value of 1 would necessitate positively charged Al sites to be adjacent to one another, contravening the cation avoidance rule. However, from the PXRD pattern data given in Fig. 7, using this co-hydration synthesis method and after 4 h reaction time it appears that phase pure LDH products with Mg/Al product ratios the same as the reactant Mg/Al ratio (*R*-value), *i.e.* 1, have formed. No reflections were observed that indicated the formation of any bayerite or gibbsite.

Results show (see Fig. S1 in ESI†) that the (110) reflections for the samples with an *R*-value of 1 are shifted to lower *d*-spacings relative to those observed in the corresponding samples with *R*-values of 2, indicating that the average cation–cation distance has decreased. This is in agreement with previously reported results, and is due to an increased M^{3+} content. However, this is the first instance where the homogeneity of the sample Mg/Al ratio has been ascertained using SEM-EDS. For the phase pure (by PXRD) products where the reactant Mg/Al ratio was 1, the bulk analysis, carried out at 500× magnification (area of 2500 $Å^2$), did indeed show an Mg/Al ratio of close to 1, or lower for the Mal1R1 sample (Table 4).

This sort of bulk measurement can be considered as analogous to the results obtained by other techniques such as atomic adsorption spectroscopy (AAS). If an area was selected at 1500 magnification and 3 to 5 selected spots within that area were analysed then the Mg/Al ratio was found to vary considerably, as can be seen in the standard deviation given in Table 4. Some areas were found to be very Al rich relative to the mean value, and others were found to be,

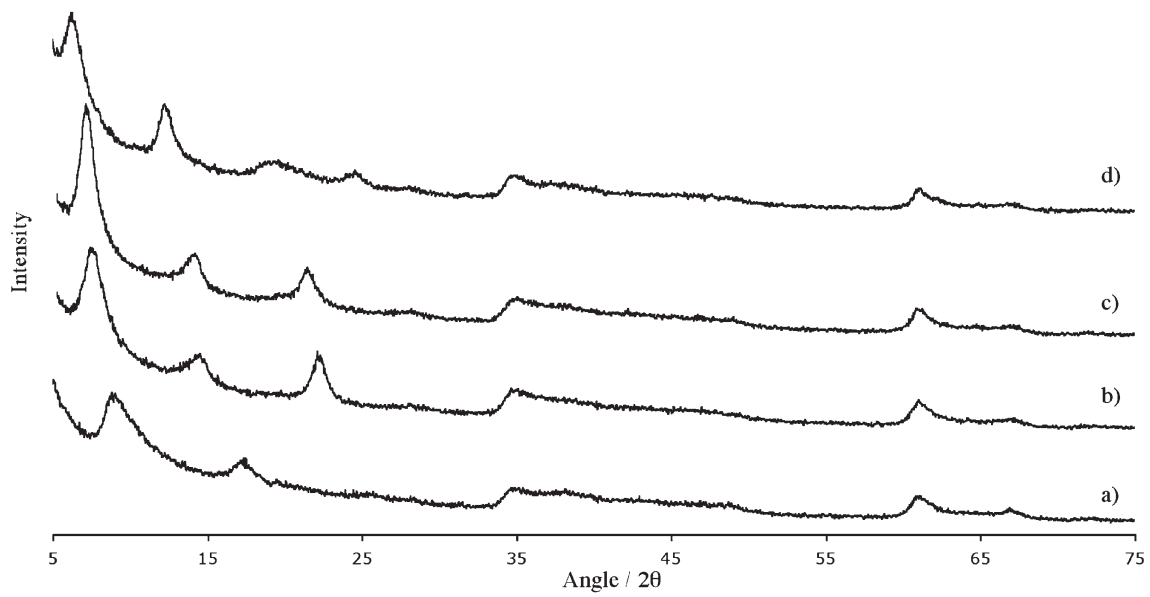

Fig. 7 PXRD patterns for 1% w/w slurry product LDH with *R*-value of 1 for (a) malonate, (b) succinate, (c) glutarate, and (d) adipate anions. Note the absence of any bayerite or gibbsite ($Al(OH)_3$) reflections.

Table 4 SEM-EDS analysis of sample composition for products formed from 1% w/w slurry with *R*-value of 1. Figures in parenthesis are the standard deviations

Sample	Bulk Mg/Al	Local Mg/Al
Mal1R1	0.83 (0.02)	1.05 (0.77)
Suc1R1	1.04 (0.02)	1.23 (0.23)
Glu1R1	0.99 (0.01)	1.23 (0.56)
Adi1R1	0.91 (0.01)	0.84 (0.47)

necessarily, Mg rich. An interesting observation arises in that morphologically different areas were found that had similar Mg/Al ratios, whilst morphologically similar areas sometimes had quite widely varying Mg/Al ratios.

In order to satisfy charge-balancing criteria the anion packing must follow the Al^{3+} site location (this may not quite be accurate as the charge on the layer may not be localized at the Al sites and hydrophobic packing may cause anion aggregation). As the products with an initial Mg/Al ratio (*R*-value) of 1 have the highest interlayer spacing, which reflects the length of the di-carboxylic acids, then the anions must be packed closer than in the samples prepared with an *R*-value of 2 or higher. It can be seen that though the Mg/Al ratio of the $R = 1$ samples varied it still remained below 2 (Table 4). Additionally, the concentration of anion in the $R = 1$ preparations was higher than in the $R = 2$ preparations. These two factors result in the formation of organo-LDHs with *R*-values of between 1 and 2 with a high anion density, resulting in a completely expanded interlayer arrangement. As in the case of the $R = 2$ samples, the Al rich areas in the SEM-EDS analysis contain amorphous alumina, as the PXRD patterns show no reflections other than the LDH.

The stepped increase (alternating between even and odd numbered carbon atom anion chains (Fig. 8)) possibly suggested in the LDH products is not exactly replicated by the crystal structure measurements. The crystal structure measurements from the CSD were taken between the terminal carboxylate oxygen atoms for all conformers of the organic acid/anion, which suggests that the arrangement of the anions within the LDH interlayer may be quite specific, consistent with few conformations of the carboxylate anion and with close packing. The slightly larger gallery height observed in the LDH products is due to the extra length of the bond distance between the carboxylate oxygen atoms and the LDH layer, suggesting that the anions are substantially perpendicular to the inorganic sheet, resulting in a completely expanded interlayer arrangement.

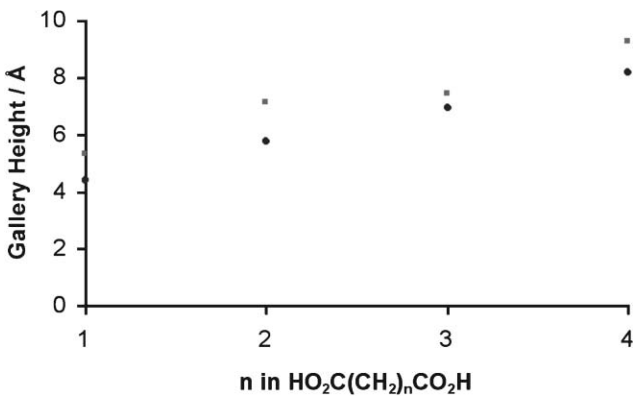

Fig. 8 Graph to illustrate the observed gallery height for the 1% weight slurry samples with an *R*-value of 1 (■) compared to the expected gallery height for an expanded interlayer arrangement based on molecular length from the CSD (●).

3.5 Sample purity in MgAl–LDHs, *R*-values greater than 2

At *R*-values above 2 other products were observed to form in addition to the organo-MgAl–LDH. The identity of these products differed depending on the particular acid. For succinic, glutaric, or adipic acid an additional phase with PXRD reflections at similar positions to brucite ($Mg(OH)_2$), though much broader, was observed (see Fig. 9, for example). In the case of the malonate MgAl–LDH samples, in addition to the organo-LDH product and the poorly crystalline brucite phase, a further phase with PXRD pattern reflections that corresponded to a layered structure, but with a larger *d*-spacing than the LDH, was observed, as well as a phase with reflections corresponding to MgO. The intensity of the non-LDH product reflections increased as the *R*-value was varied from 3 to 6, as shown for the Adi1Rx samples in Fig. 9.

3.6 Composition and interlayer arrangement of the organo-LDH when the *R*-value was 3 or above

The LDHs formed when the *R*-value was 3 or above, for all anions, were found to have approximately the same Mg/Al ratio as determined from the (110) reflections (Fig. 9), which correlates with the increasing quantity of additional, poorly crystalline, $Mg(OH)_2$ phase. Thus the LDH phase is in all cases of similar composition, with the product Mg/Al ratio between 2 and 3, and if the reactant Mg/Al ratio is increased above this commensurately more $Mg(OH)_2$ is formed. This suggests that either the LDH product with an Mg/Al ratio of 2 is the thermodynamically favoured form using the co-hydration method of synthesis, or perhaps that when larger quantities of basic MgO are utilised the higher pH of the slurry results in the $Mg(OH)_2$ phase being favoured.

The interlayer spacing, calculated from the basal reflections in the PXRD patterns, of the MgAl–LDH phases formed when the initial Mg/Al ratio was greater than 2 were found to be similar (Fig. 6 and Fig. 9). The interlayer arrangement, inferred from the calculated gallery height, corresponded to the collapsed (C) configuration as described in Fig. 4(b). The intermediate (I) phase formed at an *R*-value of 2 is clearly evident when compared to the expanded (E) interlayer arrangement at an *R*-value of 1, or the collapsed interlayer arrangement at *R*-values of 3 and above.

Upon closer inspection it was observed that the collapsed interlayer arrangement basal spacing still varied proportionally with anion length (Table 5). The variation was not large enough to be attributed to overlapping of the organic anions, forming a collapsed bilayer as seen in organo-cationic clays, and was considered to be due to the longer carbon atom chain anions having more coiled, bulkier conformations.

The fact that only a seemingly very narrow range of Mg/Al, close to 2, is favoured suggests that the co-hydration method of LDH synthesis might proceed by a different path to the

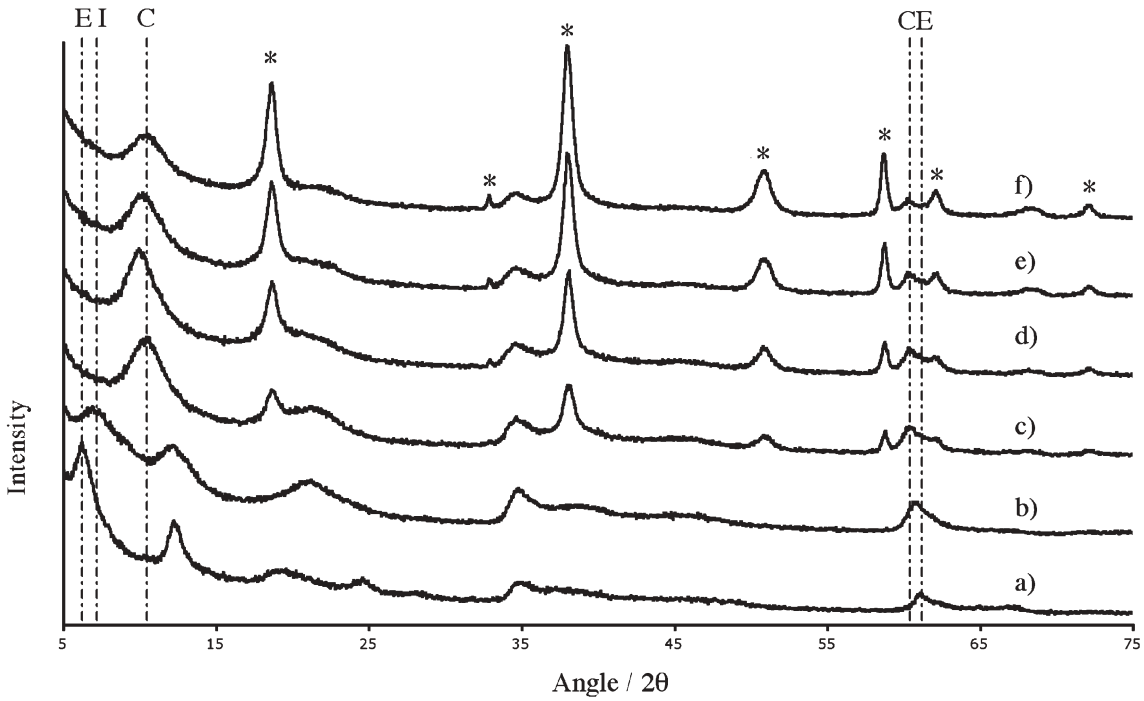

Fig. 9 PXRD patterns for adipate MgAl–LDH samples from 1% w/w slurry with *R*-values of (a) 1, (b) 2, (c) 3, (d) 4, (e) 5, and (f) 6. * Indicates brucite impurity, E = expanded, I = intermediate, and C = collapsed interlayer arrangement. PXRD data collected under atmospheric conditions.

Table 5 Summary of PXRD data for samples from 1% w/w slurry, *R*-value of 5

	d-spacing/Å	
Sample	003 LDH	110 LDH
Mal1R5	7.95	1.53
Suc1R5	8.23	1.54
Glu1R5	8.61	1.53
Adi1R5	8.93	1.54

co-precipitation method, perhaps by an insertion mechanism, rather than a dissolution/precipitation route, though this can not be definitely stated since other factors, such as the pH, may also play an important role in product selectivity.

4 Conclusions

In summary, LDH phases containing organic anions were formed at all the *R*-values tested. The LDHs formed at *R*-values of 1 and 2 were observed to be phase pure by PXRD analysis. However, accurate and full characterisation of the organo-LDHs was difficult, and the absence of impurities in the PXRD pattern of organo-LDHs was not, by itself, sufficient to confirm the samples to be phase pure. Subsequent SEM-EDS analysis showed the samples from an *R*-value of 1 to be heterogeneous, with amorphous alumina present. This has implications for earlier reported preparations of Al rich LDHs, which were deemed pure on the basis of PXRD analysis.

The organic acid used was found to have an effect on the product formed, with the succinate– and adipate–LDHs with an *R*-value of 2 being the most homogenous samples prepared. FTIR spectroscopy proved useful for detecting the presence of brucite and carbonate impurities and confirming that all the organic acid was present as an anion.

At *R*-values in excess of 2 the LDH formed were accompanied by a poorly crystalline brucite phase. A range of LDH interlayer spacings and arrangements were encountered, from expanded at *R*-values of 1, through an intermediate spacing at *R*-value of 2, to a collapsed phase when the *R*-value was 3 or above.

Further work should focus on the use of higher slurry weights, which are more amenable to industry scaled manufacture. Additionally, the effect of reaction time on the products formed and the possible avoidance of by-products will be required. Experiments in which the organic acid is initially used to peptise the Al source may also be examined to enhance product yields/selectivity.

Acknowledgements

We acknowledge the EPSRC, and the Isaac Newton Trust, Cambridge (part funded by Akzo Nobel), for funding of HCG. We also acknowledge the help of Dr D. Vowles, Department of Material Science and Metallurgy, University of Cambridge, with the SEM-EDS analysis.

References

1 F. Cavani, F. Trifiro and A. Vaccari, *Catal. Today*, 1991, **11**, 173.
2 F. Basile and A. Vaccari, in *Layered Double Hydroxides: Present and Future*, ed. V. Rives, NovaScience Publishers Inc., New York, 2001, pp. 285–322.
3 B. M. Choudary, M. L. Kantam, B. Kavita, C. V. Reddy and F. Figueras, *Tetrahedron*, 2000, **56**, 9357.
4 B. M. Choudary, M. L. Kantam and B. Kavita, *J. Mol. Catal. A: Chem.*, 2001, **169**, 193.

5 B. M. Choudary, B. Kavita, N. S. Chowdari, B. Sreedhar and M. L. Kantain, *Catal. Lett.*, 2002, **78**, 373.
6 T. J. Pinnavaia and G. W. Beall, *Polymer–Clay Nanocomposites*, Wiley, New York, 2000.
7 F. Leroux, P. Aranda, J. P. Besse and E. Ruiz-Hitzky, *Eur. J. Inorg. Chem.*, 2003, 1242.
8 H. B. Hsueh and C. Y. Chen, *Polymer*, 2003, **44**, 1151.
9 W. T. Reichle, *Solid State Ionics*, 1986, **22**, 135.
10 S. P. Newman and W. Jones, *New J. Chem.*, 1998, **22**, 105.
11 M. Ogawa and S. Asai, *Chem. Mater.*, 2000, **12**, 3253.
12 E. Traversa, P. Nunziante and G. Chiozzini, *Thermochim. Acta*, 1992, **199**, 25.
13 M. Tsuji, G. Mao, T. Yoshida and Y. Tamaura, *J. Mater. Res.*, 1993, **8**, 1137.
14 T. Sato, T. Wakabayashi and M. Shimada, *Industrial and Engineering Chemistry Product Research and Development*, 1986, **25**, 89.
15 J. Valim, B. M. Kariuki, J. King and W. Jones, *Mol. Cryst. Liq. Cryst.*, 1992, **211**, 271.
16 G. Mascolo and O. Marino, *Mineral. Mag.*, 1980, **43**, 619.
17 I. Pausch, H. H. Lohse, K. Schurmann and R. Allmann, *Clays Clay Miner.*, 1986, **34**, 507.
18 C. Misra and A. J. Perrotta, *Clays Clay Miner.*, 1992, **40**, 145.
19 C. P. Kelkar and A. A. Schutz, *Microporous Mater.*, 1997, **10**, 163.
20 M. Adachi-Pagano, C. Forano and J. P. Besse, *J. Mater. Chem.*, 2003, **13**, 1988.
21 H. C. Greenwell, W. Jones, D. N. Stamirez, M. F. Brady and P. O'Connor, *Green Chem.*, 2006, **8**, 1067.
22 S. Miyata and T. Kumura, *Chem. Lett.*, 1973, 843.
23 E. Narita and T. Yamagishi, in *Proceedings of the 9th International Clay Conference, Strasbourg 1989*; ed. V. C. Farmer and Y. Tardy, *Sci. Geol., Mem.*, Strasbourg, 1990, vol. 86, pp. 145–154.
24 S. P. Newman, PhD thesis, University of Cambridge, 1999.
25 J. T. Kloprogge and R. L. Frost, in *Layered Double Hydroxides: Present and Future*, ed. V. Rives, Nova Science Publishers Inc., New York, 2001, pp. 139–192.
26 C. P. Kelkar, A. Schutz and L. A. Cullo, in *Synthesis of Porous Materials: Zeolites, Clays, and Nanostructures*, ed. M. L. Occelli and H. Kessler, Marcel Dekker Inc., New York, 1997, vol. 69, pp. 691–704.
27 R. V. Gaines, *Dana's new mineralogy: the system of mineralogy of James Dwight Dana and Edward Salisbury Dana*, Wiley, New York, 8th edn, 1997.

Implementing objectives of sustainability into ionic liquids research and development

Dana Kralisch,* Denise Reinhardt* and Günter Kreisel

Received 8th June 2007, Accepted 8th August 2007
First published as an Advance Article on the web 23rd August 2007
DOI: 10.1039/b708721g

This paper proposes the ECO (ecological and economic optimisation) method to accompany and optimise early stage development work in chemical research and development (R&D) regarding the principles of ecological and economic sustainability. The ECO method is a screening tool that uses a simplified life cycle assessment (SLCA) approach, in combination with an optimisation procedure. All life cycle stages from the production of reactants, solvents *etc.*, synthesis and work-up, recycling and disposal are considered within this methodology. They are evaluated regarding three main objectives: the factors for energy demand (*EF*), risks concerning human health and environment (*EHF*) and costs (*CF*). During each process step, a variation of process parameters (*e.g. T*, *t*, *c*, *n* : *n*, solvent, reactant alternatives) will be compared using an outranking algorithm, in order to find the most efficient combinations. At this stage, all objectives will be assessed with respect to an input-benefit ratio. Using this approach, the search for sustainable chemical compounds, synthesis pathways, or processes can already be applied during the R&D stage. This will be demonstrated on the example of ionic liquids, which may have a remarkable potential to improve a wide range of chemical syntheses. Thus, their application may lead to environmental and cost improvements, when compared to commonly used volatile organic solvents. However, the preparation and work-up of ionic liquids are presently not environmentally benign. The application of the ECO method to ionic liquids R&D can help to overcome this problem.

Introduction

Our motivation for developing a new method for environmental impact and cost optimisation of chemical synthesis pathways or processes suitable for the research and development (R&D) stage was the increased academic and industrial interest in ionic liquids. These compounds have strongly gained importance during the last decade. Due to their negligible vapour pressure and non-flammability, ionic liquids are considered as a substitute for commonly used volatile organic solvents. Furthermore, they feature specific solubility properties in mono, bi- and multi-phase reactions. Since ionic liquids are able to dissolve a wide range of organic, inorganic and polymeric materials, they have been investigated as solvents as well as auxiliaries in a great number of organic and organometallic syntheses, *e.g.* Heck reactions, hydrogenations, Diels–Alder reactions, catalytic oxidations *etc.*[1–6] Additionally, ionic liquids are used as solvents for extractions,[7] biocatalytic reactions,[8] asymmetric catalysis[9] as well as electrolytes in electrochemistry.[10]

Until a few years ago, ionic liquids were uncritically referred to in the context of green chemistry.[11,12] Then, results on their partial toxicity, production effort and environmental impact have induced a more differentiated point of view. Nowadays, it is widely accepted that the greenness of ionic liquids heavily depends on their application, toxicological properties and on the environmental impact resulting from the production process. Especially, the last aspect is presently not environmentally benign, and has not been optimised yet.[13]

This raises the question of how synthesis pathways for ionic liquids can be optimised regarding ecological sustainability. In terms of a future applicability of these results, economic as well as ecological aspects should be included in such an optimisation strategy.

For this purpose, special methods for decision support and optimisation are necessary. A number of evaluation methods already exist to assess the environmental impact of (chemical) products or processes. They range from easily calculable metrics, to complex life cycle approaches. Best known and widely approved is the life cycle assessment (LCA) methodology.[14] It is normalised by the International Standard Organisation (ISO) and defined as the "compilation and evaluation of the inputs, outputs and environmental impacts of a product system throughout its life cycle".[15] This holistic approach includes the extraction of resources, the production of all materials, energies used in the product system, the usage through to products recycling, reuse and disposal. During the third step of a LCA, the life cycle impact assessment (LCIA), the calculated mass and energy flows are assigned to different environmental impact categories. Examples are resource depletion, global warming, acidification, human and ecotoxicity potential, as well as land use. Thus, a wide range of actual

Institute for Technical Chemistry and Environmental Chemistry, Friedrich-Schiller-University Jena, Lessingstr. 12, D-07743 Jena, Germany. E-mail: dana.kralisch@uni-jena.de; D.Reinhardt@uni-jena.de; Fax: +49-0361-948402; Tel: +49-3641-948457

environmental problems is covered. Several LCA studies still have been performed in the context of chemical processes (*e.g.* Jödicke,[16] Burgess and Brennan,[17] Hellweg[18]). The results obtained from the LCA methodology are well-founded and comprehensive, but its application is very time-consuming and needs an extensive data-base. The same is valid for the life cycle costing (LCC) methodology, which has been developed to aid more sustainable business practices.[19] However, data and time are limited during the R&D phase. Therefore, LCA/LCC are often not feasible at this stage. Nevertheless, a fundamental change from end of pipe to inherent environmentally benign design strategies can only be realised if the rethinking starts during the stage of R&D. To implement ecological as well as economic criteria into decision-making already at this stage, single or only a few simple metrics are normally used to compare different synthesis pathways, reactants *etc.* Up-stream and down-stream processes are mostly not included into the calculation.

Sheldon was one of the pioneers in the field of ecological assessment of alternative synthesis pathways by metrics. He suggested the E–factor, which characterises the mass of waste produced per unit mass of product.[20] A similar approach is the calculation of mass loss indices (MLI).[21] In this case, the masses of all substances used in a process, are related to the product mass. In addition, metrics related to the environment have been suggested, *e.g.* by Trost,[22] Heinzle and Hungerbühler,[23] Cano-Ruiz and McRae,[24] as well as by Eissen and Metzger.[25] In general, the majority of environment-related metrics are mass-based.[26] Metrics are usually easy to calculate and therefore they are widely used.

The linkage between the complex LCA methodology on the one hand and simple metrics, which cover only parts of the system, on the other hand, can be attained by a simplified LCA (SLCA). SLCA is lower in cost, time and effort to run the assessment,[27] and allows for the exclusion of certain life cycle stages, system inputs/outputs, or impact categories, as well as the use of generic data modules to fill data gaps. SLCA is usually utilised for screening purposes (see *e.g.* Fleischer and Schmidt,[28] Gadasi[29]). Typical screening indicators used in a SLCA are the cumulative energy demand (CED), material intensity per service unit (MIPS)[30] or single impact categories like the global warming potential (GWP).[27] For the incorporation of ecological, and especially toxicological aspects, a semi-quantitative ABC/XYZ-valuation has been suggested by Fleischer and Schmidt.[28] Although the ABC/XYZ-approach is useful for a rough identification of ecological hot spots, a weighting of different effects is not feasible. Alternatively, a quantitative estimation of risks to human health and the environment at an early stage of process design can be realised *e.g.* by the environmental health and safety (EHS) method, developed by Koller *et al.*[31] This method allows for the consideration of environmental, health and safety aspects. A special characteristic of the EHS method is that the so called SHE-effects can be assessed using different data-bases. This facilitates the application already at the R&D stage. The priority of the data-bases is ranked regarding their quality and significance.

Another approach was introduced by Jastorff *et al.*[32] They assessed the sustainability of products or processes by defining risk potentials for humans (toxicophore) and the environment (ecotoxicophore) regarding technical constrains (technicophore). On the example of ionic liquids, they where able to demonstrate that information on resulting risk potentials are already available at the stage of product design. They reason that this can be used to assist the development of green ionic liquids.

Generally, two possible fields to apply evaluation methods during both R&D and the industrial process, or product design stage, have to be differentiated. On the one hand, they can be used to compare several alternatives. This application has already been discussed before. On the other hand, they can be used to directly search for optimal configurations. An example is the waste reduction (WAR) algorithm. It was developed by Young *et al.*[33] to calculate potential environmental impact (PEI) configurations, which are determined by a minimum of resulting waste. If more than one objective is incorporated in the procedure, a multi-objective optimisation problem occurs, and therefore the problem of comparing several alternatives with respect to several objectives arises. This problem configuration is well-known in mathematics,[34] and can be solved using standardised algorithms for identifying pareto–optimal[35] solution candidates. A solution candidate is defined to be pareto-optimal if no objective can be improved without worsening the value of some other objective. In contrast, the so called dominated alternatives can be differentiated, which are worse with respect to any other objective. This definition can be used to identify pareto-optimal alternatives, which then constitute the basis for a total ranking *e.g.* by using the AHP process[36] or by using a partial ranking (outranking) procedure. Partial ranking procedures have the advantage that no compensation of good and bad degrees of performance regarding the objective function takes place. Therefore, no information is lost. Furthermore, indifferent, contradictory and incompletely assessed alternatives can be integrated by outranking procedures. The outranking methods ELECTRE by Roy[37] and the PROMETHEE by Brans *et al.*[38] are world-wide established and frequently used for multi-objective decision support. In both cases, a pair wise comparison of objective values can be performed.

In the context of environmental benign process design, Kheawhom and Hirao[39] proposed an approach combining the optimisation of the metrics: environmental performance and economic performance. This optimisation is based on a synthesis problem as well as a range of objectives and constraints defined beforehand. The calculation of the economic performance is based on the summation of fixed and operational costs. The proceeds are subtracted. The environmental performance depends on the sustainable process index (SPI). The SPI comprises the area which is necessary to implement the process sustainably into the environment. Stefanis *et al.*[40] apply a similar approach. Further work has been done in this context, *e.g.* by Sakizlis *et al.*[41] and Sikdar and Subhas.[42]

Furthermore, Azapagic and Clift[43] dealt with the coupling of multi-objective optimisation and LCA to facilitate the decision-making process. The system under investigation is simultaneously optimised on a number of environmental

objective functions defined and quantified through the LCA approach.[44] Azapagic and Clift[43] integrated economic performance into the optimisation process as well, thus enabling the choice of the best practicable environmental option (BPEO) and the best available technique not entailing excessive cost (BATNEEC). This so-called decision-aid tool-optimum LCA performance (OLCAP) methodology, based on the results of a LCA study as a starting point of the optimisation procedure, refers to a predefined optimisation problem. Sugiyama *et al.* and Alexander *et al.*[45] likewise presented the coupling of LCA and economic evaluation with a multi-objective evaluation to aid process design.

In summary, a wide range of methodologies, which partly overlap as well as supplement each other, still exist in the context of environmental benign process design. However, especially during the R&D stage, the influence of single parameter variations on the objectives under consideration is of great importance to guide future development. At this stage, the analysis of dependencies and proportionalities is much more important for a detailed understanding of the system under investigation than the exact determination of values which may be outperformed during the next step of development. The existing optimisation approaches strongly aggregate to the data-base before and during the optimisation procedure. Thus, a detailed look at single factors is not possible leading to results that cannot clearly be justified. Therefore, the ECO method is herewith proposed, which is based on the well-known approaches in the context of process design discussed above, but which is adjusted to the requirements and limitations during R&D.

The ECO method

Over the last decades the maximisation of yield and selectivity has been the key objectives in chemical R&D. However, due to the increased importance of environmental aspects, new objectives in the context of sustainability have become more and more important during the last couple of years. Additional complexity arises from the fact that some of these objectives may be conflicting. Thus, designing a new synthesis route, work-up procedure *etc.* leads to a highly complex multi-objective decision and optimisation problem, the exact solution of which is not feasible in practice.

For these reasons, a screening procedure based on the ECO method is proposed, which can be used to search for optimal configurations in an iterative process. In order to represent terms of ecological, as well as economic sustainability, three objective functions which incorporate (i) energy demand (*EF*), (ii) risks concerning human health and the environment (*EHF*) and (iii) costs (*CF*), were defined. They have to be minimised during the optimisation process to maximise the benefit regarding ecological and economic sustainability. Then, the decision-making process is guided by an outranking of pareto-optimal solution candidates, referring to these three key objectives.

All of them incorporate the evaluation of the entire process chain. As mentioned above, there is a lack of relevant data concerning preliminary and post processes if simple metrics, such as the E–factor, are used to describe the environmental impacts resulting from a chemical process. Often, consequences of a modification become apparent at a later process step. Otherwise, the environmental burden resulting from the production of a reactant may dominate the overall balance. Against this background, the life cycle approach is essential for a well-founded assessment,[29,46] and is valid for the R&D stage as well. However, the LCA methodology is both too complex, and based on data which are partially not available at the R&D stage. Therefore, the determination of the three objective functions is based on the SLCA approach,[27] extended by economic issues. This will be explained in more detail in the following sections.

In order to limit the extent of the required data-base, for both the evaluation as well as the calculation effort, this approach utilises the local optimisation of single process steps. The selection of preferred parameter values for each single step is resulted. The additional benefit of this approach is that detailed information about dependencies between the different parameters under investigation are provided. In addition, information about deselected parameter values is kept available, in case a rethinking is necessary under specific constraints at a later process step (may be disclosed in further research work). The summation of these results over the entire process chain allows searching for a local optimum regarding ecological and economic sustainability. At the end, a number of preferable parameter configurations are received for each process step.

The key objectives

Important requirements concerning a screening method for the R&D-level includes both an available data-base and its validity and correctness. Considering these requirements, key objectives are developed which comprise a wide range of relevant aspects. Their determination is based on data available already in R&D. At this, the loss of information in comparison to LCA and LCC has been kept as low as possible. They are introduced below.

Energy factor (*EF*)

As mentioned before in the context of the SLCA approach, the CED can be used as an indicator, reflecting most other impact categories of the LCA.[27,28,47,48] This observation also corresponds to our own experiences. The only exceptions constitute the impact categories human and ecotoxicity.[28,49] Thus, the CED was chosen to be one of the objectives considered by the ECO method. With the help of this metric, the variation of the energy demand of different alternatives can be regarded. This also allows for an implicit evaluation of the variations of the impact categories, such as abiotic resource depletion, global warming, stratospheric ozone depletion, tropospheric photooxidant formation, acidification and eutrophication.

The energy factor† *EF* is directly coherent with the CED tailored to the evaluation of chemical synthesis strategies. It is

† This metric is equal to the "energy efficiency factor" [E_{EF}] proposed in Kralisch *et al.* in 2005.[13] We decided to rename this metric to avoid misunderstandings.

defined as the energy demand (E), related to a product-based benefit *e.g.* the product molarity (eqn (1)) or the product mass. E incorporates the cumulative energy demand resulting from (i) the supply of the reactants, solvents and auxiliaries (E^S), (ii) the performance of the reaction (E^R), (iii) the energy demand necessary for the work-up (E^W), (iv) the application of the products (E^A) and (v) the disposal of waste (E^D).

$$EF = \frac{\sum_{i=1}^{x_S} E_i^S + \sum_{i=1}^{x_R} E_i^R + \sum_{i=1}^{x_W} E_i^W + \sum_{i=1}^{x_A} E_i^A + \sum_{i=1}^{x_D} E_i^D}{n_{\text{product}}} \quad (1)$$

Environmental and human health factor (*EHF*)

As mentioned above, the CED cannot be applied in all cases to reflect the impact concerning human and ecotoxicity resulting from alternative chemical processes. Nevertheless, toxicity potentials are important aspects of an environmental benign synthesis pathway. Thus, the identification of potential risks for humans and ecosystems is essential during R&D. Consequently, metrics representing risks regarding human and ecotoxicity resulting from the chemicals used are needed.

One-point models, such as the eco-indicator 99,[50] cannot provide detailed information about the cause of hazards. Furthermore, the assessment of chemical substances is only feasible if the according eco-points already exist. Similarly, the assessment of human and ecotoxicity impacts within the LCA methodology can be problematic. Extensive data gaps can occur when newly developed synthetic pathways (with unknown disposal strategies) or novel chemicals (without defined characterisation factors) are evaluated.

In contrast, the EHS method developed by Koller *et al.*[31] is a suitable approach to assess risks resulting from the handling of chemicals. It facilitates the estimation of the risks at an early stage of process design. The methodology incorporates eleven categories ranging from environmental over health to safety risks. Despite the significance of each of the eleven proposed categories, the complexity of simultaneously optimising all of these is immense. Hence, an assortment of suitable categories, especially concerning the LCA impact potentials for human and ecotoxicity, has been made. For an adequate representation, the SHE categories acute toxicity (AcT), chronic toxicity (ChT) and water-mediated effects (WmE), have been selected. According to Koller *et al.*[31] the risk potentials can be estimated by calculating the remaining potential of danger ($RPoD_{ij}$).

Thus, the second criterion is defined as the environmental and human health factor (*EHF*). The *EHF* allows a comparison of different chemical substances used, *e.g.* as reactants, solvents or auxiliaries regarding the resulting risks for humans and the environment during (i) their supply ($RPoD^S$), (ii) product synthesis ($RPoD^R$), (iii) product work-up ($RPoD^W$), (iv) product application ($RPoD^A$) and (v) disposal ($RPoD^D$). *EHF* sums up the $RPoD_{ij}$, calculated according to Koller *et al.*,[31] and relates this input to the molarity (or mass) of the product (eqn (2)). The *EHF* is divided into three sub-objectives: *EHF*(AcT), *EHF*(ChT) and *EHF*(WmE), referring to the categories acute toxicity, chronic toxicity and water-mediated effects, respectively. Their calculation is demonstrated using the example of *EHF*(AcT) in eqn (2). With the aid of *EHF*, the development of toxicologically benign chemical processes can be facilitated.

$$EHF(\text{AcT}) = \frac{\sum_{i=1}^{x_S} RPoD(\text{AcT})_i^S + \sum_{i=1}^{x_R} RPoD(\text{AcT})_i^R}{n_{\text{product}}} + \frac{\sum_{i=1}^{x_W} RPoD(\text{AcT})_i^W + \sum_{i=1}^{x_A} RPoD(\text{AcT})_i^A + \sum_{i=1}^{x_D} RPoD(\text{AcT})_i^D}{n_{\text{product}}} \quad (2)$$

Cost factor (*CF*)

Ecological advantageous alternatives will only be adopted into industrial processes if they are economically competitive. Hence, the third criterion of the ECO method is defined as the cost factor *CF*.

The calculation is similar to current approaches of LCC analyses, again tailored to the evaluation of chemical synthesis strategies. *CF* includes (i) the costs of the supply of reactants, solvents and auxiliaries (C^S); (ii) costs resulting from synthesis (C^R), (iii) work-up (C^W), (iv) application (C^A) and (v) disposal (C^D). Again, this effort is related to the molarity (or mass) of the product (eqn (3)).

$$CF = \frac{\sum_{i=1}^{x_S} C_i^S + \sum_{i=1}^{x_R} C_i^R + \sum_{i=1}^{x_W} C_i^W + \sum_{i=1}^{x_A} C_i^A + \sum_{i=1}^{x_D} C_i^D}{n_{\text{product}}} \quad (3)$$

Although personnel costs are neither facile to standardise in R&D, nor transferable to later production processes, it was decided to take them into account, since they point out work-intensive process steps.

When comparing different process techniques, costs resulting from equipment, devices *etc.* have to be considered as well. They can be determined by their acquisition costs and lifetime.

The evaluation and optimisation procedure

The evaluation is carried out in close collaboration with an expert on the particular field of R&D or by the researcher himself. At the beginning, a preselection of optimisation parameters and a range of parameter variations is made, which at this point rarely represents a starting configuration, and can be varied by considering actual results at any time.

After the starting configuration has been specified, the experiments required to characterise the system are performed. Parallel to this, freely accessible or commercial data-bases are explored in inventory data-bases (*e.g.* ecoinvent data-base by Frischknecht *et al.*,[51] SimaPro 7[52] or PROBAS[53]) for energy issues, from safety data sheets[54] or from software tools like EPIWIN v.3.11[55] for toxicological criteria and from market prices for cost issues. Having the experimental data resulting from a parameter variation on hand, the calculation of the sustainability factors can be executed. Finally, the values of all factors are collected in a performance matrix (Fig. 1). This performance matrix constitutes the basis of optimisation. Its compilation is an iterative process and it may change significantly during the optimisation process. The ranking of alternatives is executed using a partial ranking procedure.

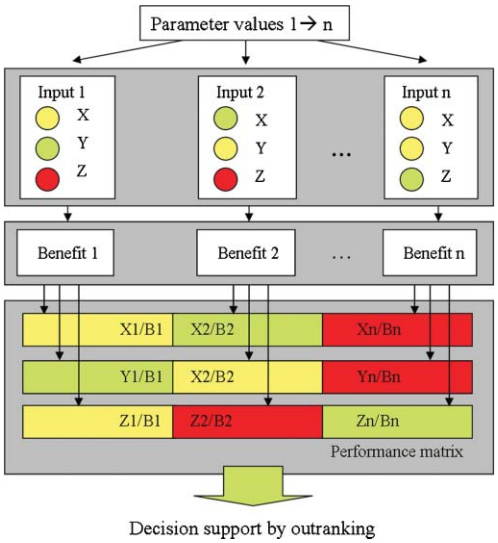

Fig. 1 Creating the performance matrix.

As discussed above, partial ranking algorithms should be preferred to total ranking algorithms. The decision between the PROMETHEE[37] and the ELECTRE[38] method fell on the former, since it features less complex calculation instructions. Partial ranking by means of the PROMETHEE method is realised by using *e.g.* the software Decision Lab 2000.[56] This decision support tool allows for the partial ranking of the parameter alternatives under investigation according to the three key objectives *EF*, *EHF* and *CF*. Thus, unfavourable (dominated) alternatives can be excluded in ongoing research work to restrict the experimental effort.

One advantage all multi-objective optimisation procedures have in common is that they do not require an *a priori* articulation of preferences. Thus, the whole set of pareto-optimal solutions can be explored by changing the preferences. The emphasis is to range the choices from a set of pareto-optimal solutions, rather than to define the preferences explicitly before analysing the alternative trade-offs. Thus, this approach shows explicitly what can be gained and lost by choosing each alternative.[44] This is necessary to understand the relationship between the levels of trade-off required.[45] Therefore, freely selectable weighting factors can be assigned to each of the objectives *EF*, *EHF* and *CF*. By this means, scenarios that reflect different decision preferences can be considered. With the help of this procedure, the expert gains insight into the interrelationship between single determining factors of the decision problem.

Optimisation of the entire process

The optimisation step discussed above results in a range of parameter values referring to a chemical compound, a synthesis pathway, a work-up procedure, or another process which is optimised regarding the objective functions, leading to new insights, which can be used to further optimise and/or identify new areas of process/product development. If this procedure is executed along the process chain, a local optimisation of the entire process regarding ecological and economic sustainability can be approximated (Fig. 2).

The ECO method provides the possibility for re-orientation at any step of the process. Based on the results of the assessment of the variation of one parameter, trends can often be detected. Therefore, both the search for new parameter values, and the selection of unsuitable parameter values can be initiated. In order to limit the time and costs for accessing experimental data, a screening on the basis of selected parameter values with a high degree of information is executed. If a comparatively high optimisation potential is detected for a specific parameter, the number of tests will be increased at this point. Besides, in some cases it can be useful to carry out an up-stream balancing, *e.g.* if the applicability or functionality of different compounds referring to a specific application task has to be tested first. Starting with a selection of the most suitable compounds, the optimisation of their synthesis and work-up procedures takes place subsequently.

In the case of data uncertainties or existing gaps, an assessment by means of similar parameter characteristics can be executed. Should this be impossible, the worst case is assumed. This happens against the background that incalculable environmental impacts, toxicological risks or costs should be pointed out. Therefore, the assumption has to be marked.

Thus, the ECO method can be seen as an instrument for decision support and optimisation in the context of an application oriented chemical R&D. It allows for an unbiased development of environmentally benign and cost-optimised synthesis pathways, work-up procedures, processes or functionalities of chemical compounds. Last but not least, the decision-making process remains with the expert of the specific R&D field, because the selection of parameter values and the weighting of the objectives require special expertise. An intense interaction between researcher and balancer is therefore an essential requirement of the proposed method.

The presented approach is not suited to provide specific values describing *e.g.* environmental impacts or costs. This is because the underlying concept of relative evaluations of a broad range of parameter variations is based on small scale preparation and simple determination methods. Nevertheless, the results allow for the detection of sensitive parameters and of hot-spots along the entire life cycle chain. In order to quantify the progress in ecological and economic sustainability achievable by the newly designed product or process, the reliability of the results needs to be proven by a detailed LCA/LCC analysis following the optimisation process.

The application of the ECO method is demonstrated below on the example of an ionic liquid synthesis.

Implementation of the ECO method into the ionic liquids R&D

The synthesis of ionic liquids is usually carried out in a two-step pathway. The first step, the alkylation of a N-, P- or S-containing organic compound, *e.g.* *N*-methylimidazole, pyridine, alkyl phosphonates or sulfonates, is followed by an anion exchange (Scheme 1). Both steps, particularly the alkylation step, involve energy and time consuming synthesis and work-up procedures. Especially, the work-up (extraction) often requires a high input of organic solvents, resulting in energy consuming distillation steps.

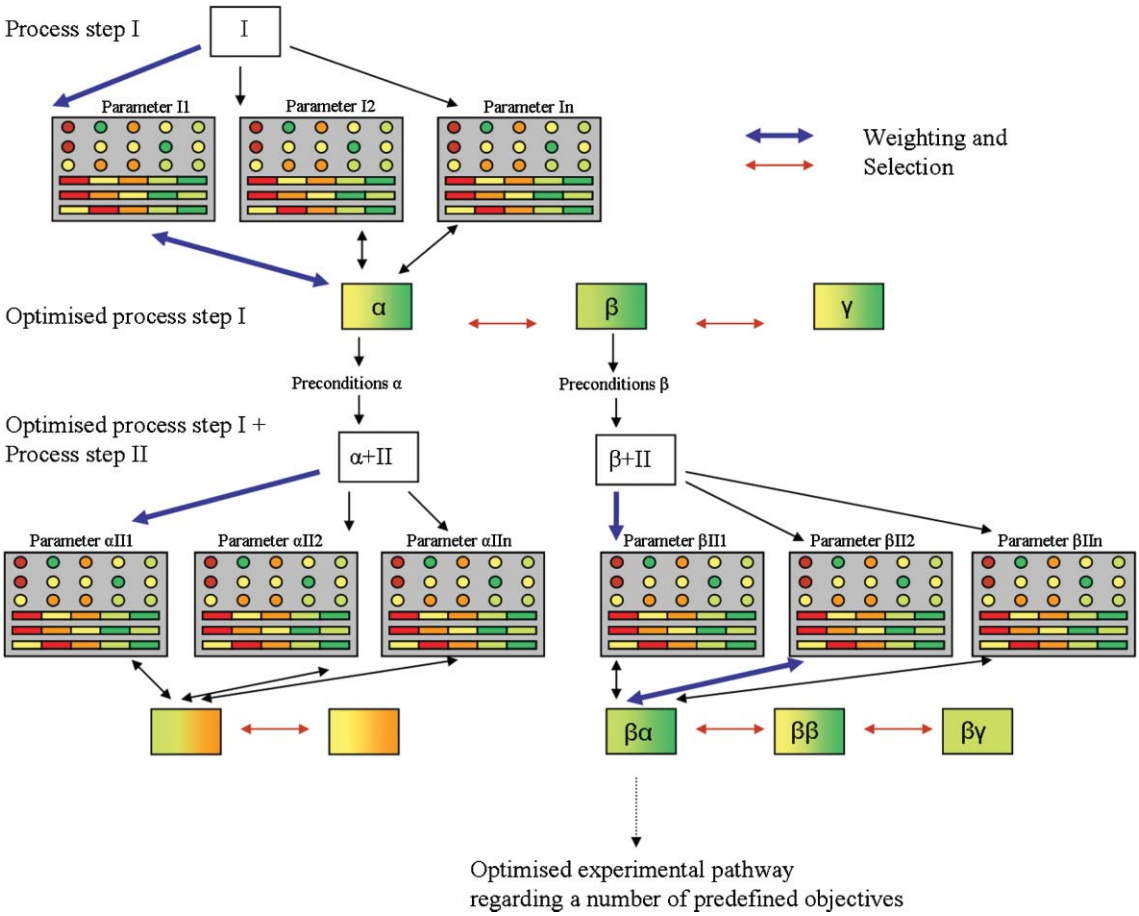

Fig. 2 Optimisation of the entire process regarding the objective function.

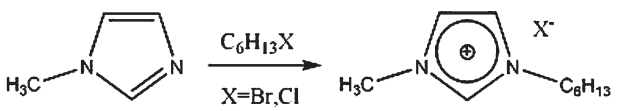

Scheme 1 Preparation of *N*-methylimidazolium based ionic liquids, alkylation step.

To pursue the development of environmentally benign synthesis routes for ionic liquids, the alkylation step (Menschutkin reaction) was first looked into. As representative experiment, the preparation of the ionic liquid 1–hexyl-3-methylimidazolium chloride ([C_6MIM]Cl) was chosen. The process parameters: temperature (*T*), solvent, concentration (*c*), molar ratio (*n* : *n*) and reaction time (*t*) were investigated. In addition, the *N*-base was altered in order to prove the transferability of the reaction parameters. The experimental setup is described below.

Experimental

All syntheses were performed in a 250 mL round bottom flask, fitted with a reflux condenser. 17.24 g (0.21 mol) of *N*-methylimidazole, *n*-hexylchloride (1.2.–1.6 equivalents) and a solvent (ethanol, xylene, cyclohexane, *n*-heptane) were combined to give a 1.6 M or 3 M concentration of *N*-methylimidazole in the reaction mixture. The stirred mixture was heated up to reaction temperature (70–100 °C), allowed to stir for 30–144 h and cooled down to room-temperature.

The work-up of the reaction mixture was carried out by decanting or distilling the solvent and by extracting reactants from the product. The extraction procedure was carried out by dissolving the crude reaction mixture in water, followed by an extraction of the remaining *N*-methylimidazole content with diethyl ether. Here, the amount of extraction solvent required to purify the product to more than 98% [C_6MIM]Cl correlates linearly with the *N*-methylimidazole content. The yield was determined after removal of all volatiles *in vacuo* (rotary evaporator, water bath $T = 80$ °C, $t = 1.5$ h, $p = 10$ mbar). The purity was checked by ^{1}H-NMR-spectroscopy and the water content by Karl Fischer titration.

In the case of solvent-free experiments, 17.24 g (0.21 mol) of *N*–methylimidazole were combined with different amounts of *n*-hexyl chloride (0.1–0.8 mol).

In the case of the synthesis of *N*-hexylpyridinium chloride, 16.61 g (0.21 mol) of pyridine reacted with 25.32 g (0.21 mol) of *n*-hexyl chloride. The work-up procedure was the same as mentioned above.

A comprehensive overview of the parameter variations performed in this context is given in Table 1. All experiments were performed as duplicates.

The energy demand for heating and stirring were determined using an energy monitoring socket (Energy Monitor 3000,

Table 1 Alkylation of *N*-methylimidazole (MIM) or pyridine (PYR), variation of $n : n$, T, t, solvent and c

Exp. number	*N*-base	$n_{N\text{-base}}$/mol	$n_{N\text{-base}} : n_{C6H13Cl}$	T/°C	t/h	Solvent	$c_{N\text{-base}}$/mol L^{-1}	Conversion (%)
1	MIM	0.21	1 : 1	70	10	—	4.6	18
2	MIM	0.21	1 : 1	70	19	—	4.6	35
3	MIM	0.21	1 : 1	70	27	—	4.6	46
4	MIM	0.21	1 : 1	70	72	—	4.6	78
5	MIM	0.21	1 : 1	70	144	—	4.6	87
6	MIM	0.21	1 : 0.5	80	30	—	6.7	50
7	MIM	0.21	1 : 0.8	80	30	—	5.3	74
8	MIM	0.21	1 : 1	80	30	—	4.6	77
9	MIM	0.21	1 : 1.6	80	30	—	3.3	73
10	MIM	0.21	1 : 3	80	30	—	2.0	52
11	MIM	0.21	1 : 4	80	30	—	1.6	40
12	MIM	0.21	1 : 1	70	30	—	4.6	49
13	MIM	0.21	1 : 1	90	30	—	4.6	94
14	MIM	0.21	1 : 1	100	30	—	4.6	98
15	MIM	0.21	1 : 1.6	80	30	xylene	1.6	16
16	MIM	0.21	1 : 1.6	80	30	cyclohexane	1.6	20
17	MIM	0.21	1 : 1.6	80	30	*n*-heptane	1.6	27
18	MIM	0.21	1 : 1.6	80	30	ethanol	1.6	25
19	MIM	0.21	1 : 1.6	80	30	ethanol	3.0	61
20	MIM	0.21	1 : 1.6	80	30	—	3.3	73
21	MIM	0.21	1 : 1.2	80	30	*n*-heptane	3.0	46
22	PYR	0.21	1 : 1	80	30	—	4.6	4

Voltcraft), and the round bottom flask was heated up to reaction temperature using a conventional oil bath.

The work-up by distillation, as well as the recycling of solvents, were carried out using a rotary evaporator fitted with a water-bath, by placing 500 g of the respective solvent in a 1000 mL round bottom flask. For ethanol, *n*-heptane, xylene and cyclohexane a temperature setting of T = 65 °C was chosen. Water and diethyl ether were distilled at T = 80 °C and T = 40 °C, respectively. The pressure decay was adjusted to the boiling point of the solvent. The electrical current necessary to run the vacuum pump, to heat the water-bath and for condensation (cryostat) was measured using an energy monitoring socket.

In all cases, a recycling and refeeding of 90% of all solvents used for syntheses and work-up was assumed.

Evaluation

The experimental work was accompanied by the application of the ECO method, in order to identify relevant variables regarding the objectives *EF*, *EHF* and *CF*. Since the experimental portfolio is very extensive, it can be used to demonstrate the proposed approach by means of some examples.

Evaluation of the energy factor (*EF*)

The *EF* was determined using the life cycle assessment software Umberto,[57] which allows for the assembly and structuring of material- and energy-flow systems. Thus, complex correlations can be mapped out and individual aspects can be analysed. The software also incorporates the data-base Ecoinvent,[51] which contains literature references as well as a pool of data on the supply of organic and inorganic chemicals, electrical energy, inert gases, *etc.*, starting from their primary sources. Some data is also available free of charge, for instance from ref. 53. If the data was not available, the energy demand for the supply of structurally similar compounds, that were available from the data-bases, was used as a first approximation.

In the case of experiments 1 to 5, the value of *EF* was investigated regarding the influence of the reaction time. As shown for the alkylation step at T = 70 °C (Fig. 3), the reaction becomes more effective concerning energy demand when the reaction time increases, however, at a certain point the required energy input exceeds the benefit. Thus, the rate of the yield is not the only performance criterion, although the demand of reactants decreases during the reaction time by a further yield increase.

In addition, the influence of the molar ratio of the educts on the resulting yield and energy demand was tested (exp. no. 6–11). Starting at $n : n$ = 1 : 1, an increase of the molar ratio of *n*-hexyl chloride results in an increasing *EF*. An equimolar reactant ratio (1 : 1) seems to be best regarding the conversion of *N*–methylimidazole, since the *EF* increases consequently at molar ratios lower than 1 (Fig. 4). This corresponds with results obtained by Kaerkkaeinen *et al.*,[58] who have investigated the microwave assisted reaction to [C_4MIM]Cl.

Furthermore, the parameter T has a significant effect on the objective *EF*. This fact becomes clear when comparing the experiments conducted at T = 70 °C and at T = 80 °C, as

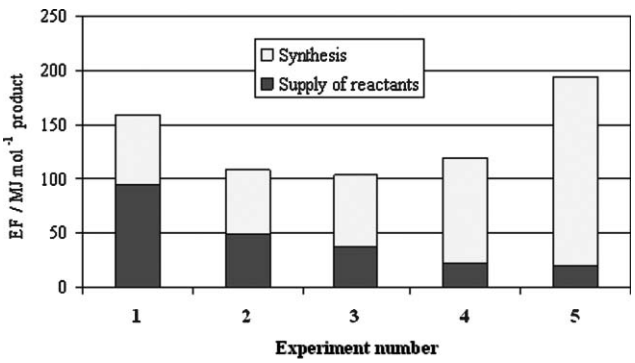

Fig. 3 Time dependence of *EF*, t = 10, 19, 27, 72, 144 h, $n_{MIM} : n_{C6H13Cl}$ = 1 : 1, T = 70 °C, see exp. no. 1–5 in Table 1.

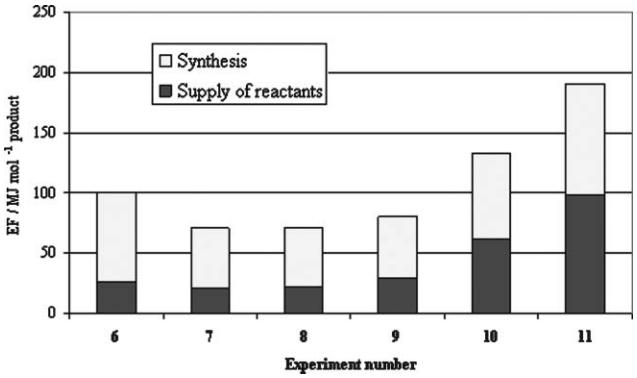

Fig. 4 Dependence of *EF* regarding n_{MIM} : $n_{C6H13Cl}$ = 1 : 0.5, 1 : 0.8, 1 : 1, 1 : 1.6, 1 : 3, 1 : 4, T = 80 °C, t = 30 h, see exp. no. 6–11 in Table 1.

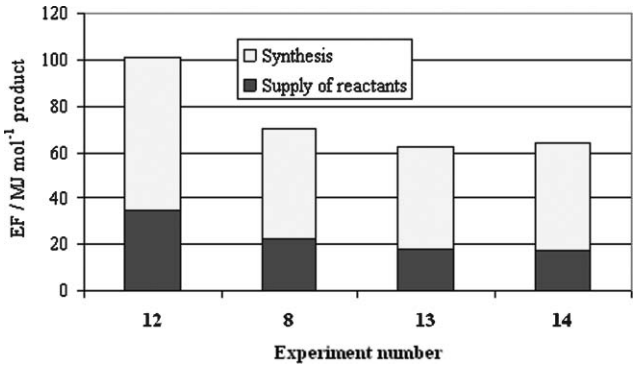

Fig. 5 Temperature dependence of *EF*, T = 70, 80, 90, 100 °C, n_{MIM} : $n_{C6H13Cl}$ = 1 : 1, t = 30 h, see exp. no. 8, 12–14 in Table 1.

discussed above. Therefore, the investigations were extended to T = 90 °C and T = 100 °C (Fig. 5). The yield increases with increasing reaction temperature; however, this tendency is limited by decomposition. The purity of the products was not influenced under the given reaction conditions, since no colour changes or additional impurities could be observed.

In the case of the temperature variation experiments, the *EF* increases similarly to the yield. However, the differences in yield when performing the reaction at T = 90 °C and T = 100 °C are marginal, so that the energy input required at higher temperatures (T > 100 °C) exceeds the benefit.

Integrating the work-up procedure, which has not been optimised yet, *EF* is mainly influenced by the supply of the solvent for extraction and its recycling (Fig. 6). In this case and for the actual state of development, the efficiency of the work-up procedure seems to be an essential performance criterion for the supply of pure [C_6MIM]Cl.

Evaluation of the environmental and human health factor (*EHF*)

As mentioned before, *EHF* is determined using the EHS-method suggested by Koller *et al.*[31] The mobility, acute and chronic toxicity, as well as environmental effects, such as degradation, accumulation and water-mediated effects of reactants, solvents and auxiliaries were included. The evaluation is based on *EC* classification, R-codes, EC50, LD50, log k_{OW} *etc.* available *e.g.* from safety data sheets[54] or from modelling software.[55]

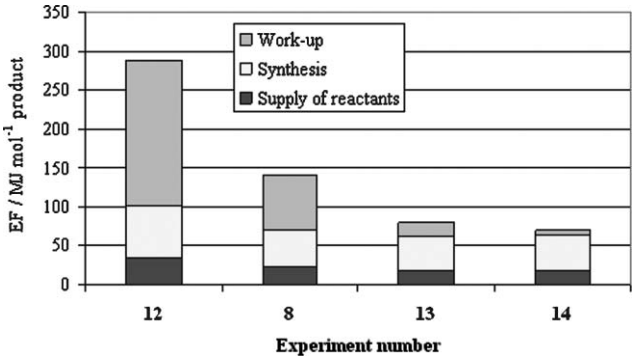

Fig. 6 Temperature dependence of *EF*, T = 70, 80, 90, 100 °C, n_{MIM} : $n_{C6H13Cl}$ = 1 : 1, t = 30 h , consideration of work-up, see exp. no. 8, 12–14 in Table 1

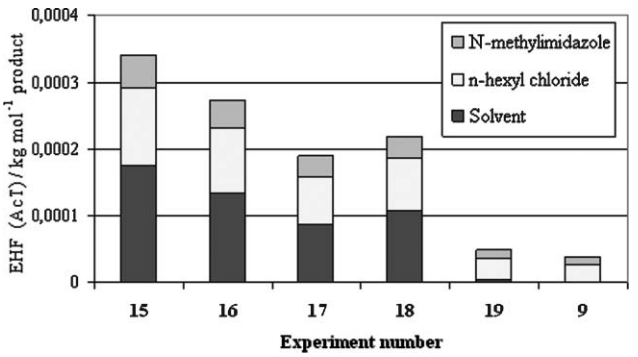

Fig. 7 Dependence of *EHF*(AcT) on the choice of solvent (xylene, cyclohexane, *n*-heptane, ethanol , solvent free) and c_{MIM} = 1.6, 3, 3.3 mol L^{-1}, T = 80 °C, t = 30 h, see exp. no. 9, 15–19 in Table 1.

The benefits of the *EHF* is demonstrated on the example of the conversion of *N*-methylimidazole in different solvents, *e.g.* ethanol, xylene, cyclohexane and *n*-heptane. Further, the reactant concentration in these solvents (see Table 1) was varied. In these experiments, the solvent-free alkylation results in better yields and energy efficiency compared to the use of solvents, due to the additional work-up step and lower conversions. Nevertheless, in other cases the use of solvents might promote the synthesis, so that the conversion is influenced positively and thus the *EHF* would be lower.

The *EHF*(AcT) concerning the solvent alternatives is displayed in Fig. 7. The *EHF* regarding chronic toxicity and water-mediated effects indicate the same trend. In highly concentrated solutions, the conversion increases after a specific reaction time, resulting in a lower reactant and solvent requirement. Therefore, the resulting *EHF*(AcT) is comparable to that calculated for the solvent-free experiment. Thus, solvents which possess a comparable high toxicity potential should not to be excluded *a priori*, since their performance significantly influences the efficiency of the synthesis.

Evaluation of the cost factor (*CF*)

The third criterion, the cost factor (*CF*), takes into account economic factors in order to allow for a comparison of the profitability of different process/product alternatives. If possible, this part of the balance should include all occurring

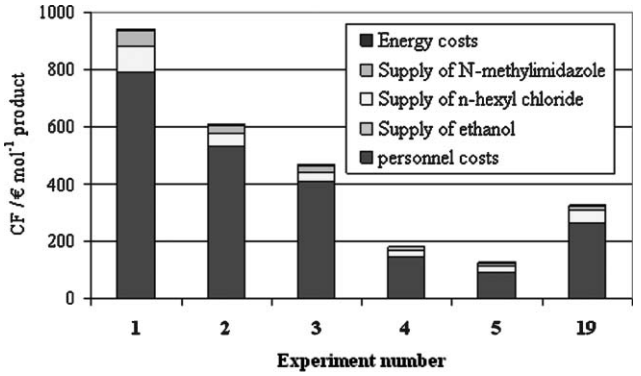

Fig. 8 Time dependence of *CF*, t = 10, 19, 27, 72, 144 h, n_{MIM} : $n_{C6H13Cl}$ = 1 : 1, T = 70 °C, solvent free and t = 30, T = 80 °C, n_{MIM} : $n_{C6H13Cl}$ = 1 : 1.6, solvent: ethanol, see exp. no. 1–5, 19 in Table 1.

costs, *i.e.* the prices of the chemicals, energy, disposal, equipment and personnel as well as process expenditure *etc.* In spite of numerous data gaps, especially in R&D, still existing, *CF* (as well as *EF* and *EHF*) can point out trends and disclose time-consuming and cost-intensive steps.

Fig. 8 depicts the *CF* related to experiments 1–5. The factor is divided into five cost sources: costs arising from energy demand, supply of reactants (*N*-methylimidazole, *n*-hexyl chloride)[59] and (extraction) solvent[59] as well as the personnel costs (preparation, monitoring, work-up). The share of personnel costs was calculated as follows: (i) gross salary: 20 € h^{-1}, (ii) preparation effort; 30 min per synthesis cycle, (iii) monitoring; 3% of reaction time, (iv) work-up; 10 min per extraction cycle. The energy-related costs are influenced by the energy required for the synthesis (reaction temperature), the work-up effort and in some cases by the refeeding of the solvent. Costs of 0.16 € per kWh were assumed to calculate the share of this cost source. In contrast to the *EF* (Fig. 4), the *CF* steadily decreases while the reaction time increases. Furthermore, one of the experiments performed in ethanol (exp. no. 19) is contrasted to the solvent-free experiments. The supply of ethanol is negligible, since a recycling and refeeding of 90% of the solvent was assumed. Therefore, the use of the solvent does not influence the *CF* in this specific case. This also applies to the energy costs.

Optimisation of the alkylation step

The experimental results discussed above represent only a small part of all investigations carried out. Besides the synthesis of [C_6MIM]Cl, the usage of different cations and anions for the preparation of ionic liquids, different extraction strategies, as well as the application of ionic liquids as solvents in organic standard reactions are considered.

In the case of the preparation of pure [C_6MIM]Cl (purity > 99%), the evaluation of these actual experimental results and the outranking of the different solution candidates resulted in the following optimal synthesis prescription: T = 100 °C, t = 30 h, n_{MIM} : $n_{C6H13Cl}$ = 1 : 1, solvent free. This parameter configuration has been found to be the best trade-off regarding *EF*, *EHF* and *CF*. With respect to the starting point of the optimisation procedure (exp. number 21: T = 80 °C, t = 30 h, n_{MIM} : $n_{C6H13Cl}$ = 1 : 1.2, $c_{N\text{-base}}$ = 3 mol L^{-1}, solvent: *n*-heptane), this synthesis protocol implies a reduction of *EF* by 78%, of *EHF* by 98% and of *CF* by 87%.

This result is valid under the following regulations: minimise *EF*, *EHF*(AcT), *EHF*(ChT), *EHF*(WmE), *CF*, weight: 33 : 11 : 11 : 11 : 33, preference function: linear, threshold unit: percent, and was determined using the software Decision Lab 2000.[56] However, it represents an interim result, since further optimisation potential still exists, especially concerning the work-up procedure.

Validation of *EF* as an indicator for several impact categories of the LCA methodology

As pointed out, the CED (and also the *EF*) is an appropriate indicator that reflects most other LCA impact categories. To visualise this coherence, a comparative LCA for alternative synthesis pathways of [C_6MIM]Cl was performed. To start with, a first experiment of the optimisation procedure, (exp. no. 21) was chosen and compared with the best trade-off solution candidate (exp. no. 14). Fig. 9 represents the reduction of the CED in contrast to the reduction of other impact categories (abiotic resource depletion potential (ADP), global warming potential (GWP), ozone depletion potential (ODP), acidification potential (AP), eutrophication potential (EP), photochemical ozone creation potential (POCP), human toxicity potential (HTP), freshwater aquatic ecotoxicity (FAETP), marine aquatic ecotoxicity potential (MAETP) and terrestrial ecotoxicity potential (TETP)) when favouring the conditions of exp. no. 14.

As discussed before, a reduction of 78% has been achieved concerning the CED (Fig. 9). The reductions within the other impact categories diverge from the CED reduction, with a median deviation of 6%. The standard deviation relating to the CED is 9.2%, thus fulfilling the requirements at a screening method during R&D. Therefore, the energy factor *EF* can be regarded as a sufficient screening factor, reflecting other environmental impacts.

As mentioned above, the CED is not applicable in all cases to reflect the impacts concerning human and ecotoxicity. In Fig. 9, these factors seem to be suitable for this task, but at this stage of development the release of the ionic liquid into the environment has not been integrated and quantified yet.

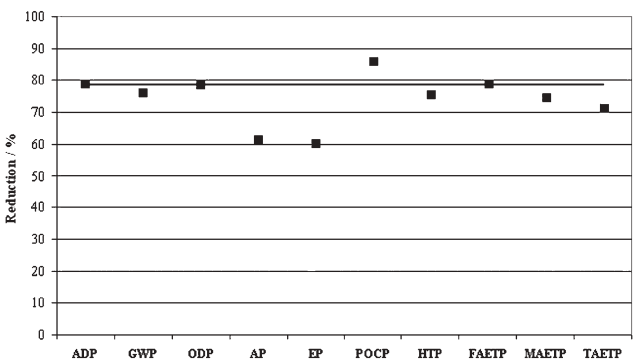

Fig. 9 Validation of *EF* as an indicator for variations within other LCA impact categories.

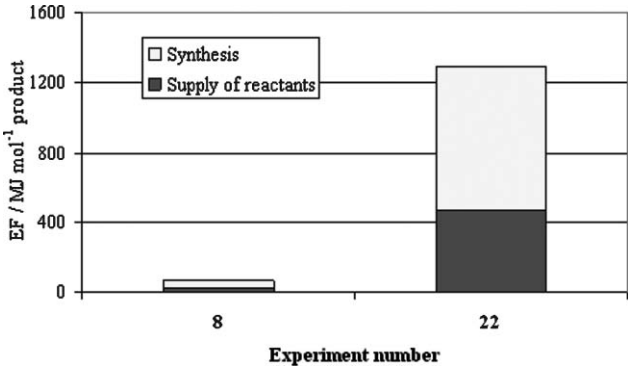

Fig. 10 *N*-base dependence of *EF*, *N*-base: [C_6MIM]Cl and [C_6Py]Cl, $n_{N\text{-base}} : n_{C6H13Cl} = 1 : 1$, $t = 30$ h, $T = 80$ °C, see exp. no. 8, 21 in Table 1.

Further, information on the future technical realisation, as well as disposal routes and the resulting emission pathway into the environment are hardly available.

Outlook: comparison of different bases, *N*–methylimidazole and pyridine

Besides the optimisation of the reaction parameters *T*, *t*, *n* : *n* and solvent, the influence of a *N*-base exchange was investigated. The optimised parameter configuration for the synthesis of [C_6MIM]Cl was chosen as a starting point for the synthesis (exp. no. 8) of [C_6Py]Cl (Table 1). With respect to the *EF*, the energy demand increases by approximately 95% to obtain 1 mol of the product (Fig. 10). From an energy point of view, the supply of pyridine is comparable to the supply of *N*-methylimidazole. Thus, the synthesis of pyridinium-based ionic liquids is not affected negatively by up-stream processes, but by the differences in conversion. Consequently, the substitution of the *N*-base results in a new optimisation problem.

Conclusion

It is not the aim of the ECO method to provide concrete values describing an environmental impact or specific costs, but to assist the implementation of sustainability aspects into the optimisation process during chemical R&D, by enabling an insight into the interrelation between several relevant aspects.

On that score, the evaluation and optimisation of synthesis pathways, work-up procedures or functionalities of chemical compounds start with the calculation of specific metrics, *EF*, *EHF* and *CF*. These metrics comprise energy demand, risks for human health and environment as well as costs. Their calculation follows a life cycle approach and comprises up- and down-stream processes. Then, the metrics will be defined as the key objective functions of ecological and economic sustainability, which have to be minimised during the optimisation process. To aid the decision-making process in a transparent and reproducible way, alternative solution candidates referring all of these objective functions are at last contrasted with the help of an outranking algorithm. Thus, beneficial parameter configurations leading to pareto-optimal configurations of the key objectives will be pointed out.

This method can be used to identify optimisation problems regarding ecological and economic sustainability already at R&D level and to find new, improved solutions which will comply to the concept of green chemistry.

In addition, on the example of selected results, the approach was demonstrated in the context of the synthesis of [C_6MIM]Cl. At the moment, the investigations are being extended to different types of ionic liquids as a function of their application area. By variation of anions/cations and alkyl chains, a huge number of ionic liquids with special properties, *e.g.* water miscibility, polarity and stability, can be synthesised. With the optimisation approach presented here, we hope to contribute to the green and efficient synthesis of ionic liquids.

Acknowledgements

Denise Reinhardt thanks the German Federal Environmental Foundation (DBU) for a graduate scholarship.

Abbreviations

[C_4MIM]Cl	1-butyl-3-methylimidazolium chloride
[C_6MIM]Cl	1-hexyl-3-methylimidazolium chloride
[C_6Py]Cl	*N*-hexylpyridinium chloride
CED	Cumulative energy demand
CF	Cost factor
EC50	Half maximal effective concentration
ECO	Ecological and economic optimisation
EF	Energy factor
EHF	Environmental and human health factor
EHF(AcT)	Environmental and human health factor regarding acute toxicity risks
EHF(ChT)	Environmental and human health factor regarding chronic toxicity risks
EHF(WmE)	Environmental and human health factor regarding risks resulting from water-mediated effects
EHS	Environmental, health and safety
LD50	Median lethal dose
LCA	Life cycle assessment
log k_{OW}	Log octanol–water partitioning coefficient
R&D	Research and development
RPoD	Remaining potential of danger
SHE	Safety, health and environment
SLCA	Simplified life cycle assessment

References

1 P. J. Dyson and D. Zhao, *Multiphase Homogeneous Catal.*, 2005, **2**, 494.
2 M. J. Earle, P. B. McCormac and K. R. Seddon, *Green Chem.*, 1999, **1**, 23.
3 E. Janus, I. Goc-Maciejewska, M. Lozynski and J. Pernak, *Tetrahedron Lett.*, 2006, **47**, 4079.
4 K. R. Seddon and A. Stark, *Green Chem.*, 2002, **4**, 119.
5 R. Sheldon, *Chem. Commun.*, 2001, **23**, 2399.
6 T. Welton, *Chem. Rev.*, 1999, **99**, 2071.
7 A. E. Visser, R. P. Swatloski and R. D. Rogers, *Green Chem.*, 2000, **2**, 1; M. L. Dietz, *Sep. Sci. Technol.*, 2006, **41**, 2047.
8 R. A. Sheldon, R. M. Lau, M. J. Sorgedrager, F. van Rantwijk and K. R. Seddon, *Green Chem.*, 2002, **4**, 147.

9 M. Gruttadauria, S. Riela, P. Lo Meo, F. D'Anna and R. Noto, *Tetrahedron Lett.*, 2004, **45**, 6113.
10 M. Galinski, A. Lewandowski and I. Stephniak, *Electrochim. Acta*, 2006, **51**, 5567; A. Fernicola, B. Scrosati and H. Ohno, *Ionics*, 2006, **12**, 95.
11 P. Wasserscheid and W. Keim, *Angew. Chem.*, 2000, **39**, 3773.
12 M. J. Earle and K. R. Seddon, *Clean Solvents*, 2002, **819**, 10.
13 D. Kralisch, A. Stark, S. Körsten, G. Kreisel and B. Ondruschka, *Green Chem.*, 2005, **7**, 301.
14 *Life Cycle Assessment – an operational guideline to the ISO standards*, ed. J. B. Guinée, Minstry of Housing, Spatial Planning and the Environment and Centre of Environmental Science, Leiden University, The Netherlands, 2001.
15 ISO 14040, *A standard on principles and framework*, European Committee for Standardisation, Brussels, Belgium, 1st edn, 1997.
16 G. Jödicke, O. Zenklusen, A. Weidenhaupt and K. Hungerbühler, *J. Cleaner Prod.*, 1999, **7**, 159.
17 A. A. Burgess and D. J. Brennan, *Chem. Eng. Sci.*, 2001, **56**, 2589.
18 S. Hellweg, U. Fischer and M. H. K. Scheringer, *Green Chem.*, 2004, **6**, 418.
19 G. Rebitzer and D. Hunkeler, *Int. J. Life Cycle Assess.*, 2003, **8**, 253–256.
20 R. A. Sheldon, *CHEMTECH*, 1994, **24**, 38.
21 G. Koller, D. Weirich, F. Brogli, E. Heinzle, V. H. Hoffmann, M. A. Verduyn and K. Hungerbuhler, *Ind. Eng. Chem. Res.*, 1998, **37**, 3408.
22 B. M. Trost, *Science, 1991*, 5037, **254**, 1471.
23 E. Heinzle, D. Weirich, F. Brogli, V. H. Hoffmann, G. Koller, M. A. Verduyn and K. Hungerbuehler, *Ind. Eng. Chem. Res.*, 1998, **37**, 3395.
24 J. A. Cano-Ruiz and G. J. McRae, *Annu. Rev. Energy Environ.*, 1998, **23**, 499.
25 M. Eissen and J. O. Metzger, *Chem.–Eur. J.*, 2002, **8**, 3580.
26 Industrial environmental performance metrics: challenges and opportunities, Committee on Industrial Environmental Performance Metrics, National Academy of Engineering, National Research Council, National Academy Press, Washington, D.C., 1999.
27 Simplifying LCA: just a cut? – *Final report of the SETAC–Europe Screening and Streamlining Working–Group*, Society of Environmental Chemistry and Toxicology (SETAC), Brussels, Belgium, 1997.
28 G. Fleischer and W.-P. Schmidt, *Int. J. Life Cycle Assess.*, 1997, **2**, 20.
29 E. Gasafi, L. Meyer and L. Schebek, *J. Ind. Ecol.*, 2004, **7**, 75.
30 F. Schmidt-Bleek, *Fresenius' Environ. Bull.*, 1993, **2**, 306.
31 G. Koller, U. Fischer and K. Hungerbühler, *Ind. Eng. Chem. Res.*, 2000, **39**, 960.
32 B. Jastorff, R. Störmann, J. Ranke, K. Mölter, F. Stock, B. Oberheitmann, W. Hoffmann, J. Hoffmann, M. Nüchter, B. Ondruschka and J. Filser, *Green Chem.*, 2003, **5**, 136.
33 D. M. Young and H. Cabezas, *Comput. Chem. Eng.*, 1999, **23**, 1477.
34 J. Horn, in *Handbook of Evolutionary Computation.*, ed. T. Bäck, D. B. Fogel and Z. Ichalewicz, Institute of Physics Publishing, Bristol (UK), 1997.
35 V. Pareto, *Cours D'Economie Politique*, F. Rouge, Lausanne, 1896.
36 T. L. Saaty, *The Analytic Hierarchy Process*, ed. McGraw-Hill, New York, NY, 1980.
37 B. Roy, *Cahiers du CERO*, 1978, **20**, 3.
38 J. P. Brans, P. Vincke and B. Mareschal, *Eur. J. Operation. Res.*, 1986, **24**, 228.
39 S. Kheawhom and M. Hirao, *Comput. Chem. Eng.*, 2004, **28**, 1715.
40 S. K. Stefanis, A. Buxton, A. G. Livingston and E. N. Pistikopoulos, *Comput. Chem. Eng.*, 1996, **20**, 1419.
41 V. Sakizlis, J. D. Perkins and E. N. Pistikopoulos, *Comput. Chem. Eng.*, 2004, **28**, 2069.
42 S. Sikdar and K. Subhas, *AIChE J.*, 2003, **49**, 1928.
43 A. Azapagic and R. Clift, *Comput. Chem. Eng.*, 1999, **23**, 1509.
44 A. Azapagic, *Chem. Eng. J.*, 1999, **73**, 1.
45 B. Alexander, G. Barton, J. Petrie and J. Romagnoli, *Comput. Chem. Eng.*, 2000, **24**, 1195.
46 P. T. Anastas and R. L. Lankey, *Green Chem.*, 2000, **2**, 289.
47 H. Sugiyama, M. Hirao, R. Mendivil, U. Fischer and K. Hungerbuhler, *Process Saf. Environ. Prot.*, 2006, **84**, 63.
48 W. Walk, J. Buchgeister and L. Schebek, 15th Annual Meeting of SETAC Europe, Lille, France, 2005.
49 D. Kralisch, Ph.D. Thesis, Friedrich-Schiller-University Jena, Germany, 2006.
50 The eco-indicator 99, *A damage oriented method for life cycle impact assessment*, 2001, PRe'Consultant.
51 ecoinvent database by Frischknecht *et al.*, v.1.3, 2006, Swiss Centre for Life Cycle Inventories, Switzerland.
52 SimaPro v.7, 2006, PRé Consultants, Netherlands.
53 http://www.probas.umweltbundesamt.de/php/index.php 2006.
54 Merck KGaA, Safety data sheets, 2006.
55 EPIWIN, v.3.11, 2000, Office of Pollution Prevention and Toxics, U.S. Environmental Protection Agency.
56 Decision Lab 2000. v. 1.01.0386, 2005, Visual Decision Inc.
57 Umberto, v. 5.5, 2006. ifu Institut für Umweltinformatik, Hamburg, ifeu Institut für Energie- und Umweltforschung, Germany.
58 J. Kaerkkaeinen, J. Asikkala, R. S. Laitinen and M. K. Lajunen, *Z. Naturforsch., B: Chem. Sci.*, 2004, **59**, 763.
59 Merck KGaA, Catalogue for chemicals and reagents, 2006.

Exploration of solvent free and/or microwave assisted syntheses of bismuth(III) thiolates

Philip C. Andrews,* Glen B. Deacon, Peter C. Junk and Nadia F. Spiccia

Received 7th June 2007, Accepted 18th September 2007
First published as an Advance Article on the web 12th October 2007
DOI: 10.1039/b708663f

A variety of synthetic approaches to the formation of bismuth(III) thiolates has been explored and compared. $BiPh_3$ was treated with a series of thiols of varying pK_a and functionality (2-mercaptobenzothiazole, 2-mercaptobenzoxazole, 2-mercaptopyrimidine, 2-mercapto-1-methylimidazole and thiosalicylic acid) in a 1:3 ratio under a variety of reaction conditions: with toluene or mesitylene under standard reflux conditions and under microwave irradiation, and solvent free with conventional and microwave heating. All reactions, except those with 2-mercapto-1-methylimidazole and thiosalicylic acid, yielded the tris-substitution product in good yield and high purity. Thiosalicylic acid gave the complex Bi_2L_3 in all reactions carried out in solvent and PhBiL when solvent free, both complexes containing the doubly deprotonated dianion (L = $O_2CC_6H_4$-2-S). Reactions carried out in the microwave reactor generally gave comparable yields to the conventional methods but in significantly shorter times. However, the solvent free microwave reactions of 2-mercaptobenzoxazole and 2-mercaptopyrimidine caused partial decomposition to give microcrystalline Bi_2S_3. The solvent free reactions conducted with conventional heating methods were highly effective in the formation of the bismuth thiolates. Reactions with 2-mercapto-1-methylimidazole were problematic in giving either no reaction products or mixtures of compounds displaying various degrees of substitution. Partial decomposition (2–7%) to the disulfide was observed for both the bismuth thiolates derived from 2-mercaptopyrimidine and thiosalicylic acid on storage of a solution over several weeks.

Introduction

Bismuth compounds, such as the subsalicylate and subcitrate, are well known for their antimicrobial activity, particularly in assisting the treatment and eradication of *helicobacter pylori*.[1] However, the hydrolytic instability of most metal–organic bismuth compounds, coupled with a high degree of insolubility, often makes it difficult to obtain complete chemical and structural characterisation, and consequently hinders a full understanding of the pathways which define their biological activity.[2] Recent investigations into bismuth(III) thiolates, $Bi(SR)_3$, indicate that they can display a relatively high level of stability in aqueous environments,[3] and are also effective as antimicrobial agents,[4–6] fungicides,[7] and anti-tumour agents,[8–10] as well as showing some potential as X-ray imaging agents.[11] Studies showing that proteins containing the sulfur bearing amino acid cysteine, and in particular the tripeptide glutathione, constitute the prime targets for biological bismuth make the thiolates important model compounds for understanding the *in vivo* action of Bi^{3+}.[12–14] However, while they constitute one of the most widely studied classes of bismuth compounds there is still a significant paucity of synthetic protocols for providing pure products in high yields. Burford and co-workers[4,15] have been seeking to establish some generally applicable synthetic methods using heterobifunctional chelating ligands, which can provide both an increase in solubility and the basis of a rational approach to studying the structure–activity relationships. Despite a recognised link between their structure and antimicrobial activity very few bismuth thiolates have been fully structurally characterised.[6] Those which have include $Bi(SC_6X_5)_3$ (X = F, Cl),[16–18] $Bi(SC_6H_5)_3$,[19] $Bi(SCH_2CH_2OH)_3$,[5,6] $[Bi\{(CH_3CH(OH)CH_2S)(CH_3CH(O)CH_2S)\}]_\infty$,[20] $Bi(S^tBu)_3$,[21] $Bi(S\text{-}4\text{-}FC_6H_4)_3$.[22]

Our current interest is in developing benign synthetic protocols for the formation of metal–organic bismuth compounds and we have previously reported the efficient and high yielding formation of bismuth carboxylates and thiolates using a solvent-free approach.[20] Rather than using a standard metathetical reaction between bismuth(III) trihalides and alkali metal thiolates,[23] which can be complicated by both salt retention[24] and the formation of anionic compounds,[23] our preferred approach is to use $BiPh_3$ as an organometallic synthon in protolysis reactions with the thiols. The air and moisture stability of $BiPh_3$, its low melting point, and its low toxicity make it an ideal reagent.[2] However, there are limitations on its reactivity, since the organic substrate has to be acidic enough for proton exchange to occur. Thiols generally have a pK_a $\leqslant$ 9 and so, notwithstanding counteracting influences such as steric hindrance, the reactions with $BiPh_3$ should be facile. Under standard reflux conditions long reaction times have been required: for example $Bi(SC_6F_5)_3$ and $Bi(SC_6Cl_5)_3$ were obtained in reasonably high yield (*ca.* 70%) after $BiPh_3$ and the appropriate thiol were reacted in refluxing toluene for 96 hours.[16,25] In earlier studies by Gilman,[26] where

School of Chemistry, Monash University, Clayton, Melbourne, Vic. 3800, Australia. E-mail: phil.andrews@sci.monash.edu.au; Fax: +61 3 9905 4597; Tel: +61 3 9905 5509

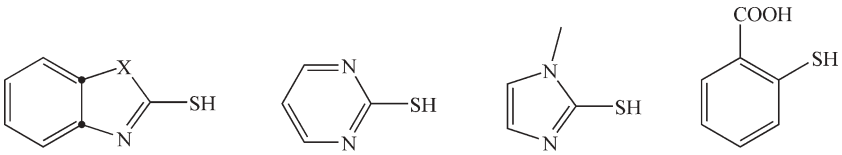

1 X = S
2 X = O

3 **4** **5**

much shorter reaction times were used, incomplete substitution usually occurred, yielding primarily the bis(thiolate), $PhBi(SR)_2$.

With the aim of establishing a synthetic methodology for the formation of pure tris-(thiolato)bismuth(III) compounds in high yield with due consideration to minimising organic solvent and energy use, we have explored and compared four sets of reaction conditions for the cleavage of $BiPh_3$ with thiols: (i) refluxing in toluene or mesitylene; (ii) solvent-free reactions in a conventional oven at 120 °C; (iii) use of toluene or mesitylene under microwave irradiation; and (iv) solvent-free reactions under microwave irradiation. Herein, we now report the results of a study comparing the efficiency and effectiveness of these methods in the reaction of $BiPh_3$ with 2-mercaptobenzothiazole (**1**), 2-mercaptobenzoxazole (**2**), 2-mercaptopyrimidine (**3**), 2-mercapto-1-methylimidazole (**4**) and thiosalicylic acid (**5**).

Results and discussion

We have previously described the successful and high yielding synthesis of bismuth carboxylates under solvent free conditions and the application of the methodology to the formation of the tris-substituted bismuth derivatives of 2-mercaptobenzothiazole (**1**) and 2-mercaptobenzoxazole (**2**).[20] The current interest in, and importance of, developing benign synthetic protocols inspired us to extend these studies to related bifunctional thiols and explore the use of microwave heating. The general synthetic pathways and reaction conditions are detailed in the Experimental section. With the exception of one reaction with thiosalicylic acid, all reactions were conducted on a 1 mmol scale in a 1:3 ratio of $BiPh_3$ to thiol under an N_2 atmosphere. The reactants and solvents were dried prior to use to prevent the possible formation of oxide from entrained water. For the solvent-free reactions the reactants were ground together prior to heating to promote efficient mixing and their thermochemical profiles were studied using DSC-TGA.

Solvent-free reactions are effective in limiting both the use of volatile organic solvents and minimising any solvent promoted side reactions.[27] Heating by conventional means in an oven or with an oil bath often requires long reaction times and higher temperatures than would be ideal to ensure adequate molecular mixing and complete protolysis of the $BiPh_3$. In contrast, microwave heating provides the opportunity of a faster heating rate to higher temperatures with a much reduced reaction time, thus minimising decomposition routes, which are promoted by *sustained* high temperatures.[28] In our study some interesting variations in reactivity and stability became apparent. Microwave heating with a solvent reaction medium generally gave comparable yields and compound purity to all the other synthetic procedures but in a fraction of the time, and this was evident for all the thiols studied except 2-mercapto-1-methylimidazole (**4**), which appears to be a special case and is discussed in more detail below. In contrast, the microwave based solvent free reactions were unpredictable and in two cases, with 2-mercaptobenzoxazole and 2-mercaptopyrimidine, partial decomposition to grey microcrystalline Bi_2S_3, as confirmed by EDX and XRD, occurred rapidly. The reaction products were characterised by ^1H and ^{13}C NMR, elemental analyses, ES-MS and FT-IR. The tris(thiolato)bismuth(III) compounds were obtained in most cases except for the reaction with thiosalicylic acid, which produced a $Bi_2(O_2CC_6H_4\text{-}2\text{-}S)_3$ complex containing the thiosalicylate dianion, and 2-mercapto-1-methylimidazole, which provided a mixture of substitution products in low yield (Table 1). Interestingly, when the synthesis with thiosalicylic acid was conducted in a 2:3 ratio, to reflect the product stoichiometry, $Bi_2(O_2CC_6H_4\text{-}2\text{-}S)_3$ was obtained when the syntheses were conducted in a solvent and $PhBi(O_2CC_6H_4\text{-}2\text{-}S)$ when carried out solvent free. Traces of $Ph_2Bi(O_2CC_6H_4\text{-}2\text{-}SH)$ ($\leqslant 4\%$) were occasionally observed in the solvent free reactions. The chemistry of the individual reactions is discussed separately below and the yields and reaction conditions are all presented in Table 1.

2-Mercaptobenzothiazole (1)

The solvent free reaction using conventional heating, described previously,[20] gave the tris-substituted product in a 97% yield after three hours at 130 °C. In the current investigation this product, a bright orange solid, was obtained in an 83% yield after heating to reflux in toluene for 5 h. Repetition in mesitylene at reflux increased the yield to 95%. With microwave dielectric heating in toluene at 120 °C for 10 min a 68% yield was obtained, while in mesitylene at 160 °C for 10 min this increased to 93%. Overall, the solvent free reactions afford good yields and in a shorter time than with conventional heating. Importantly, higher yields are obtained when the reactions are carried out at higher temperatures in mesitylene. The yield achieved in toluene after 10 min of microwave heating is lower (68%) presumably because of the slow loss of the final phenyl group from $BiPh_3$ at 120 °C, as was previously noted in the TGA-DSC analysis of the solvent free reactions.[20] In mesitylene at 160 °C the rate of release of this group is fast enough for rapid conversion to BiL_3.

2-Mercaptobenzoxazole (2)

The most unusual result with **2** by comparison with **1** is the rapid partial decomposition of the reaction product under solvent free conditions in the microwave reactor. That the reaction itself occurs readily is confirmed by a yield of 38% of BiL_3 after only 2 min (excluding ramping time). However, this

Table 1 Comparisons of reaction conditions and yields in the synthesis of bismuth thiolates

Thiol	Product	Method[c]	Time	Yield (%)
2-Mercaptobenzothiazole	BiL_3	A	5 h	75
		B	5 h	95
		C	10 min	68
		C	30 min	87
		C	1 h	94
		D	10 min	93
		E	15 min	75
		F	3 h	97[20]
2-Mercaptobenzoxazole	BiL_3	A	5 h	70
		B	5 h	85
		C	10 min	62
		C	30 min	85
		C	1 h	95
		D	10 min	82
		D	20 min	94
		E	2 min	Decomp. BiL_3 (38); Bi_2S_3 (16)
		F	3 h	88[20]
2-Mercaptopyrimidine	BiL_3	A	5 h	30
		A (90 °C)	1 week	63
		B	5 h	35
		C	20 min	15
		C	1 h	29
		D	1 h	33
		E	2 min	Decomp. BiL_3 (16); Bi_2S_3 (31)
		F	7 h	50
2-Mercapto-1-methylimidazole	Mixtures[a]	A	5 h	BiL_3 (5), Ph_2BiL (3)
		C	10 min	BiL_3 (3), $PhBiL_2$ (3)
		D	10 min	BiL_3 (6), $PhBiL_2$ (35), Ph_2BiL (6)
		F	8 h	BiL_3 (12), $PhBiL_2$ (14), Ph_2BiL (7)
Thiosalicylic acid	$Bi_2(O_2CC_6H_4\text{-}2\text{-}S)_3$	A	5 h	87
		B	5 h	96
		C	10 min	85
		C	30	87
		C	1 h	92
		D	10 min	95
		E	10 min	46
		F	7 h	78
	$PhBi(O_2CC_6H_4\text{-}2\text{-}S)$[b]	F	7 h	77

[a] Product distribution based on NMR spectroscopy. [b] Reaction stoichiometry, 2:3 $BiPh_3$:thiol. [c] A, reflux in toluene; B, reflux in mesitylene; C, microwave–toluene (120 °C); D, microwave–mesitylene (160 °C); E, microwave–solvent free (120 °C); F, solvent free conventional heating (120 °C).

is accompanied by the formation of Bi_2S_3 in a 16% yield. In contrast, the solvent free reaction with conventional heating gives 88% of BiL_3 after 3 h at 130 °C with no signs of decomposition.[20] The origin of this incongruity is not yet understood. Notably, the solvent free formation of Bi and Bi_2S_3 nanoparticles from long chain bismuth alkanethiolates has been the focus of some interest in the recent literature.[29,30] A yield of 16% compares well with that of 20–30% obtained through conventional furnace heating in the temperature range 150–225 °C for 1 h,[29,30] though our results with 2-mercaptopyrimidine, described below, show even more promise as an approach to the controlled and rapid formation of Bi_2S_3.

Conventional reflux in toluene for 5 h gave the mustard coloured tris(thiolato) product in a 70% yield, while a comparable yield of 62% yield was obtained after 10 min at 120 °C using microwave heating. When the reaction was repeated in mesitylene at 160 °C an 85% yield was achieved after 5 h using conventional heating, and a similar yield was obtained with microwave heating after 10 min at 160 °C. As for the reaction with **1**, the conventional solvent free synthesis is higher yielding than the solvent based syntheses conducted with toluene, and comparable with those in mesitylene. Again, microwave heating achieves high yields in much shorter times.

2-Mercaptopyrimidine (3)

The reactions with 2-mercaptopyrimidine **3** proved to be more problematic and lower yielding than those with **1** and **2**, but the same pattern of reactivity and product formation across almost all the synthetic methods is discernable. The one major exception to this is the formation of Bi_2S_3 as a decomposition product in the solvent free microwave reaction. The yield of Bi_2S_3 is 31%, double that from **2**, and is directly comparable with the other reported methods[29,30] but requires a reaction time of only 2 min. To understand the overall reactivity of the system, and in particular the solvent free methods, TGA and DSC measurements were carried out (Figs. 1(a) and 1(b)). The TGA trace appears more complex than was observed for **1** and **2**.[20] The melting of $BiPh_3$ is clearly evident at 79 °C and two exothermic processes, corresponding to a weight loss of the first two Ph groups, are observed at 164 °C and 171 °C. However, a second endothermic melting phase is observed at 208 °C, most likely corresponding to $PhBiL_2$, before the third

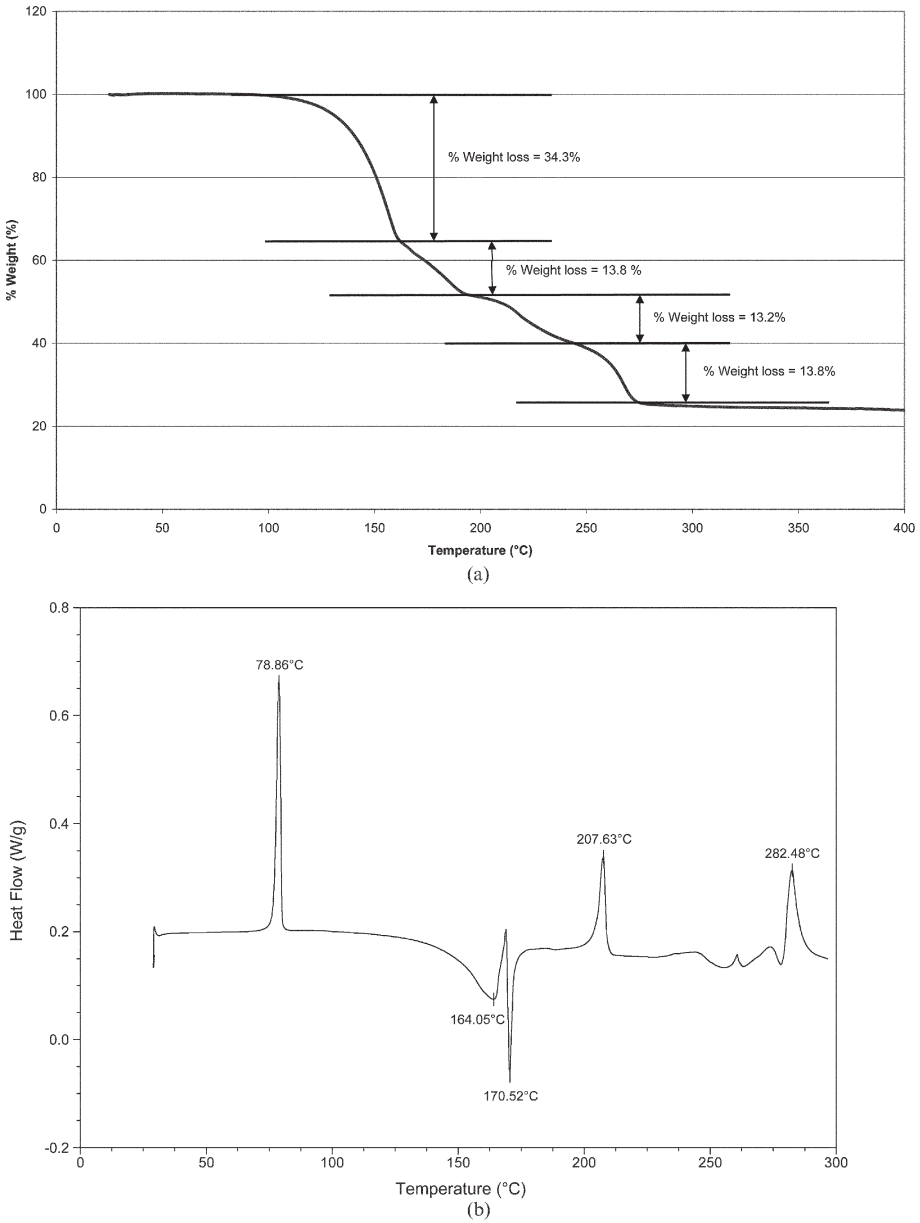

Fig. 1 (a) TGA analysis of the reaction of $BiPh_3$ with 2-mercaptopyrimidine. (b) DSC analysis of the reaction of $BiPh_3$ with 2-mercaptopyrimidine.

Ph group is lost over a broad temperature range around 250 °C. Melting of the product of the overall reaction occurs at 282 °C.

A TGA trace of the pure thiol, Fig. 2, surprisingly indicated weight loss beginning at *ca* 90 °C despite a reported literature melting point of 230 °C.[31] The almost complete evaporation of the ligand by 180 °C indicates that, under solvent free conditions at 120 or 160 °C, low yields are likely due to some sublimation from the reaction mixture and a lack of reactivity before *ca* 140 °C.

Stoyanov[32] found that 2-mercaptopyrimidine is easily oxidised to the disulfide at ambient temperatures. In solution this process is strongly concentration dependent and requires the presence of dissolved O_2. Furthermore, attempts to prepare the bismuth complex of 2-mercaptopyrimidine from bismuth hydroxide in the absence of an inert atmosphere at room temperature produced instead the disulfide.[33] No oxidation was observed when experiments were carried out in de-gassed solvents. Hence, the use of an inert atmosphere in this present study. Indeed, attempted recrystallisation of the tris(thiolato) product from the reaction of **3** with $BiPh_3$ from acetone in air yielded only the disulfide as yellow needles, as confirmed by ^1H NMR spectroscopy and a unit cell determination of a single crystal.

Synthesis of the tris(thiolato) product was achieved in toluene heated at reflux for 5 h in a 30% yield. A slightly higher yield of 35% was achieved with a comparable reaction in mesitylene. By repeating the reaction in toluene for 168 h at the lower temperature of 90 °C, the product formed in a 63% yield. Use of microwave heating for 10 min in toluene at 120 °C and mesitylene at 160 °C produced little product (<5%), although

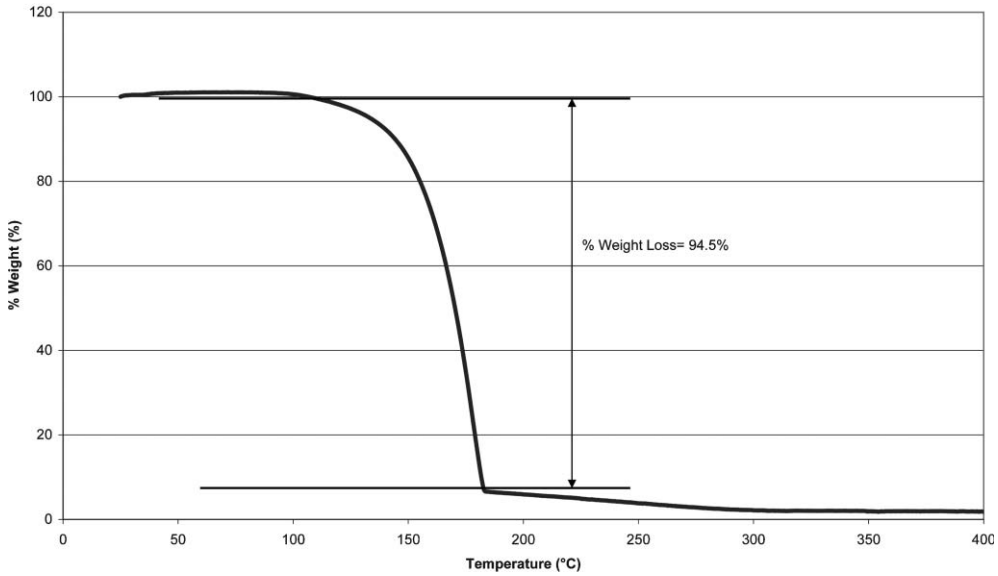

Fig. 2 TGA analysis of 2-mercaptopyrimidine.

comparable yields with reflux were obtained in both solvents after 1 h rather than 5 h.

Overall, the reaction is much lower yielding than for **1** and **2** and requires longer reaction times even to achieve lower conversions. While TGA-DSC reveals that a high temperature is required to cleave the final Ph group, this is no higher than that required for **1**, where almost complete conversion is achieved. It is generally accepted that for such reactions to occur the thiol/thioamide must be more acidic than benzene (pK_a 43) for proton exchange to occur.[16,25] The reported pK_a values for **1** and **3** are 7.86[34] and 7.20,[35] respectively, therefore this is an unlikely explanation for the difference in yields.

Formation of the tris(pyrimidinethiolato)bismuth(III) product was confirmed by the ^{1}H NMR spectrum, which showed the presence of two resonances at δ 8.26 ($H^{4,6}$) and 6.81 (H^5) in the integration ratio of 2:1, respectively, as expected for the presence of the thiolate without residual Ph groups. The ^{13}C NMR spectrum concurred with the product formulation having ligand resonances for C,[2] $C^{4,6}$ and C^5 at δ 181.5, 154.7 and 110.9, respectively. Electrospray mass spectroscopy (ES-MS) showed a peak corresponding to $[M + Na]^+$ in the positive mode while in negative mode peaks were assigned to $[M + Cl]^-$ and $[L_4Bi]^-$ species. Microanalysis was consistent with the proposed BiL_3 composition. The IR spectrum displayed absorptions due to *ν*(Ar–H) (3049 cm^{-1}), aromatic *ν*(C=C) (1563 cm^{-1} and 1534 cm^{-1}) and out plane C–H bending (739 cm^{-1}) vibrations.

2-Mercapto-1-methylimidazole (4)

All the synthetic approaches employed for the formation of the tris(thiolato) compound resulted either in no reaction or the isolation and identification of a complex mixture of products including at least two of the possible substitution products (Table 1). Both standard reflux in toluene and mesitylene produced only very low yields of the substitution products. The highest yield of any thiolate was that of the bis-substitution species $PhBiL_2$, which was produced from mesitylene in 35% yield after 10 min in the microwave reactor. Poor to moderate yields of all three possible substitution complexes, BiL_3 12%, $PhBiL_2$ 14%, Ph_2BiL 7%, were obtained by a conventional solvent free reaction. The reason for this low degree of reactivity is not readily apparent. To gain some insight into the reaction process TGA-DSC analyses were performed. The TGA trace, Fig. 3(a), indicates that the first two equivalents of benzene are lost from $BiPh_3$ after melting (78.8 °C) and before *ca* 140 °C with the final equivalent of benzene being lost around 180 °C. Interestingly, an endotherm is observed in the DSC curve at *ca* 160 °C, Fig. 3(b). This possibly corresponds to the melting of the bis-substitution product $PhBiL_2$. After 250 °C, there are several endotherms, presumably corresponding to the phase changes of various product components. These results at least support the observation that the reaction produces a variety of products, as indicated in Table 1.

Thiosalicylic acid (5)

Interestingly, the products of the reactions with thiosalicylic acid were highly sensitive to the synthetic method. All the solvent based reactions produced $Bi_2(O_2CC_6H_4\text{-}2\text{-}S)_3$ containing the thiosalicylate dianion, as did the solvent free reaction conducted using the standard 1:3 ratio of reactants. This is consistent with dianionic ligands in the solid state structures of $[(NH_4)_3[Bi(tsal)_3{\cdot}2H_2O]$[36] and $[Bi_8(tsal)_{12}(DMF)_6]{\cdot}6DMF$,[37] though these complexes were derived from inorganic bismuth salts in the presence of a base. Changing the stoichiometry in the solvent free reaction to 2:3 $BiPh_3$:thiol resulted in $PhBi(O_2CC_6H_4\text{-}2\text{-}S)$ being isolated as the predominant product in a 77% yield. This observation supports earlier studies by Gilman[26] who obtained $PhBi(O_2CC_6H_4\text{-}2\text{-}S)$ through a 1:1 reaction of $BiPh_3$ with **5** at 150 °C for 1 h.

Synthesis in toluene heated to reflux gave a yield of 87% of Bi_2L_3 after 5 h, while in refluxing mesitylene a 96% yield was produced in the same time frame. Reactions using microwave heating in toluene at 120 °C gave an 85% yield and in

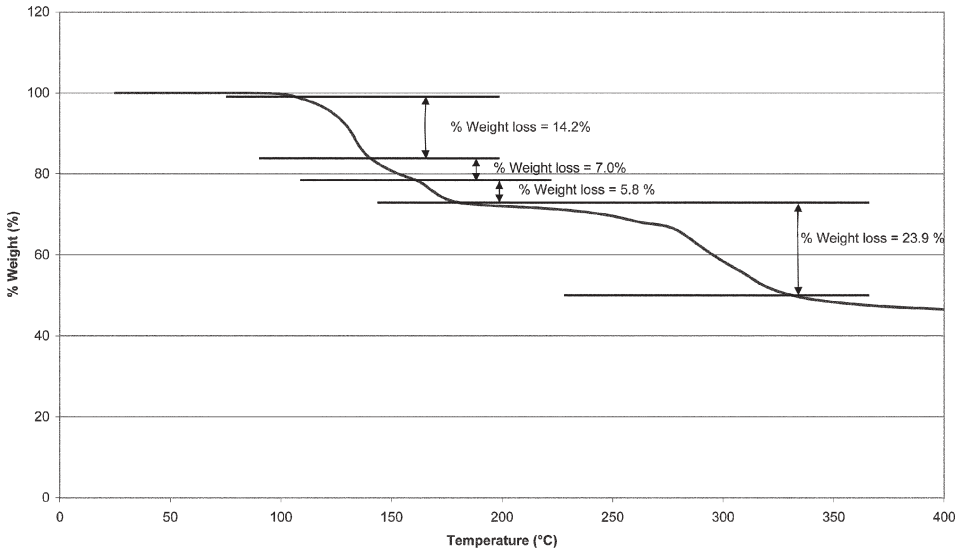

(a)

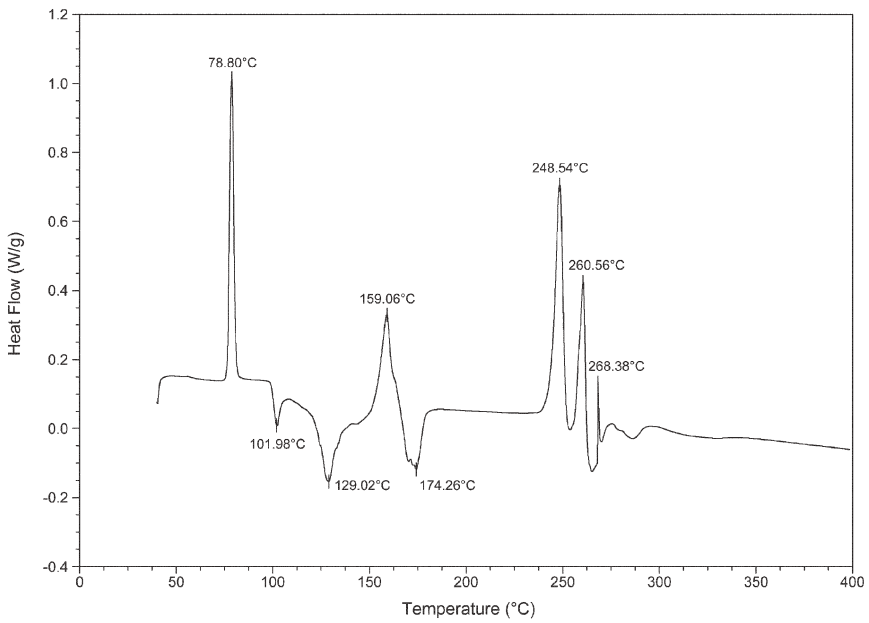

(b)

Fig. 3 (a) TGA analysis of the reaction of $BiPh_3$ with 2-mercapto-1-methylimidazole. (b) DSC analysis of the reaction of $BiPh_3$ with 2-mercapto-1-methylimidazole.

mesitylene at 160 °C a 91% yield after a 10 min reaction time. Comparing these results, it can be concluded once again that carrying out the reactions in solvents that allow higher temperatures is advantageous in increasing the yield to almost quantitative. Furthermore, microwave dielectric heating is as effective as conventional heating, but delivers greater efficiency through shorter reaction times. The reaction of $BiPh_3$ with salicylic acid (H_2sal) in the absence of an additional Lewis donor gives solely the mono-deprotonated carboxylate, $Bi(Hsal)_3$, under all conditions, indicating the higher acidity of the SH group over the phenolic OH.[38–40]

The composition of the Bi_2L_3 products was confirmed by elemental analysis, NMR and mass spectrometry. Importantly, the IR spectrum showed the absence of peaks corresponding to S–H stretching (2519 cm^{-1}) and C=O stretching (1668 cm^{-1}), absorptions that are observed in the 2-thiosalicylic acid spectrum indicating double deprotonation in the product. Positive ion ES-MS gave peaks at *m*/*z* 515 and 875, corresponding to $[Bi(LH)_2]^+$ and $[Bi_2L_2(LH)]^+$, respectively. The latter is of particular interest since it corresponds to a feature which was previously unassigned in Burford's mass spectroscopic study of the products obtained from the reaction of $BiCl_3$ and thiosalicylic acid in ethanol.[41]

Compound stability

Bismuth compounds are susceptible to oxidation and hydrolysis resulting in bismuth oxide or ligated oxo-clusters. It is

generally accepted that the higher affinity of Bi for thiolate ligands over oxygen and nitrogen donors results in the higher thermal and hydrolytic stability of the Bi–S bond.[12,15,37,42] However, Barton[43] found that bismuth thiolates can decompose to their corresponding disulfides catalysed by the presence of O_2. For example, bismuth thiophenolate undergoes a 5% decomposition to the disulfide when heated under argon for 24 h at 135 °C, while after 1 h in air 84% decomposition had occurred.[43] Bochmann[44] noted that solutions are prone to oxidation with formation of the corresponding diaryl disulfides and it was found that under thermolysis conditions at low pressures the air stable compound $Bi(S(2,4,6\text{-}Me_3C_6H_2))_3$ decomposed into elemental bismuth and the diaryl disulfide.

In the present work, it was found that recrystallisation of tris(pyrimidinethiolato)bismuth(III) from acetone in air yielded the disulfide as the only crystalline product. On leaving the reaction product for six months in a sealed vial (under air) ^{1}H NMR analysis showed that approximately 7% had decomposed into the disulfide. Interestingly, Jensen[33] reported that this disulfide was the sole product from a reaction between 2-mercaptopyrimidine and bismuth hydroxide.

In light of these results, the stability of the products in solution was monitored using ^{1}H NMR spectroscopy. After eleven days in air a deuterated DMSO solution of tris-(pyrimidinethiolato)bismuth(III) had undergone a 5% decomposition to the disulfide, while the solution of $Bi_2(O_2CC_6H_4\text{-}2\text{-}S)_3$ gave 6% of the disulfide that had formed. A solid sample of the latter compound contained 2% of the disulfide after being left in a sample vial for six months, while no decomposition of the 2-mercaptobenzothiazole and 2-mercaptobenzoxazole complexes had occurred either in solution after two weeks or as solids in sample vials after six months.

Conclusions

In comparing solvent free and microwave assisted approaches to the synthesis of heterobifunctional bismuth thiolates with conventional heating and solvent reflux methods it has been established that the most favourable reaction condition for maximising both yield and purity is with the use of mesitylene as a solvent medium, heated to reflux, in the microwave reactor. While the solvent based syntheses give equally good yields with both traditional and microwave heating, the microwave based reactions achieve these yields in a fraction of the time and so can be considered more time and energy efficient. The solvent free reactions using traditional heating methods, while giving comparable yields to those observed with mesitylene, unfortunately still require relatively long reaction times. So, although the reduction in the use of organic solvents is welcome the long reactions times impact slightly on the overall benefit of this method. The use of microwave heating for the solvent free reactions produced unpredictable results. While the reactions with 2-mercaptobenzothiazole and thiosalicylic acid were relatively successful, the products from 2-mercaptobenzoxazole and 2-mercaptopyrimidine gave only low yields and underwent rapid partial decomposition to microcrystalline Bi_2S_3. This highlights a possible problem in this approach with heat dissipation, although the importance of forming nanostructured Bi_2S_3 warrants further development of this approach.

Experimental section

Reagents obtained from suppliers (97% purity or better) were dried before use. Toluene was dried prior to use with an MBraun-SPS-800 solvent purification system and stored over molecular sieves (4Å) under N_2. Mesitylene, DMSO and d_6-DMSO were dried and distilled from CaH_2 and stored over molecular sieves (4Å) under N_2. Acetone was dried by stirring over anhydrous K_2CO_3 and distilled and stored over 4Å molecular sieves under N_2. Triphenylbismuth was prepared from PhMgBr and $BiCl_3$ in diethyl ether and recrystallised from ethanol. Its purity was checked by NMR and melting point (78 °C).

Syntheses and manipulations were carried out under inert atmosphere techniques. All reactions were carried out under an atmosphere of dry nitrogen using standard Schlenk or dry box techniques and oven dried glassware.

Elemental analyses were performed by the University of Otago, Dunedin, New Zealand. ^{1}H and ^{13}C NMR spectra were recorded on a Bruker DPX-300 spectrometer or Bruker Avance DRX 400 spectrometer in d_6-DMSO. Infrared (IR) spectra were recorded on a Bruker IFS55 Equinox FTIR Spectrometer using a Golden Gate ATR cell (cm^{-1} scale) as solid samples. Mass spectra were recorded on a Micromass Platform II (now Waters) QMS quadropole fitted with a Waters Alliance autosampler. Melting points were recorded on a Stuart Scientific melting point apparatus, SMP3. Microwave heating was performed in a Biotage Initiator Sixty Microwave Synthesiser. Thermogravimetric analysis (TGA) was carried out using a Perkin-Elmer Pyris TGA and differential scanning calorimetry (DSC) was carried out using a TA Q100 DSC between 30° and 300 °C, with a temperature ramp rate of 10° min^{-1}.

General synthetic procedures

Any variations in the general procedures described here are noted in Table 1. Reactions were conducted under a dry N_2 atmosphere using 1 mmol of $BiPh_3$ and 3 mmol of thiol. All yields are given in Table 1.

Heating under reflux: $BiPh_3$ and the thiol were added to a Schlenk flask with 15 ml of solvent. The mixture was allowed to reflux in toluene (120 °C) or mesitylene (160 °C) for 5 h. ***Solvent free reactions under conventional heating***: crystalline $BiPh_3$ was ground together with the thiol and heated in a 25 ml pear-shaped flask suspended in an oil bath for between 3–8 h at 120 °C, or alternatively placed in a conventional oven at 120 °C. ***Microwave heating with solvents***: reagents were placed in an Emery microwave vial followed by 4 ml of solvent. The reaction temperatures and times are given in Table 1. ***Microwave heating—solvent free reactions***: crystalline $BiPh_3$ was ground together with the thiol and added to an Emery microwave vial. The mixture was heated to 120 °C for the times specified in Table 1.

Tris(benzothiazol-2-ylthiolato)bismuth(III)[20]

The bright yellow–orange precipitate formed was washed with toluene and then acetone until the filtrate was colourless to yield the compound; mp 324–325 °C (dec). (lit.[20] 325 °C dec.)

(found: C, 35.20; H, 1.77; N, 5.81. Calculated for $C_{21}H_{12}BiN_3S_6$: C, 35.64; H, 1.71; N, 5.94%); ν_{max}/cm^{-1} 3054 w, 1689 m, 1588 m, 1560 m, 1501 w, 1446 m, 1402 s, 1311 m, 1275 m, 1239 m, 1075 m, 1022 s, 996 s, 933 m, 747 s, 721 m, 678 m; δ_H (400 MHz, d_6-DMSO, 30 °C): 7.75 (3H, d, *H*C^8), 7.46 (3H, m, *H*C^5), 7.22 (6H, m, *H*C^{6,7}).

Tris(benzoxazol-2-ylthiolato)bismuth(III)[20]

The mustard coloured precipitate was collected washed with acetone and toluene and dried to yield the compound; mp 261–262 °C (lit.[20] 260–261 °C) (found: C, 37.00; H, 1.83; N, 6.09. Calculated for $C_{21}H_{12}BiN_3S_3O_3$: C, 37.24; H, 1.83; N, 6.37%); ν_{max}/cm^{-1} 3040 w, 1671 w, 1594 w, 1525 w, 1501 w, 1475 w, 1437 s, 1361 w, 1283 w, 1243 s, 1220 s, 1091 s, 1002 m, 970 w, 923 m, 890 m, 849 w, 802 m, 734 s, 629 w; δ_H (400 MHz, d_6-DMSO, 30 °C): 7.41 (3H, br, *H*C^8), 7.20 (9H, m, *H*C^{5,6,7}).

Tris(pyrimidin-2-ylthiolato)bismuth(III)

The yellow precipitate that formed was collected and washed with hot toluene to yield BiL_3 in yields as specified; mp 278 °C (dec) (found: C, 26.59; H, 1.80; N, 15.15. Calculated for $C_{12}H_9BiN_6S_3$: C, 26.57; H, 1.67; N, 15.49%); ν_{max}/cm^{-1} 3053 w, 1602 s, 1561 s, 1539 s, 1422 w, 1369 m, 1323 s, 1212 m, 1174 s, 1044 m, 976 m, 789 m, 733 s, 640 w; δ_H (400 MHz, d_6-DMSO, 30 °C): 8.26 (6H, d, J = 5.2, *H*C^{4,6}), 6.81 (3H, t, J = 5.2, *H*C^5). δ_C (400 MHz, d_6-DMSO, 30 °C): 181.5 (C^2), 154.7 (C^{4,6}), 110.9 (C^5); *m*/*z* (ESI) 565 $[BiL_3Na]^+$, 577 $[BiL_3Cl]^-$, 653 $[BiL_4]^-$.

Tris(2-thiosalicylato)dibismuth(III), Bi_2L_3

The yellow precipitate was filtered and washed with toluene and acetone to yield the compound; mp 318 °C (dec) (found: C, 28.57; H, 1.47. Calculated for $C_{21}H_{12}Bi_2O_6S_3$: C, 28.84; H, 1.38%); ν_{max}/cm^{-1} 3050 w, 1567 m, 1483 s, 1424 m, 1368 m, 1306 s, 1245 m, 1130 m, 1030 m, 850 s, 799 w, 734 s, 723 s, 646 m; δ_H (400 MHz, d_6-DMSO, 30 °C): 7.58 (3H, d, J = 7.6, *H*C^6), 7.23 (3H, t, J = 7.6, *H*C^3), 7.05 (3H, d, J = 7.7, *H*C^4), 6.99 (3H, t, J = 7.5, *H*C^5); δ_C (400 MHz, d_6-DMSO, 30 °C): 171.5 (C=O), 138.8 (C–S), 138.1 (C^4), 135.8 (C^6), 129.9 (C^3), 128.6 (C^1), 125.4 (C^5); *m*/*z* (ESI) 515 $[Bi(LH)_2]^+$, 875 $[BiL_3H]^+$.

Phenylbis(2-thiosalicylato)bismuth(III), PhBiL

The yellow precipitate was filtered and washed with toluene and acetone to yield the compound. Yield 77%, mp 260 °C (dec). δ_H (400 MHz, d_6-DMSO, 30 °C): 8.68 (2H, d, J = 7.6, *o*-Ph), 7.79 (2H, d, J = 7.6, *m*-Ph) 7.57 (2H, d, J = 7.6, *H*C^6), 7.38 (1H, d, J = 7.6, *p*-Ph) 7.21 (2H, t, J = 7.6, *H*C^3), 7.04 (2H, d, J = 7.7, *H*C^4), 6.99 (2H, t, J = 7.5, *H*C^5). *m*/*z* (ESI) 899 $[Ph_2Bi_2L_2Na]^+$, 877 $[Ph_2Bi_2L_2H]^+$, 439 $[PhBiLH]^+$; 911 $[Ph_2Bi_2L_2Cl]^-$.

Complexes from 2-mercapto-1-methylimidazole

^{1}H NMR on product mixture: δ_H (400 MHz, d_6-DMSO, 30 °C); **BiL$_3$** 6.98 (3H, s, *H*C^5), 6.79 (3H, s, *H*C^4), 3.41 (9H, s, Me); **PhBiL$_2$** 8.75 (2H, d, *o*-Ph), 7.62 (2H, t, *m*-Ph), 7.31 (1H, m, *p*-Ph) 6.98 (2H, s, *H*C^5), 6.79 (2H, s, *H*C^4), 3.41 (6H, s, Me); **Ph$_2$BiL** 8.21 (4H, d, *o*-Ph), 7.53 (4H, t, *m*-Ph), 7.28 (2H, m, *p*-Ph) 6.98 (1H, s, *H*C^5), 6.79 (1H, s, *H*C^4), 3.41 (3H, s, Me). *m*/*z* (ESI) 912 $[Ph_2Bi_2L_3]^+$, 839 $[Ph_4Bi_2L]^+$, 477 $[Ph_2BiLH]^+$, 431 $[PhBiL(MeOH)]^+$, 399 $[PhBiL]^+$.

Acknowledgements

We would like to thank the Australian Research Council, the Centre for Green Chemistry at Monash University and Mr Rod Mackie from the Centre for X-Ray Physics & Imaging (CXPI) at Monash for financial and technical support.

References

1 G. G. Briand and N. Burford, *Chem. Rev.*, 1999, **99**, 2601.
2 *Organobismuth Chemistry*, eds. H. Suzuki and Y. Matano, Elsevier, Amsterdam, 2001; H. Sun, H. Li and P. J. Sadler, *Chem. Ber.*, 1997, **130**, 669.
3 G. G. Briand, N. Burford, M. D. Eelman, T. S. Cameron and K. N. Robertson, *Inorg. Chem.*, 2003, **42**, 3136.
4 L. Agocs, G. G. Briand, N. Burford, M. D. Eelman, N. Aumeerally, D. MacKay, K. N. Robertson and T. S. Cameron, *Can. J. Chem.*, 2003, **81**, 632.
5 L. Agocs, G. G. Briand, N. Burford, T. S. Cameron, W. Kwiatkowski and K. N. Robertson, *Inorg. Chem.*, 1997, **36**, 2855.
6 G. G. Briand, N. Burford, T. S. Cameron and W. Kwiatkowski, *J. Am. Chem. Soc.*, 1998, **120**, 11374.
7 T. Klapotke, *Polyhedron*, 1987, **6**, 1593.
8 P. Kopf-Maier and T. Klapotke, *Inorg. Chim. Acta*, 1988, **152**, 49.
9 *US Pat. Appl. Publ.*, 2001016600, A1, 2001.
10 H. Li, C. S. Lai, J. Wu, P. C. Ho, D. de Vos and E. R. T. Tiekink, *J. Inorg. Biochem.*, 2007, **101**, 809.
11 L. O. Rosik, *U. S. Patent*, Mallinckrodt Medical, Inc., 1995, A61B 005/055.
12 P. J. Sadler, H. Li and H. Sun, *Coord. Chem. Rev.*, 1999, **185–186**, 689.
13 H. A. Phillips, M. D. Eelman and N. Burford, *J. Inorg. Biochem.*, 2007, **101**, 736.
14 S. Ahmad, A. A. Isab, S. Ali and A. R. Al-Arfaj, *Polyhedron*, 2006, **25**, 1633.
15 G. G. Briand, N. Burford, M. D. Eelman, T. S. Cameron and K. N. Robertson, *Inorg. Chem.*, 2003, **42**, 3136.
16 K. M. Anderson, C. J. Baylies, A. H. M. Monowar Jahan, N. C. Norman, A. G. Orpen and J. Starbuck, *Dalton Trans.*, 2003, 3270.
17 M. Muller, R. J. H. Clark and R. S. Nyholm, *Transition Met. Chem.*, 1978, **3**, 369.
18 J. P. H. Charmant, A. H. M. Monowar Jahan, N. C. Norman and A. G. Orpen, *Inorg. Chim. Acta*, 2005, **358**, 1358.
19 M. Wieber and U. Baudis, *Z. Anorg. Allg. Chem.*, 1976, **423**, 47.
20 P. C. Andrews, G. B. Deacon, W. R. Jackson, M. Maguire, N. Scott, B. W. Skelton and A. H. White, *J. Chem. Soc., Dalton Trans.*, 2002, 4634–4638; P. C. Andrews, G. B. Deacon, P. C. Junk, I. Kumar and M. Silberstein, *Dalton Trans.*, 2006, 4852.
21 A. F. Janson, O. C. Vaidya and C. J. Willis, *J. Inorg. Nucl. Chem.*, 1981, **43**, 1469.
22 S. C. Hergett and M. E. Peach, *J. Fluorine Chem.*, 1988, **38**, 367.
23 L. J. Farrugia, F. J. Lawlor and N. C. Norman, *Polyhedron*, 1995, **14**, 311.
24 K. A. Smith, G. B. Deacon, W. R. Jackson and J. M. Miller, *Aust. J. Chem.*, 1996, **49**, 231.
25 W. Clegg, M. R. J. Elsegood, L. J. Farrugia, F. J. Lawlor, N. C. Norman and A. J. J. Scott, *J. Chem. Soc., Dalton Trans.*, 1995, 2129.
26 H. Gilman and H. L. Yale, *J. Am. Chem. Soc.*, 1951, **73**, 2880.
27 M. D. Bala and N. J. Coville, *J. Organomet. Chem.*, 2007, **692**, 709.
28 *Microwave Methods in Organic Synthesis*, eds. M. Larhed and K. Olofssonq, Springer-Verlag, Berlin and Heidelberg, Germany, 2006.
29 J. Chenn, L.-M. Wu and L. Chen, *Inorg. Chem.*, 2007, **46**, 586.
30 M. B. Sigman, Jr and B. A. Korgel, *Chem. Mater.*, 2005, 1655.
31 R. A. Mathes, *J. Am. Chem. Soc.*, 1953, **75**, 1747.

32 S. Stoyanov, T. Stoyanova, L. Antonov, P. Karagiannidis and P. Akrivos, *Monatsh. Chem.*, 1996, **127**, 495.
33 G. B. Jensen, G. Smith, D. S. Sagatys, P. C. Healy and J. M. White, *Acta Crystallogr.*, 2004, **E60**, 2438.
34 A. A. Boraei and I. T. Ahmed, *J. Chem. Eng. Data*, 1996, **41**, 787.
35 A. Albert and G. B. Barlin, *J. Chem. Soc.*, 1959, 3610.
36 E. Asato, K. Katsura, T. Arakaki, M. Mikuriya and T. Kotera, *Chem. Lett.*, 1994, 2123.
37 R. M. McCarrick, P. J. Squattrito, R. N. Singh, R. N. Handa and S. N. Dubey, *Acta Crystallogr.*, 1999, **C55**, 2111.
38 V. Stavila, J. C. Fettinger and K. H. Whitmire, *Organometallics*, 2007, DOI: 10.1021/om070115c.
39 P. C. Andrews, G. B. Deacon, C. M. Forsyth, P. C. Junk, I. Kumar and M. Maguire, *Angew. Chem., Int. Ed.*, 2006, **45**, 5638.
40 J. H. Thurston, E. M. Marlier and K. H. Whitmire, *Chem. Commun.*, 2002, 2834.
41 N. Burford, M. D. Eelman and T. S. Cameron, *Chem. Commun.*, 2002, 1402.
42 H. Sun, L. Hongyan, A. B. Mason, R. C. Woodworth and P. J. Sadler, *J. Biol. Chem.*, 2001, **276**, 8829.
43 D. H. R. Barton, H. Dadoun and A. Gourdon, *Nouv. J. Chim.*, 1982, **6**, 53.
44 M. Bochmann, X. Song, M. B. Hursthouse and A. Karaulov, *J. Chem. Soc., Dalton Trans.*, 1995, 1649.

New ionic liquid-modified silica gels as recyclable materials for L-proline- or H–Pro–Pro–Asp–NH_2-catalyzed aldol reaction

Carmela Aprile,[a] Francesco Giacalone,[b] Michelangelo Gruttadauria,*[b] Adriana Mossuto Marculescu,[b] Renato Noto,[b] Jefferson D. Revell[c] and Helma Wennemers[c]

Received 21st June 2007, Accepted 17th September 2007
First published as an Advance Article on the web 3rd October 2007
DOI: 10.1039/b709471j

L-proline and the tripeptide H–Pro–Pro–Asp–NH_2 (**1**) have been supported, by adsorption, onto the surface of modified silica gels functionalized with a monolayer of covalently attached 1,2-dimethyl-imidazolium chloride, tetrafluoroborate or hexafluorophosphate ionic moieties, respectively. Three different linkers were used to attach the ionic liquid moiety to the surface of these supports. The resulting materials have been used as catalysts for the aldol reaction between acetone and several substituted benzaldehydes. Good yields and enantioselectivities, comparable to or better than those obtained under homogeneous conditions, were obtained. These materials are easily recovered by filtration, and studies regarding their re-use have been carried out. Studies performed using L-proline-supported materials have shown that the re-use of these materials is dependent on the nature of the linker. The supported tripeptide H–Pro–Pro–Asp–NH_2 gave higher enantioselectivities than those obtained with supported-proline. Recycling investigations using tripeptide-supported materials showed continued good selectivities but diminishing conversions over consecutive runs. L-proline-supported materials however, can be used at least nine times without loss of either conversion or selectivity.

Introduction

In recent years, two research fields have received a paramount interest: organocatalysis[1] and ionic liquids.[2] Catalysis of reactions by simple metal-free organic molecules (organocatalysis) is a very attractive approach, especially for asymmetric conversions. Among the many organocatalysts that have been developed so far, proline has received a great deal of attention, since it is able to catalyse a wide range of reactions enantioselectively.[3] The first, and probably most important reaction in which proline was used as a catalyst, is the aldol reaction.[4] The aldol reaction is one of the most important carbon–carbon bond-forming reactions, also providing high "atom-economy".[5] The advantage of using an organocatalyst can be higher if an efficient recovery and re-use of the catalyst can be carried out, so improving the greenness of the process.

In order to get higher stereoselectivities in the aldol reaction than those observed using L-proline, a vast number of elaborate and more expensive proline derivatives have been synthesized,[6] among them, the tripeptide H–Pro–Pro–Asp–NH_2 (**1** – Fig. 1).[7] With tripeptide **1** only 1 mol% is necessary to obtain aldol products in yields and selectivities that are comparable or higher to those achieved with 30 mol% of proline. These results demonstrated that the higher complexity of **1** is a good trade-off for higher activity.[7]

Room-temperature ionic liquids (RTILs) have become very useful solvents for synthesis and catalysis. They may easily be recycled, and can be used to dissolve and immobilize the catalyst. The large number of possible cation and anion combinations allow the synthesis of tailor-made ionic liquids with which catalytic species may be immobilized. In addition, ionic liquids can be functionalized and used for a variety of reactions, providing "task specific ionic liquids".[8] Moreover, ionic liquid-supported reagents and catalysts have also been reported.[9] Ionic liquid anchored hydroxyproline has been used in the direct asymmetric aldol reaction with good results.[10] Also, chiral ionic liquids have been prepared and used as reaction media for several organic reactions.[11] Recently, we have focused our efforts on the development of new materials for stereoselective synthesis.[12] An ionic liquid moiety is covalently attached as a monolayer to the surface of a silica gel support. Indeed, ionic liquids are expensive, hence it is desirable to minimize the quantity used in typical biphasic reaction systems. To the covalently-attached ionic liquid monolayer, the organocatalyst (*e.g.* L-proline) is supported with or without additional adsorbed ionic liquid. Good enantioselectivities and yields were obtained in the reaction

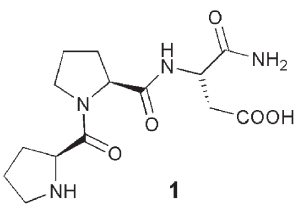

1

Fig. 1 H–Pro–Pro–Asp–NH_2.

[a]*Departamento de Química, Universidad Politecnica de Valencia, Camino de Vera s/n, 46022 Valencia, Spain*
[b]*Dipartimento di Chimica Organica "E.Paternò", Università di Palermo, Viale delle Scienze, Pad. 17, 90128, Palermo, Italy. E-mail: mgrutt@unipa.it; Fax: +39 091 596825; Tel: +39 091 596919*
[c]*Department of Chemistry, University of Basel, St. Johanns Ring 19, CH-4056 Basel, Switzerland*

between acetone and several aldehydes. The catalytic system can be recovered easily by conventional filtration and later re-used. Moreover, since proline is adsorbed, it can be removed and replaced with fresh proline. One of these supports was used in up to 13 cycles.[12b]

Since the discovery of proline as a useful organocatalyst, several publications have described its immobilization and recovery.[4b,13] However, in several cases, diminishing yields and enantioselectivities were observed following re-use of the supported catalyst, and in only one case, up to ten reaction cycles were possible.[13i] Recently, ourselves[14] and others[15] have reported the synthesis and use of polymer-supported proline or proline derivatives[16] which may be used in aqueous media. The tripeptide H–Pro–Pro–Asp–NH_2 **1** has also recently been immobilized on solid support.[17]

In our previous work, we examined different cations (1-propyl-2,3-dimethylimidazolium, 1-propyl-4-methyl-pyridinium, 1-propyl-4-aza-1-azoniabicyclo[2.2.2]octane) in combination with a variety of anions (Cl^-, BF_4^-, PF_6^-). We found good results when proline was adsorbed on imidazolium tetrafluoroborate-modified silica gel with additional bmimBF_4 (1-butyl-3-methylimidazolium tetrafluoroborate) ionic liquid.[12b] A propyl linker was used between the cation and the surface of silica gel. Herein, we report the effects that different linkers have on the course of proline-catalyzed aldol reactions, considering factors including conversion, enantioselectivity and re-use of the catalytic system. Furthermore, tripeptide **1**-supported materials have also been prepared and used as recyclable catalysts in the above reaction.

Results and discussion

In order to find the best support, we prepared the imidazolium-modified silica gels **4**, **7** and **12** (Scheme 1). These supports were used to immobilize L-proline. Modified silica gel **4** was prepared, as reported in our previous work, by condensation of 1-(3-trimethoxysilylpropyl)-2,3-dimethylimidazolium tetrafluoroborate **3** with silica gel (Merck 0.063−0.2 mm).[12b] Modified silica gels **7** and **12** were prepared by reaction between the 3-mercaptopropyl silica gel **14** and the tetrafluoroborate salt **6** or **9** in dichloromethane solution in the presence of α,α'-azoisobutyronitrile (AIBN). These compounds were obtained by reaction between 1,2-dimethyl imidazole and 6-chloro-1-hexene or 4-vinylbenzylchloride affording the chlorides **5** and **8**. The chlorides **5** and **8** were treated with sodium tetrafluoroborate in acetone to give the corresponding derivatives **6** and **9**.

In our previous work we observed better results using the BF_4 anion than PF_6 or Cl. We also prepared modified-silica gels **11** and **13** using the same linker but different anions.

The modified silica gels were characterized by ^{13}C NMR, elemental analysis and morphological properties (BET surface area, BJH average pore diameter and cumulative pore volume). The solid state ^{13}C NMR spectrum of **7** (Fig. 2a) showed similar signals to those of **6** (see Experimental) except for the complete absence of signals corresponding to the vinyl group. These results confirm that the reaction between the vinyl group of **6** and the surface thiol groups of the modified silica gel **14** proceeded to completion. Moreover, the main

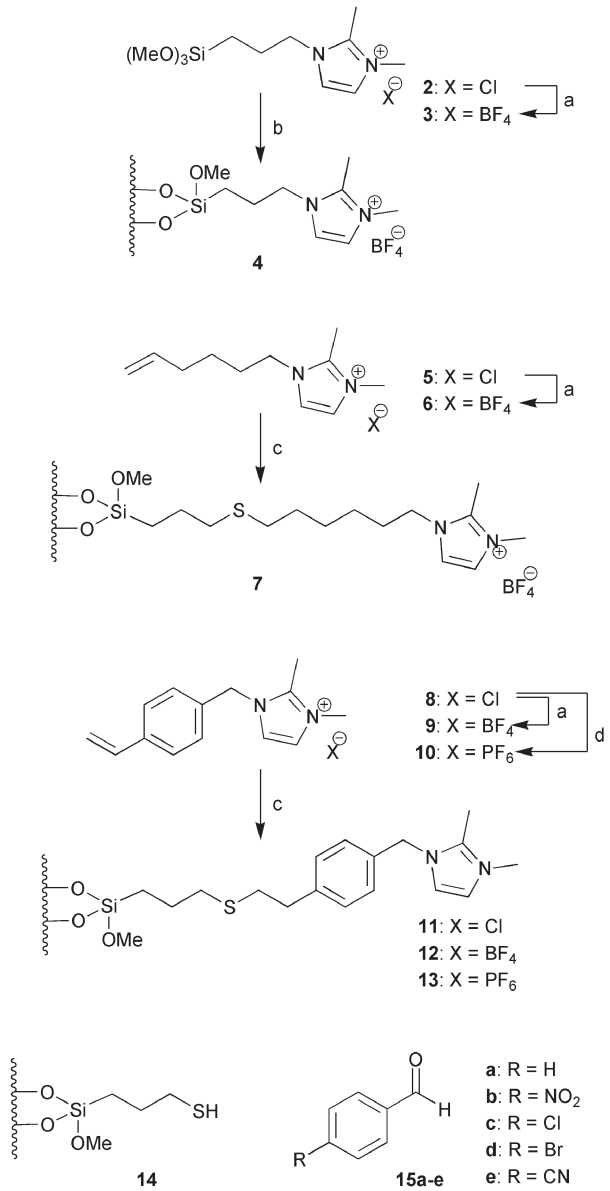

Scheme 1 Reagents and conditions: (a) $NaBF_4$ acetone, rt, 3 days; (b) SiO_2, $CHCl_3$, 65 °C, 26 h; (c) **14**, AIBN, CH_2Cl_2, reflux, 24 h; (d) $NaPF_6$ acetone, rt, 3 days.

structure of **6** is maintained after the grafting process. The same results can be deduced from analysis of the ^{13}C NMR spectrum of silica gel **12** (Fig. 2b).

Table 1 gives the morphological properties and elemental analyses of these modified silica gels. Modification of the starting silica gel (entry 6) with covalently attached ionic liquid (entries 1–5) gave materials with a lower surface area. Modified silica gel **7**, bearing a longer alkyl linker, and **11–13** bearing more sterically demanding aryl–alkyl linkers showed, as expected, lower surface area, pore diameter and pore volume than silica gel **4**.

Next, we started preliminary investigations of our supported materials. The proline-catalyzed aldol reaction between acetone and benzaldehyde was used as a probe reaction and monitored by ^1H NMR (Table 2). During the course of

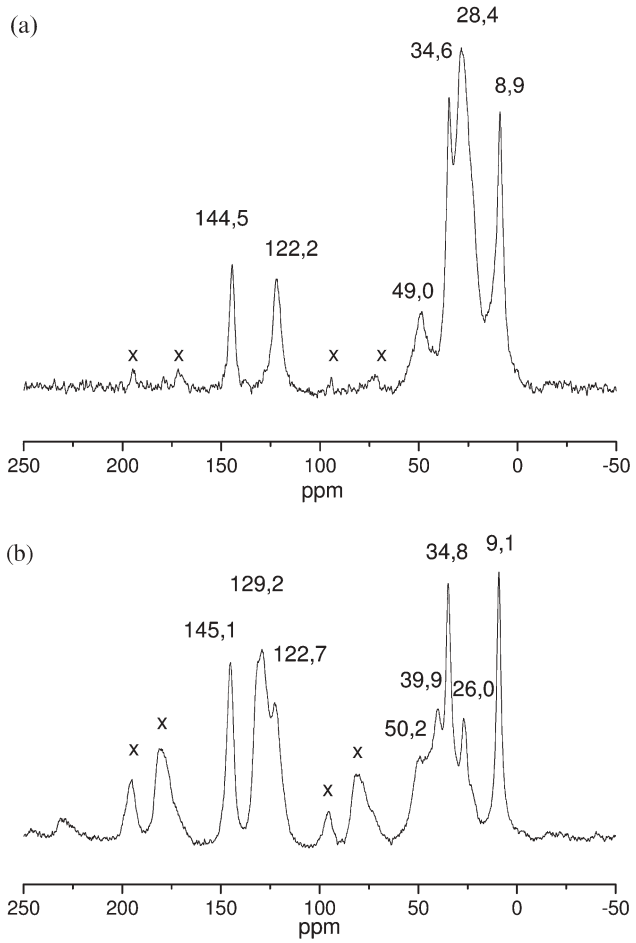

Fig. 2 Solid state ^{13}C NMR spectrum of: (a) **7**; (b) **12**. Side bands (x).

previous studies[12b] we observed different enantiomeric excess values arising from supported catalysts which were prepared using solvents during the catalyst adsorption stage, *e.g.* L-proline, adsorbed from a methanol solution rather than from water–acetonitrile solution. In order to select the most efficient solvent parameters, we adsorbed L-proline onto support **4**, both from methanol and water–acetonitrile solutions. Following removal of the solvent under reduced pressure, a powder was obtained (**4**–pro). Thermogravimetric analysis of **4**–pro materials obtained from proline adsorbed from water–acetonitrile and from methanol was then performed. Thermogravimetric analysis showed the presence of a first peak centred at around 100 °C, corresponding to water (moisture) desorption, and a second peak observed only in the case of the solid prepared from water–acetonitrile, centred at 220 °C, indicating the presence of coordinating water molecules. In all cases, we observed at around 400 °C the loss of the organic part of the modified silica compounds.

Table 2 Aldol reaction between acetone and benzaldehyde (**15a**) and recycling studies

Entry	Catalytic system	Cycle	**15a** (%)[a]	**16a** (%)[a]	e.e. **16a** (%)[b]
1[c]	**4**–pro	—	30	60	64
2	**4**–pro	1st	44	52	74
3	**4**–pro	2nd	52	44	72
4	**4**–pro	3rd	57	39	70
5	**4**–pro	4th	63	37	72
6	**7**–pro	1st	46	47	72
7	**7**–pro	2nd	43	51	71
8	**7**–pro	3rd	51	49	72
9	**7**–pro	4th	52	48	72
10	**12**–pro	1st	43	57	74
11	**12**–pro	2nd	47	53	74
12	**12**–pro	3rd	45	55	74
13	**12**–pro	4th	44	56	74

[a] Determined by ^1H NMR, the remaining amount is α,β-unsaturated product, mean values of duplicate experiments. [b] Determined by chiral HPLC, (*R*) configuration. [c] Proline adsorbed from water–acetonitrile solution.

The reaction was carried out by mixing the supported L-proline (30 mol%) with acetone and benzaldehyde at room temperature for 24 h. In order to minimize the amount of α,β-unsaturated product, we used a more dilute aldehyde solution with respect to our previous investigations (0.25 M instead of 0.5 M). The supported proline on silica gel **4** (**4**–pro from water–acetonitrile) gave the aldol product in 64% ee (Table 2, entry 1). The reaction conducted in the presence of **4**–pro (from methanol) afforded the aldol product with improved enantioselectivity (74%, Table 2, entry 2). The difference in these results can be ascribed to the water retained on the surface of modified silica gel when proline is adsorbed from water–acetonitrile solution. Indeed, it has already been reported that the addition of water severely compromises enantioselectivity in this process.[4b,18] For this reason, we decided to adsorb the proline on the modified silica gels from a methanolic solution. In order to examine the effect of the linker, additional adsorbed ionic liquid was temporarily omitted.[12]

We then investigated re-use of the supported catalyst. At the end of each reaction cycle, diethyl ether was added to the reaction mixture, and the modified silica gel was removed by filtration under reduced pressure. The organic filtrate was concentrated *in vacuo* affording the desired aldol products, and the supported catalyst was dried briefly under reduced pressure

Table 1 Morphological properties and elemental analyses of modified silica gels **4**, **7**, **11**, **12** and **13**

Entry	Modified silica gel	SSA[a]/m^2 g^{-1}	Average pore diameter[b]/Å	Cumulative pore volume/cm^3 g^{-1}	C (%)	H (%)	N (%)	S (%)
1	**4**	279	60	0.47	11.08	1.78	3.08	—
2	**7**	163	42	0.22	11.24	1.81	1.73	2.27
3	**11**	180	42	0.23	19.71	2.81	2.65	2.56
4	**12**	178	43	0.24	15.43	2.06	1.96	2.73
5	**13**	170	43	0.24	12.19	1.89	1.37	2.84
6	SiO_2 Merck	453	59	0.62				

[a] BET specific surface area. [b] BJH.

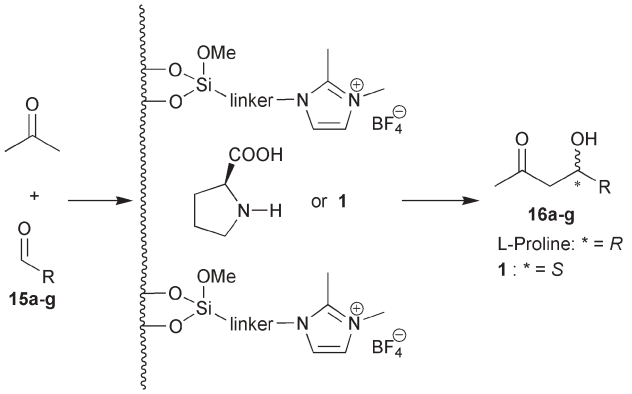

Scheme 2 Supported ionic liquid asymmetric catalysis.

before it was re-used. Three further reaction cycles were made using the catalyst isolated in this way. Each cycle gave similar ee values but a decreasing conversion was observed for the **4**–pro system. In Table 2 are reported the amount of product and unreacted aldehyde as determined by ^{1}H NMR. Very low amounts of the corresponding α,β-unsaturated products were observed. These results show that, probably at this stage, **12**–pro could be the most promising material. Noteworthily, the ee observed with **12**–pro (74%) is comparable to that obtained in pure ionic liquid[13c,d] and higher than that observed in neat acetone.[10] These results suggest that the covalently-attached monolayer of ionic liquid behaves as a bulk ionic liquid medium (Scheme 2).

In order to further evaluate the efficiency of these three materials as catalysts, we performed other aldol reactions using different aldehydes.

In the first cycle, we used p-nitrobenzaldehyde. Excellent yields, higher with respect to the reaction carried out in DMSO[4b] or ionic liquid,[13c] and good ee values were obtained (Table 3, entries 1–3). A second reaction cycle was performed using p-chlorobenzaldehyde (Table 3, entries 4–6). The three materials gave similar enantioselectivities and yield, except **7**–pro, which gave a higher yield. A third reaction cycle performed using p-bromobenzaldehyde (Table 3, entries 7–9) again showed no difference with regard to the enantioselectivity. The ee values obtained are comparable to those observed in DMSO[4b] or in ionic liquid.[13d] However, in this case **7**–pro and **12**–pro gave better yields than **4**–pro. A fourth cycle performed using p-cyanobenzaldehyde (Table 3, entries 10–12) gave different results between the supported catalysts. **12**–pro proved to be the best catalyst system and **4**–pro the worst, both in terms of yield and enantioselectivity. The ee obtained with **12**–pro (70%) is comparable to that obtained using proline in ionic liquid.[13c] In order to investigate if the catalytic systems work with the same efficiency, a fifth reaction cycle was carried out using again p-nitro-benzaldehyde, as was for the first reaction cycle (Table 3, entries 13–15). Again, the materials displayed different behaviour, mainly with regard to their relative catalytic activities. Indeed, each system gave similar enantioselectivities, which were almost identical to those obtained in the first reaction cycle. However, only the **12**–pro system afforded the product in excellent yield, whereas **4**–pro and **7**–pro gave poor conversion. In order to further assess the activity of catalyst system **12**–pro, we carried out two further reaction cycles. Again, excellent yields and reproducible ee values were obtained (Table 3, entries 16–17). In order to demonstrate the robustness of this system, two other reactions were carried out using cyclohexylaldehyde (**15f**) and isobutyraldehyde (**15g**) (Table 3, entries 18–19). Good results were obtained. Reactions between acetone and p-nitrobenzaldehyde in the presence of **11**–pro and **13**–pro were also carried out. Excellent yields and slightly lower ee values, compared to that obtained using **12**–pro, were observed.

Table 3 Aldol reaction between acetone and substituted benzaldehydes (**15b–g**) and recycling studies

Entry	Catalytic system	**15**	Cycle	**15** (%)[a]	**16** (%)[a]	e.e. **16** (%)[b]
1	**4**–pro	**b**	1st	—	99	70
2	**7**–pro	**b**	1st	—	93	70
3	**12**–pro	**b**	1st	—	96	73
4	**4**–pro	**c**	2nd	42	51	63
5	**7**–pro	**c**	2nd	13	79	66
6	**12**–pro	**c**	2nd	47	50	66
7	**4**–pro	**d**	3rd	52	43	69
8	**7**–pro	**d**	3rd	28	67	69
9	**12**–pro	**d**	3rd	30	65	70
10	**4**–pro	**e**	4th	30	67	54
11	**7**–pro	**e**	4th	12	83	64
12	**12**–pro	**e**	4th	—	99	70
13	**4**–pro	**b**	5th	73	27	72
14	**7**–pro	**b**	5th	70	30	70
15	**12**–pro	**b**	5th	—	97	70
16	**12**–pro	**b**	6th	—	98	70
17	**12**–pro	**b**	7th	—	98	70
18	**12**–pro	**f**	8th	—	60	85
19	**12**–pro	**g**	9th	—	94	95
20	**11**–pro	**b**	1st	—	98	71
21	**13**–pro	**b**	1st	—	99	68
22	**11**–pro	**b**	2nd	—	97	69
23	**11**–pro	**b**	3rd	10	90	70
24	**11**–pro	**b**	4th	27	73	69

[a] Isolated yield. [b] Determined by chiral HPLC, (*R*) configuration.

Recycling studies using **11**–pro showed a decreased conversion after four cycles, although enantioselectivities were unchanged. Comparison of selectivity values with those observed in pure acetone[10] showed that in our case, higher enantioselectivities can be realized. These ee values are similar to those obtained in pure ionic liquid or ionic liquid-anchored-proline.

The catalytically active tripeptide H–Pro–Pro–Asp–NH_2 (**1**) is more expensive than L-proline, and hence its recovery and re-use is of still higher value, from an economical point of view. Given the interesting results obtained using L-proline, we were intrigued to evaluate the properties of **1** immobilized on modified silica gels **12** (**12**–**1**). In order to draw an accurate comparison between the immobilized proline catalysts, we supported tripeptide **1** on modified silica gels **11**, **12** and **13** (**11**–**1**, **12**–**1**, **13**–**1**).

Catalytic system **12**–**1** was used four times at 25 °C. The catalyst loading was 5 mol% and the reaction was stopped after four hours. The first and the second reaction cycles gave excellent yields while the following two cycles gave lower conversion (Table 4, entries 1–4). However, reproduction of good enantioselectivity was observed in all reaction cycles. These ee values are slightly lower than that observed with the unsupported peptide.[7] When the reaction was carried out at −20 °C the enantioselectivity increased (Table 4, entries 5–8).

Table 4 Aldol reaction between acetone and p-nitrobenzaldehyde with catalytic systems **12**–**1**, **11**–**1** and **13**–**1**

Entry	Cycle	Catalytic system[a]	*T*/°C	*t*/h	**16b** (%)[b]	**15b** (%)[b]	e.e. **16b** (%)[c]
1	1	**12**–**1**	25	4	99	—	74
2	2	**12**–**1**	25	4	99	—	75
3	3	**12**–**1**	25	4	64	35	72
4	4	**12**–**1**	25	4	57	43	73
5	1	**12**–**1**	−20	24	91	6	83
6	2	**12**–**1**	−20	24	75	25	83
7	3	**12**–**1**	−20	24	54	46	82
8	4	**12**–**1**	−20	24	42	58	82
9	1	**11**–**1**	25	4	99	—	80
10	2	**11**–**1**	25	4	40	60	80
11	3	**11**–**1**	25	4	35	65	80
12	4	**11**–**1**	25	4	26	73	74
13	1	**11**–**1**	−20	24	99	—	86
14	2	**11**–**1**	−20	24	38	62	83
15	1	**13**–**1**	25	4	99	—	78
16	2	**13**–**1**	25	4	30	70	68
17	3	**13**–**1**	25	4	33	67	62
18	4	**13**–**1**	25	4	30	70	58

[a] Catalyst loading 5 mol%. [b] Isolated yield. [c] Determined by chiral HPLC, (*S*) configuration.

Once more, we observed stable enantioselectivities after four reaction cycles, albeit with a decreasing conversion. The use of a different counter ion (Cl^-, **11**–**1**) improved the ee value, especially at 25 °C, but the conversion after four reaction cycles was low (Table 4, entries 9–12). At −20 °C the conversion was low even in the second reaction cycle (Table 4, entries 13–14). In the case of PF_6-modified material (**13**–**1**), both yields and ee values decreased after four cycles (Table 4, entries 15–18).

Conclusions

We have investigated the preparation of a number of novel surface modified silica gels functionalized with ionic liquids, and their application as valuable supports for 2 different organocatalysts. We have used these supports for the immobilization of L-proline, and demonstrated that better enantioselectivities are obtained when the catalyst is adsorbed from a methanol solution, rather than from aqueous solutions. Moreover, both enantioselectivities and yields are comparable or better than those obtained under homogeneous conditions. Comparison of our data with literature values shows that the monolayer of covalently-attached ionic liquid behaves as a bulk ionic liquid. It is worthy to mention that our system gave higher enantioselectivities with respect to those obtained in pure acetone. These results indicate that **12**–pro material is superior to both **4**–pro and **7**–pro. This difference is clearly seen after at least three reaction cycles. The lower performance as support of silica gel **4** may be due to its different morphological properties. The different performances of silica gels **11**, **12** and **13** may be due to the different nature of the anion. Silica gel **7**, which has the same anion and similar morphological properties with respect to **12**, showed similar results, at least in the first four cycles. Tripeptide H–Pro–Pro–Asp–NH_2 was supported on silica gel **12** because of the better overall performance of this support. The use of chloride- or hexafluorophosphate-modified silica gels **11** and **13** gave higher enantioselectivities in the first reaction cycle. However, recycling studies further indicated that silica gel **12** was indeed the best support. Comparison between proline- and tripeptide-supported catalysts showed that the former material is more recyclable. Indeed, the L-proline-supported material **12**–pro can be used at least up to nine times with unchanged yield and selectivity. Studies are in progress for further application of these supported catalysts.

Experimental

General

^{1}H NMR and ^{13}C NMR spectra were recorded on a Bruker AC-E series 250 MHz spectrometer. FT-IR spectra were registered with a Nicolet 710 or with a Shimadzu FTIR 8300 infrared spectrophotometer. Carbon, hydrogen and nitrogen content was determined by combustion analysis in a Fisons EA 1108 elemental analyzer. Specific surface area and pore size distributions were measured by recording the nitrogen adsorption/desorption isotherms at liquid N_2 temperature using a Micromeritics ASAP 2010 system. Pore size distribution was determined from the desorption branch of the isotherm by the BJH (Barrett–Joyner–Halenda) method using Halsey equation. Solid-state ^{13}C MAS NMR spectra were recorded on a Bruker AV 400, 400 MHz spectrometer with samples packed in zirconia rotors spinning at 5 kHz. Chiral HPLC were performed using a Shimadzu LC-10AD pump with a SPD-M10A UV detector and Daicel columns.[12b] Compounds **16a–e** showed spectroscopic and analytical data in agreement with their structures.[12b]

1-(5-hexen)- 2,3-dimethyl-imidazolium chloride (5)

A mixture of 1,2-dimethyl-imidazole (1.92 g, 0.02 mol) and 6-chloro-1-hexene (2.75 mL, 0.02 mol) was heated under argon atmosphere at 95 °C for 18 h. After cooling a viscous brown oil was formed. The oil was washed several times with diethyl ether, then dried under reduced pressure to give **5** as a light brown oil (4.24 g, 96%). ^{1}H NMR (CD_3OD) δ 1.41–1.53 (m, 2H), 1.77–1.90 (m, 2H), 2.09–2.18 (m, 2H), 2.63 (s, 3H), 3.83 (s, 3H), 4.17 (t, J = 7.2 Hz, 2H), 4.94–5.08 (m, 2H), 5.73–5.90 (m, 1H), 7.49 (d, J = 2.1 Hz, 1H), 7.53 (d, J = 2.1 Hz, 1H). ^{13}C NMR (CD_3OD) δ 9.5, 26.5, 30.1, 34.0, 35.4, 49.2, 115.6, 122.1, 123.6, 139.0, 145.8. (liquid film) ν = 1640, 1589 cm^{-1}. Anal. calcd. for $C_{11}H_{19}ClN_2$: C, 61.53, H, 8.92, N, 13.05. Found: C, 61.70; H, 8.99; N, 13.10.

1-(5-hexen)-2,3-dimethyl-imidazolium tetrafluoroborate (6)

Salt **5** (4.2 g, 0.0196 mol) was dissolved in methanol (6 mL), then acetone (90 mL) was added followed by sodium tetrafluoroborate (2.26 g, 0.0205 mol) in one portion. The mixture was stirred at room temperature for 3 days. After this time the mixture was filtered and the solution evaporated under reduced pressure. A yellow oil was obtained. The oil was dissolved in a small amount of acetone and filtered again under reduced pressure on a short pad of silica gel. The solution was evaporated under reduced pressure to give **6** (4.5 g, 86%) as a pale yellow oil. ^{1}H NMR (acetone-d_6) δ 1.43–1.53 (m, 2H), 1.81–1.92 (m, 2H), 2.07–2.15 (m, 2H), 2.73

(s, 3H), 3.89 (s, 3H), 4.26 (t, J = 7.2 Hz, 2H), 4.92–5.05 (m, 2H), 5.73–5.88 (m, 1H), 7.55 (d, J = 1.9 Hz, 1H), 7.59 (d, J = 1.9 Hz, 1H). ^{13}C NMR (acetone-d_6) δ 10.0, 26.4, 30.3, 34.1, 35.8, 49.2, 115.8, 122.2, 123.7, 139.5, 146.0. IR (nujol) ν = 1640, 1590, 1538 cm^{-1}. Anal. calcd. for $C_{11}H_{19}BF_4N_2$: C, 49.65, H, 7.20, N, 10.53. Found: C, 49.72; H, 7.24; N, 10.88.

1-(4-vinylbenzyl)- 2,3-dimethyl-imidazolium chloride (8)

A mixture of 1,2-dimethyl-imidazole (3.84 g, 0.04 mol) and 4-vinylbenzylchloride (8.15 mL, 0.052 mol) in chloroform (33 mL) was heated under argon atmosphere at 50 °C for 8 h. After cooling, the solvent was removed under reduced pressure to give a viscous oil. Diethyl ether was added, and after mechanical stirring with a spatula, a white solid was formed. It was filtered off and washed with more diethyl ether. White igroscopic solid (9.3 g, 93%). ^{1}H NMR ($CDCl_3$) δ 2.60 (s, 3H), 3.80 (s, 3H), 5.16 (d, J = 10.9 Hz, 1H), 5.43 (s, 2H), 5.63 (d, J = 17.5 Hz, 1H), 6.54 (dd, J = 17.5 and 10.9 Hz, 1H), 7.18–7.27 (m, 4H), 7.58–7.62 (m, 2H). ^{13}C NMR ($CDCl_3$) δ 10.5, 35.5, 51.6, 114.9, 121.5, 122.7, 126.7, 128.3, 132.7, 135.6, 137.8, 144.0. IR (nujol) ν = 1589, 1537 cm^{-1}. Anal. calcd. for $C_{14}H_{17}ClN_2$: C, 67.60, H, 6.89, N, 11.26. Found: C, 67.70; H, 6.99; N, 11.50.

1-(4-vinylbenzyl)- 2,3-dimethyl-imidazolium tetrafluoro-borate (9)

Salt **7** (8.00 g, 0.032 mol) was dissolved in methanol (10 mL), then acetone (150 mL) was added followed by sodium tetrafluoroborate (3.69 g, 0.0336 mol) in one portion. The mixture was stirred at room temperature for 3 days. After this time the mixture was filtered and the solution evaporated under reduced pressure. A white solid was obtained. The solid was dissolved in a small amount of acetone and filtered again. The solvent was removed under reduced pressure to give **9** as a white solid (9.00 g, 94%). M.p. 93–95 °C. ^{1}H NMR (acetone-d_6) δ 2.79 (s, 3H), 3.96 (s, 3H), 5.28 (d, J = 10.6 Hz, 1H), 5.53 (s, 2H), 5.85 (d, J = 18.4 Hz, 1H), 6.77 (dd, J = 18.4 and 10.6 Hz, 1H), 7.38 (d, J = 8.2 Hz, 2H), 7.53 (d, J = 8.2 Hz, 2H), 7.64 (s, 2H). ^{13}C NMR (acetone-d_6) δ 10.6, 36.2, 52.6, 115.8, 122.8, 124.3, 128.3, 129.8, 135.3, 137.6, 139.5, 146.7. IR (nujol) ν = 1591, 1541 cm^{-1}. Anal. calcd. for $C_{14}H_{17}BF_4N_2$: C, 56.03, H, 5.71, N, 9.33. Found: C, 56.20; H, 5.77; N, 9.50.

1-(4-vinylbenzyl)- 2,3-dimethyl-imidazolium hexafluoro-phosphate (10)

Following the above procedure compound **10** was obtained in 90% yield. M.p. 84–87 °C. ^{1}H NMR (acetone-d_6) δ 2.73 (s, 3H), 3.91 (s, 3H), 5.28 (d, J = 10.9 Hz, 1H), 5.47 (s, 2H), 5.85 (d, J = 17.7 Hz, 1H), 6.76 (dd, J = 17.7 and 10.9 Hz, 1H), 7.37 (d, J = 8.2 Hz, 2H), 7.52 (d, J = 8.2 Hz, 2H), 7.55 (s, 2H). ^{13}C NMR (acetone-d_6) δ 10.5, 36.1, 52.6, 115.9, 122.7, 124.2, 128.3, 129.7, 135.0, 137.6, 139.5, 146.6. IR (nujol) ν = 1593, 1541 cm^{-1}. Anal. calcd. for $C_{14}H_{17}F_6N_2P$: C, 46.93, H, 4.78, N, 7.82. Found: C, 47.08; H, 4.85; N, 7.91.

Synthesis of thiol functionalized silica gel (14)

Silica gel (Merck, 0.063–0.2 mm, 4.0 g) was pre-activated by heating the material for 3 h at 300 °C under vacuum. After cooling, toluene (15 mL) and 3-mercaptopropyltrimethoxy silane (10 mmol, 1.9 mL) were sequentially added. The mixture was stirred for 24 h at reflux temperature, then cooled, and the solvent was filtered off. The residual unreacted silane was removed by soxhlet extraction of the solid with methanol.

General synthesis for the ionic liquid modified silica gels

Thiol functionalized silica gel (2.0 g) was suspended in dichloromethane (10 mL) and the appropriate ionic liquid (4.0 mmol) was added. The mixture was stirred, under argon, in the presence of a catalytic amount of AIBN at reflux temperature. After cooling, the solvent was filtered off and the possible unreacted ionic liquid was removed by soxhlet extraction of the silica with dichloromethane.

Imidazolium-modified silica gel **7**: solid state ^{13}C NMR δ: 8.9, 28.4, 34.6, 49.0, 122.2, 144.5.

Imidazolium-modified silica gel **12**: solid state ^{13}C NMR δ: 9.1, 26.0, 34.8, 39.9, 50.2, 122.2, 129.2, 145.1.

General procedure for the supported proline materials

In a round bottom flask L-proline (17.5 mg, 0.15 mmol) was dissolved in methanol (0.9 mL). To this solution the modified silica gel was added (500 mg). The mixture was shaken for a few minutes then evaporated under reduced pressure for 25 h to give a free-flowing powder.

General procedure for the supported peptide materials

In a round bottom flask trifluoroacetic acid salt of peptide **1** (22 mg, 0.05 mmol) was dissolved in methanol (2.0 mL). To this solution the modified silica gel was added (200 mg). The mixture was shaken for a few minutes then evaporated under reduced pressure for 25 h to give a free-flowing powder.

General procedure for aldol reaction

A solution of aldehyde (0.5 mmol) in acetone (2 mL) was added to **4**/pro (or **7**/pro or **12**/pro) system (520 mg, L-proline 30% mol). The mixture was stirred at room temperature for 24 h. After this time the modified silica gel was taken up with diethyl ether and filtered under reduced pressure. The solution was evaporated, checked by NMR and finally purified by chromatography (light petroleum/ethyl acetate) to give the aldol product. The catalytic system was dried for a few minutes and then re-used. In the case of supported peptide materials to a solution of aldehyde (1 mmol) in acetone (4 mL), *N*-methylmorpholine (0.05 mmol) was added.

Acknowledgements

This work was supported by the Swiss National Science Foundation and BACHEM, from the University of Palermo (Funds for selected topics) and Italian MIUR within the National Project "Catalizzatori, metodologie e processi innovativi per il regio- e stereocontrollo delle sintesi organiche".

References

1 (*a*) *Asymmetric Organocatalysis: From Biomimetic Concepts to Applications in Asymmetric Synthesis*, ed. A. Berkessel and

H. Gröger, Wiley-VCH, Weinheim, 2005; (*b*) P. I. Dalko and L. Moisan, *Angew. Chem., Int. Ed.*, 2004, **43**, 5138–5175; (*c*) J. Seayad and B. List, *Org. Biomol. Chem.*, 2005, **3**, 719–724; (*d*) G. Guillena and D. J. Ramón, *Tetrahedron: Asymmetry*, 2006, **17**, 1465–1492; (*e*) Other interesting recent examples can be find in the following issues devoted to organocatalysis: *Acc. Chem. Res.*, 2004, **37**, 8, pp. 631–847; *Adv. Synth. Catal.*, 2004, **346**, 9–10, pp. 1007–1249; *Tetrahedron*, 2006, **62**, 2–3, pp. 243–502.

2 (*a*) T. Welton, *Chem. Rev.*, 1999, **99**, 2071–2084; (*b*) D. Zhao, M. Wu, Y. Kou and E. Min, *Catal. Today*, 2002, **74**, 157–189; (*c*) *Ionic Liquids in Synthesis*, ed. P. Wasserscheid and T. Welton, Wiley-VCH, Weinheim, 2003.

3 (*a*) B. List, *Tetrahedron*, 2002, **58**, 5573–5590; (*b*) E. R. Jarvo and S. J. Miller, *Tetrahedron*, 2002, **58**, 2481–2495.

4 (*a*) B. List, R. A. Lerner and C. F. Barbas, III, *J. Am. Chem. Soc.*, 2000, **122**, 2395–2396; (*b*) K. Sakthivel, W. Notz, T. Bui and C. F. Barbas, III, *J. Am. Chem. Soc.*, 2001, **123**, 5260–5267; (*c*) Selected recent examples on proline-catalyzed aldol reactions: C. Grondal and D. Enders, *Tetrahedron*, 2006, **62**, 329–337; (*d*) J. T. Suri, D. B. Ramachary and C. F. Barbas, III, *Org. Lett.*, 2005, **7**, 1383–1385; (*e*) R. I. Storer and D. W. C. MacMillan, *Tetrahedron*, 2004, **60**, 7705–7714; (*f*) J. Casas, H. Sundén and A. Córdova, *Tetrahedron Lett.*, 2004, **45**, 6117–6119; (*g*) Q. Pan, B. Zou, Y. Wang and D. Ma, *Org. Lett.*, 2004, **6**, 1009–1012; (*h*) A. B. Northrup, I. K. Mangion, F. Hettche and D. W. C. MacMillan, *Angew. Chem., Int. Ed.*, 2004, **43**, 2152–2154.

5 (*a*) B. M. Trost, *Science*, 1991, **254**, 1471–1477; (*b*) B. M. Trost, *Angew. Chem., Int. Ed.*, 1995, **34**, 259–281.

6 (*a*) D. Gryko, M. Zimnicka and R. Lipiński, *J. Org. Chem.*, 2007, **72**, 964–970; (*b*) S. Samanta and C.-C. Zhao, *Tetrahedron Lett.*, 2006, **47**, 3383–3386; (*c*) J.-F. Zheng, Y.-X. Li, S.-Q. Zhang, S.-T. Yang, X.-M. Wang, Y.-Z. Wang, J. Bai and F.-A. Liu, *Tetrahedron Lett.*, 2006, **47**, 7793–7796; (*d*) Z. Thang, Z.-H. Yang, X.-H. Chen, L.-F. Cun, A.-Q. Mi, Y.-Z. Jiang and L.-Z. Gong, *J. Am. Chem. Soc.*, 2005, **127**, 9285–9289; (*e*) Z. Thang, F. Jiang, L.-T. Yu, X. Cui, L.-Z. Gong, A.-Q. Mi, Y.-Z. Jiang and Y.-D. Wu, *J. Am. Chem. Soc.*, 2003, **125**, 5262–5263; (*f*) Z. Tang, Z.-H. Yang, L.-F. Cun, L.-Z. Gong, A.-Q. Mi and Y.-Z. Jiang, *Org. Lett.*, 2004, **6**, 2285–2287; (*g*) S. Samanta, J. Liu, R. Dodda and C.-G. Zhao, *Org. Lett.*, 2005, **7**, 5321–5323; (*h*) A. Berkessel, B. Koch and J. Lex, *Adv. Synth. Catal.*, 2004, **346**, 1141–1146.

7 P. Krattiger, R. Kovasy, J. D. Revell, S. Ivan and H. Wennemers, *Org. Lett.*, 2005, **7**, 1101–1103.

8 For review, see: J. H. Davis, *Chem. Lett.*, 2004, **33**, 1072–1077.

9 (*a*) J. Fraga-Dubreuil and J. P. Bazureau, *Tetrahedron Lett.*, 2001, **42**, 6097–6100; (*b*) J. Fraga-Dubreuil and J. P. Bazureau, *Tetrahedron*, 2003, **59**, 6121–6130; (*c*) Q. Yao and Y. Zhang, *Angew. Chem., Int. Ed.*, 2003, **42**, 3395–3398; (*d*) S. T. Handy and M. Okello, *Tetrahedron Lett.*, 2003, **44**, 8399–8402; (*e*) M. De Kort, A. W. Tuin, S. Kuiper, H. S. Overkleeft, G. A. Van der Marel and R. C. Buijsman, *Tetrahedron Lett.*, 2004, **45**, 2171–2175; (*f*) S. Anjaiah, S. Chandrasekhar and R. Gree, *Tetrahedron Lett.*, 2004, **45**, 569–571; (*g*) S. T. Handy and M. Okello, *J. Org. Chem.*, 2005, **70**, 2874–2877; (*h*) F. Yi, Y. Peng and G. Song, *Tetrahedron Lett.*, 2005, **46**, 3931–3933; (*i*) X.-E. Wu, L. Ma, M.-X. Ding and L.-X. Gao, *Synlett*, 2005, 607–610.

10 W. Miao and T.-H. Chan, *Adv. Synth. Catal.*, 2006, **348**, 1711–1718.

11 For review, see: (*a*) J. Ding and D. W. Armstrong, *Chirality*, 2005, **17**, 281–292; (*b*) C. Baudequin, J. Baudoux, J. Levillain, D. Cahard, A.-C. Gaumont and J.-C. Plaquevent, *Tetrahedron: Asymmetry*, 2003, **14**, 3081–3093; (*c*) Selected recent examples: B. Pegot, G. Vo-Thanh, D. Gori and A. Loupy, *Tetrahedron Lett.*, 2004, **45**, 6425–6428; (*d*) Z. Wang, Q. Wang, Y. Zhang and W. Bao, *Tetrahedron Lett.*, 2005, **46**, 4657–4660; (*e*) J. Ding, V. Desikan, X. Han, T. L. Xiao, R. Ding, W. S. Jenks and D. W. Armstrong, *Org. Lett.*, 2005, **7**, 335–337.

12 (*a*) M. Gruttadauria, S. Riela, P. Lo Meo, F. D'Anna and R. Noto, *Tetrahedron Lett.*, 2004, **45**, 6113–6116; (*b*) M. Gruttadauria, S. Riela, C. Aprile, P. Lo Meo, F. D'Anna and R. Noto, *Adv. Synth. Catal.*, 2006, **348**, 82–92.

13 (*a*) M. Benaglia, M. Cinquini, F. Cozzi, A. Puglisi and G. Celentano, *Adv. Synth. Catal.*, 2002, **344**, 533–542; (*b*) M. Benaglia, G. Celentano and F. Cozzi, *Adv. Synth. Catal.*, 2001, **343**, 171–175; (*c*) P. Kotrusz, I. Kmentová, B. Gotov, Š. Toma and E. Solčániová, *Chem. Commun.*, 2002, 2510–2511; (*d*) T.-P. Loh, L.-C. Feng, H.-Y. Yang and J.-Y. Yang, *Tetrahedron Lett.*, 2002, **43**, 8741–8743; (*e*) A. Córdova, *Tetrahedron Lett.*, 2004, **45**, 3949–3952; (*f*) S. Chandrasekhar, Ch. Narsihmulu, N. Ramakrishna Reddy and S. Shameen Sultana, *Tetrahedron Lett.*, 2004, **45**, 4581–4582; (*g*) G. Szöllősi, G. London, L. Baláspiri, C. Somlai and M. Bartók, *Chirality*, 2003, **15**, S90–S96; (*h*) F. Calderón, R. Fernández, F. Sánchez and A. Fernández-Mayoralas, *Adv. Synth. Catal.*, 2005, **347**, 1395–1403; (*i*) S. Chandrasekhar, N. Ramakrishna Reddy, S. Shameen Sultana, Ch. Narsihmulu and K. Venkatram Reddy, *Tetrahedron*, 2006, **62**, 338–345.

14 (*a*) F. Giacalone, M. Gruttadauria, A. Mossuto Marculescu and R. Noto, *Tetrahedron Lett.*, 2007, **48**, 255–259; (*b*) M. Gruttadauria, F. Giacalone, A. Mossuto Marculescu, P. Lo Meo, S. Riela and R. Noto, *Eur. J. Org. Chem.*, 2007, 4688–4698.

15 D. Font, C. Jimeno and M. A. Pericás, *Org. Lett.*, 2006, **8**, 4653–4655.

16 K. Akagawa, S. Sakamoto and K. Kudo, *Tetrahedron Lett.*, 2005, **46**, 8185–8187.

17 J. D. Revell, D. Gantenbein, P. Krattiger and H. Wennemers, *Biopolymers*, 2006, **84**, 105–113.

18 In some cases addition of water may have a beneficial effect: see (*a*) P. M. Pihko, K. M. Laurikainen, A. Usano, A. I. Nyberg and J. A. Kaavi, *Tetrahedron*, 2006, **62**, 317–328; (*b*) For organocatalytic aldol reactions in water see: N. Mase, Y. Nakai, N. Ohara, H. Yoda, K. Takabe, F. Tanaka and C. F. Barbas, III, *J. Am. Chem. Soc.*, 2006, **128**, 734–735; (*c*) Y. Hayashi, T. Sumiya, J. Takahashi, H. Gotoh, T. Urushima and M. Shoji, *Angew. Chem., Int. Ed.*, 2006, **45**, 958–961 and references 14 and 15.

"On water" organic synthesis: a highly efficient and clean synthesis of 2-aryl/heteroaryl/styryl benzothiazoles and 2-alkyl/aryl alkyl benzothiazolines†

Asit K. Chakraborti,* Santosh Rudrawar, Kirtikumar B. Jadhav, Gurmeet Kaur and Sunay V. Chankeshwara

Received 9th July 2007, Accepted 17th September 2007
First published as an Advance Article on the web 10th October 2007
DOI: 10.1039/b710414f

A convenient and clean "on water"-mediated synthesis of benzothiazoles/benzothiazolines is reported. Aromatic, heteroaromatic, and styryl aldehydes are converted to 2-substituted benzothiazoles in high yields in a one-pot reaction with 2-aminothiophenol in water at 110 °C (oil-bath). Alkyl and aryl alkyl aldehydes afforded the benzothiazolines. The reaction is highly chemoselective with no competitive thia-Michael addition, *O*-dealkylation/debenzoylation, reduction of the nitro or the α,β-unsaturated carbonyl groups, and substitution of the halogen atom or the nitro group. The reaction is found to be general with respect to the 2-aminothiophenol substrate through the reaction of a few substituted 2-aminothiophenols with a few representative aromatic and aliphatic aldehydes. The procedure does not involve the use of any additional reagent/catalyst, produces no waste, and represents a green synthetic protocol.

Inroduction

There has been growing concern over the environmental impact of chemicals so that cleaner green reaction conditions in synthetic processes have been advocated. The tight legislation to maintain greenness requires us to prevent the generation of waste, avoid use of auxiliary substances (*e.g.*, organic solvents, additional reagents) and minimize the energy requirement.[1] In this context, the use of water as the reaction medium offers several advantages as: (i) it is cheap, non-inflammable, non-toxic and safe for use; (ii) it eliminates the additional efforts required to make the substrates/reagents dry before use and thus reduces/eliminates the consumption of drying agents, energy and time; (iii) the unique physical and chemical properties of water often increase the reactivity or selectivity unattainable in organic solvents;[2] and (iv) the product may be easily isolated by filtration. Thus, reactions in aqueous medium have gained considerable momentum.[3–5] We have focused our attention on the development of a green synthesis of benzothiazoles due to their wide ranges of application, *e.g.*, potential therapeutic agents for various diseases,[6] enzyme inhibitors,[7] plant growth regulator,[8] *in vivo* imaging,[9] fluorescence material,[10] and dyes.[11]

The various reported methodologies (Scheme 1 and ref. 12) have one or more disadvantages such as the requirement of: (i) stringent reaction conditions, *e.g.*, heating in the presence of excess of PPA at 150–220 °C for 2–4 h or P_2O_5–$MeSO_3H$ at 70 °C for 10 h, heating at 160 °C for 5 h or reflux in toluene for 24 h in the presence of 4 equiv of Me_3Al, microwave heating in ionic liquids or in the presence of excess of *p*-TsOH adsorbed on SiO_2/K 10 and graphite, treatment with stoichiometric amounts of oxidizing agents such as $K_3Fe(CN)_6$ at 90 °C under basic conditions and excess of $Mn(OAc)_3$ in AcOH at 110 °C for 4 h; (ii) prolonged reaction time (2 h to 4 d); (iii) additional reagents/catalysts, high boiling solvents that are difficult to recover; (iv) costly, air sensitive, and toxic substances; and (v) lack of the ease of availability/preparation of the starting material/reagent, *etc.* In many cases the acidic/metallic wastes are generated and mixed with the effluent water. These necessitate the development of a more efficient/convenient and environmentally friendly methodology.

Results and discussion

We report herein an efficient synthesis of 2-substituted benzothiazoles/thiazolines in water in the absence of any acid/base catalyst. The reaction of aryl, heteroaryl, and styryl aldehydes with 2-aminothiophenol afforded the benzothiazoles in excellent yields (Table 1). Alkyl and aryl alkyl aldehydes gave the benzothiazolines. As comparable results were obtained in tap and distilled water, the reactions were carried out in tap water so that the efforts and the consumption of energy needed to prepare distilled water are avoided. In general, the products settled down on cooling the reaction mixture (room temperature or ice–water bath) and were

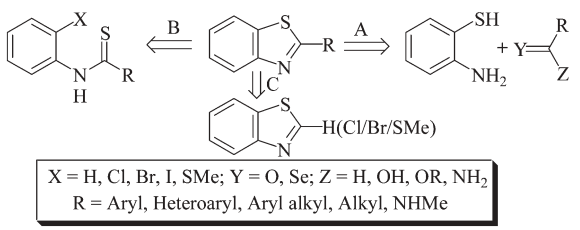

Scheme 1 Strategies for the synthesis of benzothiazoles.

Department of Medicinal Chemistry, National Institute of Pharmaceutical Education and Research (NIPER), Sector 67, S. A. S. Nagar 160 062, Punjab, India. E-mail: akchakraborti@niper.ac.in; Fax: +91 (0)172 2214692; Tel: +91 (0)172 2214683
† Electronic supplementary information (ESI) available: spectral data of all compounds and solvent study. See DOI: 10.1039/b710414f

Table 1 Synthesis of benzothiazoles/benzothiazolines by reaction of aldehydes with 2-aminothiophenol in water[a]

Entry	Aldehyde	Time/h	Yield (%)[b,c]	Entry	Aldehyde	Time/h	Yield (%)[b,c]
	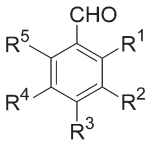			26	$R^1 = R^4 = R^5 = H$; $R^2 = OBu^n$; $R^3 = OMe$	4	85
1	$R^1 = R^2 = R^3 = R^4 = R^5 = H$	2.5	94[d,e,f]	27	$R^1 = R^4 = R^5 = H$; $R^2 = OCH_2CH{=}CH_2$; $R^3 = OMe$	4	90
2	$R^1 = R^2 = R^4 = R^5 = H$; $R^3 = Me$	3	95	28	$R^1 = R^4 = R^5 = H$; $R^2 = OCH_2CH{=}C(CH_3)_2$; $R^3 = OMe$	5	85
3	$R^1 = R^2 = R^4 = R^5 = H$; $R^3 = OMe$	3	98	29	$R^1 = R^4 = R^5 = H$; $R^2 = OC_5H_9$[c]; $R^3 = OMe$	6	82
4	$R^1 = R^2 = R^4 = R^5 = H$; $R^3 = NO_2$	3	96	30	$R^1 = R^4 = R^5 = H$; $R^2 = OMe$; $R^3 = OC_5H_9$[c]	6	88
5	$R^1 = R^2 = R^4 = R^5 = H$; $R^3 = F$	3	94	31	$R^1 = R^4 = R^5 = H$; $R^2 = R^3 = OCHF_2$	3	85
6	$R^1 = R^2 = R^4 = R^5 = H$; $R^3 = Cl$	3	96	32	$R^1 = R^4 = R^5 = H$; $R^2 = OCHF_2$; $R^3 = OCH_2CH(CH_2)_2$	3	88
7	$R^1 = R^2 = R^4 = R^5 = H$; $R^3 = NMe_2$	3	89	33	$R^1 = R^4 = R^5 = H$; $R^2 = OMe$; $R^3 = OCOPh$	3	85
8	$R^1 = R^2 = R^4 = R^5 = H$; $R^3 = OH$	3	85		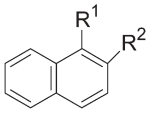		
9	$R^1 = R^3 = R^4 = R^5 = H$; $R^2 = OH$	3	83	34	$R^1 = CHO$; $R^2 = H$	3	91
10	$R^1 = R^2 = R^4 = R^5 = H$; $R^3 = CN$	3	93	35	$R^1 = H$; $R^2 = CHO$	3	95
11	$R^1 = R^4 = R^5 = H$; $R^2 = R^3 = OH$	3	82		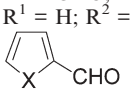		
12	$R^1 = R^4 = OH$, $R^2 = R^3 = R^5 = H$	3	80	36	X = O	3	82
13	$R^1 = R^2 = OMe$; $R^3 = R^4 = R^5 = H$	3	89	37	X = S	3	88
14	$R^1 = R^4 = R^5 = H$; $R^2 = R^3 = OMe$	3	90		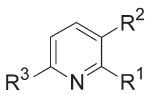		
15	$R^1 = R^5 = H$; $R^2 = R^3 = R^4 = OMe$	3	81	38	$R^1 = CHO$; $R^2 = R^3 = H$	3	93
16	$R^1 = R^4 = R^5 = H$; $R^2 = OH$, $R^3 = OMe$	3	86	39	$R^1 = R^3 = H$; $R^2 = CHO$	3	88
17	$R^1 = R^4 = R^5 = H$; $R^2 = OMe$ $R^3 = OH$	3	81	40	$R^1 = R^3 = Cl$; $R^2 = CHO$	4	90
18	$R^1 = R^5 = H$; $R^2 = R^4 = OMe$, $R^3 = OH$	3	90	41	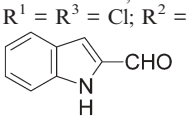	4	85
19	$R^2 = R^3 = R^5 = H$; $R^1 = OH$; $R^4 = NO_2$	3	86	42	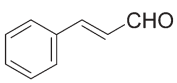	3	80
20	$R^1 = R^3 = R^5 = Br$; $R^2 = OH$; $R^4 = H$	7	94[g]		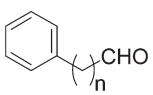		
21	$R^1 = R^4 = R^5 = H$; R^2, $R^3 = OCH_2O$	3	93	43	n = 1	3	88[h,i,j,k]
22	$R^1 = R^4 = R^5 = H$; $R^2 = R^3 = OCH_2Ph$	3	81	44	n = 2	3	89[h,i,l,m]
23	$R^1 = R^4 = R^5 = H$; $R^2 = OPr^i$; $R^3 = OMe$	4	86		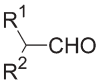		
24	$R^1 = R^4 = R^5 = H$; $R^2 = OBu^i$; $R^3 = OMe$	4	92	45	$R^1 = R^2 = Me$	3	85[h,i,n]
25	$R^1 = R^4 = R^5 = H$; $R^2 = OCH_2Ph$; $R^3 = OMe$	3	91	46	$R^1 = R^2 = (CH_2)_5$	3	98[h,o,p]

[a] The aldehyde (3 mmol) was treated with 2-aminothiophenol (3 mmol) in water at 110 °C (oil-bath). [b] Characterized by IR, NMR and MS. [c] Yield of the purified thiazole (except for entries 43–46). [d] Comparable results were obtained on carrying out the reaction using tap and distilled water. [e] The starting materials remained unchanged (TLC) on carrying out the reaction at room temperature for 12 h. [f] A 98% yield was obtained after 1 h by bubbling oxygen into the reaction mixture. [g] A 90% yield was obtained after 2.5 h by bubbling oxygen into the reaction mixture. [h] The thiazoline was the isolated product. [i] A mixture of the thiazole and the thiazoline was obtained on carrying out the reaction in water at 110 °C for 3 h by bubbling oxygen gas to the reaction mixture. [j] The thiazoline was obtained in 85% in carrying out the reaction in water at 110 °C for 10 h. [k] The thiazoline was obtained in 85% on carrying out the reaction in water at 110 °C until complete consumption of 2-aminothiophenol (20 min, TLC). [l] The thiazoline was obtained in 85% yield on carrying out the reaction in water at 110 °C for 10 h. [m] The thiazoline was obtained in 83% yield on carrying out the reaction in water at 110 °C until complete consumption of 2-aminothiophenol (30 min, TLC). [n] The thiazoline was obtained in 86% yield on carrying out the reaction in water at 110 °C until complete consumption of 2-aminothiophenol (30 min, TLC). [o] The thiazoline was obtained in 90% yield on carrying out the reaction in water at 110 °C for 10 h. [p] The thiazoline was obtained in 96% yield on carrying out the reaction in water at 110 °C until the complete consumption of 2-aminothiophenol (20 min, TLC).

isolated in pure form (spectral data) after decanting off the water and air drying.

When the supernatant water retained the product as a colloidal form, resulting in lower yields, the product was isolated by extraction of the reaction mixture with Et_2O. In most cases, the isolated product was pure (spectral data) and did not require additional efforts at purification. Where required, the purification was achieved by crystallization (EtOAc–hexane). When the residue obtained after decanting off the water was not free-flowing and stuck to the walls of the reaction flask, the product was isolated by dissolving the residue in Et_2O. Liquid products were isolated by solvent extraction (Et_2O). Purification, if required, was performed by column chromatography (silica gel, 2–5% EtOAc in hexane). The reactions were chemoselective and no substitution of the halogen atom[13] (entries 5, 6, and 20) or the nitro group[14] (entries 4 and 19), dealkylation[15a]/debenzoylation[15b,15c,16] (entries 3, 13–18 and 21–33), and reduction of the nitro group (entries 4 and 19)[17] took place although thiols are good nucleophiles and SET agents.[18] Cinnamaldehyde (entry 42) afforded the benzothiazole without any Michael addition,[4,19] or reduction of the double bond.[20] The cyano group (entry 10) was not involved in thiazole formation.[21] Although the dithioacetal formation is a common reaction of aldehydes with thiols,[22] no competitive dithioacetal formation was observed under the present conditions. The amino (entry 7) and hydroxyl (entries 8, 9, 11, 12, 16–20) groups did not interfere. The reactions of alkyl and aryl alkyl aldehydes (entries 43–46) afforded the benzothiazolines.

To ensure that any metal ion leaching out from the glass reaction vessel did not provide catalytic assistance, the reaction of 4-chlorobenzaldehyde (3 mmol) with 2-aminothiophenol (3 mmol) was carried out in a plastic vessel in water for 3 h at 110 °C (oil-bath) and the corresponding thiazole was obtained in 90% yield. Further, the reaction of 4-methoxybenzaldehyde (3 mmol) with 2-aminothiophenol (3 mmol) was carried out separately in distilled water, tap water, and saturated brine.[23] No significant difference was observed either in the reaction time or in the product yields. The benzothiazole was obtained in 96, 98, 97 and 95% yields, respectively, after 3 h at 110 °C (oil-bath). Further, to prove that the trace amounts of metallic impurities that might be present in the tap water are not the actual catalytic species, the reaction was performed in de-ionized water. The thiazole was obtained in 94% yield and no appreciable rate retardation was observed.

To demonstrate the generality, a few aromatic aldehydes and cyclohexanecarboxaldehyde were treated with 2-amino-4-chlorobenzenethiol and 2-amino-4-(trifluoromethyl)benzenethiol hydrochloride as representatives of substituted 2-aminothiophenol (Table 2).

The reactions of aromatic aldehydes with 2-amino-4-chlorobenzenethiol and 2-amino-4-(trifluoromethyl)benzenethiol (as the hydrochloride) afforded the corresponding thiazoles in excellent yields (entries 1–8, Table 2). The reactions of cyclohexanecarboxaldehyde with 2-amino-4-chlorobenzenethiol afforded the thiazoline after 40 min. No appreciable formation of the thiazole took place in carrying out the reaction for 8 h. However, the treatment of cyclohexanecarboxaldehyde with 2-amino-4-(trifluoromethyl)benzenethiol (available as hydrochloride) for 20 min afforded the thiazole and the thiazoline in 96% yield in a ratio of 6:94 (based on the integral values of the C-4 aromatic proton at δ 8.23 ppm of the benzenoid ring of the thiazole and the CH proton at δ 5.18 ppm of the thiazoline moiety). The pure thiazoline was obtained in 92% yield after crystallisation of the mixture from hexane containing a few drops of EtOAc. When the reaction was carried out for 40 min the thiazole and the thiazoline were formed as a 16:84 mixture in 88% yield. The increase in the formation of the thiazole from 6 to 16% by increasing the reaction time from 20 to 40 min encouraged us to achieve a

Table 2 Thiazole/thiazoline formations from substituted 2-aminothiophenols[a]

Entry	Aldehyde	2-Aminothiophenol[b]	Time/h	Yield (%)[b,c]
	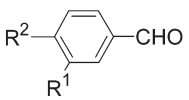	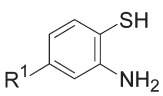		
1	$R^1 = R^2 = OMe$	$R^1 = CF_3$	4	85
2	$R^1 = OH$; $R^2 = OMe$	$R^1 = CF_3$	5	92
3	$R^1 = OCHMe_2$; $R^2 = OMe$	$R^1 = CF_3$	4	71
4	$R^1 = R^2 = OCHF_2$	$R^1 = CF_3$	6	87
5	$R^1 = OCH_2CH(CH_2)_2$; $R^2 = OCHF_2$	$R^1 = CF_3$	6	75
6	$R^1 = R^2 = OMe$	$R^1 = Cl$	6	87
7	$R^1 = OCHMe_2$; $R^2 = OMe$	$R^1 = Cl$	5	80
8	$R^1 = OCH_2CH(CH_2)_2$; $R^2 = OCHF_2$	$R^1 = Cl$	5	76
	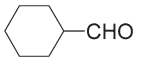			
9		$R^1 = Cl$	40 min	90[e,f]
10		$R^1 = CF_3$	20 min	92[g,h,i]

[a] The aldehyde (3 mmol) was treated with the 2-aminothiophenol dvt (3 mmol) in water (10 mL) at 110 °C (oil-bath). [b] The 2-amino-4-(trifluoromethyl)benzenethiol was available as hydrochloride and was used as such. [c] Characterized by IR, NMR and MS. [d] Yield of the purified thiazole (except for entries 9 and 10). [e] Yield of the thiazoline. [f] The thiazoline was isolated in 86% yield after carrying out the reaction for 8 h and no thiazole formation was observed (^{1}H NMR). [g] The isolated product was obtained in 96% yield as a 6:94 mixture of the thiazole and the thiazoline (^{1}H NMR) and the pure thiazoline was isolated by crystallisation. [h] The isolated product was obtained in 88% yield as a 16:84 mixture of the thiazole and the thiazoline (^{1}H NMR) when the reaction was carried out for 40 min. [i] The product was obtained in 90% yield as a 30:70 mixture of the thiazole and the thiazoline (^{1}H NMR) after 8 h.

Table 3 The time required for the complete consumption (TLC) of 2-aminothiophenol during the reaction of 4-chlorobenzaldehyde with 2-aminothiophenol in various solvents and under neat conditions[a]

Entry	Solvent	Time/min[b,c,d]
1	Neat	50
2	DMSO	60
3	EtOH	90
4	THF	120
5	PhMe	120
6	Dioxane	180
7	NMP	40
8	Water	20

[a] The mixture of 4-chlorobenzaldehyde (3 mmol) and 2-aminothiophenol (3 mmol) in the appropriate solvent (10 mL except for entry 1) was heated at 110 °C (oil-bath). [b] The time required for the complete consumption of 2-aminothiophenol (TLC). [c] The product formed after the complete consumption of 2-aminothiophenol was different from the thiazole (TLC). [d] In each occasion, the reaction was continued for 3 h after which the product was isolated and analysed by GC-MS (date provided in Table 4).

Table 4 The reaction of 4-chlorobenzaldehyde with 2-aminothiophenol in various solvents and under neat conditions[a]

Entry	Solvent	Ratio[b,c]
1	Neat	80:15
2	DMSO	91:9
3	EtOH	23:61
4	THF	40:51
5	PhMe	75:18
6	Dioxane	63:19
7	NMP	90:10
8	Water	100:0
9	Water	67:24[d]

[a] The mixture of 4-chlorobenzaldehyde (3 mmol) and 2-aminothiophenol (3 mmol) in the appropriate solvent (10 mL except for entry 1) was heated for 3 h at 110 °C (oil-bath, except for entry 9). [b] Ratio of the corresponding thiazole and thiazoline as determined by GC-MS of the isolated reaction mixture without further purification. [c] The remaining constituents of the reaction mixture were the unreacted 4-chlorobenzaldehyde and the 2-aminothiophenol. [d] The reaction mixture was under heated for 5 min in a domestic microwave oven using 600 W output power.

clean formation of the thiazole by further increasing the reaction time. However, the thiazole and the thiazoline were formed as a 30:70 mixture (^{1}H NMR) in 90% yield on carrying out the reaction for 8 h.

To find out if water provides a kinetic advantage over the neat condition and other solvents, the progress of the reaction of 4-chlorobenzaldehyde with 2-aminothiophenol in various solvents and under solvent-free conditions at 110 °C (oil-bath) was monitored (TLC) (Table 3). Since 4-chlorobenzaldehyde and the corresponding thiazoline had close R_f values, the consumption of 2-aminothiophenol was considered.

Complete consumption (TLC) of 2-aminothiophenol took place after 20, 60, 90, 120, 120, 180, 40 and 50 min in water, DMSO, EtOH, THF, PhMe, dioxane, NMP, and in the neat state, respectively. A graphical representation of the time required for the complete consumption of 2-aminothiophenol is provided in Fig. 1

In each case the product formed after the complete consumption of the 2-aminothiophenol was different from the thiazole and we presumed it to be the thiazoline on the basis of MS. The conversion of the thiazoline to the thiazole took a longer time (~3 h), after which the product was isolated and subjected to GCMS analyses (data provided in Table 4). No disulfide of 2-aminothiophenol was detected (GC-MS of the reaction mixture isolated after 3 h).

To find the effect of the reaction medium, 4-chlorobenzaldehyde was treated with 2-aminothiophenol in the neat state and in various solvents at 110 °C (oil-bath) for 3 h (Table 4).

In each case, the isolated product was analysed by GC-MS. In the case of the reaction in water, a quantitative conversion to the thiazole took place. The isolated products from the reactions under the neat condition and in other solvents revealed the presence of another constituent with 2 Da higher mass than that of the thiazole along with the unreacted starting materials (in some cases) and the thiazole. The new/additional constituent in the reaction mixtures was presumed to be the thiazoline. The thiazole/thiazoline ratio (GC-MS) was found to be 100/0, 91/9, 23/61, 40/51,75/18, 63/19, 90/10, and 80/15, in water, DMSO, EtOH, THF, PhMe, dioxane, NMP, and in neat condition, respectively (Table 4). A graphical representation of the thiazole:thiazoline content of the products obtained under various reaction media is provided in Fig. 2. The distinct advantages in using water alone as the reaction medium for

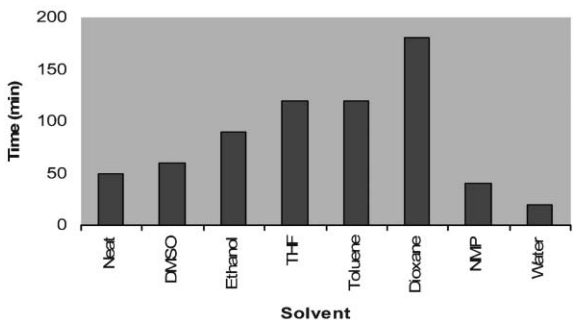

Fig. 1 Graphical representation of the time (min) required for complete consumption of 2-aminothiophenol (TLC) during the reaction of 4-chlorobenzaldehyde (2.5 mmol) with 2-aminothiophenol (2.5 mmol) under various reaction media (data provided in Table 3).

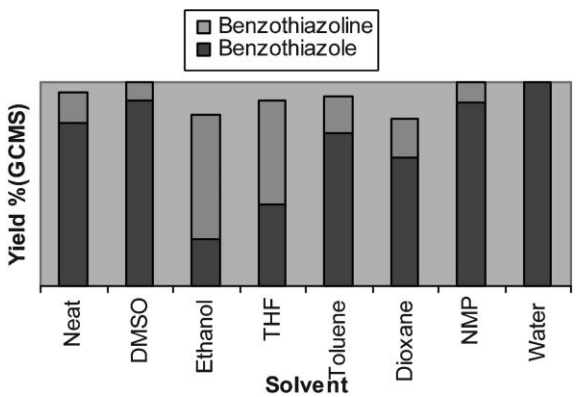

Fig. 2 Graphical representation of the thiazoline/thiazole formation (GC-MS) under various conditions (data provided in Table 4) during the reaction of 4-chlorobenzaldehyde (2.5 mmol) with 2-aminothiophenol (2.5 mmol).

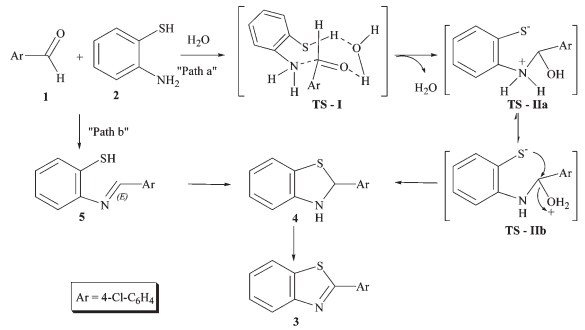

Scheme 2 The role of water in benzothiazole synthesis.

reactants that are insoluble make this methodology ''on water'' synthesis.[24]

The formation of the benzothiazole is depicted in Scheme 2. Water plausibly exhibits an ambiphilic dual activation catalysis[25] by cooperative hydrogen bond formation with the aldehyde carbonyl oxygen and the SH hydrogen of 2-aminothiophenol (TS-I), followed by cyclocondensation to form the thiazoline† (path a) which, on dehydrogenation, is converted to the thiazole so that the heterocyclic moiety attains aromatic character/stabilisation. The conjugation effect of the 2-aryl/heteroaryl/styryl group with the imine bond of the thiazole moiety may also play a significant/critical role in the conversion of the thiazoline to the thiazole. The lack of such a stabilising interaction with the incipiently formed imine bond of the thiazole moiety might be the reason for formation of thiazolines as an end product in case of alkyl and aryl alkyl aldehydes. The dissolved oxygen in water may act as the hydrogen acceptor to facilitate the dehydrogenation† and is corroborated by the faster rate of formation of the thiazole while bubbling oxygen gas into the reaction mixture.

The faster rate of reaction in water compared with that in other solvents and in the neat state† indicates that water plays a specific role (probably through the TS–I) in promoting the condensation of 2-aminothiophenol with the aldehyde. The longer time (1 h 40 min) required for the complete consumption of 2-aminothiophenol during the reaction with 2,4,6-tribromo-3-hydroxybenzaldehyde was due to the steric factor exhibited by the two bromine atoms adjacent to the aldehyde group for the formation of the corresponding transtion state (TS–I). The alternate path (path b) involving formation of the imine followed by intramolecular nucleophilic attack of the SH group to the C=N of the imine is probably not followed as no imine was detected after 6 h at 110 °C (oil-bath) when 3,4-dimethoxybenzaldehyde was treated with 4-aminothiophenol in water.

Conclusions

We have described herein an efficient, cleaner, green methodology for ''on water''-mediated synthesis of benzothiazoles/benzothiazolines. The advantages such as (i) no requirement of additional reagent/catalyst, (ii) non-inflammable and non-toxic reaction medium, (iii) high yields, (iv) excellent chemoselectivity, (v) virtually no waste generation, and (vi) ease of product isolation/purification fulfil the triple bottom line philosophy of green chemistry and make the present methodology environmentally benign.‡

Acknowledgements

The authors thank DST, New Delhi, India and OPCW, The Hague, for financial support.

References

1 P. Tundo, P. Anastas, D. S. Black, J. Breen, T. Collins, S. Memoli, J. Miyamoto, M. Polyakoff and W. Tumas, *Pure Appl. Chem.*, 2000, **72**, 1207.
2 K. Manabe, S. Limura, X.-M. Sun and S. Kobyashi, *J. Am. Chem. Soc.*, 2002, **124**, 11971, and references cited therein.

‡ **Typical procedure for the synthesis of 2-substituted benzothiazole: 2-(4-methoxyphenyl)benzothiazole** (Table 1, entry 3). The magnetically stirred mixture of 4-methoxybenzaldehyde (408 mg, 3 mmol) and 2-aminothiophenol (375 mg, 3 mmol) in water (10 mL) was heated at 110 °C (oil-bath). The progress of the reaction was monitored by TLC. After completion of the reaction (3 h), the reaction mixture was cooled to room temperature, the water was decanted off, the residue was extracted with Et_2O (5 mL) and purified by passing through a column of silica-gel and eluting with hexane:EtOAc (95:5) to give 2-(4-methoxyphenyl)benzothiazole (700 mg, 98%) as a white solid (98%). Mp: 120 °C; IR (KBr) ν 2996, 2936, 2836, 1606, 1592, 1575, and 1557 cm^{-1}; ^1H NMR ($CDCl_3$, 300 MHz) δ 3.86 (s, 3 H), 6.99 (d, 2 H, J = 8.8 Hz), 7.34 (t, 1 H, J = 7.35 Hz), 7.46 (t, 1 H, J = 7.35 Hz), 7.86 (d, 1 H, J = 7.8 Hz), 8.01–8.04 (m, 3 H). APCI MS: m/z = 242 (MH^+). These properties are identical with those of an authentic compound.[26] The remaining reactions were carried out following this general procedure. On each occasion, the spectral data (IR, NMR and MS) of known compounds were found to be identical with those reported in the literature. All unknown compounds were characterized by the spectral data (IR, ^1H and ^{13}C NMR, and MS) and gave satisfactory elemental analyses. A representative example of the reaction using a substituted 2-aminothiophenol is given below. **2-(3,4-Dimethoxyphenyl)-5-trifluoromethylbenzothiazole (Table 2, entry 1)**. The treatment of 3,4-dimethoxybenzaldehyde (498 mg, 3 mmol) with 2-amino-4-(trifluoromethyl)benzenethiol hydrochloride (687 mg, 3 mmol) in water (10 mL) at 110 °C (oil-bath) for 4 h afforded 2-(3,4-dimethoxyphenyl)-5-trifluoromethylbenzothiazole (865 mg, 85%) as a white solid, mp 112–113 °C. ^1H NMR ($CDCl_3$, 300 MHz) δ 3.96 (s, 3 H), 4.02 (s, 3 H), 6.94 (d, 1 H, J = 8.36 Hz), 7.56–7.60 (m, 2 H), 7.70 (d, 1 H, J = 1.84 Hz), 7.95 (d, 1 H, J = 8.35 Hz), 8.28 (s, 1 H). ^{13}C NMR ($CDCl_3$, 75 MHz) δ 56.6, 56.6, 110.3, 111.5, 120.4, 120.4, 121.6, 121.7, 121.9, 122.6, 122.9, 126.5, 129.2, 129.6, 138.8, 149.9, 152.6, 154.3, 170.4. APCI MS m/z 340 (MH^+). Analysis calculated for (%) $C_{16}H_{12}F_3NO_2S$: C, 56.63; H, 3.56; F, 16.80; N, 4.13; S, 9.45. Found: C, 56.60; H, 3.57; N, 4.12; S 9.46. **Benzothiazole synthesis by bubbling oxygen gas into the reaction mixture. 3-Benzothiazol-2-yl-2,4,6-tribromophenol (Table 1, entry 20, footnote)**. Oxygen was bubbled into the magnetically stirred mixture of 2,4,6-tribromo-3-hydroxybenzaldehyde (718 mg, 2 mmol) and 2-aminothiophenol (250 mg, 2 mmol) in water (10 mL) at 100 °C. The progress of reaction was monitored by TLC. After some time (~30 min) complete consumption of the starting materials took place with the appearance of a new spot (expected to be of the intermediate thiazoline). On further continuation of the reaction, a separate spot (expected to be of the thiazole formed by oxidation of the intermediately formed thiazoline) appeared in the TLC. After the complete disappearance of the thiazoline (TLC, 2.5 h) the reaction mixture was cooled to room temperature, the precipitated solid was filtered, and then air dried to give the desired thiazole as a white solid (830 mg; 90%), mp 230 °C (decomp.). IR (KBr) ν 2929, 1591, 1556, 1496, 1447, 1432, 1358, 1316, 1261, 1205, 1099, 1011, 910, 864 cm^{-1}; ^1H NMR (DMSO-d_6, 300 MHz) δ 7.71–7.78 (m, 2 H), 8.31–8.41 (m, 3 H). ^{13}C NMR (75 MHz) δ 113.0, 114.8, 114.9, 122.8, 123.8, 126.4, 126.9, 135.0, 135.6, 136.1, 151.6, 152.6, 165.3. MS (APCI): m/z = 464 (MH^+). Analysis calculated for (%) $C_{13}H_6Br_3NOS$: C, 33.65; H, 1.30; Br, 51.67; N, 3.02; O, 3.45; S, 6.91. Found C, 33.64; H, 1.30; N, 3.03; S 6.90.

3 S. V. Chankeshwara and A. K. Chakraborti, *Org. Lett.*, 2006, **8**, 3259.
4 G. L. Khatik, R. Kumar and A. K. Chakraborti, *Org. Lett.*, 2006, **8**, 2433.
5 H. C. Hailes, *Org. Process Res. Dev.*, 2007, **11**, 114, and references cited therein.
6 M. Yoshida, I. Hayakawa, N. Hayashi, T. Agatsuma, Y. Oda, F. Tanzawa, S. Iwasaki, K. Koyama, H. Furukawa, S. Kurakata and Y. Sugano, *Bioorg. Med. Chem. Lett.*, 2005, **15**, 3328.
7 S.-J. Choi, H. J. Park, S. K. Lee, S. W. Kim, G. Han and H.-Y. P. Choo, *Bioorg. Med. Chem.*, 2006, **14**, 1229.
8 D. Loos, E. Sidoova and V. Sutoris, *Molecules*, 1999, **4**, 81, and references cited therein.
9 D. Alagille, R. M. Baldwin and G. D. Tamagnan, *Tetrahedron Lett.*, 2005, **46**, 1349.
10 S.-J. Ji and H.-B. Shi, *Dyes Pigm.*, 2006, **70**, 246.
11 A. C. Razus, L. Birzan, N. M. Surugiu, A. C. Corbu and F. Chiraleu, *Dyes Pigm.*, 2007, **74**, 26.
12 A few recent examples are: (*a*) T. Itoh and T. Mase, *Org. Lett.*, 2007, **9**, 3687; (*b*) G. Evindar and R. A. Batey, *J. Org. Chem.*, 2006, **71**, 1802; (*c*) Y. Heo, Y. S. Song, B. T. Kim and J.-N. Heo, *Tetrahedron Lett.*, 2006, **47**, 3091; (*d*) X.-J. Mu, J.-P. Zou, R.-S. Zeng and J.-C. Wu, *Tetrahedron Lett.*, 2005, **46**, 4345; (*e*) S. Rostamizadeh and S. A. G. Housaini, *Phosphorus, Sulfur Silicon Relat. Elem.*, 2005, **180**, 1321; (*f*) S. Rudrawar, A. Kondaskar and A. K. Chakraborti, *Synthesis*, 2005, 2521, and references cited therein; (*g*) A. K. Chakraborti, C. Selvam, G. Kaur and S. Bhagat, *Synlett*, 2004, 851; (*h*) A. K. Chakraborti, S. Rudrawar, L. Sharma and G. Kaur, *Synlett*, 2004, 1533; (*i*) For review see C. A. Zificsak and D. J. Hlasta, *Tetrahedron*, 2004, **60**, 8991.
13 P. Cogolli, F. Maiolo, L. Testaferri, M. Tingoli and M. Tiecco, *J. Org. Chem.*, 1979, **44**, 2642.
14 P. Cogolli, L. Testaferri, M. Tingoli and M. Tiecco, *J. Org. Chem.*, 1979, **44**, 2636.
15 (*a*) A. K. Chakraborti, L. Sharma and M. K. Nayak, *J. Org. Chem.*, 2002, **67**, 6406; (*b*) A. K. Chakraborti, L. Sharma and M. K. Nayak, *J. Org. Chem.*, 2002, **67**, 2541; (*c*) A. K. Chakraborti, M. K. Nayak and L. Sharma, *J. Org. Chem.*, 2002, **67**, 1776; (*d*) M. K. Nayak and A. K. Chakraborti, *Tetrahedron Lett.*, 1996, **38**, 8749.
16 A. K. Chakraborti, M. K. Nayak and L. Sharma, *J. Org. Chem.*, 1999, **64**, 8027.
17 M.-J. Shiao, L.-L. Lai, W.-S. Ku, P.-Y. Lin and J. R. Hwu, *J. Org. Chem.*, 1993, **58**, 4742.
18 P. S. Surdha and D. A. Armstrong, *J. Phys. Chem.*, 1986, **90**, 5915, and references cited therein.
19 (*a*) S. K. Garg, R. Kumar and A. K. Chakraborti, *Tetrahedron Lett.*, 2005, **46**, 1721; (*b*) S. K. Garg, R. Kumar and A. K. Chakraborti, *Synlett*, 2005, 1370; (*c*) G. L. Khatik, G. Sharma, R. Kumar and A. K. Chakraborti, *Tetrahedron*, 2007, **63**, 1200; (*d*) G. Sharma, R. Kumar and A. K. Chakraborti, *J. Mol. Catal. A: Chem.*, 2007, **263**, 143.
20 M. Belley and R. Zamboni, *J. Org. Chem.*, 1989, **54**, 1230.
21 A. Abbotto, S. Bradamante, A. Facchetti and G. A. Pagani, *J. Org. Chem.*, 2002, **67**, 5753.
22 (*a*) S. Rudrawar, R. C. Besra and A. K. Chakraborti, *Synthesis*, 2006, 2767; (*b*) R. C. Besra, S. Rudrawar and A. K. Chakraborti, *Tetrahedron Lett.*, 2005, **46**, 6213.
23 N. Mase, K. Watanabe, H. Yoda, K. Takabe, F. Tanaka and C. F. Barbas, III, *J. Am. Chem. Soc.*, 2006, **128**, 4966.
24 (*a*) S. Narayan, J. Muldoon, M. G. Finn, V. V. Fokin, H. C. Kolbe and K. B. Sharpless, *Angew. Chem., Int. Ed.*, 2005, **44**, 3275; (*b*) J. E. Klijn and J. B. F. N. Engberts, *Nature*, 2005, **435**, 746.
25 V. K. Aggarwal, D. K. Dean, A. Mereu and R. Williams, *J. Org. Chem.*, 2002, **67**, 510.
26 V. I. J. Cohen, *Heterocycl. Chem.*, 1979, **16**, 13.

Mannich type reactions of chlorophosphites, phosphoramides and aldehydes (ketones) under solvent-free and catalyst-free conditions—synthesis of *N*-phosphoramino α-aminophosphonates†

Jianfeng Zhang, Zhanwei Cui, Fei Wang, Yadan Wang, Zhiwei Miao* and Ruyu Chen*

Received 2nd July 2007, Accepted 26th September 2007
First published as an Advance Article on the web 11th October 2007
DOI: 10.1039/b710008f

A convenient and rapid method was developed for the synthesis of various *N*-phosphoramino α-aminoalkylphosphonates through Mannich type reactions under catalyst- and solvent-free conditions with excellent yields.

Introduction

α-Aminophosphonic acids have received great attention in synthetic organic chemistry due to their structural analogy to natural α-amino acids, and therefore have biological importance either in themselves or as building blocks for peptides.[1] Because of their versatile biological activities, a number of methods for the synthesis of α-aminophosphonic acids have been developed during the past two decades. Of these methods, three-component Mannich type reactions starting from aldehydes, amines and phosphites catalysed by Lewis acids such as $InCl_3$,[2a] $ZrCl_4$,[2b] lanthanide triflates,[2c] $TaCl_5$–SiO_2,[2d] SmI_2,[2e] $Mg(ClO_4)_2$,[2f] I_2,[2f] or acetyl chloride[3] are common strategies. However, many of those methods utilize toxic organic solvents and in some cases the catalyst is used in stoichiometric amounts. Recently, organic reactions under solvent-free conditions have attracted significant attention[4] for the advantages they offer in terms of green chemistry.[5] However, in most cases, the solvent-free reaction requires microwave irradiation in the presence of a catalyst.[6]

More recently, the direct and solvent-free synthesis of α-aminophosphonates in the presence of catalysts such as Brønsted acids,[7] $LiClO_4$,[8] $Mg(ClO_4)_2$[9] and NBS/CBr_4[10] have been reported. Ranu and Hajra[11] described a practical green alternative for the synthesis of α-aminophosphonates by a three-component condensation of carbonyl compounds (aldehydes and ketones), amines and diethyl phosphite at 75–80 °C neat without any solvent and catalyst. Subsequently, Swamy *et al.*[12] reported the synthesis of α-aminophosphonates using cyclic chlorophosphites as scaffolds under solvent-free conditions. Although the synthesis of α-aminophosphonates under solvent- and catalyst-free conditions is worth studying, reports detailing these types of reactions have been rare and are far less commonly exploited.

1,3,2-Dioxaphosphorinane derivatives are interesting compounds due to their biological activities and are widely used to connect with biologically active nucleoside analogs to form a prodrug with higher lipophilicity.[13] This class of compounds can overcome difficulties associated with the intracellular delivery of nucleoside analogs since it becomes easier for the prodrug to pass through a membrane than the free nucleoside analogs. Moreover, the prodrug can be readily hydrolyzed to release the biologically active nucleoside analogs under physiological conditions.

We have designed and synthesized the corresponding *N*-phosphoramino cyclic α-aminophosphonates that might improve the lipophilicity of the biologically active α-aminophosphonates, which are very interesting probes in biochemistry and medicinal chemistry as they selectively inhibit various enzyme,[14] depending on the *N*-substituent.

Results and discussion

Three-component Mannich type reactions starting from aldehydes (ketones), amines and phosphites have proved to be a facile method for the preparation of various α-aminoalkylphosphonate compounds. Here we have developed a more practical and rapid method for the synthesis of various *N*-phosphoramino α-aminophosphonates. The general procedure involved reacting aldehydes or ketones with diethyl phosphoramidate and cyclic trivalent chlorophosphite at 50–60 °C neat without any solvent and catalyst for a corresponding time, in order to produce the title compounds with good yields (Scheme 1). It was found that this reaction was obviously exothermic.

Various substituted aldehydes and ketones were tested, and aromatic and heteroaromatic aldehydes were found to produce much better yields than ketones. However, only trace amounts of the expected products were obtained when conjugated aliphatic aldehydes were used, and we failed to obtain any of the expected products using aliphatic aldehydes and ketones (Table 1).

The reactions are, generally, very fast, clean and atom economical. No side reactions were observed during the process. Additionally, the catalyst- and solvent-free reactions described here are more practical and environmentally benign. In particular, none of the expected products were detected when the reactions were carried out in a solvent such as acetyl chloride or THF, while yields were very low when the reactions were carried out under benzene-reflux conditions.

State Key Laboratory of Elemento-Organic Chemistry, Research Institute of Elemento-Organic Chemistry, Nankai University, Tianjin, China. E-mail: miaozhiwei@nankai.edu.cn; Fax: +86 22 2350 3627; Tel: +86 22 2350 8857

† CCDC reference number 645802. For crystallographic data in CIF or other electronic format see DOI: 10.1039/b710008f

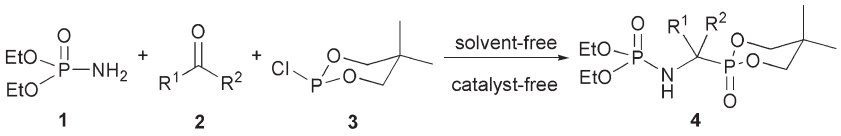

1 2 3 4

Scheme 1 Reaction of diethyl phosphoramidate **1**, ketones or aldehydes **2** and 2-chloro-5,5-dimethyl-1,3,2-dioxaphosphane **3** under solvent- and catalyst-free conditions.

Table 1 Synthesis of α-aminophosphonates

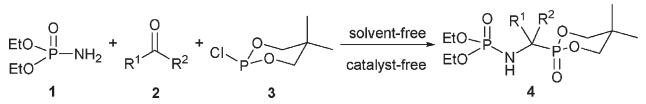

1 2 3 4

4	R^1	R^2	Time	Yield (%)[a]
4a	Ph	H	<1 min	90 (100[b])
4b	*p*-ClC_6H_4	H	1 min	89
4c	*p*-$MeOC_6H_4$	H	20 s	91
4d	*o*-BrC_6H_4	H	1 min	85
4e	*p*-MeC_6H_4	H	30 s	88
4f	*o*-OHC_6H_4	H	20 s	94
4g	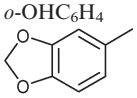	H	1 min	90
4h	*p*-$NO_2C_6H_4$	H	1 min	79
4i	*p*-BrC_6H_4	H	30 s	83
4j	*m*-$NO_2C_6H_4$	H	30 s	86
4k	*o*-$NO_2C_6H_4$	H	1 min	81
4l	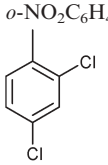	H	5 min	85
4m	Ph	CH_3	90 min	70
4n		H	1 min	77
4o	$CH_3CH_2CH_2$	H	2 h	n.r.[b]
4p	Cyclopentanone		2 h	n.r.[b]
4q	Citral		1 min	Trace[b]

[a] After purification by column chromatography (1 mmol scale). [b] Determined by ^{31}P NMR.

The ^{31}P NMR spectra showed that both of the two P atoms exhibited doublets due to the P–P splitting, with coupling constants of about 33 Hz. The ^{31}P NMR spectra exhibited two peaks at around $\delta = 15$ and 8 ppm, with the first one attributed to the P-atom of the dioxaphosphinyl group, and the second one to the P-atom of the *N*-phosphoryl group. From the ^1H NMR spectra, the CHP protons clearly showed multiple peaks due to the splitting of the two P atoms and the protons of the NH group.

The possible mechanism for the reactions is shown in Scheme 2. *N*-phosphoramino α-aminophosphonates **4** were synthesized *via* Mannich type reactions of diethyl phosphoramidate **1**, aldehydes (ketones) **2** and 2-chloro-5,5-dimethyl-1,3,2-dioxaphosphane **3**. Diethyl phosphoramidate and aldehydes (ketones) could undergo an addition reaction to form intermediates **5**, which could then be dehydrated to generate imines **6** in the presence of 2-chloro-5,5-dimethyl-1,3,2-dioxaphosphane **3**, which served as a dehydrating agent.

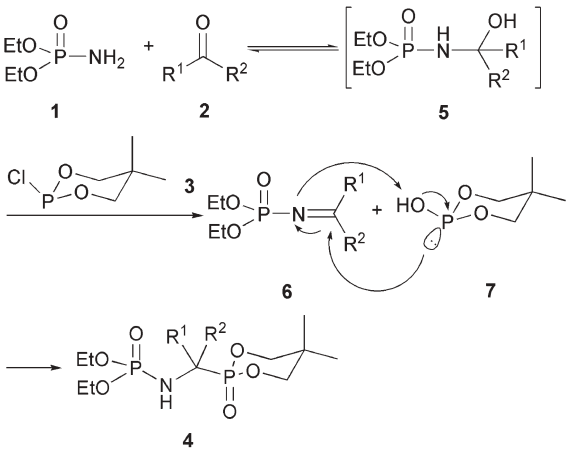

1 2 5 3 6 7 4

Scheme 2 Possible reaction mechanism for the synthesis of the α-aminophosphonates **4**.

As a result, **3** was converted to 5,5-dimethyl-1,3,2-dioxaphosphinane 2-oxide **7**. Then **7** and imines **6** underwent a nucleophilic addition to generate *N*-phosphoramino α-aminophosphonates **4**. Since reactions of phosphites as reaction reagents are generally sluggish, the HCl may act as an activating agent.[11,12]

Conclusions

In conclusion, we have developed a convenient and rapid method for the synthesis of various *N*-phosphoramino α-aminoalkylphosphonates under catalyst-free and solvent-free conditions. All types of aromatic aldehydes produce the corresponding target compounds with excellent yields. The reactions described here have several advantages: they are generally rapid, clean, atom economical and environmentally benign. Therefore, this protocol challenges the existing procedures for synthesis of *N*-phosphoramino α-aminoalkylphosphonates using solvents and catalysts.

Experimental

General procedure

Ketones or aldehydes (1 mmol) were added to a stirred mixture of diethyl phosphoramidate **1** (1 mmol), 2-chloro-5,5-dimethyl-1,3,2-dioxaphosphane **3**[15] (1 mmol) at 50–60 °C. After stirring for the corresponding amount of time (Table 1), the mixtures went slimy and the reactions were stopped. The crude products were purified by flash chromatography on silica gel (started with ethyl acetate–petroleum ether 4 : 1, and then pure ethyl acetate as eluent). Their structures were characterized by ^1H NMR, ^{31}P NMR, ^{13}C NMR and element

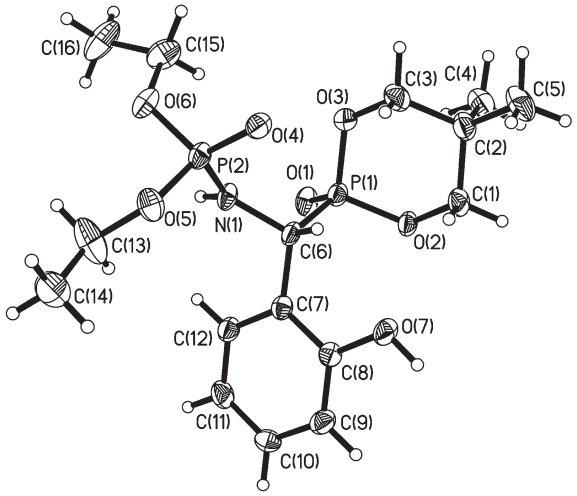

Fig. 1 ORTEP presentation of **4f**, with 50% probability displacement ellipsoids.

analysis. An X-ray crystal structure has been obtained for compound **4f** from methanol (Fig. 1).† All of the title compounds are new and previously unreported.

1-(*N*-diethoxyphosphorylamino)phenylmethyl-5,5-dimethyl-1,3,2λ^5-dioxaphosphorinane-2-oxide 4a

White solid. mp 183–185 °C; δ_P(162 MHz; $CDCl_3$; 85% H_3PO_4): 17.09 (d, *J* 33.9), 7.97(d, *J* 33.9); δ_H(400 MHz; $CDCl_3$; Me_4Si): 7.45–7.26 (5H, m, Ph), 4.80–4.69 (1H, m, PC*H*NH), 4.27–3.75 (9H, m, 4 × OCH_2 and NH), 1.16 (3H, t, *J* 7.0, OCH_2*Me*), 1.10 (3H, s, Me), 1.09 (3H, t, *J* 7.0, OCH_2*Me*), 0.90 (3H, s, Me); δ_C(100 MHz; $CDCl_3$; Me_4Si): 136.40, 128.85, 128.45, 128.08 (d, *J* 6.0), 76.83 (d, *J* 6.4), 76.77 (d, *J* 6.4), 62.78 (d, *J* 4.8), 62.68 (d, *J* 4.8), 51.36 (d, *J* 150.3, P*C*N), 32.70 (d, *J* 6.7), 21.92, 21.22, 16.19 (d, *J* 7.5), 16.06 (d, *J* 7.5). (Found: C, 49.23; H, 7.02; N, 3.69. $C_{16}H_{27}N_2O_6P_2$ requires C, 49.11; H, 6.95; N, 3.58%).

1-(*N*-diethoxyphosphorylamino)(4-chlorophenyl)methyl-5,5-dimethyl-1,3,2λ^5-dioxaphosphorinane-2-oxide 4b

White solid. mp 197–198 °C; δ_P(162 MHz; $CDCl_3$; 85% H_3PO_4): 17.79 (d, *J* 33.5), 7.86 (d, *J* 33.5); δ_H(400 MHz; $CDCl_3$; Me_4Si): 7.42–7.26 (4H, m, Ph), 4.81–4.71 (1H, m, PC*H*NH), 4.35–3.80 (9H, m, 4 × OCH_2 and NH), 1.19 (3H, t, *J* 7.1, OCH_2*Me*), 1.15 (3H, t, *J* 7.0, OCH_2*Me*), 1.12 (3H, s, Me), 0.95 (3H, s, Me); δ_C(100 MHz; $CDCl_3$; Me_4Si): 135.06, 134.39 (d, *J* 2.7), 129.49 (d, *J* 6.1), 129.02, 76.83 (d, *J* 5.5), 76.80 (d, *J* 5.5), 62.90 (d, *J* 5.0), 62.80 (d, *J* 5.0), 50.78 (d, *J* 149.4, P*C*N), 32.74 (d, *J* 6.8), 21.88, 21.26, 16.21(d, *J* 7.4),16.14 (d, *J* 7.4). (Found: C, 45.23; H, 7.02; N, 3.69. $C_{16}H_{26}ClNO_6P_2$ requires C, 45.13; H, 6.15; N, 3.29%).

1-(*N*-diethoxyphosphorylamino)(4-methoxyphenyl)methyl-5,5-dimethyl-1,3,2λ^5-dioxaphosphorinane-2-oxide 4c

White solid. mp 139–140 °C; δ_P(162 MHz; $CDCl_3$; 85% H_3PO_4): 19.94 (d, *J* 33.5), 8.31 (d, *J* 33.5); δ_H(400 MHz; $CDCl_3$; Me_4Si): 7.69–7.32 (4H, m, Ph), 4.79–4.64 (2H, m, PC*H*NH and NH), 4.07–3.70 (8H, m, 4 × OCH_2), 3.63(3H, s, PhO*Me-p*), 1.16–1.04 (6H, m, 2 × OCH_2*Me*), 1.02 (3H, s, Me), 0.79(3H, s, Me); δ_C(100 MHz; $CDCl_3$; Me_4Si): 159.49, 129.35 (d, *J* 5.7), 128.54, 114.05, 76.86 (d, *J* 6.1), 76.80 (d, *J* 6.1), 62.55 (d, *J* 4.5), 62.46 (d, *J* 4.5), 55.33, 50.42(d, *J* 150.1, P*C*N), 32.57(d, *J* 7.0), 21.91, 20.94, 16.11 (d, *J* 7.0), 16.04 (d, *J* 7.0). (Found: C, 48.13; H, 7.32; N, 3.70. $C_{17}H_{29}NO_7P_2$ requires C, 48.46; H, 6.94; N, 3.32%).

1-(*N*-diethoxyphosphorylamino)(2-bromophenyl)methyl-5,5-dimethyl-1,3,2λ^5-dioxaphosphorinane-2-oxide 4d

White solid. mp 140–142 °C; δ_P(162 MHz; $CDCl_3$; 85% H_3PO_4): 16.39 (d, *J* 34.1), 7.47 (d, *J* 34.1); δ_H(400 MHz; $CDCl_3$; Me_4Si): 7.67–7.10 (4H, m, Ph), 5.34–5.23 (1H, m, PC*H*NH), 4.44–3.62 (9H, m, 4 × OCH_2 and NH), 1.18 (3H, t, *J* 7.0, OCH_2*Me*), 1.09 (3H, s, Me), 1.03 (3H, t, *J* 7.0, OCH_2*Me*), 0.91 (3H, s, Me); δ_C(100 MHz; $CDCl_3$; Me_4Si): 136.54, 132.82, 130.48 (d, *J* 3.4), 129.89, 128.29, 123.84 (d, *J* 9.1), 77.24 (d, *J* 6.4), 76.77 (d, *J* 6.4), 62.68 (2 × C, d, *J* 4.9), 50.21 (d, *J* 150.3, P*C*N), 32.67 (d, *J* 7.0), 21.91, 21.29, 16.24 (d, *J* 7.3), 16.01 (d, *J* 7.3). (Found: C, 40.63; H, 5.49; N, 2.86. $C_{16}H_{26}BrNO_6P_2$ requires C, 40.87; H, 5.57; N, 2.98%).

1-(*N*-diethoxyphosphorylamino)(4-methylphenyl)methyl-5,5-dimethyl-1,3,2λ^5-dioxaphosphorinane-2-oxide 4e

White solid. mp 149–150 °C; δ_P(162 MHz; $CDCl_3$; 85% H_3PO_4): 17.34 (d, *J* 33.5), 7.97 (d, *J* 33.5); δ_H(400 MHz; $CDCl_3$; Me_4Si): 7.32–7.09 (4H, m, Ph), 4.75–4.65 (1H, m, PC*H*NH), 4.09–3.75 (9H, m, 4 × OCH_2 and NH), 2.28 (3H, s, Ph*Me-p*), 1.16 (3H, t, *J* 7.0, OCH_2*Me*), 1.11 (3H, t, *J* 7.0, OCH_2*Me*), 1.09 (3H, s, Me), 0.91 (3H, s, Me); δ_C(100 MHz; $CDCl_3$; Me_4Si): 138.23, 133.29, 129.55, 127.94 (d, *J* 6.2), 76.76 (d, *J* 5.1), 76.71 (d, *J* 5.1), 62.75 (d, *J* 5.0), 62.64 (d, *J* 5.0), 50.97 (d, *J* 151.8, P*C*N), 32.68 (d, *J* 6.7), 21.92, 21.33, 21.24, 16.17 (d, *J* 7.7), 16.08 (d, *J* 7.7). (Found: C, 50.53; H, 7.32; N, 3.64. $C_{17}H_{29}NO_6P_2$ requires C, 50.37; H, 7.21; N, 3.46%).

1-(*N*-diethoxyphosphorylamino)(2-hydroxylphenyl)methyl-5,5-dimethyl-1,3,2λ^5-dioxaphosphorinane-2-oxide 4f

White solid. mp 223–225 °C; δ_P(162 MHz; CD_3OD; 85% H_3PO_4): 18.71 (d, *J* 34.1), 9.46 (d, *J* 34.1); δ_H(400 MHz; CD_3OD; Me_4Si): 7.49–6.80 (4H, m, Ph), 5.48–5.40 (1H, m, PC*H*NH), 4.41–3.88 (8H, m, 4 × OCH_2), 1.22–1.17 (9H, m, 2 × OCH_2*Me* and Me), 0.90 (3H, s, Me); δ_C(100 MHz; CD_3OD; Me_4Si): 155.78 (d, *J* 6.5), 130.43 (d, *J* 4.2), 130.33, 124.00, 120.91, 116.13, 79.03 (d, *J* 6.3), 78.64 (d, *J* 6.3), 63.94 (d, *J* 5.4), 63.86 (d, *J* 5.4), 44.94 (d, *J* 151.8, P*C*N), 33.36 (d, *J* 7.3), 22.00, 20.67, 16.39 (d, *J* 6.7), 16.30 (d, *J* 6.7). (Found: C, 47.20; H, 6.79; N, 3.68. $C_{16}H_{27}NO_7P_2$ requires C, 47.18; H, 6.68; N, 3.44%).

1-(*N*-diethoxyphosphorylamino)anisylmethyl-5,5-dimethyl-1,3,2λ^5-dioxaphosphorinane-2-oxide 4g

White solid. mp 162–164 °C; δ_P(162 MHz; $CDCl_3$; 85% H_3PO_4): 17.27 (d, *J* 33.5), 8.23 (d, *J* 33.5); δ_H(400 MHz; $CDCl_3$; Me_4Si): 7.00–6.71 (3H, m, Ph), 5.90 (2H, s, OCH_2O), 4.73–4.63 (1H, m, PC*H*NH), 4.31–3.82 (9H, m, 4 × OCH_2 and NH), 1.19–1.11 (9H, m, 2 × OCH_2*Me* and Me), 0.93 (3H, s,

Me); δ_C(100 MHz; $CDCl_3$; Me_4Si): 148.09, 147.79, 130.19, 121.80 (d, *J* 7.1), 108.63 (d, *J* 5.0), 108.50, 104.41, 76.87 (d, *J* 5.7), 76.81 (d, *J* 5.7), 62.86 (d, *J* 4.3), 62.75 (d, *J* 4.3 Hz), 50.99 (d, *J* 150.4, P*C*N), 32.71 (d, *J* 6.5), 21.95, 21.26, 16.23 (d, *J* 7.6), 16.15 (d, *J* 7.6). (Found: C, 46.69; H, 6.23; N, 3.25. $C_{17}H_{27}NO_8P_2$ requires C, 46.90; H, 6.25; N, 3.22%).

1-(*N*-diethoxyphosphorylamino)(4-nitrophenyl)methyl-5,5-dimethyl-1,3,2λ^5-dioxaphosphorinane-2-oxide 4h

White solid. mp 227–228 °C; δ_P(162 MHz; $CDCl_3$; 85% H_3PO_4): 15.62 (d, *J* 32.3), 7.76 (d, *J* 32.3); δ_H(400 MHz; $CDCl_3$; Me_4Si): 8.16–7.67 (4H, m, Ph), 5.02–4.85 (2H, m, PC*H*NH and NH), 4.23–3.84 (8H, m, 4 × OCH_2), 1.20 (3H, t, *J* 7.0, OCH_2*Me*), 1.14 (3H, t, *J* 7.0, OCH_2*Me*), 1.13 (3H, s, Me), 0.95 (3H, s, Me); δ_C(100 MHz; $CDCl_3$; Me_4Si): 147.85, 144.06, 129.12 (d, *J* 5.2), 123.82, 77.06 (d, *J* 6.7), 76.99 (d, *J* 6.7), 62.99 (d, *J* 5.5), 62.93 (d, *J* 5.5), 51.22 (d, *J* 147.5, P*C*N), 32.79 (d, *J* 6.6), 21.87, 21.17, 16.22 (d, *J* 6.6), 16.16 (d, *J* 6.6). (Found: C, 44.09; H, 6.26; N, 6.25. $C_{16}H_{26}N_2O_8P_2$ requires C, 44.04; H, 6.01; N, 6.42%).

1-(*N*-diethoxyphosphorylamino)(4-bromophenyl)methyl-5,5-dimethyl-1,3,2λ^5-dioxaphosphorinane-2-oxide 4i

White solid. mp 181–182 °C; δ_P(162 MHz; $CDCl_3$; 85% H_3PO_4): 16.39 (d, *J* 33.2), 7.97 (d, *J* 33.2); δ_H(400 MHz; $CDCl_3$; Me_4Si): 7.42–7.34 (4H, m, Ph), 4.82–4.60 (2H, m, PC*H*NH and NH), 4.17–3.79 (8H, m, 4 × OCH_2), 1.16 (3H, t, *J* 7.0, OCH_2*Me*), 1.13 (3H, t, *J* 7.0, OCH_2*Me*), 1.11 (3H, s, Me), 0.91 (3H, s, Me); δ_C(100 MHz; $CDCl_3$; Me_4Si): 135.70, 131.87, 129.86 (d, *J* 5.9), 122.41, 76.91 (d, *J* 5.8), 76.85 (d, *J*5.8), 62.83 (d, *J* 5.0), 62.73 (d, *J* 5.0), 50.82 (d, *J* 149.3, P*C*N), 32.71 (d, *J* 7.0), 21.92, 21.16, 16.19 (d, *J* 7.0), 16.12 (d, *J* 7.0). (Found: C, 40.58; H, 5.51; N, 2.86. $C_{16}H_{26}BrNO_6P_2$ requires C, 40.87; H, 5.57; N, 2.98%).

1-(*N*-diethoxyphosphorylamino)(3-nitrophenyl)methyl-5,5-dimethyl-1,3,2λ^5-dioxaphosphorinane-2-oxide 4j

White solid. mp 188–189 °C; δ_P(162 MHz; $CDCl_3$; 85% H_3PO_4): 15.76 (d, *J* 32.9 Hz), 7.81 (d, *J* 32.9); δ_H(400 MHz; $CDCl_3$; Me_4Si): 8.39–7.46 (4H, m, Ph), 5.14–4.94 (2H, m, PC*H*NH and NH), 4.27–3.84 (8H, m, 4 × OCH_2), 1.19 (3H, t, *J* 7.0, OCH_2*Me*), 1.14 (3H, s, Me), 1.13 (3H, t, *J* 7.0, OCH_2*Me*), 0.93 (3H, s, Me); δ_C(100 MHz; $CDCl_3$; Me_4Si): 148.48, 139.09, 134.33 (d, *J* 4.8), 129.67, 123.21, 123.09 (d, *J* 5.9), 77.10 (d, *J* 6.9), 77.00 (d, *J* 6.9), 62.97 (2 × C, d, *J* 5.5), 51.01 (d, *J* 148.7, P*C*N), 32.79 (d, *J* 7.2), 21.89, 21.12, 16.21 (d, *J* 7.7), 16.13 (d, *J* 7.7). (Found: C, 44.14; H, 6.41; N, 6.50. $C_{16}H_{26}N_2O_8P_2$ requires C, 44.04; H, 6.01; N, 6.42%).

1-(*N*-diethoxyphosphorylamino)(2-nitrophenyl)methyl-5,5-dimethyl-1,3,2λ^5-dioxaphosphorinane-2-oxide 4k

White solid. mp 185–186 °C; δ_P(162 MHz; $CDCl_3$; 85% H_3PO_4): 15.40 (d, *J* 34.9), 7.17 (d, *J* 34.9); δ_H(400 MHz; $CDCl_3$; Me_4Si): 7.91–7.39 (4H, m, Ph), 5.86–5.75 (1H, m, PC*H*NH), 4.67–4.58 (1H, m, NH), 4.15–3.65 (8H, m, 4 × OCH_2), 1.21 (3H, t, *J* 7.0, OCH_2*Me*), 1.10 (3H, s, Me), 1.01 (3H, t, *J* 7.0, OCH_2*Me*), 0.93 (3H, s, Me); δ_C(100 MHz; $CDCl_3$; Me_4Si): 148.44 (d, *J* 6.9), 133.89, 132.44, 130.84 (d, *J* 4.0), 129.04, 124.95, 77.37 (d, *J* 6.8), 76.75 (d, *J* 6.8), 62.84 (2 × C, d, *J* 5.1), 46.17 (d, *J* 150.9, P*C*N), 32.74 (d, *J* 7.2), 21.93, 21.21, 16.23 (d, *J* 7.3), 15.97 (d, *J* 7.3). (Found: C, 44.19; H, 6.11; N, 6.55. $C_{16}H_{26}N_2O_8P_2$ requires C, 44.04; H, 6.01; N, 6.42%).

1-(*N*-diethoxyphosphorylamino)(2,4-dichlorophenyl)methyl-5,5-dimethyl-1,3,2λ^5-dioxaphosphorinane-2-oxide 4l

White solid. mp 160–161 °C; δ_P(162 MHz; $CDCl_3$; 85% H_3PO_4): 15.69 (d, *J* 33.6), 7.65 (d, *J* 33.6); δ_H(400 MHz; $CDCl_3$; Me_4Si): 7.68–7.17 (3H, m, Ph), 5.29–5.18 (1H, m, PC*H*NH), 4.87–4.80 (1H, m, NH), 4.15–3.69 (8H, m, 4 × OCH_2), 1.17 (3H, t, *J* 7.0, OCH_2*Me*), 1.08 (3H, s, Me), 1.07 (3H, t, *J* 7.0, OCH_2*Me*), 0.91 (3H, s, Me); δ_C(100 MHz; $CDCl_3$; Me_4Si): 134.67, 133.86 (d, *J* 8.4), 133.66, 131.48 (d, *J* 3.2), 129.12, 127.93, 77.29 (d, *J* 6.4), 76.89 (d, *J* 6.4), 62.73 (2 × C, d, *J* 4.7), 47.22 (d, *J* 151.7, P*C*N), 32.66 (d, *J* 6.6), 21.83, 21.23, 16.19 (d, *J* 7.2), 16.03 (d, *J* 7.2). (Found: C, 41.56; H, 5.46; N, 2.92. $C_{16}H_{25}NO_6P_2$ requires C, 41.76; H, 5.48; N, 3.04%).

1-(*N*-diethoxyphosphorylamino)(phenylmethyl)methyl-5,5-dimethyl-1,3,2λ^5-dioxaphosphorinane-2-oxide 4m

White solid. mp 106–107 °C; δ_P(162 MHz; $CDCl_3$; 85% H_3PO_4): 20.49 (d, *J* 46.1), 5.40 (d, *J* 46.1); δ_H(400 MHz; $CDCl_3$; Me_4Si): 7.65–7.27 (5H, m, Ph), 4.17–3.57 (9H, m, 4 × OCH_2 and NH), 2.06 (3H, d, *J* 17.5, PhC*Me*), 1.31 (3H, t, *J* 7.0, OCH_2*Me*), 1.08 (3H, t, *J* 7.0, OCH_2*Me*), 0.95 (3H, s, Me), 0.92 (3H, s, Me); δ_C(100 MHz; $CDCl_3$; Me_4Si): 140.16, 128.07, 127.71, 127.08 (d, *J* 4.7), 77.95 (2 × C, d, *J* 7.2), 62.47 (d, *J* 4.7), 62.41 (d, *J* 4.7), 57.09 (d, *J* 152.9, P*C*N), 32.63 (d, *J* 6.7), 21.56, 21.43, 20.43, 16.03 (d, *J* 7.3), 15.84 (d, *J* 7.3). (Found: C, 50.46; H, 7.48; N, 3.42. $C_{17}H_{29}NO_6P_2$ requires C, 50.37; H, 7.21; N, 3.46%).

1-(*N*-diethoxyphosphorylamino)furylmethyl-5,5-dimethyl-1,3,2λ^5-dioxaphosphorinane-2-oxide 4n

Yellow solid. mp 127–129 °C; δ_P(162 MHz; $CDCl_3$; 85% H_3PO_4): 13.85 (d, *J* 29.9), 7.72 (d, *J* 29.9); δ_H(400 MHz; $CDCl_3$; Me_4Si): 7.33–6.28 (3H, m, furyl), 4.97–4.86 (1H, m, PC*H*NH), 4.12–3.86 (9H, m, 4 × OCH_2 and NH), 1.18 (3H, t, *J* 7.0, OCH_2*Me*), 1.17 (3H, t, *J* 7.0, OCH_2*Me*), 1.14 (3H, s, Me), 0.87 (3H, s, Me); δ_C(100 MHz; $CDCl_3$; Me_4Si): 149.34, 142.92, 110.99, 109.03 (d, *J* 6.3), 77.24 (2 × C, d, *J* 7.0), 62.89 (d, *J* 5.3), 62.79 (d, *J* 5.3), 45.36 (d, *J* 155.2, P*C*N), 32.60 (d, *J* 7.2), 22.00, 20.93, 16.18 (d, *J* 4.1), 16.11 (d, *J* 4.1). (Found: C, 44.46; H, 6.50; N, 3.62. $C_{14}H_{25}NO_7P_2$ requires C, 44.10; H, 6.61; N, 3.67%).

X-ray crystallographic study

Crystallographic data were collected at 113(2) K using a Bruker SMART 1000 CCD diffractometer and Mo-Kα radiation (λ = 0.71070 Å). The structure was solved by direct methods using SHELXS and refined using SHELXL-97 software.

Crystal data for **4f**:† $C_{16}H_{27}NO_7P_2$, *M*r = 407.33, triclinic, space group *P*-1, *a* = 9.955(9), *b* = 10.404(9), *c* = 10.839(9) Å, α = 97.689(9), β = 98.771(7), γ = 111.382(16)°, *V* = 1011.0(15) Å^3, *T* = 113(2) K, *Z* = 2, D_c = 1.338 g cm^{-3},

μ(Mo-Kα) = 0.251 mm^{-1}, F(000) = 432. Least-squares refinement based on 10348 reflections with $I > 2\sigma(I)$ (out of 3551 unique reflections) led to final value of R_1 = 0.0574 for 2931 observed reflections. The final $wR(F^2)$ was 0.1388 (all data).

Acknowledgements

We thank the Committee of Science and Technology of Tianjin (07JCZDJC04800) and Nankai University (J02044 to Z. W. Miao) for financial support.

References

1 For a review see: V. P. Kukhar, H. R. Hudson, *Aminophonic and Aminophinic Acids Chemistry and Biological Activity*, John Wiley & Sons Ltd, Chichester, 2000.
2 (*a*) B. C. Ranu, A. Hajra and U. Jana, *Org. Lett.*, 1999, **1**, 1141; (*b*) J. S. Yadav, B. V. S. Reddy, K. S. Raj, K. B. Reddy and A. R. Prasad, *Synthesis*, 2001, 2277; (*c*) S. Lee, J. H. Park, J. Kang and J. K. Lee, *Chem. Commun.*, 2001, 1698; (*d*) S. Chandrasekhar, S. J. Prakash, V. Jagadeshwar and C. Narsihmulu, *Tetrahedron Lett.*, 2001, **42**, 5561; (*e*) F. Xu, Y. Q. Luo, M. Y. Deng and Q. Shen, *Eur. J. Org. Chem.*, 2003, 4728; (*f*) J. Wu, W. Sun, H. G. Xia and X. Y. Sun, *Org. Biomol. Chem.*, 2006, **4**, 1663.
3 (*a*) C. Y. Yuan, S. J. Chen and G. H. Wang, *Synthesis*, 1991, 490; (*b*) Z. W. Miao, B. Wang, G. H. Zhang and R. Y. Chen, *Bioorg. Chem.*, 2006, **34**, 167.
4 For a review of solvent-free reaction see: (*a*) R. S. Varma, *Green Chem.*, 1999, **1**, 43; (*b*) G. W. V. Cave, C. L. Raston and J. L. Scott, *Chem. Commun.*, 2001, 2159.
5 P. T. Anastas and J. C. Warner, *Green Chemistry—Theory and Practice*, Oxford University Press, New York, 1998.
6 (*a*) J. S. Yadav, B. V. S. Reddy and C. Madan, *Synlett*, 2001, 1131; (*b*) B. Kaboudin and R. Nazari, *Tetrahedron Lett.*, 2001, **42**, 8211; (*c*) A. K. Bhattacharya and T. Kur, *Synlett*, 2007, 745.
7 T. Akiyama, M. Sanada and K. Fuchibe, *Synlett*, 2003, 1463.
8 N. Azizi, F. Rajabi and M. R. Saidi, *Tetrahedron Lett.*, 2004, **45**, 9233.
9 S. Bhagat and A. K. Chakraborti, *J. Org. Chem.*, 2007, **72**, 1263.
10 J. Wu, W. Sun, X. Y. Sun and H. G. Xia, *Green Chem.*, 2006, **8**, 365.
11 B. C. Ranu and A. Hajra, *Green Chem.*, 2002, **4**, 551.
12 K. C. K. Swamy, S. Kumaraswamy, K. S. Kumar and C. Muthiah, *Tetrahedron Lett.*, 2005, **46**, 3347.
13 (*a*) C. Meier, *Angew. Chem., Int. Ed. Engl.*, 1996, **35**, 70; (*b*) For a review see: C. Meier, *Eur. J. Org. Chem.*, 2006, 1081; (*c*) N. Gisch, J. Balzarini and C. Meier, *J. Med. Chem.*, 2007, **50**, 1658.
14 (*a*) J. Oleksyszyn and J. C. Power, *Biochemistry*, 1991, **30**, 485; (*b*) J. Oleksyszyn, B. Boduszek, C. M. Cam and J. C. Powers, *J. Med. Chem.*, 1994, **37**, 226; (*c*) B. Boduszek, J. Oleksyszyn, C. M. Cam, J. Selzer, R. E. Smith and J. C. Powers, *J. Med. Chem.*, 1994, **37**, 3969; (*d*) J. A. Bertrand, J. Oleksyszyn, C. M. Kam, B. Boduszek, S. Presnell, R. R. Plaskon, F. L. Suddath, J. C. Powers and L. D. Williams, *Biochemistry*, 1996, **35**, 3147; (*e*) A. Belyaev, X. M. Zhang, K. Augustyns, A. M. Lambeir, I. D. Meester, I. Vedernikova, S. Scharpe and A. Haemers, *J. Med. Chem.*, 1999, **42**, 1041; (*f*) A. Mucha and P. Kafarski, *Tetrahedron*, 2002, **58**, 5855; (*g*) J. Joossens, P. Van der Veken, A. M. Lambeir, K. Angustyns and A. Haemers, *J. Med. Chem.*, 2004, **47**, 2411.
15 R. M. Matos, L. C. G. Lima, E. Souza, A. L. A. B. Souza, M. B. G. Lima and D. S. Raslan, *Phosphorus, Sulfur Silicon Relat. Elem.*, 2002, **177**, 2859.

Development of new SILP catalysts using chitosan as support

Jérôme Baudoux,[a] Katy Perrigaud,[b] Pierre-Jean Madec,[a] Annie-Claude Gaumont*[a] and Isabelle Dez*[a]

Received 18th June 2007, Accepted 26th September 2007
First published as an Advance Article on the web 16th October 2007
DOI: 10.1039/b709226a

New SILP catalysts based on chitosan-supported ionic liquid were successfully applied to allylic substitution reactions. A high level of activity combined with recyclability and reusability were obtained in the amination reaction. No organic solvent was used. The scope and limitations of the reaction using these new SILP catalysts were estimated.

Introduction

In industrial processes, heterogeneous catalysis is generally preferred to homogeneous catalysis as the extraction of the product and recovering of the catalyst are made easier.[1] However, in various examples of heterogeneous catalysis, mass or heat transfer limitations in the solid catalyst may lead to decreased activity. Furthermore, lower chemo- and stereoselectivities are often encountered compared with homogeneous catalysis.[2] Obviously, a catalytic system making it possible to secure the advantages of both homogeneous and heterogeneous catalyses (*i.e.*, good activity, selectivity, easy extraction of the product and recovery of the catalyst) would greatly enhance the interest of industry in catalysis. In recent years, ionic liquids (ILs) have attracted considerable interest in catalysis as replacement media for volatile organic solvents.[3,4] They are ideal reaction media for biphasic reactions with organic substrates (easy product and catalyst separation). However, biphasic IL/organic liquid systems generally require significant amounts of IL, which is unattractive from an economical point of view due to the high cost of many ILs. Furthermore, a considerable number of extractions are usually required to recover the product from the polar IL. Lastly, after a limited number of recyclings, a leaching occurred leading to the deactivation of the catalytic phase.[5] To overcome these problems, an approach using the concept of supported ionic liquid phase (SILP) has recently been proposed.[6] In these SILP systems, a thin film of ionic liquid containing the homogeneous catalyst is immobilized on the surface of a solid support. This combination makes easier the separation of the product from the catalyst phase and the use of very small amounts of IL is possible. Immobilisation of ILs by adsorption or grafting onto a silica surface has been used with success in various reactions such as hydrogenation,[7] hydroformylation[8] and Friedel–Crafts acylations.[9] Organic polymers have also been used as supports for nucleophilic substitution reactions.[10] For the development of clean processes, it is likely that renewable polymeric supports occurring from the biofeedstocks will play a key role in the future. To the best of our knowledge, the use of natural polymers such as polysaccharides to immobilize the IL layer has never been proposed. Chitosan, an enantiopur biopolymer, which consists of 2-amino-2-deoxy-(1,4)-β-D-glucopyranose residues (D-glucosamine units) with no or a small amount of *N*-acetyl-D-glucosamine units, is characterised by its strong affinity towards transition metals.[11] This biopolymer, which is derived mainly from the shells of crustaceans, is produced in considerable amounts each year. Our current interest in the development of new chitosan based materials,[12] and the recent works dealing with the use of this biopolymer in the field of heterogeneous catalysis[13] and in supported aqueous phase (SAP) catalysis,[14] led us to explore its application as an IL phase-support. The main advantages in using chitosan as catalytic support are: high sorption capacities, stability of metal anions (such as Pt and Pd) on chitosan, physical and chemical versatility of the biopolymer and chirality. In this article, we report the synthesis of new chitosan-SILP catalysts and their application in a model reaction, the palladium catalysed allylic substitution, one of the most important reactions for carbon–carbon and carbon–heteroatom bond formation.[15]

Results and discussion

The chitosan–SILP catalytic system is reported in Fig. 1.

Typically, such a catalytic system is prepared by impregnation of the chitosan with an ionic liquid ([bmim][BF_4]) in the presence of 0.05 equiv. of the palladium catalyst [$Pd(OAc)_2$] and 0.2 equiv. of PPh_3 as ligand with a polymer concentration of 14.3% (w/v). After stirring at room temperature for 30 min, the chitosan–SILP catalyst is ready for use. Its potential was investigated in a model reaction: the allylic substitution between morpholine and *(E)*-1,3-diphenyl-3-acetoxyprop-1-ene **1** (Scheme 1).

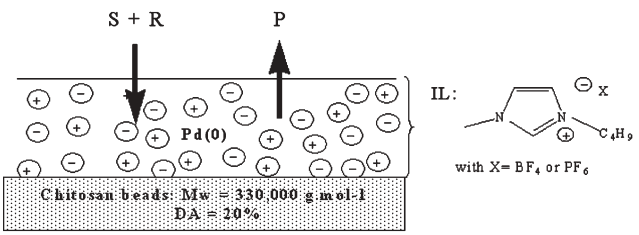

Fig. 1 Chitosan–SILP catalytic system.

[a]*Laboratoire de Chimie Moléculaire et Thio-organique, ENSICAEN, Université de Caen Basse-Normandie, CNRS, 6 boulevard du Maréchal Juin, 14050 Caen, France. E-mail: dez@ensicaen.fr; gaumont@ensicaen.fr; Fax: +33 2 31 45 28 77; Tel: +33 2 31 45 28 42*
[b]*Subatech, Ecole des Mines de Nantes, 4 rue Alfred Kastler, BP 20722, 44307 Nantes Cedex 3, France*

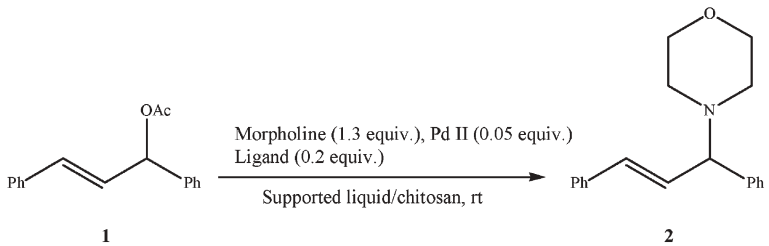

1 2

Scheme 1 Palladium catalysed allylic substitution.

Table 1 Allylic substitution reaction carried out with chitosan-supported ionic liquid phase and chitosan–SAP[a]

	Supported liquid phase	Palladium source	Ligand	Time/h	Isolated yield (%)
1	[bmim][BF_4]	$Pd(OAc)_2$	PPh_3	1	94
2	[bmim][BF_4]	$PdCl_2$	PPh_3	1	95
3	[bmim][PF_6]	$Pd(OAc)_2$	PPh_3	1	93
4	[bmim][BF_4]	$Pd(OAc)_2$	TPPTS	1	91
5	H_2O[a]	$PdCl_2$	TPPTS	60	20

[a] SAP: supported aqueous phase.

Compound **2** was obtained in a good yield (94%) when using this new catalytic system under mild conditions (rt for 1 hour) (Table 1, entry 1). It is worth noting that in the absence of the phosphine ligand (PPh_3), the reaction was unsuccessful, indicating that the complexation of the Pd to the chitosan did not occur or that the organometallic complex formed was inactive. These preliminary results compare satisfactorily to those obtained under similar conditions in monophasic [bmim][BF_4] (92% yield), indicating that the chitosan support does not limit the activity of the catalyst.

Exchanging $Pd(OAc)_2$ with palladium dichloride as the palladium source afforded quite similar results: the reaction was completed in 1 hour and the coupling product **2** was obtained in 95% yield (Table 1, entry 2). The influence of the nature of the ionic liquid anion was next examined. For this purpose, a SILP catalyst was prepared, with a more hydrophobic IL ([bmim][PF_6]). This new chitosan–SILP catalyst applied to the Tsuji–Trost reaction afforded **2** with an excellent yield (93%) (Table 1, entry 3), comparable to those obtained with the catalyst based on [bmim][BF_4].

One of the main advantages of the chitosan–SILP system is the easy product/catalyst separation. By using the chitosan-supported [bmim][BF_4] catalyst, and after nine extractions with 1 mL of ether, the crude yield of product amounted to 100%, corresponding to an isolated yield of 91%, whereas reactions conducted in monophasic [bmim][BF_4] required at least twenty extractions. Recovering and re-usability of the catalyst are the other main advantages of the new chitosan-SILP catalysts. Recycling tests showed that the chitosan-SILP catalyst could be successfully re-used until the fifth cycle with a good conversion (>98%) (Table 2), although a decrease in the activity was observed after the third run. Thus, two hours were required in the fourth run for a complete conversion instead of one in the three firsts and 20 hours for the following trials. In the 6th and 7th cycles, conversion dropped to respectively 14 and 5%. Examination by ^{31}P NMR of the organic phase after extraction did not allow the detection of the catalyst. However, traces of triphenylphosphine oxide (δ_{31P} = 30 ppm) were observed, indicating that a partial decomplexation of the ligand followed by its oxidation has occurred. Detection of palladium by ICP-MS in the extraction phases showed important leaching of metal in the two first cycles (Table 2), explaining the decrease of the conversion after the fifth cycle. Addition of 0.2 equivalent of fresh PPh_3 ligand in the SILP system allowed the partial recovering of the catalytic performance (50% in the 8th run compared with 5% in the 7th one) (Table 2).

To get a better anchoring of the Pd complex and to avoid the catalyst leaching from the ionic liquid to the organic phase, the neutral triphenylphosphine ligand was replaced by the ionic TPPTS ligand ($P(m\text{-}C_6H_4SO_3Na)_3$). The new [bmim][$BF_4$] chitosan SILP catalyst was evaluated in the model reaction described in Scheme 1 under the conditions used previously (rt, 1 h). An excellent conversion was achieved (100%), leading to the expected product **2** in good yield (91%). A similar conversion was even obtained after only 3 min at rt (TOF > 500 mol (mol h)$^{-1}$), showing the great efficiency of the new catalytic system (Table 1, entry 4).

Recycling and re-use were next examined. As expected, the replacement of the neutral PPh_3 ligand by the ionic TPPTS afforded a great improvement in the catalyst recycling. The chitosan–SILP catalytic system could be recycled and re-used at least 10 times without any decrease in activity (conversion higher than 98% in 1 h), see Table 3. Except for the first cycle, where the Pd extracted amounted 9%, the palladium detected by ICP-MS in the ether phases after extraction of the product was very low (<3% of introduced Pd) (Table 3). This leaching

Table 2 Recycling and re-use of Chitosan–SILP catalyst with PPh_3 in the allylic substitution of **1** with morpholine

Cycle	1	2	3	4	5	6	7	8[b]	9[b]
Reaction time/h	1	1	1	2	20	20	20	10	20
Conversion (%)	>98	>98	>98	>98	>98	14	<5	50	15
Pd (%)[a]	35	20	3	1	0.2	—	—	—	—

[a] Percentage palladium leached in the ether as compared with the total palladium introduced in the chitosan–SILP catalyst. [b] Addition of 0.2 equiv. of PPh_3.

Table 3 Recycling and re-use of Chitosan–SILP with TPPTS as ligand in the allylic substitution of **1** with morpholine

Cycle	1	2	3	4	5	6	7	8	9	10
Reaction time/h	1	1	1	1	1	1	1	1	1	1
Conversion (%)	>98	>98	>98	>98	>98	>98	>98	>98	>98	>98
Pd (%)[a]	9	2	3	2	1	0.1	1	0.5	0.3	0.4

[a] Percentage of palladium leached in the ether as compared to total palladium introduced in the chitosan–SILP catalyst.

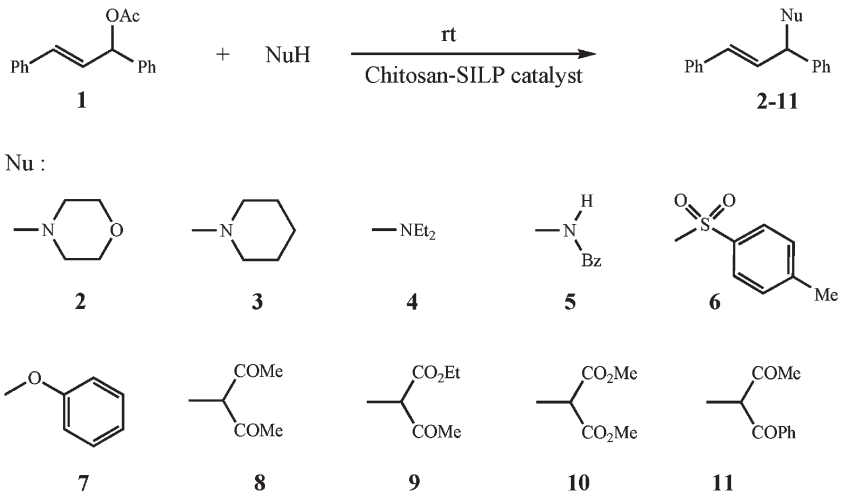

Scheme 2

does not seem to affect the activity of the catalyst since a complete conversion was observed in each cycle. After the 8th cycle, leaching fell down to a value lower than 0.5% and a full conversion was still observed. This low leaching of the catalyst is in agreement with the better anchoring of the catalyst in the ionic liquid phase when an ionic ligand is used.

The SILP system was then compared with another heterogeneous catalytic system, the chitosan–SAP (supported aqueous phase) system. A great decrease in activity for the chitosan–SAP system compared with the chitosan-supported [bmim][BF_4] system was noticed (isolated yield in coupling product 20% for SAP catalyst compared with 91% for SILP catalyst) (Table 1, entries 5 and 4 respectively). The low activity observed in the chitosan–SAP system is in good agreement with investigations reported earlier by Quignart.[16] The increase in catalytic activity for the chitosan–SILP can be correlated to a higher mobility of the organometallic complex in the IL layer than in the water layer.

Finally, the new chitosan–SILP catalysts were applied to a series of different nucleophiles using $Pd(OAc)_2$ as palladium source and the low cost PPh_3 as ligand (Scheme 2).

Reactions using piperidine, diethylamine and benzylamine as nucleophiles were successfully conducted with the chitosan-supported [bmim][BF_4] catalyst (Table 4). With various other nucleophiles, such as sodium *p*-toluenesulfinate and phenol/Et_3N couple, moderate to good yields (68%–72%) were obtained using either [bmim][BF_4] or [bmim][PF_6] as the ionic liquid source. The allylic alkylations with soft carbon nucleophiles, which required additional base, proceeded readily to give the corresponding products with good yields (80–90%). With acetylacetone and 1-phenyl-1,3-butanedione, K_2CO_3 was first solubilised in a small amount of water because of its poor solubility in the IL layer. It is worth noting that for the synthesis of **8**, a better yield was obtained when using the chitosan–SILP catalyst compared with the monophasic IL system (80% instead of 54%).[17]

Table 4 Allylic substitution reactions

Nucleophile	Ionic liquid	Base	Isolated yield (%)
Piperidine	[bmim][BF_4]	—	97
Diethylamine	[bmim][BF_4]	—	92
Benzylamine	[bmim][BF_4]	—	90
p-Me–C_6H_4–SO_2Na	[bmim][BF_4]	—	72
Phenol	[bmim][PF_6]	Et_3N	68
Acetylacetone	[bmim][PF_6]	K_2CO_3[a]	80
Ethyl acetoacetate	[bmim][PF_6]	Et_3N	89
Dimethyl malonate	[bmim][PF_6]	Et_3N	89
1-Phenylbutane-1,3-dione	[bmim][PF_6]	K_2CO_3[a]	90

[a] 0.2 mL of water was added to solubilize the base.

Another advantage of these new catalytic systems is their great stability in time. They can be left under nitrogen for at least one week after a series of reactions and then re-used without any decrease in activity. The new chitosan–SILP system could also be used subsequently with two different nucleophiles, affording in each case only the expected product without any traces of the previous one, indicating that no contamination of the SILP system by the product occurred.

Conclusion

In conclusion, we have shown that chitosan–SILP catalysts can be successfully applied to the Tsuji–Trost reactions. This preliminary study showed the high flexibility of the new systems, which can be used under various conditions (Pd source, phosphine ligand, IL, nucleophiles). The main advantages of these catalysts are: the small amount of IL

which is required, the use of a biopolymer as support, the ease of product extraction, the efficient recycling and re-use of the catalytic system (>10 cycles with TPPTS as ligand). Further studies dealing with the exploration of the behaviour of these chitosan–SILP catalysts for asymmetric reactions are currently under way.

Experimental

Chitosan obtained from Fluka was purified by dissolution in aqueous hydrochloric acid (0.2%) to get a solution with a polymer concentration of 1% (w/v) and was precipitated in aqueous NaOH solution (pH > 7). The residue was washed several times with de-ionized water to attain the water conductivity and finally freeze-dried. The viscosity-average molar mass is 330 000 g mol^{-1} (determined by viscosimetry) and the degree of deacetylation determined by ^1H NMR is 80%.

Ionic liquids were supplied by Solvionic. All commercially available compounds were used as received. Thin layer chromatography was performed on silica gel 60 F-254 plates (0.1 mm, Merck) with UV detection. Chromatographic separations were achieved on silica gel columns (60, 40–63 μm, Merck). All NMR spectra were recorded on a Bruker Avance DPX 250 instrument (250 MHz ^1H, 62 MHz ^{13}C) using $CDCl_3$ and TMS as solvent and reference, respectively. Chemical shifts (δ) are given in parts per million and coupling constants (*J*) in hertz. Mass and high resolution mass spectra (HRMS) were obtained on a Waters-Micromass Q-Tof micro-instrument. IR spectra were recorded on a PerkinElmer 16 PC FT-IR spectrometer. Analytical data were performed with a Thermoquest NA 2500 instrument and ICP-MS analysis with a PQ-Exel–VG Elemental apparatus.

1. Preparation of the chitosan–SILP catalyst (general procedure)

Pre-degassed [bmim][PF_6] or [bmim][BF_4] (0.5 mL) was slowly added to the palladium source (0.02 mmol, 0.05 equiv.), the phosphine (0.09 mmol, 0.2 equiv.) and the purified chitosan (100 mg). The resulting mixture was stirred at room temperature under N_2 atmosphere for 30 min. The SILP system having a chitosan concentration of 14.3% (w/v) is then ready for application in catalysis.

2. General procedure for the Pd-catalysed allylic substitution of (rac)-*(E)*-1,3-diphenyl-3-acetoxyprop-1-ene with nitrogen nucleophile

(E)-1,3-Diphenyl-3-acetoxyprop-1-ene (105 mg, 0.42 mmol, 1 equiv.) and nitrogen nucleophile (0.6 mmol, 1.4 equiv.) were successively added to the chitosan–SILP catalyst. The mixture was stirred at room temperature under N_2 for 5 h. The solution was then extracted 9 times with 1 mL of diethyl ether (monitored by TLC). The combined diethyl ether extracts were washed with water (1 mL), dried over $MgSO_4$, filtered and concentrated to give the desired products **2** to **5**.

***(E)*-3-Morpholino-1,3-diphenylprop-1-ene 2.** 93% yield. Mp (DSC) 64–65 °C. ^1H NMR (250 MHz, $CDCl_3$,) δ 2.21–2.33 (m, $2H^{CH_2}$); 2.39–2.47 (m, $2H^{CH_2}$); 3.58 (m, $4H^{2*CH_2}$); 3.65 (d, *J* = 8.8 Hz, $1H^{CH}$); 6.16 (dd, *J* = 15.8 Hz, *J* = 8.8 Hz, $1H^{CH}$); 6.44 (d, *J* = 15.8 Hz, $1H^{CH}$); 7.03–7.37 (m, $10H^{CHar}$), ^{13}C NMR ($CDCl_3$, 62.5 MHz) δ 52.7 ($2*CH_2$); 67.6 ($2*CH_2$); 75.3 (CH); 126.9 (2*CH); 127.5 (CH); 128.1 (CH); 128.5 (2*CH); 129.1 (2*CH); 129.5 (2*CH); 131.4 (CH); 132.1 (CH); 137.3 (C_q); 142.1 (C_q). ν_{max}: 3025.8; 2955.6; 2851.3; 2803.6; 1493.6; 1449.5; 1270.0; 1114.9; 1005.1; 965.6; 879.6; 743.1; 692.1. Anal. calcd for $C_{19}H_{21}NO$: 81.68 (C) 7.58 (H) 5.01 (N); found 81.39 (C) 7.77 (H) 4.78 (N). HRMS (ESI) calculated for $C_{19}H_{22}NO$ $[M–H]^+$ 280.1701; found 280.1712.

***(E)*-3-Piperidyl-1,3-diphenylprop-1-ene 3.** 97% yield. Mp (DSC) 102–104 °C. ^1H NMR (250 MHz, $CDCl_3$) δ 1.34 (m, $2H^{CH_2}$); 1.47 (m, $4H^{2*CH_2}$); 2.24 (m, $2H^{CH_2}$); 2.37 (m, $2H^{CH_2}$); 3.70 (d, *J* = 8.5 Hz, $1H^{CH}$); 6.24 (dd, *J* = 15.8 Hz, *J* = 8.5 Hz, $1H^{CH}$); 6.42 (d, *J* = 15.8 Hz, $1H^{CH}$); 7.06–7.31 (m, $10H^{CHar}$). ^{13}C NMR ($CDCl_3$, 62.5 MHz) δ 25.2 (CH_2); 26.6 ($2*CH_2$); 53.2 ($2*CH_2$); 75.2 (CH); 126.8 (2*CH); 127.4 (CH); 127;8 (CH); 128.5 (2*CH); 128.9 (2*CH); 129.0 (2*CH); 131.4 (CH); 132.7 (CH); 137.5 (Cq); 142.9 (Cq). ν_{max}: 3028.7; 2931.3; 2790.1; 2748.1; 1739.9; 1489.9; 1448.3; 1231.5; 1098.2; 979.9; 744.9; 692.4. Anal. calcd for $C_{20}H_{23}N$ 86.59 (C) 8.36 (H) 5.05 (N); found 86.33 (C) 8.44 (H) 4.77 (N). HRMS (ESI) calculated for $C_{20}H_{24}N$ $[M–H]^+$ 278.1909; found 278.1922.

***(E)*-*N*,*N*-Diethyl-1,3-diphenylallylamine 4.** 92% yield. Mp (DSC) 41–43 °C. ^1H NMR (250 MHz, $CDCl_3$,) δ 0.91 (t, *J* = 7.1 Hz, $6H^{2*CH_3}$); 2.52 (m, $4H^{2*CH_2}$); 4.20 (d, *J* = 8.7 Hz, $1H^{CH}$); 6.26 (dd, *J* = 15.8 Hz, *J* = 8.7 Hz, $1H^{CH}$); 6.44 (d, *J* = 15.9 Hz, $1H^{CH}$); 7.07–7.36 (m, $10H^{CHar}$). ^{13}C NMR ($CDCl_3$, 62.5 MHz) δ 12.1 ($2*CH_3$); 43.5 ($2*CH_2$); 69.2 (CH); 126.8 (2*CH); 127.3 (CH); 127.8 (CH); 128.4 (2*CH); 128.8 (2*CH); 129. 0 (2*CH); 131.5 (CH); 132.0 (CH); 137.6 (Cq); 143.5 (Cq). ν_{max}: 3024.6; 2968.4; 2824.1; 1741.9; 1491.1; 1448.0; 1231.6; 1024.7; 977.9; 743.8; 699.8. Anal. calcd for $C_{19}H_{23}N$ 85.99 (C) 8.74 (H) 5.28 (N); found 86.20 (C) 8.84 (H) 4.85 (N). HRMS (ESI) calculated for $C_{19}H_{24}N$ $[M–H]^+$ 266.1909; found 266.1914.

***(E)*-*N*-Benzyl-1,3-diphenylallylamine 5.** 90% yield. Oil. ^1H NMR (250 MHz, $CDCl_3$,) δ 3.74 (s, $2H^{CH_2}$); 4.35 (d, *J* = 7.3 Hz, $1H^{CH}$); 6.28 (dd, *J* = 15.8 Hz, *J* = 7.4 Hz, $1H^{CH}$); 6.55 (d, *J* = 15.9 Hz, $1H^{CH}$); 7.20–7.39 (m, $15H^{CHar}$). ^{13}C NMR ($CDCl_3$, 62.5 MHz) δ 51.6 (CH_2); 64.8 (CH); 126.6 (2*CH); 127.2 (CH); 127.5 (CH); 127.6 (2*CH); 127.7 (CH); 128.4 (2*CH); 128.6 (2*CH); 128.7 (2*CH); 128.8 (2*CH); 130.5 (CH); 132.8 (CH); 137.1 (Cq); 140.6 (Cq); 143.4 (Cq). ν_{max}: 3059.9; 3025.9; 2918.8; 2849.3; 1737.4; 1600.0; 1493.5; 1450.8; 1233.7; 1027.1; 964.3; 742.6; 692.2. Anal. calcd for $C_{22}H_{21}N$ 88.25 (C) 7.07 (H) 4.68 (N); found 88.50 (C) 7.49 (H) 4.29 (N). HRMS (ESI) calculated for $C_{22}H_{22}N$ $[M–H]^+$ 300.1752; found 300.1767.

3. Synthesis of *(E)*-3-(sulfonyl-4-methylbenzene)-1,3-diphenylprop-1-ene 6

p-Toluenesulphinic acid sodium salt (107 mg, 0.6 mmol, 1.4 equiv.) and *(E)*-1,3-diphenyl-3-acetoxyprop-1-ene (105 mg, 0.42 mmol, 1 equiv.) were successively added to the chitosan–SILP catalyst. The mixture was stirred at room temperature

under N_2 for 20 h. The solution was then extracted with 1 mL of diethyl ether (monitored by TLC). The combined diethyl ether extracts were washed with water (1 mL), dried over $MgSO_4$ and filtered. Evaporation of the solvent gave a residue, which was purified by column chromatography on silica gel (petroleum ether/ether: 9/1 to 7/3) to give 6 as a white solid in 73% yield. Mp (DSC) 157–159 °C. ^{1}H NMR (250 MHz, $CDCl_3$,) δ 2.29 (s, $3H^{CH_3}$); 4.74 (d, J = 7.2 Hz, $1H^{CH}$); 6.40–6.55 (m, $2H^{2*CH}$); 7.10 (d, J = 8.2 Hz, $2H^{CHar}$); 7.14–7.28 (m, $10H^{CHar}$); 7.45 (d, J = 8.1 Hz, $2H^{CHar}$). ^{13}C NMR ($CDCl_3$, 62.5 MHz) δ 21.6 (CH_3); 75.3 (CH); 120.2 (CH); 126.4 (2*CH); 128.5 (CH); 128.6 (2*CH); 128.7 (2*CH); 128.9 (CH); 129.3 (4*CH); 129.7 (2*CH); 132.5 (Cq); 134.4 (Cq); 136.0 (Cq); 138.0 (CH); 144.6 (Cq). ν_{max}: 3060.8; 3027.6; 2922.1; 1493.5; 1454.6; 1310.6; 1287.6; 1141.3; 1083.5; 977.1; 746.1; 692.3. Anal. calcd for $C_{22}H_{20}O_2S$ 75.83 (C) 5.79 (H) 9.20 (S); found 76.13 (C) 5.98 (H) 8.63 (S). HRMS (ESI) calculated for $C_{22}H_{20}NaO_2S$ $[M–Na]^+$ 371.1082; found 371.1083.

4. Synthesis of *(E)*-3-phenoxy-1,3-diphenylprop-1-ene 7

Phenol (56 mg, 0.6 mmol, 1.4 equiv.) in [bmim][PF_6] (0.5 mL), *(E)*-1,3-diphenyl-3-acetoxyprop-1-ene (105 mg, 0.42 mmol, 1 equiv.) then Et_3N (69 μL, 0.5 mmol, 1.2 equiv.) were successively added to the chitosan–SILP catalyst which was stirred at room temperature under N_2 for 20 h. The solution was then extracted with diethyl ether (monitored by TLC). The combined diethyl ether extracts were washed with water (1 mL), dried over $MgSO_4$ and filtered. Evaporation of the solvent gave a residue, which was purified by column chromatography on silica gel (petroleum ether/ether: 9/1) to give **7** in 68% yield. Mp (DSC) 61–63 °C. ^{1}H NMR (250 MHz, $CDCl_3$,) δ 5.72 (d, J = 6.2 Hz, $1H^{CH}$); 6.36 (dd, J = 15.9 Hz, J = 6.3 Hz, $1H^{CH}$); 6.60 (d, J = 15.9 Hz, $1H^{CH}$); 6.86 (m, $3H^{CHar}$); 7.12–7.32 (m, $10H^{CHar}$); 7.39 (m, $2H^{CHar}$). ^{13}C NMR ($CDCl_3$, 62.5 MHz) δ 80.7 (CH); 116.3 (2*CH); 121.0 (CH); 126.7 (4*CH); 127.9 (2*CH); 128.6 (2*CH); 128.7 (2*CH); 129.3 (CH); 129.4 (2*CH); 131.5 (CH); 136.4 (Cq); 140.4 (Cq); 158.0 (Cq). ν_{max}: 2969.6; 2901.6; 1584.9; 1489.4; 1222.8; 1076.0; 1027.1; 961.5; 748.1; 688.7. Anal. calcd for $C_{21}H_{18}O$ 88.08 (C) 6.34 (H); found 88.22 (C) 6.47 (H). HRMS (ESI) calculated for $C_{21}H_{18}OK$ $[M–K]^+$ 325.0995; found 325.0943.

5. Synthesis of *(E)*-3-(1,3-diphenylallyl)-pentane-2,4-dione 8

Acetylacetone (62 μL, 0.6 mmol, 1.4 equiv.), *(E)*-1,3-diphenyl-3-acetoxyprop-1-ene (105 mg, 0.42 mmol, 1 equiv.), then K_2CO_3 (82 mg, 0.6 mmol, 1.4 equiv.) and water (0.2 mL) were successively added to the chitosan–SILP catalyst which was stirred at room temperature under N_2 for 20 h. The solution was then extracted with diethyl ether (monitored by TLC). The combined diethyl ether extracts were washed with water (1 mL), dried over $MgSO_4$ and filtered. Evaporation of the solvent gave a residue, which was purified by column chromatography on silica gel (petroleum ether/ether: 9/1) to give 8 in 80% yield. Mp (DSC) 82–84 °C. ^{1}H NMR (250 MHz, $CDCl_3$) δ 1.85 (s, $3H^{CH_3}$); 2.18 (s, $3H^{CH_3}$); 4.27 (m, $2H^{CH}$); 6.12 (dm, J = 16.2 Hz, $1H^{CH}$); 6.36 (d, J = 16.0 Hz, $1H^{CH}$); 7.10–7.37 (m, $10H^{CHar}$). ^{13}C NMR ($CDCl_3$, 62.5 MHz) δ 29.7 (CH_3); 30.0 (CH_3); 49.2 (CH); 74.5 (CH); 126.3 (2*CH); 127.3 (CH); 127.7 (CH); 127.9 (2*CH); 128.5 (2*CH); 129.0 (2*CH); 129.2 (CH); 131.6 (CH); 136.5 (Cq); 140.1 (Cq); 202.7 (CO); 202.9 (CO). ν_{max}: 2987.8; 2901.5; 1721.3; 1695.3; 1494.5; 1358.8; 1268.7; 1136.7; 1066.6; 967.1; 742.0; 692.9. Anal. calcd for $C_{20}H_{20}O_2$ 82.16 (C) 6.89 (H); found 82.19 (C) 7.36 (H). HRMS (ESI) calculated for $C_{20}H_{20}O_2Na$ $[M–Na]^+$ 315.1361; found 315.1375.

6. Synthesis of *(E)*-2-(1,3-diphenylallyl)-3-oxobutyric acid ethyl ester 9

Ethyl acetoacetate (78 mg, 0.6 mmol, 1.4 equiv.), *(E)*-1,3-diphenyl-3-acetoxyprop-1-ene (105 mg, 0.42 mmol, 1 equiv.) then Et_3N (69 μL, 0.5 mmol, 1.2 equiv.) were successively added to the chitosan–SILP catalyst, which was stirred at room temperature under N_2 for 20 h. The solution was then extracted with diethyl ether (monitored by TLC). The combined diethyl ether extracts were washed with water (1 mL), dried over $MgSO_4$ and filtered. Evaporation of the solvent gave a residue, which was purified by column chromatography on silica gel (petroleum ether/ether: 9/1) to give 9 in 89% yield. ^{1}H NMR (250 MHz, $CDCl_3$,) δ 0.88–1.15 (t, J = 7.2 Hz, $3H^{CH_3}$, both diastereoisomers); 1.94–2.21 (s, $3H^{CH_3}$, both diastereoisomers); 3.84–4.21 (m, $2H^{CH_2+CH}$, both diastereoisomers); 6.18–6.36 (m, $2H^{2*CH}$, both diastereoisomers); 7.06–7.21 (m, $10H^{CHar}$). ^{13}C NMR ($CDCl_3$, 62.5 MHz) δ 13.8 (2*CH_3); 30.0 (2*CH_3); 48.8 (2*CH); 61.5 (2*CH_2); 65.4 (2*CH); 126.4 (4*CH); 127.2 (2*CH); 127.7 (2*CH); 128.0 (4*CH); 128.5 (4*CH); 128.8 (4*CH); 129.4 (2*CH); 131.7 (2*CH); 136.7(2*Cq); 140.3 (2*Cq); 167.7 (2*CO); 201.6 (2*CO). ν_{max}: 3060.1; 3028.2; 2981.5; 1739.1; 1713.8; 1494.5; 1356.4; 1297.6; 1170.9; 1139.3; 964.6; 744.3; 693.4. Anal. calcd for $C_{21}H_{22}O_3$ 78.23 (C) 6.88 (H); found 78.30 (C) 7.35 (H). HRMS (ESI) calculated for $C_{21}H_{22}O_3Na$ $[M–Na]^+$ 345.1467; found 345.1476.

7. Synthesis of *(E)*-2-(1,3-diphenylallyl)-malonic acid dimethyl ester 10

Dimethyl malonate (68.6 μL, 0.6 mmol, 1.4 equiv.), *(E)*-1,3-diphenyl-3-acetoxyprop-1-ene (105 mg, 0.42 mmol, 1 equiv.), then Et_3N (69 μL, 0.5 mmol, 1.2 equiv.), were successively added to the chitosan–SILP catalyst which was stirred at room temperature under N_2 for 20 h. The solution was then extracted with diethyl ether (monitored by TLC). The combined diethyl ether extracts were washed with water (1 mL), dried over $MgSO_4$ and filtered. Evaporation of the solvent gave a residue, which was purified by column chromatography on silica gel (petroleum ether/ether: 9/1) to give 10 in 89% yield. Mp (DSC) 66–68 °C. ^{1}H NMR (250 MHz, $CDCl_3$) δ 3.42 (s, $3H^{CH_3}$); 3.60 (s, $3H^{CH_3}$); 3.87 (d, J = 10.9 Hz, $1H^{CH}$); 4.19 (dd, J = 10.9 Hz, J = 8.3 Hz, $1H^{CH}$); 6.24 (dd, J = 15.7 Hz, J = 8.3 Hz, $1H^{CH}$); 6.40 (d, J = 15.8, $1H^{CH}$); 7.07–7.25 (m, $10H^{CHar}$). ^{13}C NMR ($CDCl_3$, 62.5 MHz) δ 49.6 (CH); 52.9 (CH_3); 53.0 (CH_3); 58.0 (CH); 126.8 (2*CH); 127.6 (CH); 128.0 (CH); 128.3 (2*CH); 128.9 (2*CH); 129.1 (2*CH); 129.5 (CH); 132.2 (CH); 137.2 (Cq); 140.6 (Cq); 168.2 (CO); 168.6 (CO). ν_{max}: 3027.4; 2955.6; 1730.9; 1428.9; 1244.7; 1153.1; 969.0; 741.8; 700.7; 690.2. Anal. calcd for $C_{20}H_{20}O_4$ 74.06 (C) 6.21 (H); found 74.03 (C) 6.65 (H). HRMS (ESI) calculated for $C_{20}H_{20}O_4Na$ $[M–Na]^+$ 347.1259; found 347.1263.

8. Synthesis of *(E)*-2-(1,3-diphenylallyl)-1-phenylbutane-1,3-dione 11

1-Phenyl-1,3-butanedione (97.3 mg, 0.6 mmol, 1.4 equiv.) in [bmim][PF_6] (0.5 mL), *(E)*-1,3-diphenyl-3-acetoxyprop-1-ene (105 mg, 0.42 mmol, 1 equiv.) then K_2CO_3 (82 mg, 0.6 mmol, 1.4 equiv.) and water (0.2 mL) were successively added to the chitosan–SILP catalyst which was stirred at room temperature under N_2 for 20 h. The solution was then extracted with diethyl ether (monitored by TLC). The combined diethyl ether extracts were washed with water (1 mL), dried over $MgSO_4$ and filtered. Evaporation of the solvent gave a residue, which was purified by column chromatography on silica gel (petroleum ether/ether: 9/1) to give 11 in 90% yield. Mp (DSC) 142–144 °C. ^{1}H NMR (250 MHz, $CDCl_3$) δ 2.25 (s, $3H^{CH_3}$); 4.60 (dd, J = 11.2 Hz, J = 8.7 Hz, $1H^{CH}$); 5.18 (d, J = 11.3 Hz, $1H^{CH}$); 6.34 (dd, J = 15.8 Hz, J = 8.7 Hz, $1H^{CH}$); 6.55 (d, J = 15.8, $1H^{CH}$); 7.10–7.37 (m, $10H^{CHar}$); 7.42 (d, J = 7.8, $2H^{CHar}$); 7.52 (t, J = 7.4, $1H^{CHar}$); 7.89 (d, J = 7.3, $2H^{CHar}$). ^{13}C NMR ($CDCl_3$, 62.5 MHz) δ 27.7 (CH_3); 49.2 (CH); 69.5 (CH); 126.4 (2*CH); 126.9 (CH); 127.7 (CH); 127.9 (2*CH); 128.5 (2*CH); 128.6 (2*CH); 128.7 (4*CH); 129.3 (CH); 131.7 (CH); 133.6 (CH); 136.6 (Cq); 136.9 (Cq); 140.7 (Cq); 194.2 (CO); 203.0 (CO). ν_{max}: 2987.6; 2901.5; 1718.2; 1667.5; 1359.1; 1279.2; 1249.4; 1075.7; 1051.5; 962.1; 742.4; 685.9. HRMS (ESI) calculated for $C_{25}H_{22}O_2Na$ $[M–Na]^+$ 377.1517; found 377.1515.

Acknowledgements

This work has been performed within the inter-regional networks: RMPP et PUNCH (Pôle Universitaire Normand). We gratefully acknowledge financial support from the ''Ministère de la Recherche et des Nouvelles Technologies'', the CNRS (Centre National de la Recherche Scientifique), the ''Région Basse-Normandie'' and the European Union (FEDER Funds).

References

1 E. Lindner, T. Schneller, F. Auer and H. A. Mayer, *Angew. Chem., Int. Ed.*, 1999, **38**, 2154.
2 I. F. J. Vankelecom and P. A. Jacobs, in *Immobilisation of Chiral Catalysts*, ed. D. De Vos, I. F. J. Vankelecom and P. A. Jacobs, VCH Weinheim, 2000, ch. 2, pp 19–42.
3 (*a*) T. Welton, *Chem. Rev.*, 1999, **99**, 2071; (*b*) R. Sheldon, *Chem. Commun.*, 2001, 2399.
4 R. D. Rogers and K. R. Seddon, *Science*, 2003, **302**, 792.
5 See for example: H. Vallette, S. Pican, C. Boudou, J. Levillain, J. C. Plaquevent and A. C. Gaumont, *Tetrahedron Lett.*, 2006, **47**, 5191.
6 (*a*) A. Riisager, R. Fehrmann, M. Haumann and P. Wasserscheid, *Eur. J. Inorg. Chem.*, 2006, 695; (*b*) A. Riisager, R. Fehrmann, M. Haumann and P. Wasserscheid, *Top. Catal.*, 2006, **40**, 91.
7 C. P. Mehnert, E. J. Mozeleski and R. A. Cook, *Chem. Commun.*, 2002, 3010.
8 C. P. Mehnert, R. A. Cook, N. C. Dispenziere and M. Afeworki, *J. Am. Chem. Soc.*, 2002, **124**, 12932.
9 M. H. Valkenberg, C. de Castro and W. F. Hölderich, *Green Chem.*, 2002, **4**, 88.
10 D. W. Kim and D. Y. Chi, *Angew. Chem., Int. Ed.*, 2004, **43**, 483.
11 N. V. Kramavera, A. Y. Stakheev, O. P. Tkachenko, K. V. Klementiev, W. Grünert, E. D. Finashina and L. M. Kustov, *J. Mol. Catal. A: Chem.*, 2004, **209**, 97.
12 (*a*) F. Lebouc, I. Dez and P. J. Madec, *Polymer*, 2005, **46**(2), 319; (*b*) F. Lebouc, I. Dez, J. Desbrières, L. Picton and P. J. Madec, *Polymer*, 2005, **46**(3), 639.
13 (*a*) E. Guibal, *Prog. Polym. Sci.*, 2005, **30**, 71; (*b*) D. J. Macquarrie and J. J. E. Hardy, *Ind. Eng. Chem. Res.*, 2005, **44**, 8499.
14 F. Quignard, A. Choplin and A. Domard, *Langmuir*, 2000, **16**, 9106.
15 J. Tsuji, in *Palladium Reagents and Catalysts*, Wiley and Sons, New York, 1995.
16 P. Buisson and F. Quignard, *Aust. J. Chem.*, 2002, **55**, 73.
17 W. Chen, L. Xu, C. Chatterton and J. Xiao, *Chem. Commun.*, 1999, 1247.

Selective oxidation of styrene to acetophenone over supported Au–Pd catalyst with hydrogen peroxide in supercritical carbon dioxide

Xueguang Wang,[a] Natarajan S. Venkataramanan,[a] Hajime Kawanami*[ab] and Yutaka Ikushima[a]

Received 7th March 2007, Accepted 16th August 2007
First published as an Advance Article on the web 7th September 2007
DOI: 10.1039/b703458j

Selective oxidation of styrene to acetophenone has been investigated for the first time over Pd–Au catalysts with H_2O_2 in CO_2 medium. The influence of the support on the catalytic activity and the product selectivity was investigated, and Al_2O_3 support showed the best catalytic performance in this system. The presence of CO_2 medium could improve the oxidation of styrene to acetophenone and inhibit the formation of by-products. The influence of substituting groups in the aromatic rings of styrene was also discussed.

Introduction

Acetophenone and its derivatives are important intermediates in the manufacture of pharmaceuticals, resins, drugs and perfumes. The classical production of acetophenone is performed by Friedel–Crafts process of benzene with acetic anhydride or acetyl chloride, using stoichiometric quantities of homogeneous acid.[1,2] The Wacker reaction is another important method for the synthesis of acetophenone, which involves the oxidation of terminal olefins to ketones over Pd(II) catalyst using excess hydrogen peroxide (H_2O_2) as oxidizing agents in the presence of acetic acid.[3,4] However, both the above processes cause problems in product separation, corrosion hazards of the reactor and a large amounts of toxic and corrosive wastes. Consequently, the development of a simple, efficient and environmentally benign method for the selective synthesis of styrene to acetophenone is still of great challenge.

Au- and Pd-based solid catalysts have received much attention due to their excellent catalytic performance in the oxidation of alcohols and carbon monoxide using molecular oxygen.[5–10] Recently, the oxidation of styrene has been reported by anhydrous *t*-butyl hydroperoxide (TBHP) over supported Au nanocatalysts in the presence of benzene solvent.[11,12] However, these catalysts hardly showed selectivity to acetophenone under reaction conditions. To the best of our knowledge, no literature is available on the efficient selective oxidation of styrene to acetophenone over an Au and/or Pd-based solid catalyst, especially through an environmentally friendly route.

In recent years, supercritical CO_2 ($scCO_2$) has been extensively used as an environmentally benign solvent and is a potential replacement for conventional hazardous solvents as it possesses a mild critical point.[13–15] Particularly, in oxidation reactions of weakly polar, water-insoluble alkenes, $scCO_2$ is advantageous for its low polarity. Moreover, the tunable physical properties with pressure and temperature may enable the improvement of reaction rates and product selectivity in the reactions.[16,17] In addition, products and solvent can be easily separated by releasing the pressure of the reaction mixtures. Here, we will report for the first time on the efficient selective oxidation of styrene to acetophenone over supported Au–Pd catalysts with H_2O_2 in $scCO_2$.

[a]*Research Center for Compact Chemical Process, AIST, 4-2-1 Nigatake, Miyagino-ku, Sendai, 983-8551, Japan. E-mail: h-kawanami@aist.go.jp; Fax: +81 22 237 5214; Tel: +81 22 237 5211*
[b]*School of Chemistry, Department of Science, University of Nottingham, University Park, Nottingham, NG7 2RD, UK*

Experimental

TiO_2, ZrO_2, Al_2O_3, and SiO_2 were purchased from Japan Aerosil. $HAuCl_4{\cdot}3H_2O$ and $PdCl_2$ were from Aldrich, and other chemicals of reagent grade were from Wako. All chemicals were used as received.

The supported Pd, Au and Pd–Au catalysts were prepared by the impregnation method according to the literature.[18] 2.5 wt% Pd/Al_2O_3, 5 wt% Pd/Al_2O_3 and 5 wt% Au/Al_2O_3 were prepared by impregnation of Al_2O_3 into aqueous solutions of $PdCl_2$ or $HAuCl_4{\cdot}3H_2O$. For a range of supported 2.5 wt% Au/2.5 wt% Pd catalysts using TiO_2, ZrO_2, Al_2O_3, CeO_2 and SiO_2 as supports, in a typical preparation, 1.14 g of $HAuCl_4{\cdot}3H_2O$ and 0.95 g of $PdCl_2$ were dissolved into 100 ml of water. 16.5 ml of the prepared solution was added into 3.8 g of support powder under vigorous stirring and kept at room temperature for 2 h, and then the mixture suspension was evaporated out at 60 °C. After this, the solid was dried at 100 °C overnight and ground to powder, and finally was calcined at 400 °C for 3 h.

The oxidation of styrene was carried out in a 50 ml high pressure reactor. The catalyst was charged into the reactor and then was flushed with 2.0 MPa CO_2 three times. The reactor was heated at the set temperature for 1 h to stabilize the temperature. Then 450 μl of 30 wt% H_2O_2 and 1 mmol of styrene were simultaneously introduced with CO_2 to the desired pressure using a high-pressure liquid pump. The reaction mixture was stirred continuously with a magnetic stirrer during the reaction. After the reaction, the reactor was cooled in ice-cold water. Finally, the products were separated by filtration and analyzed by a gas chromatograph with a capillary column. The selectivity was calculated as molar percentage of the consumed styrene to a certain product per mol of reacted

Table 1 The results of the oxidation of styrene over supported Pd and/or Au catalyst with H_2O_2 in $scCO_2$

Entry	Catalyst	Conversion of styrene (mol%)	Selectivity to acetophenone (mol%)	Selectivity to benzaldehyde (mol%)	Selectivity to benzoic acid (mol%)	Selectivity to others (mol%)
1	5 wt% Au/Al_2O_3	4	35	65	0	0
2	2.5 wt% Pd/Al_2O_3	53	83	6	7	4
3	5 wt% Pd/Al_2O_3	54	81	6	7	6
4	2.5 wt% Pd/2.5 wt% Au/Al_2O_3	68	87	5	7	1
5	2.5 wt% Pd/2.5 wt% Au/ZrO_2	28	60	11	7	22
6	2.5 wt% Pd/2.5 wt% Au/CeO_2	29	78	13	3	6
7	2.5 wt% Pd/2.5 wt% Au/SiO_2	73	46	25	11	18
8	2.5 wt% Pd/2.5 wt% Au/TiO_2	56	63	16	14	7
9[a]	2.5 wt% Pd/2.5 wt% Au/Al_2O_3	39	84	11	0	5
10[b]	2.5 wt% Pd/2.5 wt% Au/Al_2O_3	29	77	14	0	9

[a] Spent entry 4 catalyst for the first run. [b] For the second run. Reaction conditions: styrene, 1 mmol; catalyst, 0.4 g; H_2O_2, 4 mmol; CO_2 pressure, 9 MPa; reaction temperature, 120 °C; reaction time, 3 h.

styrene. The used catalyst was washed with diethyl ether and calcined at 300 °C for 2 h, and then it was reused for the subsequent oxidation of styrene.

Results and discussion

5 wt% Au/Al_2O_3, 2.5 wt% Pd/Al_2O_3, 5 wt% Pd/Al_2O_3 and 2.5 wt% Au/2.5 wt% Pd/Al_2O_3 were first evaluated for the oxidation of styrene with H_2O_2 as oxidant in $scCO_2$ at 120 °C for 3 h and the reaction results are shown in Table 1. Au/Al_2O_3 catayst (Table 1, entry 1) has a very poor activity of 4% and a low acetophenone selectivity of 35%. Supported Pd catalysts (Table 1, entry 2 and 3) show good conversions and high acetophenone selectivities, but the increase in Pd loading from 2.5% to 5% in catalyst has little influence on the conversion and the selectivity to acetophenone. After addition of Au to Pd/Al_2O_3 catalyst, the catalytic activity and the acetophone selectivity (Table 1, entry 4) are increased from 53% and 83% to 68% and 87%, respectively, indicating that Au can improve the catalytic performance of Pd/Al_2O_3 as reported for the selective oxidation of alcohols.[7]

The catalytic performance of 2.5 wt% Au/2.5 wt% Pd/Al_2O_3 catalyst as a function of reaction period was examined at 120 °C in $scCO_2$ and the results are shown in Fig. 1. In this reaction, styrene can be oxidized to form acetophenone, benzaldehyde, benzoic acid and traces of other by-products. The conversion of styrene increases to 68% with the reaction time up to 3 h. As the reaction time is prolonged, the conversion remains constant, possibly due to the exhaustion of H_2O_2. However, the acetophenone selectivity has little change for the first 3 h, but then shows a slight decrease at 4 h. Over the whole course of the catalytic reaction, the benzaldehyde selectivity decreases, and correspondingly, the selectivity to benzoic acid gradually increases, but the total selectivity to benzaldehyde and benzoic acid show no change, staying around 12%. These results imply that the formation of acetophenone and benzaldehyde might proceed in parallel pathways. The trace amounts of other by-products were formed by the further reaction of acetophenone. The possible pathways of the reactions occurring on the surface of Pd–Au catalyst are proposed in Scheme 1.

The effect of the support materials on the activity and selectivity of the catalysts were investigated over Pd–Au catalysts. As shown in Fig. 2, all the supported Pd–Au catalysts have certain catalytic activities and selectivity to acetophenone. The Al_2O_3 support shows both good catalytic activity and high selectivity to acetophenone, with an acetophenone yield of 59%. The TiO_2 support has the highest conversion of 73%. However, the selectivity to acetophenone is very low with large amounts of benzaldehyde or benzoic acid and other by-products, as seen in Table 1, entry 7. ZrO_2 and CeO_2 supports show good selectivity to acetophenone ($\geqslant$60%), but the conversions of styrene are 28% and 29%,

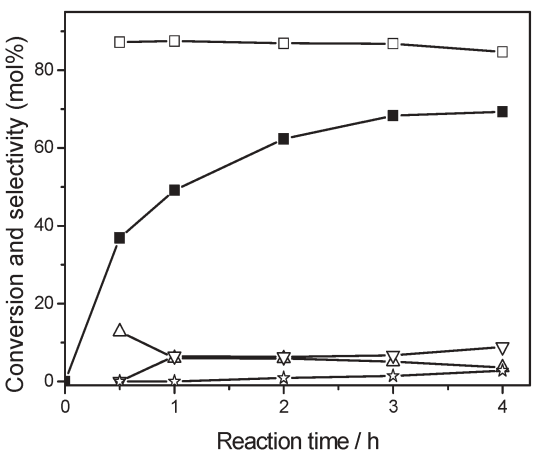

Fig. 1 The dependence of reaction time on styrene conversion and product selectivity over 2.5 wt% Au/2.5 wt% Pd/Al_2O_3 catalyst: (■) conversion of styrene, (□) selectivity to acetophenone, (△) selectivity to benzaldehyde, (▽) selectivity to benzoic acid, and (☆) other by-products. Reaction conditions: styrene, 1 mmol; catalyst, 0.4 g; H_2O_2, 4 mmol; CO_2 pressure, 9 MPa; reaction temperature, 120 °C.

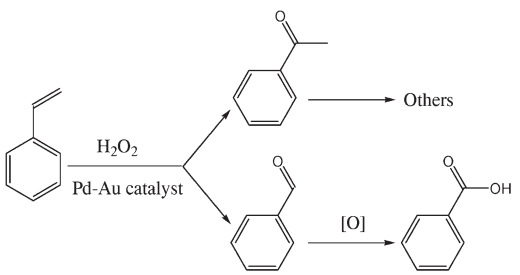

Scheme 1 Reaction scheme for the oxidation of styrene over supported Pd–Au catalyst.

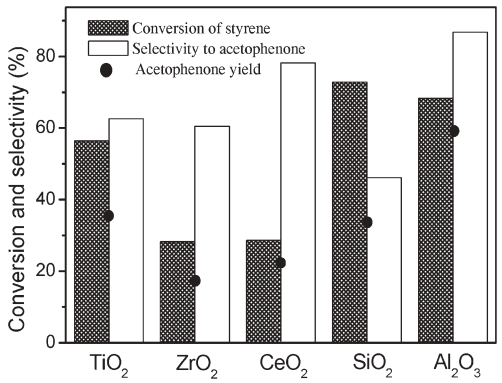

Fig. 2 Results of the selective oxidation of styrene to acetophenone over different support catalysts in $scCO_2$. *Reaction conditions*: styrene, 1 mmol; catalyst, 0.4 g; H_2O_2, 4 mmol; CO_2 pressure, 9 MPa; reaction temperature, 120 °C; reaction time, 3 h.

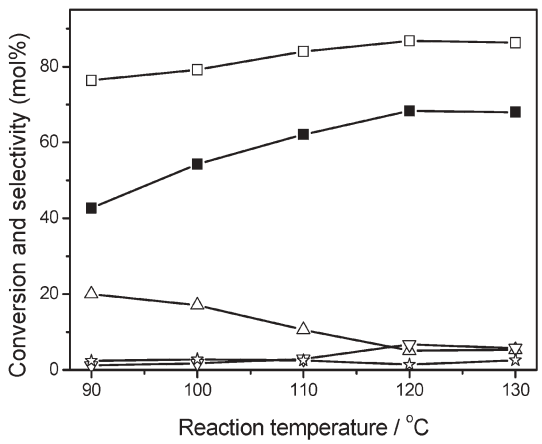

Fig. 3 Effect of reaction temperature on the reaction performance over 2.5 wt% Au/2.5 wt% Pd/Al_2O_3 catalyst: (■) conversion of styrene, (□) selectivity to acetophenone, (△) selectivity to benzaldehyde, (▽) selectivity to benzoic acid, and (☆) other by-products. *Reaction conditions*: styrene, 1 mmol; catalyst, 0.4 g; H_2O_2, 4 mmol; CO_2 pressure, 9 MPa; reaction time, 3 h.

respectively, much less than the 68% for Al_2O_3. The order of acetophenone yields over different supports for the selective oxidation of styrene is Al_2O_3 (59%) > TiO_2 (35%) > SiO_2 (34%) > CeO_2 (23%) > ZrO_2 (17%). The results reveal that the nature of the support has a strong influence on both the activity of Pd–Au catalysts and the selectivity to acetophenone, and Al_2O_3 is the best support of Pd–Au catalysts for the selective oxidation of styrene with H_2O_2 in $scCO_2$.

The effect of reaction temperature on conversion of styrene and acetophenone selectivity was examined in $scCO_2$ over 2.5 wt% Au/2.5 wt% Pd/Al_2O_3 and the results are illustrated in Fig. 3. It was found that the conversion of styrene increases gradually with the reaction temperature from 43% at 90 °C to 68% at 120 °C, and the selectivity to acetophenone was also increased from 76% to 87%. As the temperature was further raised to 130 °C, the conversion of styrene and the acetopheone selectivity show little change. Fig. 3 displays that the total selectivity of benzaldehyde and benzoic acid decrease with the reaction temperature. This indicates that the elevated temperature favours the selective oxidation of styrene to acetophenone, and, relatively, reduces the reaction of styrene to benzaldehyde.

The effect of CO_2 pressure on the activity and the product selectivity was investigated over 2.5 wt% Au/2.5 wt% Pd/Al_2O_3 for the oxidation of styrene at 120 °C for 3 h and the results are shown in Table 2. Compared with the results without CO_2, the catalyst in the presence of CO_2 has higher conversion of styrene, indicating that the CO_2 medium can promote the oxidation of styrene. The styrene conversion hardly changes with the increase in CO_2 pressure from 4 MPa to 16 MPa. However, the acetophenone selectivity increases with the increase in CO_2 pressure and reaches a maximum at 9 MPa. As seen in Table 2, the selectivity to benzaldehyde decreases and the selectivity to benzoic acid increases with the CO_2 pressure in the lower pressure region, but the total selectivity of benzaldehyde and benzoic acid changes little. At the same time, other by-product selectivity dramatically decreases from 18% to 1%. These results imply that CO_2 medium in the proper pressure region might promote the further oxidation of benzaldehyde to benzoic acid, but inhibit the transformation of acetophenone to other by-prodcuts.

The oxidation reaction of some substituted styrenes was carried out over 2.5 wt% Au/2.5 wt% Pd/Al_2O_3 in $scCO_2$ at 120 °C for 3 h. The results are summarized in Table 3. All the results show relatively high conversions of styrene and very high selectivities to the corresponding acetophenones. The substituting groups in the aromatic rings have great influence on the conversion and the product selectivity. The presence of the electron-donating group ($-CH_3$) at the *para*-position of styrene increases the conversion of styrene, while the electron-withdrawing group ($-NO_2$) at the *meta*-position of styrene decreases both the conversion and the selectivity to acetophenone, but favours the formation of benzaldehyde and other by-products.

2.5 wt% Au/2.5 wt% Pd/Al_2O_3 catalyst was recycled after being washed with diethyl ether and the results are given in Table 1, entry 9 and 10. It can be seen that the conversion of

Table 2 The effect of CO_2 pressure on the activity of 2.5 wt% Au/2.5 wt% Pd/Al_2O_3 and the product selectivity

Entry	CO_2 pressure/MPa	Conversion of styrene (mol%)	Selectivity to acetophenone (mol%)	Selectivity to benzaldehyde (mol%)	Selectivity to benzoic acid (mol%)	Selectivity to others (mol%)
1	0	53	70	10	3	17
2	4	69	79	4	8	11
3	6	70	84	1	8	8
4	9	68	87	5	7	1
5	13	71	78	6	10	6
6	16	67	74	10	10	6

[a] Reaction conditions: styrene, 1 mmol; catalyst, 0.4 g; H_2O_2, 4 mmol; reaction temperature, 120 °C; reaction time, 3 h.

Table 3 Selective oxidation of styrene with substituting groups over 2.5 wt% Au/2.5 wt% Pd/Al_2O_3 with H_2O_2 in $scCO_2$ at 120 °C for 3 h

Entry	Substrate	Conversion of styrene (mol%)	Selectivity to acetophenone (mol%)	Selectivity to benzaldehyde (mol%)	Selectivity to benzoic acid (%)	Selectivity to others (mol%)
1	Styrene	68	87	5	7	1
2	*p*-Methylstyrene	79	88	7	2	2
3	3-Nitrostyrene	55	61	26	0	13

[a] Reaction conditions: styrene, 1 mmol; catalyst, 0.4 g; H_2O_2, 4 mmol; CO_2 pressure, 9 MPa; reaction temperature, 120 °C; reaction time, 3 h.

styrene shows a significant decrease after the first reaction. The reason for deactivation is still under investigation.

Conclusions

A supported Pd–Au catalyst is efficient for the selective oxidation of styrene to acetophenone with H_2O_2 in $scCO_2$. The presence of the CO_2 medium can increase the conversion of styrene and enhance the selectivity to acetophenone and, at the same time, inhibit the formation of other by-products. The nature of the support has great influence on the catalytic performance of Pd–Au catalysts. Al_2O_3 is the best support for the selective oxidation of styrene in $scCO_2$. The substituting groups in the aromatic rings of styrene also affect the catalytic performance. An electron-donating group at the *para*-position of styrene increases the conversion of styrene, but an electron-withdrawing group at the *meta*-position of styrene decreases both the conversion and the selectivity to acetophenone. Although this reaction system can not currently be recycled due to partial deactivation, supported Pd–Au catalyst will still be promising and worthy of investigation for the selective oxidation of styrene to acetophenone from an environmentally benign point of view.

Acknowledgements

This research is partly supported by Development of Microspace and Nanospace Reaction Environment Technology for Functional Materials Project under NEDO (New Energy and Industrial Technology Development Organization).

References

1 G. A. Olah, *Friedel–Crafts and Related Reactions*, Wiley-Interscience, New York, 1963.
2 S. K. Jana, P. Wu and T. Tatsumi, *J. Catal.*, 2006, **240**, 268.
3 V. V. Namboodiri, R. S. Varma, E. Sahle-Demessie and U. R. Pillai, *Green Chem.*, 2002, **4**, 170.
4 N. Alandis, I. Ricolattes and A. Lattes, *New J. Chem.*, 1994, **18**, 1147.
5 K. Mori, T. Kara, T. Mizugaki, K. Ebitani and K. Kaneda, *J. Am. Chem. Soc.*, 2004, **126**, 10657.
6 B. Karimi, S. Abedi, J. H. Clark and V. Budarin, *Angew. Chem., Int. Ed.*, 2006, **45**, 4776.
7 D. I. Enache, J. K. Edwards, P. Landon, B. Solsona-Espriu, A. F. Carley, A. A. Herzing, M. Watanabe, C. J. Kiely, D. W. Knight and G. J. Hutchings, *Science*, 2006, **311**, 362.
8 H. Wu, Q. Zhang and Y. Wang, *Adv. Synth. Catal.*, 2005, **347**, 1356.
9 M. S. Chen and D. W. Goodman, *Science*, 2004, **36**, 252.
10 A. M. Venezia, L. F. Liotta, G. Pantaleo, V. La Parola, G. Deganello, A. Beck, Zs. Koppany, K. Frey, D. Horvath and L. Guczi, *Appl. Catal., A*, 2003, **251**, 359.
11 N. S. Patil, R. Jha, B. S. Uphade, S. K. Bhargava and V. R. Choudhary, *Appl. Catal., A*, 2004, **275**, 87.
12 N. S. Patil, B. S. Uphade, P. Jana, S. K. Bharagava and V. R. Choudhary, *J. Catal.*, 2004, **223**, 236.
13 E. Sahle-Demessie, M. A. Gonzalez, J. Enriquez and Q. Zhao, *Ind. Eng. Chem. Res.*, 2000, **39**, 4858.
14 G. Jenzer, D. Sueur, T. Mallat and A. Baiker, *Chem. Commun.*, 2000, 2247.
15 M. Caravati, J. D. Grunwaldt and A. Baiker, *Catal. Today*, 2004, **91**, 1.
16 H. Jiang, L. Jia and J. Li, *Green Chem.*, 2000, **2**, 161.
17 N. Theyssen, Z. Hou and W. Leitner, *Chem.–Eur. J.*, 2006, **12**, 3401.
18 J. K. Edwards, B. E. Solsona, P. Landon, A. F. Carley, A. Herzing, C. J. Kiely and G. J. Hutchings, *J. Catal.*, 2005, **236**, 69.

Cross-metathesis of fatty acid derivatives with methyl acrylate: renewable raw materials for the chemical industry†

Anastasiya Rybak and Michael A. R. Meier

Received 9th August 2007, Accepted 28th September 2007
First published as an Advance Article on the web 16th October 2007
DOI: 10.1039/b712293d

The cross-metathesis of fatty acid esters derived from plant oils as renewable raw materials with methyl acrylate was studied, revealing high conversions for the synthesis of α,ω-dicarboxylic acid esters, depending on the choice of catalyst. A series of unsaturated α,ω-diesters (1,8-, 1,11-, 1,12-, 1,15-, and 1,20-), as well as unsaturated α-esters, was thus prepared and fully characterized. The obtained results can significantly contribute to a sustainable supply of monomers for polyester and polyamide synthesis, as well as for detergents.

Introduction

Fats and oils are important renewable raw materials for the chemical industry.[1] Cross-metathesis of unsaturated fatty acid derivatives has been known for many decades. However, until now only unfunctional cross-metathesis reaction partners, such as ethylene or 2-butene, were investigated with a variety of catalysts.[2–5] Such approaches can not only contribute to a sustainable development, due to the utilization of renewable raw materials, but also offer the opportunity to obtain desired platform chemicals and other products in high yields with relatively low catalyst loadings. Currently, Materia Inc. and Cargill are on the way to commercialize the cross-metathesis of natural fats and oils (and their derivatives) with ethylene in order to obtain a variety of products ranging from waxes to defined platform chemicals.[6] As already discussed in the early 1990s by Warwel *et al.*, 9-decenoic acid (which can be derived by the metathetical ethenolysis of oleic acid) can be such a platform chemical for the sustainable production of a variety of polymers, including polyesters, polyamides, polyethers, as well as polyolefins.[4] In our approach, methyl acrylate (**MA**) was studied as a cross-metathesis co-reactant for the direct synthesis of α,ω-dicarboxylic acid derivatives. This approach has the advantage of a direct access to desirable monomers and detergent intermediates in high yields, without the production of undesired byproducts, taking full advantage of the synthetic potential of renewable raw materials.

The cross-metathesis of electron deficient substrates, such as acrylic acid and its esters, is possible with second generation metathesis catalysts and is frequently used as a synthetic approach to a variety of interesting compounds.[7,8] However, usually high catalysts loadings of 5 mol% and up to 20 mol% and/or longer reaction times were required to perform these reactions successfully.[8–11] Special care has to be taken for the choice of catalyst, whereby second generation ruthenium based catalysts developed by Grubbs and Hoveyda-Grubbs are reported to tolerate a wide range of chemical functionalities. Therefore, we studied the commercially available second generation catalysts **C2** and **C3** for these cross-metathesis reactions and compared the results to the widely studied Grubbs first generation catalyst **C1** (compare Fig. 1). Generally, Grubbs *et al.* recently introduced a classification due to which acrylates are considered as type II substrates that undergo self-metathesis only at slow reaction rates with the Grubbs second generation catalyst.[7] On the other hand, the internal double bonds of unsaturated fatty acid derivatives can be considered as type I reactants, since they readily undergo self-metathesis with generation 1 and generation 2 types of catalysts. Therefore, it should be possible to obtain the desired α,ω-dicarboxylic acid derivatives *via* cross-metathesis.

University of Applied Sciences Oldenburg/Ostfriesland/Wilhelmshaven, Constantiaplatz 4, 26723, Emden, Germany.
E-mail: michael.meier@fh-oow.de; www.meier-michael.com
† Electronic supplementary information (ESI) available: Additional gas chromatography results and analytical data. See DOI: 10.1039/b712293d

Results and discussion

We started our investigations with methyl oleate (**1**) as the model substrate. As others before us,[12] we observed a facile self-metathesis of this substrate with all studied catalysts, leading to a statistical mixture of methyl oleate, 9-octadecene and dimethyl-9-octadecene-1,18-dioate, if methyl oleate was metathesized. The obtained products were isolated from the mixtures and analyzed by GC-MS, ESI-MS, as well as NMR, in order to identify all substances and were subsequently used as identification standards for the cross-metathesis reactions. Table 1 summarises the cross-metathesis results of methyl oleate with methyl acrylate, whereas Fig. 2 depicts the corresponding reaction scheme.

From the results in Table 1, it can be concluded that the cross-metathesis reaction of **1** with methyl acrylate proceeds smoothly only with the second generation catalysts **C2** and **C3**, for reasons discussed above. Products **2** and **3** were identified by GC-MS, ESI-MS, as well as ^{1}H NMR experiments, and later on isolated for a complete analysis. Both products are useful for the chemical industry, since **2** is a α,ω-diester that can be applied for the synthesis of polycondensation polymers (*e.g.* polyesters or polyamides) and **3** is a valuable starting material for detergents.[13]

Generally, lower loadings of catalyst led to an increase in self-metathesis products (compare, *e.g.*, entries 4 and 5,

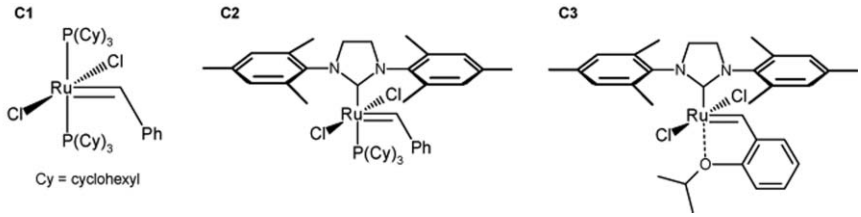

Fig. 1 Studied metathesis catalysts (initiators).

Table 1 Cross-metathesis results of methyl oleate with methyl acrylate (**MA**) (T = 50 °C, reactions performed with 0.5 g **1** in bulk)

	Catalyst (mol%)	C (%)[a]	SM (%)[b]	Yield CM (%)[c]	time	x =[d]
1	**C1** (10)	0	0	0	72 h	10
2	**C2** (5)	71	60	43	72 h	10
3	**C2** (5)	82	68	66	72 h	5
4	**C3** (5)	99	0	99	30 min	10
5	**C3** (1)	95	5	90	30 min	10
6	**C3** (0.2)	97	5	92	18 h	10
7	**C3** (0.1)	79	22	69	20 h	10
8	**C3** (1)	95	5	90	30 min	5

[a] Conversion of **1** in % (by GC); [b] % self-metathesis products of all products (GC estimate); [c] Yield[14] of cross-metathesis products in % (GC estimate); [d] Ratio of **MA** : **1** (compare Fig. 2)

Table 1) and optimization reactions with the most promising catalyst **C3** revealed that a loading of only 0.2 mol% with ten equivalents of methyl acrylate led to full conversion of **1**, while the self-metathesis of **1** was still almost completely suppressed under these conditions (entry 6, Table 1). Interestingly, when performing the same reaction with only five equivalents of methyl acrylate, considerable amounts of self-metathesis products were observed. From GC analysis, we also estimated the yields of the desired cross-metathesis products,[14] clearly revealing that even at low catalyst loadings, high yields can be obtained. Moreover, we observed that reactions performed under a N_2 atmosphere generally led to 10–20% higher conversions, and that increasing the equivalents of methyl acrylate slightly decreased conversions. In addition, ^{1}H NMR investigations of **2** and **3** revealed a high stereoselectivity of the reaction, since the high coupling constant of the alkenyl protons ($J \sim 15$ Hz) in combination with a high chemical shift ($\delta \sim 7$ and $\delta \sim 5.8$ ppm) of these protons indicate that only trans isomers were formed.[15] This observation is further supported by ^{13}C NMR measurements, where only two peaks for the olefinic carbons were detected at ~150 and 120 ppm. It is also very important to note here that our investigations were performed in bulk and that this synthetic approach did not only significantly increase the observed conversions and the reaction rate but is also beneficial in terms of green chemistry, since solvent waste can be avoided.[16] These results represent a significant improvement of currently known literature procedures and are even more valuable if the contribution to a sustainable development due to the use of renewable raw materials is considered.

Inspired by these results, we investigated the cross-metathesis of methyl erucate (**4**) and methyl petroselinate (**5**) with **C3** under similar conditions (Fig. 3). However, first we

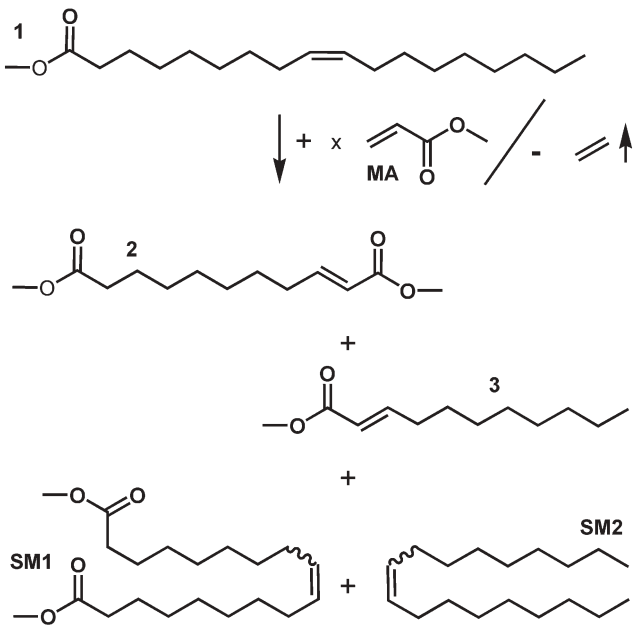

Fig. 2 Cross-metathesis of methyl oleate (**1**) with methyl acrylate (**SM1** and **SM2** are self-metathesis side products).

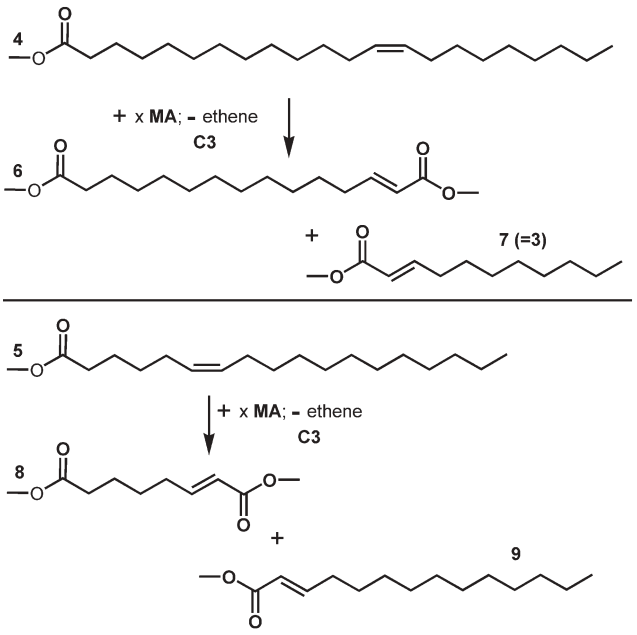

Fig. 3 Cross-metathesis of methyl erucate and methyl petroselinate with methyl acrylate. (Note: self-metathesis products are omitted for simplicity.)

Table 2 Self- and cross-metathesis results of methyl 10-undecenoate with methyl acrylate (**MA**) (T = 50 °C, reactions performed with 0.5 g **10** in bulk)

	Catalyst (mol%)	C (%)[a]	SM (%)[b]	Yield CM (%)[c]	time	x =[d]
1	**C1** (1)	69	100	—	30 min	0
2	**C2** (1)	98	100	—	30 min	0
3	**C3** (1)	95	100	—	30 min	0
4	**C1** (1)	13	90	1	72 h	5
5	**C2** (1)	98	5	93	30 min	5
6	**C2** (0.5)	95	7	88	30 min	5
7	**C2** (0.5)	87	15	74	30 min	2
8	**C2** (0.2)	80	8	74	30 min	5
9	**C2** (0.1)	79	12	70	30 min	2
10	**C3** (1)	98	1	97	30 min	5
11	**C3** (0.2)	98	0	98	30 min	10
12	**C3** (0.1)	99	0	99	30 min	10
13	**C3** (0.1)	99	3	96	30 min	5

[a] Conversion of **10** in % (GC); [b] % self-metathesis products of all products (GC estimate); [c] Yield[14] of cross-metathesis products in % (GC estimate); [d] Ratio of **MA** : **10** (compare Fig. 4 and 5)

investigated their self-metathesis in order to have model compounds for GC analysis in our hands and in order to understand these reactions completely. As for methyl oleate, the self-metathesis of **4** and **5** with 1 mol% **C1** and 0.1 mol% **C2** led to a statistical mixture of alkene, starting material and diester, which could all be successfully identified by GC-MS and ESI-MS. The subsequently studied cross-metathesis of **4** and **5** with methyl acrylate (see Fig. 3) led to the desired products **6** and **7** as well as **8** and **9**, respectively. As already observed for the cross-metathesis of **1**, also the cross-metathesis of **4** and **5** was unsuccessfull with **C1** as a catalyst, whereas **C2** and especially **C3** provided similarly high conversions and product yields as for **1**. Therefore, not only the 1,11-diester (**2**), but also the 1,15-diester (**6**) and the 1,8-diester (**8**) can be obtained from renewable raw materials by this approach. As already observed for **2** and **3**, the NMR data of **6** and **7** only showed trans configured double bonds, once more indicating the high stereoselectivity of these reactions. The accompanying byproducts **7** and **9** are again valuable starting materials for detergent applications.[13]

Last, but not least, we studied the self- and cross-metathesis of methyl 10-undecenoate (**10**), which can be obtained from the pyrolysis of ricinoleic acid from castor oil.[17,18] The self-metathesis of **10** proceeded smoothly with all investigated catalysts, as shown in Table 2, revealing that the second generation catalysts are more active than **C1**, as expected. The resulting product **11** (Fig. 4), a 1,20-diester, could be obtained in high conversion and yields with all studied catalysts (compare entries 1–3, Table 2).

The cross-metathesis of **10** with methyl acrylate resulted in the formation of the 1,12-diester (**12**), as shown in Fig. 5. A

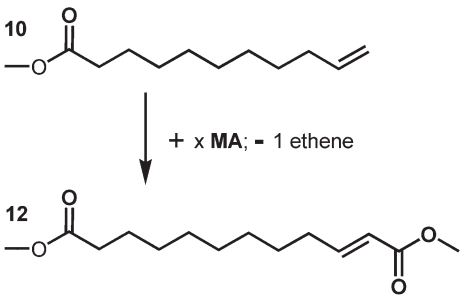

Fig. 5 Cross-metathesis of methyl 10-undecenoate with methyl acrylate.

catalyst loading of only 1 mol% resulted in full conversion with both **C2** and **C3** after only 30 min reaction time (entries 5 and 10, Table 2). These reactions also showed that **C3** tends to produce fewer self-metathesis products than **C2**. This trend gets even more pronounced if lower catalyst loadings are applied. Moreover, even **C1** was able to catalyze this reaction, albeit not very efficiently, since GC analysis showed a large excess of the self-metathesis products if compared to the cross-metathesis products. Remarkably, **C2** could still provide almost full conversion at an even lower catalyst loading of 0.5 mol% in a relatively clean reaction without the observation of large amounts of byproducts (entry 6, Table 2). However, if the catalyst loading of **C2** was further decreased, conversions dropped and more self-metathesis products were observed (entries 8 and 9, Table 2). This observation is not valid for **C3** and thus reactions with this catalyst proceeded smoothly without the observation of self-metathesis products even at 0.1 mol% of catalyst loading (entries 12 and 13, Table 2). The advantage of this reaction is of course the equimolar liberation of ethene in the course of the reaction, in combination with the high reactivity of the terminal type I olefin with all catalysts that drives the equilibrium easily to the side of the products. These observations are in complete agreement with literature and are due to the higher reactivity of the terminal olefin, if compared to the internal double bonds of **1**, **4**, and **5**. Catalyst **C2** did not produce any side products, as was sometimes the case for **C3** with a loading of 1 mol% or higher that showed considerable amounts (up to ~30%) of unidentified side products in GC traces, that were most likely a result of isomerisation reactions.[19] However, when **C3** was applied in very low loadings of 0.1 or 0.2 mol%, full conversions without the observation of side products was observed. Fig. 6 depicts the gas chromatography analysis of such a reaction, clearly showing that full conversion can be achieved without observation of the formation of self-metathesis side products (the self-metathesis product **11** would be observed at 19.9 min under these GC conditions and was not detectable).

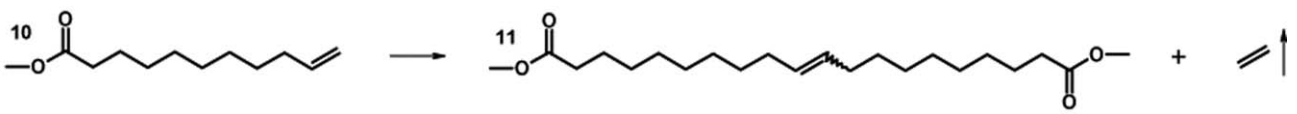

Fig. 4 Self-metathesis of methyl 10-undecenoate.

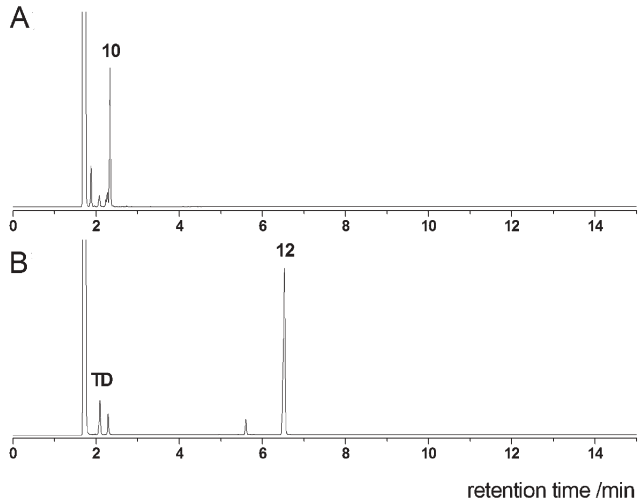

Fig. 6 Gas chromatograms of (A) methyl 10-undecenoate (**10**) starting material and (B) cross-metathesis crude reaction mixture of **12** after 30 min reaction time (see Fig. 5, x = 10, 0.2 mol% **C3**). TD: tetradecane (internal standard).

Conclusions

In conclusion, we demonstrated the synthesis of α,ω-diesters from renewable resources by the facile cross-metathesis of plant oil derived fatty acid methyl esters with methyl acrylate. It should be noted here that acrylic acid is currently made from fossil resources, mostly *via* direct oxidation of propene but can in the future also be obtained from natural resources by, for instance, the dehydration of lactic acid.[20] Moreover, diesters can also be prepared from fatty acids in other ways (as described in the literature[21,22]) and a comparison of all relevant parameters concerning the sustainability of the chosen approach will be necessary in the future. Here, different metathesis catalysts (or more correctly initiators) were investigated, revealing that the second generation catalysts **C2** and **C3** provided good to excellent results, whereas **C3** was more active providing considerably better results than both **C1** and **C2,** allowing for complete conversions without the observation of side products, with only 0.1 mol% of the catalyst. Nevertheless, **C2** also provided good results, especially for the more reactive terminal double bond of **10**, provided that catalyst loadings of 0.5 mol% or higher were applied. Therefore, middle to long chain unsaturated α,ω-diesters (1,8-, 1,11-, 1,12-, 1,15-, and 1,20-) were obtained, which are valuable renewable monomers for, *e.g*, polyesters and polyamides. The unsaturation in these monomers can of course be hydrogenated in order to obtain the saturated analogues but it might also be interesting to polymerise these monomers as such and use the unsaturated sites for post-polymerisation modification reactions (*e.g.* epoxidation and subsequent cross-linking). Apart from the desired α,ω-diester monomers, a variety of unsaturated esters was obtained as byproducts. However, these byproducts are also valuable for the chemical industry as starting materials for detergent applications. Therefore, we introduced a new and efficient catalytic approach for the synthesis of fine chemicals starting from plant oil natural resources, thereby contributing to a sustainable development.[21,23]

Experimental

Experimental procedures and details

Materials. Methyl oleate (Aldrich, 99%), undecylenic acid (Aldrich, 98%), petroselinic acid (Sigma, ⩾99%), erucic acid (Cognis, 92%), benzylidene-bis(tricyclohexylphosphine) dichlororuthenium (**C1**) (Grubbs Catalyst 1st generation, Aldrich), benzylidene[1,3-bis(2,4,6-trimethylphenyl)-2-imidazolidinylidene]dichloro(tricyclohexylphosphine)ruthenium (**C2**) (Grubbs Catalyst 2nd generation, Aldrich) and (1,3-bis-(2,4,6-trimethylphenyl)-2-imidazolidinylidene)dichloro(o-isopropoxyphenylmethylene)ruthenium (**C3**) (Hoveyda-Grubbs Catalyst 2nd generation, Aldrich) were used as received. Methyl acrylate (Aldrich, 99%) was purified by filtration over aluminium oxide. Methyl erucate (**4**), methyl petroselinate (**5**) and methyl 10-undecenoate (**10**) were prepared by esterification with methanol from corresponding fatty acids according to a literature procedure.[24] 1,18-Dimethyl-octadec-9-enedioate, 1,20-dimethyl-eicos-10-enedioate (**11**) and 1,26-dimethyl-hexacos-13-enedioate were synthesized as described earlier[12] and were used as references for GC experiments.

Analytical equipment and methods. Thin layer chromatography (TLC) was performed on silica gel TLC-cards (layer thickness 0.20 mm, Fluka). Compounds were visualized by permanganate or iodine reagents. For column chromatography, silica gel 60 (0.035–0.070 mm, Fluka) was used.

Infrared (IR) spectra were obtained using a Bruker EQUINOX 55 FTIR spectrometer fitted with an ATR cell. Data are presented as the frequency of absorption (cm^{-1}). ^{1}H NMR (^{13}C NMR) spectra were recorded in $CDCl_3$ on a Bruker AVANCE DPX spectrometer operating at 300 (75.5) MHz. Chemical shifts (δ) were reported in parts per million, relative to the internal standard tetramethylsilane (TMS, δ = 0.00 ppm).

Analytical GC characterization of mixtures was carried out with a Shimadzu GC-2010 equipped with a fused silica capillary column (Stabilwax®, 30 m × 0.25 mm × 0.25 μm, Restek), using flame ionization detection. The oven temperature program was: initial temperature 200 °C, ramp at 8 °C min^{-1} to 250 °C, hold for 15 min. Measurements were performed in the split-split mode (split ratio 45 : 1) using hydrogen as the carrier gas (linear velocity of 31.4 cm s^{-1} at 220 °C).

GC-MS (EI) spectra were recorded using a Hewlett-Packard HP 5890 Series II instrument with a capillary column DB-5 (30 m × 0.25 mm × 0.25 μm, Agilent) and a Finnigan MAT 95 mass detector set to scan from 40 to 650 *m/z* at rate of 1.5 scans s^{-1}. The oven temperature program was: initial temperature 160 °C, ramp at 20 °C min^{-1} to 300 °C, hold for 15 min. Measurements were performed in the splitless and split-split mode (split ratio 50 : 1) using helium as the carrier gas (flow rate 1.0 ml min^{-1}).

Mass spectra (ESI) were recorded on Q-Tof Premier™ spectrometer from Waters-Micromass.

Solvent-free cross-metathesis reaction (general procedure)

(A) In a typical small-scale experiment, between 0.5 and 1 ml of fatty acid methyl ester **1**, **4**, **5** or **10** and an excess of methyl

acrylate (2–10 equivalents) were used. Tetradecane (olefin free, 10% of the volume of fatty acid ester) was used as an internal standard for GC measurements. The reaction mixture was stirred magnetically at 50 °C and degassed with nitrogen. A respective solid Grubbs catalyst, **C1–C3**, was then added to the solution, in the range of 0.1–5 mol%. No additional solvents were added. Samples were taken periodically for conversion analysis by GC.

(B) Scale-up syntheses were performed in order to obtain a considerable quantity of compounds for NMR measurements.

A mixture of methyl acrylate (0.16 mol, 14 g) and respective fatty acid methyl ester **1**, **4** or **10** (14–16 mmol) was degassed with nitrogen for 30 min. (1,3-bis-(2,4,6-trimethylphenyl)-2-imidazolidinylidene)dichloro(o-isopropoxyphenylmethylene)-ruthenium (**C3**, 0.032 mmol, 19.8 mg), a second generation Hoveyda-Grubbs catalyst, was then added. The reaction mixture was stirred magnetically at 50 °C under nitrogen atmosphere. After a 20 h reaction, the excess of methyl acrylate was evaporated *in vacuo* and a small amount of the white solid **13** began to precipitate from the reaction mixture. This solid byproduct was removed and recrystallized from acetone. The residue was purified and separated by column chromatography with hexane–diethyl ether (8 : 2) as eluate.

Analytic data†

The reason for the comparably low isolated yields (compared to the GC yields) is due to a very similar retention of the mono and diesters during column chromatography. Reported are only the isolated yields of the pure collected fractions; considerable amounts of products were detected (by GC) in the other fractions collected from the column.

1,11-Dimethyl-undec-2-enedioate (2)

Isolated yield: 2 g (50.4%). IR: ν = 2930, 2861, 1723, 1656, 1435, 1269, 1170, 980 cm^{-1}. ^{1}H NMR (300 MHz, $CDCl_3$): δ = 7.02–6.92 (m, 1H, –C*H*=CH–$COOCH_3$), 5.85–5.79 (d, J = 15.6 Hz, 1H, –CH=C*H*–$COOCH_3$), 3.73 (s, 3H, –CH=CH–$COOCH_3$), 3.68 (s, 3H, –$COOCH_3$), 2.29–2.34 (t, J = 7.4 Hz, 2H, –CH_2COOCH_3), 2.24–2.17 (dt, J = 7.4 and 14.2 Hz, 2H, CH_2–CH=CH–$COOCH_3$), 1.68–1.58 (m, 2H, CH_2), 1.51–1.42 (m, 2H, CH_2), 1.32 (br. s, 6H, 3CH_2) ppm. ^{13}C NMR (75.5 MHz, $CDCl_3$): δ = 174.1 (s, –*C*$OOCH_3$), 167.1 (s, –*C*$OOCH_3$), 149.5 (s, –*C*H=CH–$COOCH_3$), 120.9 (s, –CH=*C*H–$COOCH_3$), 51.4 (s, –CH=CH–COO*C*H_3), 51.3 (s, –COO*C*H_3), 34.0 (s, CH_2), 32.1 (s, CH_2), 31.9 (s, CH_2), 29.0 (s, CH_2), 28.9 (s, CH_2), 28.0 (s, CH_2), 24.9 (s, CH_2) ppm. MS (EI): m/z (%) 242.2 ($M^{+\cdot}$, 1), 210.2 (74), 150.2 (100), 133.2 (24), 113.1 (18), 108.1 (42), 87.1 (38), 81.1 (60), 59.0 (39), 55.1 (59). MS (ESI-positive, CH_2Cl_2): m/z 243.2 (MH^+, calc. 243.16).

1-Methyl-undec-2-enoate (3 = 7)

Isolated yield: 1.7 g (53.6%). The isolated yield of compound **7** was 1.9 g (68.4%). IR: ν = 2924, 2854, 1725, 1657, 1435, 1268, 1171, 1126, 1039, 980 cm^{-1}. ^{1}H NMR (300 MHz, $CDCl_3$): δ = 7.0–6.92 (m, 1H, –C*H*=CH–$COOCH_3$), 5.84–5.79 (d, J = 15.7 Hz, 1H, –CH=C*H*–$COOCH_3$), 3.72 (s, 3H, –CH=CH–COO*C*H_3), 2.23–2.15 (dt, J = 7.2 and 14.2 Hz, 2H, –CH_2–CH=CH–$COOCH_3$), 1.48–1.41 (m, 2H, CH_2), 1.27 (br. s, 10H, 5CH_2), 0.88 (t, J = 7.1, 3H, CH_3) ppm. ^{13}C NMR (75.5 MHz, $CDCl_3$): δ = 167.2 (s, –*C*$OOCH_3$), 149.8 (s, –*C*H=CH–$COOCH_3$), 120.8 (s, –CH=*C*H–$COOCH_3$), 51.4 (s, –COO*C*H_3), 32.2 (s, CH_2), 31.6 (s, CH_2), 29.4 (s, CH_2), 29.2 (s, CH_2), 28.0 (s, CH_2), 22.7 (s, CH_2), 14.1 (s, CH_3) ppm. MS (EI): m/z (%) 198.3 ($M^{+\cdot}$, 30), 167.2 (2), 155.2 (3), 127.2 (5), 113.1 (27), 99.2 (9), 85.1 (37), 71.1 (56), 57.1 (100). MS (ESI-positive, CH_2Cl_2): m/z 199.2 (MH^+, calc. 199.17).

1,15-Dimethyl-pentadec-2-enedioate (6)

Isolated yield: 2.8 g (67.0%). IR: ν = 2919, 2851, 1727, 1655, 1437, 1252, 1201, 1168, 990 cm^{-1}. ^{1}H NMR (300 MHz, $CDCl_3$): δ = 7.02–6.92 (m, 1H, –C*H*=CH–$COOCH_3$), 5.85–5.79 (d, J = 14.2 Hz, 1H, –CH=C*H*–$COOCH_3$), 3.72 (s, 3H, –CH=CH–COO*C*H_3), 3.66 (s, 3H, –COO*C*H_3), 2.32–2.27 (t, J = 7.6, 2H, –CH_2COOCH_3), 2.23–2.16 (dt, J = 7.5 and 14.0 Hz, 2H, CH_2–CH=CH–$COOCH_3$), 1.64–1.57 (m, 2H, CH_2), 1.45–1.40 (m, 2H, CH_2), 1.27 (br. s, 14H, 7CH_2) ppm. ^{13}C NMR (75.5 MHz, $CDCl_3$): δ = 174.2 (s, –*C*$OOCH_3$), 167.1 (s, –*C*$OOCH_3$), 149.7 (s, –*C*H=CH–$COOCH_3$), 120.8 (s, –CH=*C*H–$COOCH_3$), 52.2 (s, –CH=CH–COO*C*H_3), 51.3 (s, –COO*C*H_3), 34.0 (s, CH_2), 32.2 (s, CH_2), 31.5 (s, CH_2), 29.5 (s, CH_2), 29.4 (s, CH_2), 29.3 (s, CH_2), 29.2 (s, CH_2), 29.1 (s, CH_2), 28.9 (s, CH_2), 28.0 (s, CH_2), 24.9 (s, CH_2) ppm. MS (EI): m/z (%) 298.4 ($M^{+\cdot}$, 2), 266.3 (72), 238.3 (100), 225.2 (13), 206.2 (23), 165.2 (19), 152.2 (47), 123.1 (20), 109.1 (26), 98.1 (54), 81.1 (68), 69.1 (37), 55.1 (80). MS (ESI-positive, CH_2Cl_2): m/z 299.2 (MH^+, calc. 299.22).

1,8-Dimethyl-oct-2-enedioate (8) and 1-methyl-tetradec-2-enoate (9)

Only small-scale reactions were performed in order to identify the cross-metathesis products. The crude reaction mixture was analyzed by GC-MS(EI). Retention time of **8** was detected at 4.3 min, retention time of **9** was 20.3 min.

MS (EI) of compound **8**: m/z (%) 200.1 ($M^{+\cdot}$, 5), 168.1 (60), 140.1 (42), 136.0 (100), 127.1 (8), 113.1 (18), 108.1 (38), 94.0 (22), 81.1 (61), 67.1 (23), 59.0 (37).

MS (EI) of compound **9**: m/z (%) 240.2 ($M^{+\cdot}$, 22), 208.1 (51), 166.1 (38), 141.1 (21), 124.1 (23), 113.0 (42), 96.0 (36), 87.0 (100), 74.0 (36), 55.0 (43).

1,20-Dimethyl-eicos-10-enedioate (11)

Isolated yield: 0.3 g (56%). IR: ν = 2913, 2849, 1736, 1469, 1434, 1382, 1244, 1205, 1163, 962 cm^{-1}. ^{1}H NMR (500 MHz, $CDCl_3$): δ = 5.39–5.37 (m, 2H, –C*H*=C*H*–), 3.66 (s, 6H, 2$COOCH_3$), 2.32–2.27 (t, J = 7.5 Hz, 4H, 2CH_2COOCH_3), 1.97 (br. s, 4H, –CH_2–CH=CH–CH_2–), 1.64–1.60 (m, 4H, 2CH_2), 1.29 (br. s, 20H, 10CH_2) ppm. ^{13}C NMR (125 MHz, $CDCl_3$): δ = 174.3 (s, –*C*$OOCH_3$), 130.3 (s, –*C*H=*C*H–), 51.8 (s, COO*C*H_3), 34.1 (s, CH_2), 32.6 (s, CH_2), 29.6 (s, CH_2), 29.3 (s, CH_2), 29.1 (s, CH_2), 24.8 (s, CH_2) ppm. MS (EI): m/z (%) 368.4 ($M^{+\cdot}$, 38), 336.4 (100), 304.3 (57), 207.1 (16), 109.1 (17), 95.1 (28), 81.1 (35), 55.1 (60). MS (ESI-positive, CH_2Cl_2): m/z 369.3 (MH^+, calc. 369.30).

1,12-Dimethyl-dodec-2-enedioate (12)

Isolated yield: 2.8 g (68.3%). IR: ν = 2931, 2859, 1727, 1660, 1439, 1272, 1174, 984 cm^{-1}. ^1H NMR (300 MHz, $CDCl_3$): δ = 7.01–6.91 (m, 1H, –C*H*=CH–$COOCH_3$), 5.84–5.79 (d, J = 15.6 Hz, 1H, –CH=C*H*–$COOCH_3$), 3.72 (s, 3H, –CH=CH–COOC*H*$_3$), 3.66 (s, 3H, –COOC*H*$_3$), 2.33–2.75 (t, J = 7.5 Hz, 2H, –C*H*$_2$$COOCH_3$), 2.23–2.16 (q, J = 7.5 and 14.1 Hz, 2H, –C*H*$_2$–CH=CH–$COOCH_3$), 1.64–1.57 (m, 2H, C*H*$_2$), 1.47–1.41 (m, 2H, C*H*$_2$), 1.30 (br. s, 8H, 4C*H*$_2$) ppm. ^{13}C NMR (75.5 MHz, $CDCl_3$): δ 174.1 (s, –*C*$OOCH_3$), 167.1 (s, –*C*$OOCH_3$), 149.6 (s, –*C*H=CH–$COOCH_3$), 120.8 (s, –CH=*C*H–$COOCH_3$), 51.3 (s, –CH=CH–COO*C*H_3), 51.2 (s, –$COOCH_3$), 34.0 (s, *C*H_2), 32.1 (s, *C*H_2), 29.1 (s, *C*H_2), 29.0 (s, *C*H_2), 28.9 (s, *C*H_2), 27.9 (s, *C*H_2), 24.9 (s, *C*H_2) ppm. MS (EI): *m/z* (%) 256.3 ($M^{+\cdot}$, 3), 224.2 (93), 192.2 (98), 164.2 (82), 150.2 (19), 123.1 (36), 95.1 (38), 87.1 (44), 81.1 (100), 59.0 (43), 55.1 (96). MS (ESI-positive, CH_2Cl_2): *m/z* 257.1 (MH^+, calc. 257.18).

Acknowledgements

This work was financially supported by the German Federal Ministry of Food, Agriculture and Consumer Protection (represented by the Fachagentur Nachwachsende Rohstoffe). The authors are grateful for the access to MS and NMR facilities at the University of Oldenburg, Germany. M. A. R. Meier kindly acknowledges support from Prof. Dr J. O. Metzger as well as financial support from BASF.

References

1 U. Biermann, W. Friedt, S. Lang, W. Lühs, G. Machmüller, J. O. Metzger, M. Rüsch gen. Klaas, H. J. Schäfer and M. P. Schneider, *Angew. Chem., Int. Ed.*, 2000, **39**, 2206–2224.
2 J. C. Mol, *Green Chem.*, 2002, **4**, 5–13.
3 J. Patel, J. Elaridi, W. R. Jackson, A. J. Robinson, A. K. Serelisb and C. Such, *Chem. Commun.*, 2005, 5546–5547.
4 S. Warwel, H.-G. Jägers and S. Thomas, *Fat Sci. Technol.*, 1992, **94**, 323–328.
5 W. A. Herrmann, W. Wagner, U. N. Flessner, U. Vokhardt and H. Komber, *Angew. Chem., Int. Ed. Engl.*, 1991, **30**, 1636–1638.
6 http://www.materia-inc.com/News/Cargill082005.html.
7 A. K. Chatterjee, T.-L. Choi, D. P. Sanders and R. H. Grubbs, *J. Am. Chem. Soc.*, 2003, **125**, 11360–11370.
8 S. J. Connon and S. Blechert, *Angew. Chem., Int. Ed.*, 2003, **42**, 1900–1923.
9 L. Ferrié, D. Amans, S. Reymond, V. Bellosta, P. Capdevielle and J. Cossy, *J. Organomet. Chem.*, 2006, **691**, 5456–5465.
10 S. Fustero, M. Sánchez-Roselló, J. F. Sanz-Cervera, J. L. Aceña, C. del Pozo, B. Fernández, A. Bartolomé and A. Asensio, *Org. Lett.*, 2006, **8**, 4633–4636.
11 S. J. Langford, M. J. Latter and C. P. Woodward, *Org. Lett.*, 2006, **8**, 2595–2598.
12 H. L. Ngo, K. Jones and T. A. Foglia, *J. Am. Oil Chem. Soc.*, 2006, **83**, 629–634.
13 The obtained mono-esters have potential use as intermediates for the synthesis of surfactants (*e.g.* carboxylates).
14 GC yields in Tables 1 and 2 were estimated from GC results; please note that an error of ~3% has to be taken into account due to the possibility of not detected side products and different detector responses of the investigated compounds.
15 D. J. Frost and F. D. Gunstone, *Chem. Phys. Lipids*, 1975, **15**, 53–85.
16 J. O. Metzger, *Angew. Chem., Int. Ed.*, 1998, **37**, 2975–2978.
17 H. Baumann, M. Bühler, H. Bochem, F. Hirsinger, H. Zoebelein and J. Falbe, *Angew. Chem., Int. Ed. Engl.*, 1988, **27**, 41–62.
18 H. Guobin, L. Zuyu, Y. Suling and Y. Rufeng, *J. Am. Oil Chem. Soc.*, 1996, **73**, 1109–1112.
19 S. H. Hong, D. P. Sanders, C. W. Lee and R. H. Grubbs, *J. Am. Chem. Soc.*, 2005, **127**, 17160–17161.
20 A. Corma, S. Iborra and A. Velty, *Chem. Rev.*, 2007, **107**, 2411–2502.
21 M. A. R. Meier, J. O. Metzger and U. S. Schubert, *Chem. Soc. Rev.*, 2007, **36**, 1788–1802.
22 K. Hill, *Pure Appl. Chem.*, 2000, **72**, 1255–1264.
23 M. Eissen, J. O. Metzger, E. Schmidt and U. Schneidewind, *Angew. Chem., Int. Ed.*, 2002, **41**, 414–436.
24 M. J. Haas, S. Bloomer and K. Scott, *J. Am. Oil Chem. Soc.*, 2000, **77**, 373–379.

Predictions of flavonoid solubility in ionic liquids by COSMO-RS: experimental verification, structural elucidation, and solvation characterization†

Zheng Guo,[a] Bena-Marie Lue,[a] Kaj Thomasen,[b] Anne S. Meyer[b] and Xuebing Xu*[a]

Received 27th June 2007, Accepted 3rd September 2007
First published as an Advance Article on the web 17th September 2007
DOI: 10.1039/b709786g

Predictions of the solubility of flavonoids in a large variety of ionic liquids (ILs) with over 1800 available structures were examined based on COSMO-RS computation. The results show that the solubilities of flavonoids are strongly anion-dependent. Experimental measurement of the solubilities of esculin and rutin in 12 ILs with varying anions and cations show that predicted and experimental results generally have a good agreement. Based on the sound physical basis of COSMO-RS, the solubility changes of flavonoids were quantitatively associated with solvation interactions and structural characteristics of ILs. COSMO-RS derived parameters, *i.e.* misfit, H-bonding and van der Waals interaction energy, are shown to be capable of characterizing the complicated multiple interactions in the IL system effectively. H-bonding interaction is the most dominant interaction for ILs (followed by misfit and van der Waals interactions) to determine the solubility of flavonoids, and the anionic part has greater effect on the overall H-bonding capability of the IL. Based on basicity of anions, ILs were categorized into 3 groups, corresponding to the classification of the solubility of flavonoid. COSMO sigma-moment descriptors, which roughly denote the characteristic properties of the ILs, might be of general value to have a fast estimation for the solubilities of flavonoids as well as those compounds with massive moieties as H-bonding donors. The results obtained in this work may be important for achieving an improved understanding of IL solvations and the tailoring of the desired structures of ILs used as the media for efficient enzymatic esterification of flavonoids.

Introduction

The effectiveness and absorption of many drugs are largely controlled by their low solubility, therefore, modification of drugs and producing so-called prodrugs is a useful method to obtain improved properties.[1–3] Flavonoids are such a group of prominent molecules with multiple physiological activities. However, their functions are limited by their low aqua- and lipo-solubility and resultant low bioavailability.[4–6] Lipophilisation of flavonoids into fatty acid esters has been proven to be an efficient way to expand functionalities and applications in human nutrition.[5,7] The presence of solvents is essential in all steps of pharmaceutical processes (reaction, separation and formulation).[8] The particular importance of a good choice of solvents for a reaction results from the fact that the medium often affects the overall reaction rate, selectivity or yield.[9,10] However, the attempts to establish an efficient enzymatic esterification of flavonoids with fatty acids using conventional solvents have been seriously upset by their low solubility.[7,11] As neoteric "green" solvents, the unique properties and tunable physical and chemical characteristics of ionic liquids (ILs) guide one to resort to these novel media for a better solution.[12,13]

The characteristics and the state of art of ILs in technology development and applications have been described in a few excellent reviews.[14,15] Among those characteristics of ILs distinguishing them from conventional solvents, the ability to tailor their properties by judicious selection of cation, anion and substituents and an extended family of available structures for selection constitutes the most interesting and attractive features of ionic liquids.[13,16] Actually, from an engineering point of view, it is the above distinct features that qualify ILs as "a designer solvent" and offer a huge potential for practical applications.[13,17] However, screening a desired structure with required properties for a particular task from a large pool of available ILs represents a big challenge facing chemists and engineers.[13,18,19] To establish an efficient IL-based enzymatic reaction system to producce lipophilic derivatives of flavonoids, there exist similar obstacles for the setup of such a reaction system to fulfil the requirement of high productivity and simultaneously being benign for enzyme activity.[20] Solubility estimation approaches could be quite valuable in reducing the time and resources required to identify a good solvent.[8,9,21] Particularly for numerous possible ILs, *a priori*

[a]*BioCentrum-DTU, Technical University of Denmark, Building 222, DK-2800 Lyngby, Denmark. E-mail: xx@biocentrum.dtu.dk; Fax: +45-45884922; Tel: +45-45252773*
[b]*Department of Chemical Engineering, Technical University of Denmark, DK-2800 Lyngby, Denmark*
† Electronic supplementary information (ESI) available: Chemical structures of the anions evaluated. See DOI: 10.1039/b709786g

screening is needed, because it is impractical to use trial and error methods to find a suitable IL from enormous number of ILs structurally possible for a given function. As reviewed elsewhere,[8,9] Hansen solubility parameters, the group contribution method (UNIFAC) and the quantitative structure–property relationship (QSPR) method *etc.* have been employed for solvent selection for solid solutes. These methods generally need property data to be experimentally available to create reliable training sets, which are currently scarce for ILs, as a group of relatively new compounds.[9,22] As a physically well-founded computational approach and independent of experimental data, COSMO-RS (conductor-like screening model for real solvent) provides a different and feasible alternative for solubility estimation in ILs.[23,24]

As a physically founded model, COSMO-RS integrates dominant interactions (electrostatic (polarity), H-bonding and van der Waals (dispersion)) among IL systems, which adequately summarize multiple solvation interactions of ILs.[23,24] Therefore, this method is able, at least qualitatively, to describe structural variations correctly. Previous publications have also demonstrated the general applicability of COSMO-RS concerning the prediction of solubilities of solids and liquids in ILs.[8,25] Importantly, COSMO-RS introduces the vivid concept of σ-profiles for a qualitative and quantitative comparison of the polarity distribution on molecular surfaces, which integrate the description of electrostatic, hydrogen-bonding and hydrophobicity of a structure. The derived interaction items from COSMO-RS calculation can be conversely used for molecular force field analysis to correlate interaction parameters with structural characteristics qualitatively and quantitatively, which is of general instruction value in the design and development of ILs for specific tasks.[20,26,27] Thus, besides presenting the predicted results of flavonoids in ILs and experimental validation of the COSMO-RS prediction, this work gives more attention to the analysis and assortment of interactions resulting from the specific environment of the ILs applied. These efforts are expected to contribute to an improved understanding of the structure–functionality relationship of ILs and serve later structural optimization of ionic liquids, possibly with high solubilities of flavonoids and benign to enzyme activity as well.

Theoretical basis of COSMO-RS for solubility calculation

Solubility denotes the solute concentration in a solution that is in thermodynamic equilibrium with the solute in the solid state. Therefore, the solubility depends on the difference of the chemical potentials of the solute in the solvent and in pure solute. For a solid solute, the energy change of a compound from the "supercooled" liquid state to the ordered solid state has to be taken into account. The solubility (x_i) at temperature T is thus expressed as a function of pure component properties of the solute (the melting temperature T_m and the free energy difference $(\mu_i^l - \mu_i^j)$ (solid state related to its liquid state) calculated from heat of fusion (ΔH_m^{fus}) and the heat capacity difference of solute in melt state and "hypothetical" "supercooled" melt state) ($C_p^m - C_p^s$) and of the interactions between the solute and solvent in the solution (the activity coefficients, ln γ_i):[28]

$$\ln x_i = \frac{1}{RT}\left(\mu_i^i - \mu_i^j\right) - \ln\gamma_i = \frac{1}{R}\left[\Delta H_m^{fus}\left(\frac{1}{T_m} - \frac{1}{T}\right) + \int_{T_m}^{T}\frac{\int_{T_m}^{T}\left(C_p^m - C_p^s\right)dT}{T^2}dT\right] - \ln\gamma_i \quad (1)$$

where R is the gas constant.

The theory of COSMO-RS has been described by Klamt and coworkers.[23,24] Briefly, COSMO-RS is a statistical thermodynamics approach based on the results of quantum chemical-COSMO calculations. Starting from the surface polarization charge densities σ from density functional theory (DFT) COSMO calculations, COSMO-RS considers all interactions, especially electrostatic interaction and H-bonding, in a liquid system as contact interactions of the molecular surfaces, which are written as pair interactions of the respective polarization change densities σ and σ' of the contacting surface. Then, the chemical potential of a surface segment with SCD (screening charge density) σ in an ensemble can be described by the normalized distribution function $p_S(\sigma')$ given by eqn (2).

$$\mu_S(\sigma) = -\frac{RT}{a_{eff}}\ln\left[\int p_S(\sigma')\exp\left\{\frac{a_{aff}}{RT}\left[\mu_S(\sigma') - E_{misfit}(\sigma,\sigma') - E_{HB}(\sigma,\sigma')\right]\right\}d\sigma'\right] \quad (2)$$

where $\mu_S(\sigma)$ is a measure for the affinity of the system S to a surface polarity σ; E_{misfit} represents the electrostatic contact interaction energy; E_{HB} represents the energy contribution from H-bonding interaction; and a_{eff} is the effective contact area between two surface segments. Not being a function of individual surface contacts, E_{vdw} is not included in eqn (2) but added to the reference energy in solution *a posteriori*. The chemical potential of compound X_i in system S is then available from integration of the σ-potential over the surface of X_i. The capability of COSMO-RS to predict the chemical potential μ_S^X of any solute X in any pure or mixed solvent S at variable temperature T enables the calculation of any thermodynamic liquid–liquid equilibrium, which also constitutes the basis of COSMO-RS for solubility estimation. In the current COSMO*therm* program, the free energy of fusion of a solid solute is estimated *via* a QSPR approach and approximated from the following COSMO*therm* descriptors:[25]

$$-\Delta G_{fus}^X = c_1\mu_i^{(H_2O)} + c_2N_i^{Ring} + c_3V_i + c_4 \quad (3)$$

where c_1 to c_4 are the QSPR parameters for the free energy of fusion of the solute. $\mu_i^{(H_2O)}$ is the chemical potential of solute i in water, N_i^{Ring} is the number of ring atoms in compound i and V_i is the molecular volume of the solute. Crystal structure prediction for drugs has to be considered as an unsolved problem. In eqn (3), COSMO-RS treats the quantity size, rigidity, polarity and number of H-bonds as plausible driving forces of crystallization. Molecular size is described by V_i, which is available in the framework of COSMO-RS. The molecular rigidity of drugs largely results from ring structures

and therefore the number of ring atoms N_i^{Ring} is used as descriptor of rigidity. $\mu_i^{(H_2O)}$ is a combined measure of polarity and H-bonding, which can be estimated by COSMO*therm*. Therefore, the chemical potential of a compound in pure water is of special importance in the computation of solubility in COSMO-RS. The parameterizations of the QSPR parameters for fully relaxed Turbomole DFT/COSMO calculations with the larger TZVP basis set (namely BP_TZVP_C21_0106.ctd) used in this calculation includes solubility parameters that are derived from a set of solubility data of 150 aqueous solubilities.[25]

Computational details and calculation sets of flavonoids and ionic liquids

The molecular structures of flavonoids (rutin, esculin, quercetin, isoquercetrin and naringin, *etc.*) (Scheme 1) were sketched as two-dimensional structures and subsequently converted to three-dimensional geometries using Chemdraw Ultra 8.0. To obtain the lowest energy conformations for each flavonoid, special care has been taken into consideration in choosing *cis-trans* and conformational isomerism of the sugar ring structures that are able to build internal hydrogen bonds. The energy of molecular conformations was minimized by MOPAC (Molecular Orbital PACkage) 2000.[26] Using the geometries thus optimized, the computation of the COSMO polarization charge densities σ of the molecular surfaces were performed with the TURBOMOLE 5.7 program package on the density functional theory level, utilizing the BP (B88-VWN-P86) functional with a triple-ζ valence polarized basis set (TZVP).[25] Most of the COSMO files of the cations and anions involved in this work adopt the provision from a latest database of BP-COSMO-IL (COSMO/logic GmbH & Co KG, Leverkusen, Germany). The COSMO files of the cations and anions of ILs excluded in this database but used in this work were generated following a procedure similar to the one we used for flavonoid molecules. All solubility calculations of flavonoids are performed using COSMOthermX_2.1 program (COSMOlogic GmbH & Co KG, Leverkusen, Germany). For flavonoid inputs, only the conformation lowest in energy was used, and for cations and anions of ILs multiple conformers were input with activated conformer treatment in the automatic computation.

In all calculations of the solubilities of flavonoids in ILs, the cation and anion of an IL are treated as separate molecules with equal molar fractions ($n_{\mathrm{cation}} = n_{\mathrm{anion}} = n_{\mathrm{IL}}$). Thus, the COSMOtherm calculation is based on a ternary mixture (cation, anion and solute), differing from an experimental determination treated as a binary system consisting of IL and solute. Therefore, a transition calculation from the solubility of a ternary system ($x_S^{\mathrm{ternary}} = n_i/(n_i + 2n_{\mathrm{ion}})$) to the solubility of a binary system ($x_S^{\mathrm{binary}} = n_i/(n_i + n_{\mathrm{IL}})$) was done to acquire the comparative datum with the experimental value. The intensive interests of this work are not placed on the discussion of methodology itself but devoted to the revelation of the dominant interactions among IL systems to govern the solubility of flavonoids. For a better comparison of solubilities of flavonoids in different types of ILs under the same conditions, all calculations (regardless of small or large solubility) were performed with a non-iterative mode, which means the solubility computed is a zeroth order approximation.

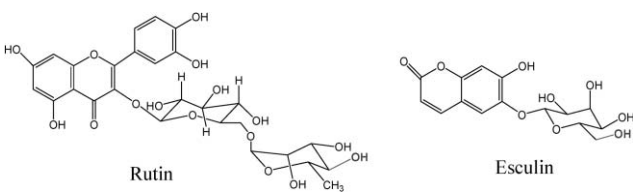

Scheme 1 Structures of rutin and esculin.

To achieve a comprehensive evaluation on the properties of ILs, the calculation set of cations involved in this work covered the most important types of possible cations, such as imidazolium, pyridinium, pyrrolidinium, ammonium, phosphonium, sulfonium, guanidinium, isoquinolinium, and isouronium, *etc.* (Scheme 2). To investigate the effects of the incorporated substituents on the hydrophobic–hydrophilic property of ILs and the subsequent influence on the solubility of flavonoids, various chain lengths of alkyl groups were appended to the parent structures at different positions, with a total of 59 structures. The anions examined include the often used types (*e.g.* PF_6^-, BF_4^- and tf_2N) and those uncommon groups[29,30] that have properties varying from "non-polar" to moderate and strong polar anions. The number of the anion types involved amounts to 32. Therefore, the calculation set of ILs in this work is 1888 combinations, which covered almost all hitherto known important commercially available ILs (not included are those functionalized ILs developed for special tasks). It should be mentioned that not all combinations lead to ionic liquids, at least some of them do not exist as liquid at room temperature. However, they are perceived as ionic liquids herein for the convenience of model processing.

The common structural nature of flavonoids is a polyphenyl ring with saccharide substituents. Therefore, rutin with a 2-phenylchromone parent structure (three phenolic rings) and disaccharide substituents and esculin with a chromone parent structure (two phenolic rings) and monosaccharide substituents were selected as the representative structures for an extensive investigation of solubility (Scheme 1). Another reason for choosing these two flavonoids is that their lipophilic derivatives have previously been shown to have improved antioxidation properties.[7]

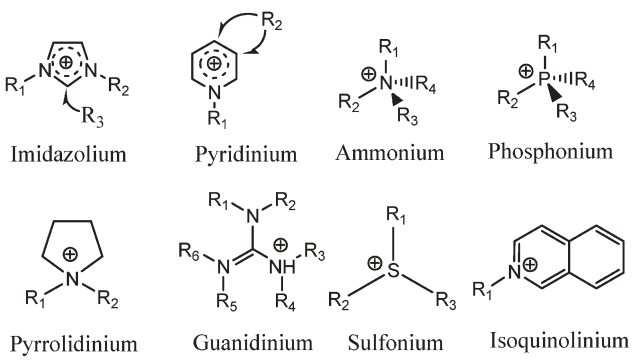

Scheme 2 Basic structures of the cations of ionic liquids evaluated in this study.

The average absolute error (*AAE*) was determined by eqn (4)

$$AAE = \sum|\log S_{\text{predict}} - \log S_{\text{exp}}|/n \quad (4)$$

and root mean square deviations (*RMSD*) from eqn (5)

$$RMSD = \left[\frac{1}{n}\sum\left(|\log S_{\text{predict}} - \log S_{\text{exp}}| - AAE\right)^2\right]^{1/2} \quad (5)$$

where log *S* are the logarithms of the molar percentage of the predicted and experimental solubility (mol%) and *n* is the number of the compounds used.

Results and discussion

COSMO-RS solubilities of esculin in ILs

The primary objective of this study is to acquire fundamental knowledge regarding what are the dominant interaction parameters that govern the solubilities of flavonoids in ILs and what are the structural characteristics behind these interactions. Therefore, a large pool of ILs (59 cations × 32 anions) was employed for solubility evaluation by COSMO-RS calculation. Fig. 1 shows the predicted solubilities of esculin in the ILs of different cations paired with differing anions (A) and in the ILs of different anions paired with varying cations (B). It is difficult to find any regularity in the plotting of the solubilities of esculin *versus* cation alteration in Fig. 1A. For most of the ILs with same cation, the solubilities of esculin (logarithm of molar fraction) varied over a wide range (from 0 to 10^{-6}) with the change of the anion paired. However, if the same data are plotted as the function of anion variation, a different and interesting observation can be visualized (Fig. 1B). That is, in the same anion interval, apart from some exceptions (examinations of the structures of ILs for the exception cases reveal that these ILs exist as solids at room

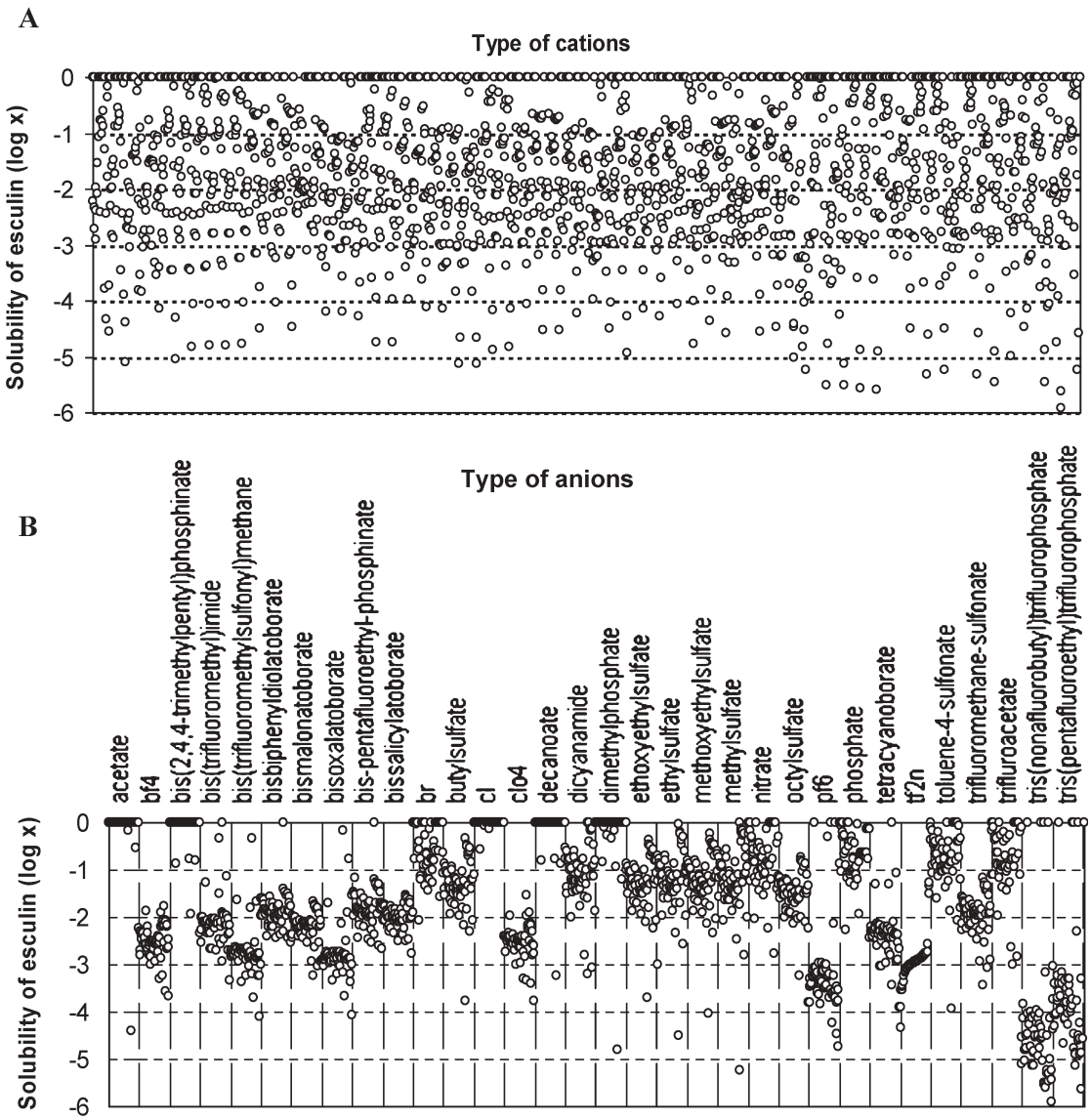

Fig. 1 COSMO-RS predictions of the solubility of esculin in 1888 types of ionic liquids (theoretically possible) created from 59 types of cations and 32 types of anions at 298.15 K. The data shown are categorized by cations (A) and by anions (B), respectively. The 59 cations have basic structures as shown in Scheme 2 but different substituents, which are not shown in this figure. The data in Fig. 1A and 1B are the same data but plotted *versus* cation and anion variation, respectively. See the ESI† for the chemical structures of the anions evaluated.

temperature, but are perceived as liquids in the prediction), the group of ILs with the same anion gave a narrow variation range of the solubilities of esculin. For instance, regardless of the structural variations of cations paired, acetate, deaconate and chlorion *etc.* based ILs generally have very high solubility of esculin (some are even theoretically mutual miscible according to COSMO-RS estimation). For PF_6^- based ILs, the solubilities of esculin varied within 10^{-3}–10^{-5} (log x) and for tris(nonafluorobutyl)trifluorophosphate based ILs the solubilities are generally lower than 10^{-4}. The results suggested that the solubilities of esculin in ILs are determined, to a greater extent, by the anion rather than the cation part of the solvent IL. In other words, the solubilities of esculin in the solvent ILs with different anion and cation combinations are largely anion-dependent. To examine whether other flavonoids have a similar tendency, a similar computation of the solubilities of rutin in a total of 1888 combinations of ILs was carried out, and the solubilities of quercetin, isoquercetrin and naringin were calculated in part of the databases (data not shown). The results demonstrated that the anion-dependency of the solubilities of flavonoids in the solvent ILs with different cation–anion pairings is universal for rutin and other test flavonoids, which indicates that there are some intrinsic interactions between flavonoid molecules and solvent ILs which deserve to be explored.

Based on the anion-dependent solubilities of esculin, the ILs examined could be classified into 3 groups (Fig. 1B). The first group dissolves flavonoids at very high concentration (log x, 0–−1), which includes the ILs with the anions of Cl^-, Br^-, decanoate, dimethylphosphate, dihydricphosphate, acetate, trifluoroacetate, bis(2,4,4-trimethylpentyl)phosphinate, and toluene-4-sulfonate *etc*. The second group of ILs have moderate solubilities (log x, −1–−2.5) and includes the anions of dicyanamide, bisbiphenyldiolatoborate, bis-pentafluoroethyl-phosphinate, bissalicylatoborate, ethoxyethylsulfate, methoxyethylsulfate, alkylsulfate (methyl-, ethyl-, butyl-, and octyl-), trifluoromethane-sulfonate, bis(trifluoromethyl)imide, bis(trifluoromethylsulfonyl)methane, *etc*. The third group of ILs, with the anions of BF_4^-, PF_6^-, bismalonatoborate, bisoxalatoborate, ClO_4^-, tetracyanoborate, tf_2N (bis(trifluoromethylsulfonyl)imide), tris(nonafluorobutyl)trifluorophosphate, tris(pentafluoroethyl) trifluorophosphate, *etc.*, have solubilities of esculin (log x) are generally less than −2 regardless of whatever cations are paired (Fig. 1B). Interestingly, the above categorization of ILs for esculin is also seen to be validated for rutin, with a few exceptions, according to our calculation (data not shown), indicating, in some way, a similar solvation behaviour between ILs with esculin and rutin. This categorization of ILs is apparently useful to quantify solute–solvent interactions and thus deserves to be further examined and investigated.

Validation of COSMO-RS predictions

To examine the accuracy of COSMO-RS predictions of the solubilities of flavonoids, 12 different types of ILs, representing different anion types and dissolution abilities as categorized above, were selected as solvents and esculin and rutin were chosen as model flavonoid molecules for evaluation

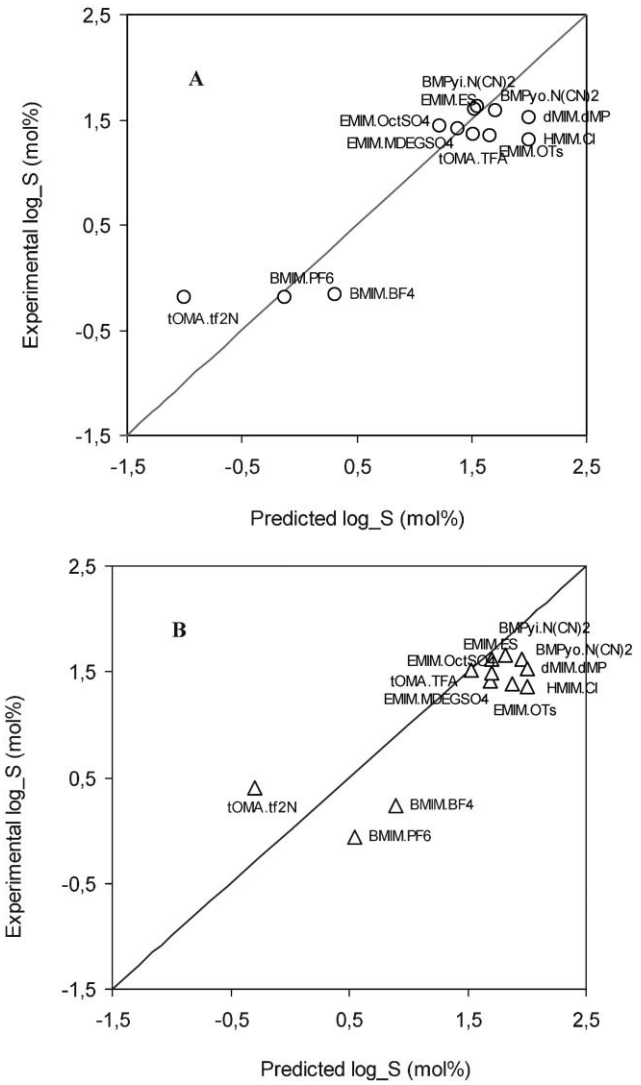

Fig. 2 COSMO-RS predictions plotted *versus* experimental values of the solubility of esculin in 12 types of ILs at 313.15 K (A) and 333.15 K (B). For abbreviations for ILs see Experimental.

(Fig. 2 and 3). Most of the ILs tested have higher viscosity, and 1-ethyl-3-methylimidazolium toluene-4-sulfonate (EMIM·OTs) is even solid at room temperature. Therefore, the measurements were conducted at 40 °C and 60 °C to accelerate dissolution. This test temperature is far from the boiling points of ILs and the evaporation of ILs can be neglected, thereby the measurements stay in a safe temperature range. The scatter plot of Fig. 2A shows a rather homogeneous error distribution of esculin solubilities at 40 °C, which means the solubilities of esculin in the ILs were not systematically overestimated or underestimated. The predicted and experimental values gave average absolute error (*AAE*) of 0.29 log-units and root mean square deviations (*RMSD*) of 0.25 log-units. These data suggested a better quality of esculin solubility prediction in ILs than a previous report concerning prediction of aqueous solubility of drugs and pesticides with COSMO-RS.[25] The predictions of esculin solubility at the temperature of 60 °C achieve an accuracy of an *AAE* of 0.39 and *RMSD* of 0.22. The accuracy is comparable with that at 40 °C. No systemic

deviation is observed, suggesting that 60 °C (the temperature range often used for lipase catalysis) is within the safety interval for COSMO-RS prediction.

Predicted and experimental data for the solubilities of rutin in 12 types of ILs at 40 and 60 °C are depicted in Fig. 3A and 3B, respectively. It is clear that for solvents BMIM.PF_6, BMIM.BF_4 and tOMA.tf_2N at either 40 or 60 °C, the experimental values are significantly higher than the predicted data. These significant differences lead to a bigger error for the total test set of 12 ILs. The average absolute error for the solubility of rutin at 40 °C is 1.41 log-units and the root mean square deviations is 1.51; while the AAE for 60 °C is 1.16 and RMSD amounts to 1.10 log-units. This result is still acceptable compared to the prediction of solid solute by other methods.[28] Inspection of the data in Fig. 3 reveals that the major errors come from the greater deviations of the predicted solubilities of rutin in BMIM.PF6, BMIM.BF4 and tOMA.tf_2N from the corresponding experimental data, which cover over 50% of the total absolute error. Interestingly, even for the solubility of esculin in tOMA.tf_2N, the predicted value also seriously deviates from the experimental datum in the same direction. This result seems to suggest that COSMO-RS did not give a sufficient and accurate description of the interaction between tOMA.tf_2N and flavonoid molecules.

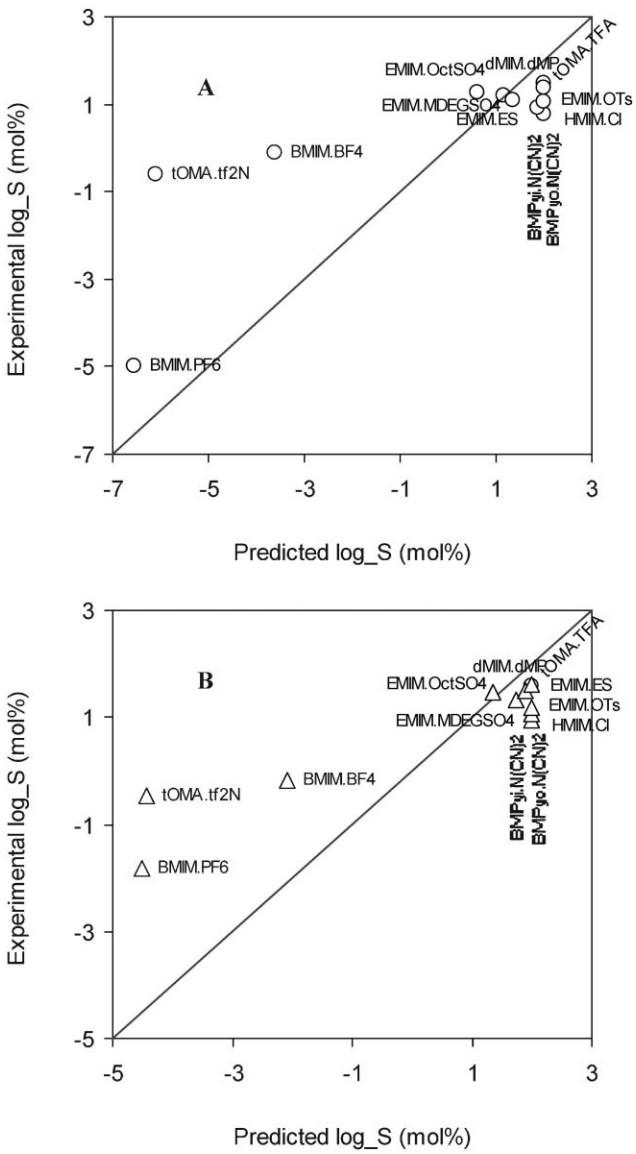

Fig. 3 COSMO-RS predictions plotted *versus* experimental values of the solubility of rutin in 12 types of ILs at 313.15 K (A) and 333.15 K (B). For abbreviations for ILs see Experimental.

It should be pointed out that an accurate measurement of flavonoids in those ILs with high viscosity is methodologically difficult. For instance, HMIM.Cl (7985 mPa s at 25 °C), EMIM.OTs (solid at 25 °C) and dMIM.dMP (391.1 mPa s at 25 °C) have high viscosity, in which both rutin and esculin have higher solubility according to COSMO-RS estimation. However, both flavonoids have bigger molecular weight and are structurally cohesive compounds. With more solute added to the solvents, the viscosity of the system becomes much greater (like semi-solid). In this case, agitation to promote dissolution is impossible and prolonging equilibrating time (over 2 months) doesn't help much for diffusion. This fact demonstrated that the presented experimental data for HMIM.Cl, EMIM.OTs and dMIM.dMP in Fig. 2 and 3 are far less than real solubilities in these solvents due to methodological impossibility, which means that the model estimation for the ILs with high solubility is actually more accurate than the shown data. This probably may explain a better agreement of experimental solubility of rutin with the predicted value at 60 °C, because the dissolution of rutin at 60 °C is observed faster than at 40 °C in high-viscosity ILs and enables the measured value to be closer to its real solubility. However, this doesn't represent the reasons accounting for greater deviation of the predictions for the solubilities of rutin in BMIM.PF_6, BMIM.BF_4 and tOMA.tf_2N, because of their relatively lower viscosity and lower solubility of flavonoids. Most likely, the solubilities of rutin in these three types of ILs could be systematically underestimated by COSMO-RS. More studies are needed to look into the issue more thoroughly.

Overall, COSMO-RS essentially gave a good prediction of the solubilities of representative flavonoid molecules in the ILs with varied cation structures and different anions, as experimentally validated. The predicted results at 60 °C give almost the same accuracy as at 40 °C, which indicates that the temperature range tested in this work is within the safety and effective prediction range of COSMO-RS prediction for ILs with high upper limit of liquidus. The prediction quality for the case of esculin is better than that for rutin (Fig. 2 and 3). The model shows a better estimation for strong solvation ionic liquids than those ILs with lower solubility (paired anions of BF_4^-, PF_6^- and tf_2N) (Fig. 2 and 3). The results demonstrated that the model is capable of producing a reasonable prediction of the solubilities in almost arbitrary cation–anion combinations existing as liquid at the test temperature range.[22,25,31] This is perhaps of particular interest to serve as a first guide in the selection of solvents from a large pool. Most importantly, being a sound physical founded model, COSMO-RS could give reasonable force field analysis in a complicated system and therefore is able to quantify the function property of the structural moiety. This function of the COSMO-RS approach is particularly useful for IL structural design for a specific task, as demonstrated in a recent work,[26] by provision of a

molecular level understanding of the structure–function relationship of ILs, which constitutes intensive contents in the following section.

Analysis of the multiple solvation interactions between esculin and ILs

It is known that ionic liquids are among the most complex solvents.[32] Clearly, single parameters like "polarity", normally used for the characterization of conventional solvents, are not sufficient to describe the structure and diversity of functionality of ILs. Several approaches have been proposed that allow one to examine and categorize the different solvent–solute interactions.[32,33] These solvatochromic or chromatographic approaches employ probe molecules to characterize the most dominant interactions of ILs, namely, polarity, hydrogen bond basicity, and dispersion, *etc*.[32,33] These efforts are capable of categorizing the types and strength of interactions of an extensive number of ILs that effectively delineate their similarities and differences. However, those descriptions could not or at least have not been associated with the quantification of the thermodynamic properties of ILs, which is just the need for a practical application.[26] As a physically well-founded computation approach, COSMO-RS integrates dominant interactions among IL systems (electrostatic (polarity), H-bonding and van der Waals (dispersion)), which adequately summarize multiple solvation interactions of ILs.[32] Importantly, this methodology provides a direct quantitative scaling of the thermodynamic properties of ILs in a specific solvation environment.[26] Therefore, it is theoretically possible to associate the specific interactions determining the solubility of flavonoids with the cationic and/or anionic part of the ILs through force field analysis of the measures derived from COSMO-RS computation.

Fig. 4 shows the predicted solubilities of esculin in BMIM-based ILs with varying anions and the corresponding solvation interaction energies. According to the solubility of esculin, the ILs (in terms of the anions paired) could be classified into 3 groups: $\log_{10}$(solu_S) of 0–1, 1–2 and >2 (Fig. 4). Among the 3 descriptor parameters (Fig. 4), van der Waals interaction is strongly negative for all ILs and varies within a narrow range of value. Misfit interaction could be regarded as a disguised form of polarity, and in COSMO-RS it is defined as electrostatic interaction between the two contacting ensembles. Actually this term integrates the molecular shape, size and charge density and distribution,[34] which reflects, to some extent, the dissimilarity and mismatching property of the two interacting molecules. Its positive value indicates the ionic nature of ILs is thermodynamically unfavourable for the dissolution of a neutral molecule (herein esculin). The declining values with the anions paired denote a decreasing polarity of the anions and corresponding ILs, and also indicates that a less polar IL favours the dissolution of esculin if judged only by this parameter. However, the decrease of

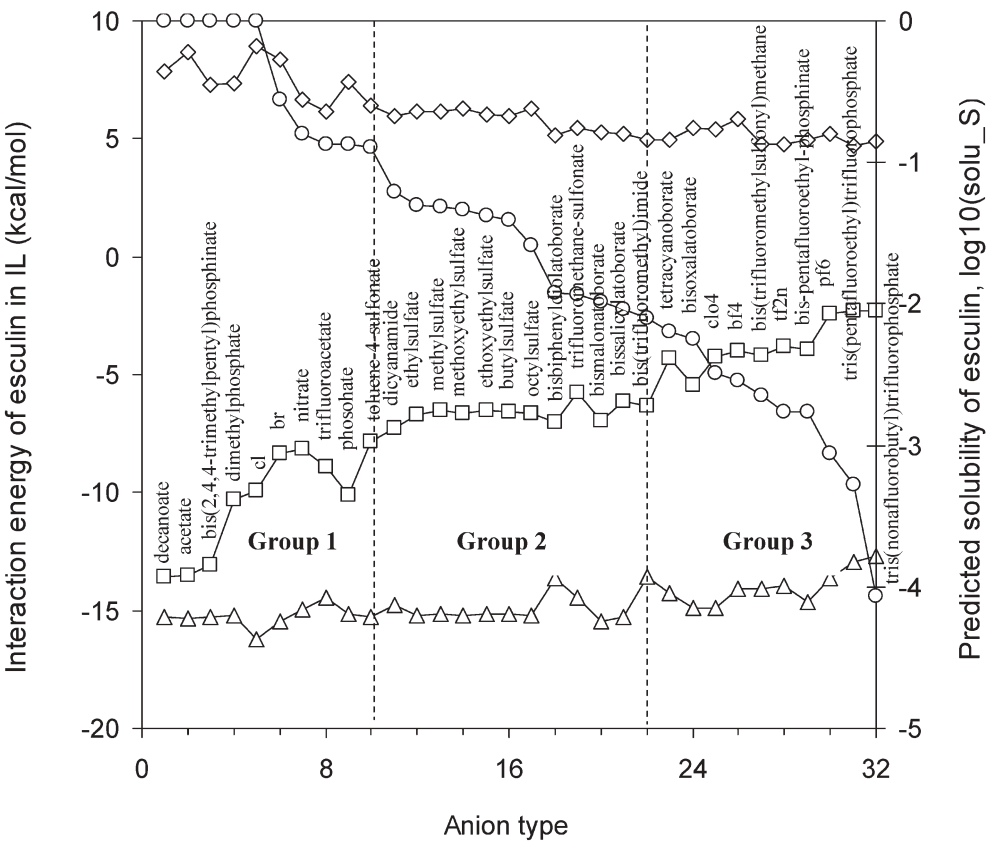

Fig. 4 COSMO-RS derived descriptors used to characterize the solvation interactions of esculin and BMIM-based ionic liquids with different anions. (○) Predicted solubility, (◇) misfit interaction energy, (□) H-bonding interaction energy and (△) van der Waals interaction energy in respective ILs at 298.15 K. All interactions are calculated at indefinite dilution. See the ESI† for the chemical structures of the anions evaluated.

misfit interaction energy is apparently not enough to compensate for the continuous reduction of the H-bonding power of ILs to stabilize the dissolved esculin (Fig. 4). Clearly, the decrease of solubility has shown a pronounced dependency of the increase of H-bonding interaction energy (Fig. 4). In the first group of ILs the dissolved esculin is stabilized by the strong H-bonding between anion and solute, yielding a very high solubility; while for the anions in the third group, like PF_6^-, the H-bonding capability attenuates seriously (H-bonding interaction energy close to 0), leading to a lower solubility of esculin. The results suggested that, for a solute with the presence of a structure (herein saccharide rings) being a good H-bonding donor, the anion part of ILs or the H-bonding capability of the anion plays a decisive role in the determination of solute solubility.

To have a close look into the effects of the structural variation of cations on the solubility of esculin, the prediction was carried out on the ionic liquids of the 4 basic structures of imidazolium, pyridinium, ammonium and phosphonium with variable substituents (Fig. 5). Acetate (A), methylsulfate (B) and PF_6^-, representing three different groups (Fig. 4), were selected as the paired anions to examine how structural changes of the cationic part influence the solvation behaviours of the ILs with different anionic properties. In agreement with the results in Fig. 1B, $\log_{10}$(solu_S) is zero no matter what substituent is incorporated into the 4 basic cation structures of the ILs when the anion is acetate (Fig. 5A); in the ILs with the anion of PF_6^- the esculin solubilities vary between −3–−4 (Fig. 5C); and in the ILs with the anion of methylsulfate the solubility has a wider fluctuating range (−0.5–−2) (Fig. 5B). As depicted in Fig. 5, for the same solute molecule of esculin, the structural variation in the cation part results in little change of the van der Waals interaction and different anions also have comparable values (around −15 kcal mol^{-1}). The strongly negative values for acetate (Fig. 5A) and less negative value for PF_6^- (Fig. 5C) of the H-bonding interaction could explain the high and low solubility of esculin in respective ILs. The case for the ILs with the anion of methylsulfate is in between that of acetate and PF_6^-, and the absolute values of the H-bonding and misfit interaction energies are very close. This probably may explain a slightly wide variation range of esculin solubility. Briefly, the results presented in Fig. 5 further demonstrate that the solubility of esculin in an ionic liquid is largely governed by the H-bonding capability of its anionic part (great difference in the orders of magnitude), and the change of the cationic part generally results in small variation of solubility (within 1 order of magnitude).

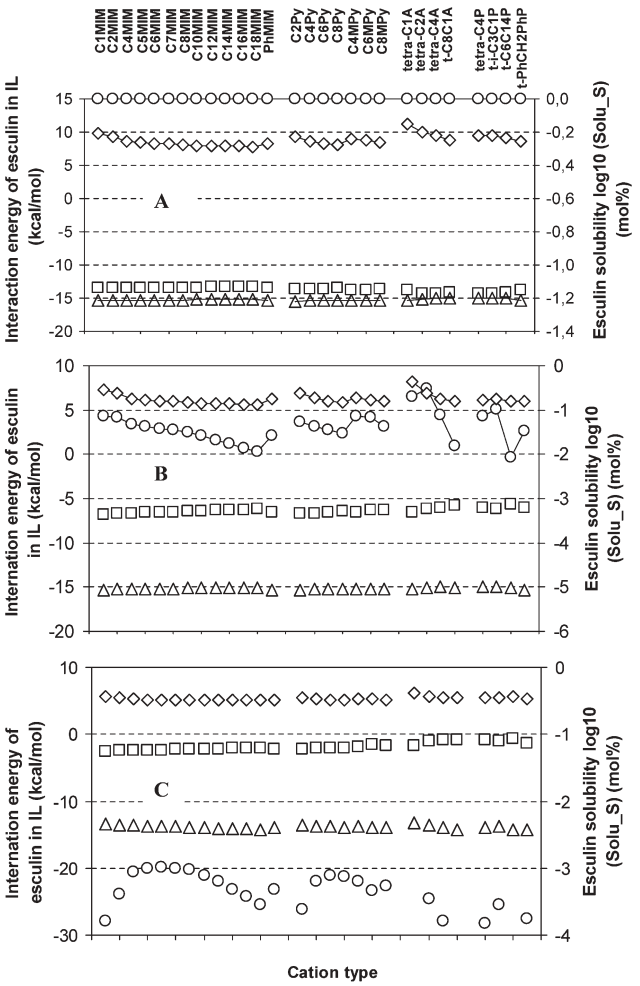

Fig. 5 Solvation interactions of esculin and acetate- (A), methylsulfate- (B) and hexaflurophosphate- (PF_6) based ionic liquids with different cations characterized by COSMO-RS derived descriptive parameters. (○) Predicted solubility, (◇) misfit interaction energy, (□) H-bonding interaction energy and (△) van der Waals interaction energy in respective ILs at 298.15 K. All interactions are calculated at indefinite dilution. Abbreviations: C1MIM to C18MIM represents 1-methyl- to octadecyl-3-methylimizadolium, respectively. PhMIM is 1-benzyl-3-methyl-imidazolium. C2Py to C8Py stand for 1-ethyl- to octyl-pyridinium, respectively, and C4MPy, C6MPy and C8MPy corresponds to 1-butyl-, hexyl- and octyl-3-methylpyridinium. Other abbreviations: Tetra-methylammonium (tetra-C1A), tetra-ethylammonium (tetra-C2A), tetra-*n*-butylammonium (tetra-C4A) and methyl-trioctyl-ammonium (t-C8C1A or tOMA). tetrabutyl-phosphonium (tetra-C4P), triisobutyl-methyl-phosphonium (t-*i*-C4C1P), trihexyl-tetradecyl-phosphonium (t-C6C14P) and benzyl-triphenyl-phosphonium (t-$PhCH_2PhP$).

Analysis of the multiple solvation interactions of rutin and ILs

Compared to esculin, rutin has 1 more phenolic ring and a disaccharide substituent. To examine the similarities and differences of the solvation behaviours of ILs between rutin and esculin, a similar computation has been conducted for solute rutin as done for esculin (Fig. 6). Fig. 6 displays that rutin has a wider varying range of solubility, and the minimum solubility (molar fraction) is around 10^{-13}. The classification of solubility by order of magnitude of the values appears to be very clear (Fig. 6). In the high solubility zone, the logarithmic solubility of rutin is zero (Group 1′); in the low solubility zone the solubility is less than 10^{-4} (Group 3′), and the solubility varies within the range of 10^{-1}–10^{-4} in the second group. Comparison of Fig. 4 and 6 reveals that the solubility of rutin decreases against anion type in a generally similar, but not totally the same order, as esculin, indicating a similar but different solvation behaviour between rutin and esculin. Similar to esculin, the van der Waals interactions for rutin are nearly constant, but the absolute values (about

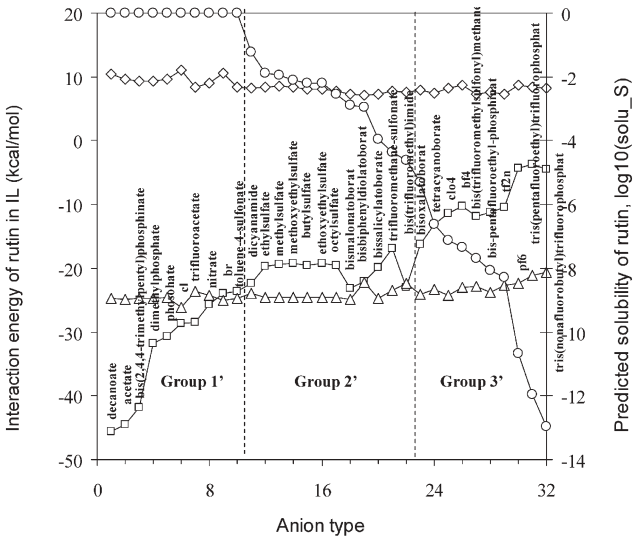

Fig. 6 COSMO-RS derived descriptors used to characterize the solvation interactions of rutin and BMIM-based ionic liquids with different anions. (○) Predicted solubility, (◇) misfit interaction energy, (□) H-bonding interaction energy and (△) van der Waals interaction energy in respective ILs at 298.15 K. All interactions are calculated at indefinite dilution. See the ESI† for the chemical structures of the anions evaluated.

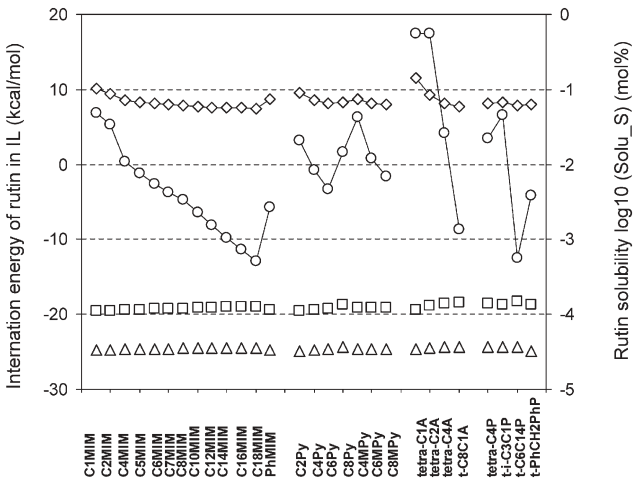

Fig. 7 Solvation interactions of rutin and methylsulfate based ionic liquids with different cations characterized by COSMO-RS derived descriptive parameters. (○) Predicted solubility, (◇) misfit interaction energy, (□) H-bonding interaction energy and (△) van der Waals interaction energy in respective ILs at 298.15 K. All interactions are calculated at indefinite dilution. The abbreviations are the same as in Fig. 5.

25 kcal mol^{-1}) are markedly higher than those for esculin (around 15 kcal mol^{-1}). This strong interaction results from the bigger molecular size and mass of rutin. Differently from esculin, the misfit interaction for rutin with anion alteration shows a smaller variability, indicating that in the same solvent environment, different solutes have different solvation or induce solvents to exhibit different polarities, as reported elsewhere.[26,32] The data in Fig. 6 show that there are strong H-bonding interactions between rutin and anions of ILs in the high solubility zone to stabilize the dissolved molecules, and this interaction is generally greater than van der Waals interaction for the ILs in this zone, except for the cases of Br^- and toluene-4-sulfonate. This result suggests that the additional saccharide ring of rutin adds much to the H-bonding interaction with ILs. However, this structural characteristic does not always generate a desirable effect for the dissolution of rutin; because more saccharide rings will result in a bigger molecular misfit or increase the molecular dissimilarity with hydrophobic ILs, and thus, lead to a significantly lower solubility of rutin in those ILs with weak H-bonding capability (Group 3′ in Fig. 6).

As we did for esculin, we also calculated the rutin solubility in the ILs having cations with varying substituents. Similar to the observations for esculin, the rutin solubility in the ILs with acetate anion is zero and in the ILs with PF_6^- anion is less than 10^{-6} (logarithm of molar fraction) regardless of substituent variation in the cation (details not shown). A greater variation range of the rutin solubility in the ILs containing methylsulfate as anion but with the alteration of substituents in the cation can be seen in Fig. 7. This change plausibly corresponds to the change of misfit interaction, indicating that rutin appears to be more sensitive to the incorporation of hydrophobic substituents due to the massive occurrence of polar saccharide rings. The increasing hydrophobicity of the cation may enhance the repulsion between IL and rutin, and counteract the H-bonding interaction that facilitates dissolution of rutin. This interaction may thus exert a more significant effect for those ILs with moderate H-bonding capability (*e.g.* methylsulfate), and leads to an evident decrease of the solubility of rutin (Fig. 7).

Concluding remarks and outlook

The primary interest of this study is not only to validate COSMO-RS predictions, but also to achieve a better understanding of the functionality of structural moieties of ILs through the powerful force field analysis function of COSMO-RS methodology based on its sound physical basis. It turns out that COSMO-RS predictions generally have a good agreement with the experimental data, compared to the predictions of the solubilities of solid solute by other approaches.[25,28] Considering that the predictions of this model cover the vast structural diversity of ILs and the calculations are performed without any specific parameter adjustment, the results and accuracy are encouraging and acceptable. The physically founded basis of COSMO-RS and validation of this work proved that the predicted results are reliable, and thus the necessary experimental efforts for quantitative determination of the solubilities of flavonoids in ILs could be reduced. The results of this work also revealed a reasonable anion-dependency of the solubility of flavonoids in ILs, and accordingly presented a first systemic categorization of anions based on flavonoid solubility. With this interesting finding, we anticipate that the grouping for anions of ILs might be generally applicable to those solutes with massive moieties as H-bonding donor. We note the reports so far concerning the ILs that are capable of dissolving cellulose,[35] carbohydrate,[36] and protein,[37] *etc*, the anions of which (Cl^-, Br^-, $H_2PO_4^-$ and

Table 1 COSMO-RS descriptor of HB_acc3 (hydrogen bonding acceptor moment indicates hydrogen bond basicity) for 32 anions of ionic liquids and classification of solvation interactions. For structural formulae, see ESI

Group I		Group II		Group III	
Anion types	HB_acc3	Anion types	HB_acc3	Anion types	HB_acc3
Acetate	39.0533	Ethylsulfate	19.2952	Bis(trifluoromethyl)imide	4.0642
Decanoate	38.2772	Octylsulfate	19.1774	Bis(trifluoromethyl sulfonyl)methane	3.8915
Bis(2,4,4-trimethyl pentyl) phosphinate	37.8887	Butylsulfate	19.1238	ClO_4	3.7574
Cl	36.6278	Methylsulfate	18.5006	Tetracyanoborate	3.4554
Phosphate	35.9622	Dicyanamide	15.5327	Bisoxalatoborate	3.0140
Dimethylphosphate	35.1611	Bisbiphenyl diolatoborate	12.7544	BF_4	2.4740
Br	29.6444	Bis-pentafluoroethyl phosphinate	12.6559	tf_2N	2.3089
Toluene-4-sulfonate	25.9431	Bissalicylatoborate	12.6200	Tris(nonafluorobutyl) trifluorophosphate	0.0747
Ethoxyethylsulfate	20.6579	Bismalonatoborate	10.8007	Tris(pentafluoroethyl) trifluorophosphate	0.0108
Methoxyethylsulfate	20.5119	Trifluoromethane-sulfonate	10.6147	PF_6	0.0000
Trifluoroacetate	20.3944				
Nitrate	19.4858				

$(CN)_2N^-$, *etc*) are exclusively included in the first group of the categorization in this study ($(CN)_2N^-$ is on the border) (Fig. 4 and 6). To confirm this interesting finding, we calculated the solubility of two repetitive units of cellulose, carbohydrate and protein (used in place of macromolecular structures) in BMIM-based ILs with the anion spectrum as in Fig. 6. The predictions give surprisingly good agreement with the categorization of anions for rutin (data not shown). The results strengthened the experimental basis of COSMO-RS, and further identified the general applicability of this physically founded model, as well as the reasonableness of a logical extension of some conclusions in this work.

Importantly, the descriptors derived from COSMO-RS are also shown to give a different, but surprisingly equivalent description of the physics of molecules and a similar quantitative scaling in the corresponding terms of another experimental based solvation model—the Abraham equation.[32,38] The overlap of chemical content of the molecular descriptors between COSMO sigma-moments of COSMO-RS and experimental descriptors in the Abraham equation has been demonstrated elsewhere.[38] COSMO sigma-moments (total 5 parameters) are molecular descriptors derived from COSMO-RS calculation, among which the second and third sigma moment (Sig2 and Sig3) and the hydrogen bond moments (HB_acc3 and HB_don3), are chemically corresponding to the measures of polarity/polarizability, H-bonding basicity and H-bonding acidity, respectively.[38] The zeroth sigma-moment is identical with the molecular surface.[38] Table 1 lists the HB_acc3 of the anions evaluated in this work. Anions are good H-bonding acceptors but negligible donors (HB_don3 is generally zero, data not shown). This parameter could be used to classify ILs into 3 groups based on basicity (Table 1). Clearly, the categorization of anions in Table 1 is similar but not the same as in Fig. 4 and 6. For example, ethoxyethylsulfate and methoxyethylsulfate (Group I) belong to Group 2 in Fig. 4 or Group 2′ in Fig. 6. The reason is that HB_acc3 is an intrinsic property of the solvent and does not change with specific solute. However, the specific interactions between IL and different solutes can be different due to varying molecular size, surface charge density and distribution, symmetry, *etc* of the solute. Therefore, misfit, H-bonding and van der Waals interaction energies employed in this work could theoretically give a more correct and accurate description for the solvation behaviour of flavonoids in ILs. Our results show a comparable visualization of the solvation behaviours of ILs in the characterization of ionic liquids as described by Anderson *et al.*[32] Namely, the anion has a greater influence on the overall H-bond basicity of ILs; hydrogen bond basicity varies significantly with anions but vary little for cation alternation; and the dispersion forces show only a slight variability for the ILs evaluated. However, as a first rough selection of ILs for flavonoid dissolution, HB_acc3 is very useful to evaluate the H-bonding capability of anions (Table 1 and Fig. 4 and 6). Based on the changes of measures from COSMO-RS *versus* cationic variation depicted in Table 2, it is also easy to reason why misfit interaction energy decreases, H-bonding changes little and the corresponding decrease of solubility of flavonoids at the small scale follows the changes of cationic substituents (Fig. 5). In brief, the results in this study demonstrated that, as an experimentally independent approach, COSMO-RS is capable of producing a high-quality characterization of multiple solvation interactions of ILs comparable to that obtained from other experimental models. The knowledge and understanding of the relationships of properties with interactions and characteristic moieties of ILs can thereby serve molecular design and structural optimization for constructing a desirable structure with high solubility of flavonoids. However, the establishment of an efficient

Table 2 COSMO-RS descriptors of molecular surface area, the second sigma moment 2 (Sig 2 indicates polarity/polarizability) and HB_don3 (hydrogen bonding donor moment indicates hydrogen bond acidity) for the cations of 1-alkyl-3-methylimidalizium (alkylMIM)

Cations	Area/Å^2	Sig 2	HB_don3
MethylMIM	143.6001	88.0259	2.0735
EthylMIM	161.7652	85.3777	2.0727
ButylMIM	201.9685	84.7111	2.0647
PentylMIM	221.9982	85.2520	2.0537
HexylMIM	241.7418	86.0083	2.0371
HeptylMIM	261.8546	86.6088	1.9864
OctylMIM	281.5146	87.3381	2.0014
DecylMIM	321.5566	88.7644	1.9834
DodecylMIM	361.3977	90.2467	1.9988
TetradecylMIM	401.0784	91.7587	1.9814
HexadecylMIM	441.0983	93.3169	1.9932
OctadecylMIM	480.4567	94.8666	1.9960

enzymatic reaction system involves some unpredictable parameters, such as enzyme activity. Fortunately, COSMO-RS can also aid our effort in some way, because our results show that some parameters, such as water activity and activity coefficients in ILs relevant to enzyme activity, could be accurately estimated by COSMO-RS. The molecular design of ILs assisted by COSMO-RS is in progress in our group.

Experimental

Esculin and rutin hydrate (with purity >99%) were purchased from Sigma–Aldrich Co. (St. Louis, USA). Dimethylsulfonate (DMSO), methanol, acetic acid and triethylamine were from Sigma–Aldrich Co. (St. Louis, USA) and of HPLC grade. 1-Hexyl-3-methylimidazolium (HMIM.Cl), 1-butyl-3-methylpyridinium dicyanamide (BMPyi.N(CN)$_2$), 1-ethyl-3-methylimidazolium toluene-4-sulfonate (EMIM.OTs), 1,3-dimethylimidazolium dimethylphosphate (dMIM.dMP), 1-ethyl-3-methylimidazolium *n*-octylsulfate (EMIM.OctSO$_4$), 1-ethyl-3-methylimidazolium 2(2-methoxyethoxy)ethylsulfate (EMIM.MDEGSO$_4$), 1-ethyl-3-methylimidazolium ethylsulfate (EMIM.ES), methyltrioctylammonium bis(trifluoromethylsulfonyl)imide (tOMA.tf$_2$N), 1-butyl-3-methylimidazolium tetrafluoroborate (BMIM.BF$_4$) and 1-butyl-3-methylimidazolium hexafluorophosphate (BMIM.PF$_6$) were procured from Solvent Innovation GmbH (Köln, Germany) and of minimum 98% purity. Methyltrioctylammonium trifluoroacetate (tOMA.TFA) is from Merck KGaA (Darmstadt, Germany) and with a purity >99.7%. 1-Butyl-1-methylpyrrolidinium dicyanamide (BMPyo.N(CN)$_2$) was purchased from IoLiTec Ionic Liquids Tchnologies GmbH & Co KG and of >98% purity (Denzlingen, Germany). The dissolution and equilibration of esculin or rutin in the solvent ILs were performed in a thermostat oven at 40 or 60 °C with ±0.1 °C accuracy. Typically, 2 mL of ionic liquid were accurately added in a 10 mL capped bottle fixed on a Variomag Telesystem with multiple magnetic stirrers (H+P Labortechnik AG, Oberschleissheim, Germany). The batchwise added esculin or rutin was dissolved with continuous magnetic stirring and the dissolution lasted over 2 months to allow sufficient equilibration. For the case of EMIM.OTs, ultrasonication was employed to assist the dissolution of rutin. The undissolved solid was removed by pressure filtration with a syringe filter (with 0.45 μm PTFE membrane) (Pall Life Science, Ann Arbor, MI, USA) at the same temperature. The resulting IL solution was immediately dissolved in DMSO for HPLC analysis.

The standard curves of esculin, rutin and different ILs were established, respectively. A series of sample concentrations of 0.05, 0.1, 0.2, 0.5, 1, 2, 3, 5 and 10 mg mL^{-1} in DMSO were used and the means of triplicate determinations were adopted. Based on the property of ILs, two elution systems were used for the HPLC analysis of esculin (rutin) dissolved in ILs. The solubility of flavonoids in BMIM.PF$_6$, BMIM.BF$_4$, tOMA.tf$_2$N and tOMA.TFA were eluted with methanol–water (containing 0.1% acetic acid); while other types of ILs use methanol–acetate-triethylamine (TEA) buffer (20 mM; pH, 4.0) elution system. The HPLC analysis was performed on a Hitachi-Merck HPLC Series 7000 (Hitachi-Merck, Japan), conjugated with a PL-ELS 2100 evaporative light scattering detector (ELSD) (Polymer Laboratories, Shropshire, UK). The reverse phase column employed was a Supelcosil LC-18 (250 mm × 4.6 mm) (Supelcosil Inc., Bellefonte, PA). The ELSD was operated at an evaporating temperature of 100 °C and a nebulizing temperature of 50 °C with air as the nebulizing gas at 1.2 SLM. For either methanol–water or methanol–buffer, the elution gradient follows the same program: starts with 30% methanol phase and increase to 100% methanol phase in 10 min; and holds for 6 min and then reduces to 30% methanol phase in 3 min, and keeps at this phase ratio for another 10 min. The mobile phase flow rate was 1.0 mL min^{-1}.

Area percentage was used as mass for solubility calculation. The measured values of the IL and flavonoid were calibrated using standard curves. All HPLC analyses were determined in triplicate and the means were used for evaluation.

Acknowledgements

The authors thank A. Klamt and M. Diedenhofen for their assistance in model processing. Financial support from Danish Research Council for Technology and Production (FTP) (274-05-0286) and Center for Advanced Food Studies (LMC) is gratefully acknowledged.

References

1 A. Wong and I. Toth, *Curr. Med. Chem.*, 2001, **8**(9), 1123–1136.
2 M. Gulati, M. Grover, S. Singh and M. Singh, *Int. J. Pharm.*, 1998, **165**(2), 129–168.
3 W. N. Charman and C. J. H. Porter, *Adv. Drug Delivery Rev.*, 1996, **19**(2), 149–169.
4 C. Rice-Evans, *Curr. Med. Chem.*, 2001, **8**(7), 797–807.
5 S. Lesser, R. Cermak and S. Wolffram, *J. Nutr.*, 2004, **134**(6), 1508–1511.
6 R. Hirano, W. Sasamoto, A. Matsumoto, H. Itakura, O. Igarashi and K. Kondo, *J. Nutr. Sci. Vitamin.*, 2001, **47**(5), 357–362.
7 S. Riva, G. Carrea, G. Ottolina, F. Secundo, B. Danieli and P. De Bellis, *Ann. N. Y. Acad. Sci.*, 1996, 712–715.
8 P. Kolář, J.-W. Shen, A. Tsuboi and T. Ishikawa, *Fluid Phase Equilib.*, 2002, **194–197**, 771–782.
9 T. C. Frank, J. R. Downey and S. K. Gupta, *Chem. Eng. Prog.*, 1999, **95**(12), 41–61.
10 C. Reichardt, *Solvents and solvent effects in organic chemistry*, 2nd edn, 1996, VCH, New York.
11 M. H. Katsoura, A. C. Polydera, L. Tsironis, A. D. Tselepis and H. Stamatis, *J. Biotechnol.*, 2006, **123**(4), 491–503.
12 R. A. Sheldon, R. M. Lau, M. J. Sorgerdrager, F. van Rantwijiknd and K. R. Seddon, *Green Chem.*, 2002, **4**, 147–151.
13 F. Brennecke and E. J. Maginn, *AIChE J.*, 2001, **47**, 2384–2389.
14 J. Dupont, R. F. de Souza and P. A. Z. Suarez, *Chem. Rev.*, 2002, **102**, 3667–3692.
15 F. van Rantwijik and R. A. Sheldon, *Chem. Rev.*, 2007, **107**, 2757–2785.
16 Z. Guo, B.-M. Lue and X. Xu, *Inform*, 2007, **18**(2), 78–82.
17 Z. Guo and X. Xu, *Org. Biomol. Chem.*, 2005, **3**, 2615–2619.
18 Z. Guo and X. Xu, *Green Chem.*, 2006, **8**, 54–62.
19 C. Jork, C. Kristen, D. Pieraccini, A. Stark, C. Chiappe, Y. A. Beste and W. Arlt, *J. Chem. Thermodyn.*, 2005, **37**(6), 537–558.
20 Z. Guo, B. Chen, R. L. Murillo, T. Tan and X. Xu, *Org. Biomol. Chem.*, 2006, **4**, 2772–2776.
21 K. Wichmann, M. Diedenhofen and A. Klamt, *J. Chem. Inf. Model.*, 2007, **47**, 228–233.
22 S. Oleszek-Kudlak, M. Grabda, E. Shibata, F. Eckert and T. Nakamura, *Environ. Toxicol. Chem.*, 2005, **24**(6), 1368–1375.
23 A. Klamt, *J. Phys. Chem.*, 1995, **99**, 2224–2235.
24 F. Eckert and A. Klamt, *AIChE J.*, 2002, **48**, 369–385.

25 A. Klamt, F. Eckert, M. Hornig, M. E. Beck and T. Bürger, *J. Comput. Chem.*, 2002, **23**, 275–281.
26 B. Chen, Z. Guo, T. Tan and X. Xu, *Biotechnol. Bioeng.*, 2007, **97**, OI 10.1002/bit.21520.
27 M. Fermeglia, P. Braiuca, L. Gardossi, S. Pricl and P. J. Halling, *Biotechnol. Prog.*, 2006, **22**, 1146–1152.
28 S. Gracin, T. Brinck and A. C. Rasmuson, *Ind. Eng. Chem. Res.*, 2002, **41**(20), 5114–5124.
29 J. L. Kaar, A. M. Jesionowski, J. A. Berberich, R. Moulton and A. J. Russell, *J. Am. Chem. Soc.*, 2003, **125**, 4125–4131.
30 S. Stolte, J. Arning, U. Bottin-Weber, M. Matzke, F. Stock, K. Thiele, M. Uerdingen, U. Welz-Biermann, B. Jastorff and J. Ranke, *Green Chem.*, 2006, **8**(7), 621–629.
31 A. Klamt, *Fluid Phase Equilib.*, 2003, **206**, 223–235.
32 L. Anderson, J. Ding, T. Welton and D. W. Armstrong, *J. Am. Chem. Soc.*, 2002, **124**, 14247–14254.
33 C. Reichardt, *Green Chem.*, 2005, **7**, 339–351.
34 A. Klamt and F. Eckert, *Fluid Phase Equilib.*, 2000, **172**, 43–72.
35 R. P. Swatloski, S. K. Spear, J. D. Holbrey and R. D. Rogers, *J. Am. Chem. Soc.*, 2002, **124**(18), 4974–4975.
36 Q. B. Liu, M. H. A. Janssen, F. van Rantwijk and R. A. Sheldon, *Green Chem.*, 2005, **7**(1), 39–42.
37 K. Fujita, D. R. MacFarlane and M. Forsyth, *Chem. Commun.*, 2005, **38**, 4804–4806.
38 A. M. Zissimos, M. H. Abraham, A. Klamt, F. Eckert and J. Wood, *J. Chem. Inf. Comput. Sci.*, 2002, **42**, 1320–1331.

Pyrolysis of cellulose catalysed by nanopowder metal oxides: production and characterisation of a chiral hydroxylactone and its role as building block

Daniele Fabbri,*[a] Cristian Torri[a] and Ines Mancini[b]

Received 30th May 2007, Accepted 16th August 2007
First published as an Advance Article on the web 5th September 2007
DOI: 10.1039/b707943e

As a bulk component of plant biomass, cellulose plays a key role in the route leading to viable chemicals from renewable resources. Pyrolysis is a thermal treatment that converts cellulose into a liquid material (bio-oil) containing dehydrated monomers, among which the anhydrosugars levoglucosan (LGA) and levoglucosenone (LGO) have been widely investigated as chiral multifunctional synthons. A chiral cyclic hydroxylactone (LAC, **1**) is also produced, but its potential as chemical intermediate has never been scrutinised, probably because it is generated only in minute amounts. In this study, experiments with a fixed bed reactor showed that the yields of LAC could be significantly increased by pyrolysing cellulose for few minutes at 350 °C in the presence of nanopowder (NP) titanium dioxide, aluminium oxide, and aluminium titanate (AlTi). When pyrolysis was conducted with NP AlTi at 500 °C, LAC became the principal anhydromonosaccharide and could be isolated from the resulting bio-oil with simple operations (6% overall yield). Its structure could be definitively assigned to the (1*R*,5*S*)-1-hydroxy-3,6-dioxabicyclo[3.2.1]octan-2-one by extensive NMR analysis and high resolution EI-MS experiments, providing a firm evidence of its previous attribution. The significance of LAC as building block for follow-up bioproducts was evaluated in some examples, including the synthesis of a suitable amide by the effective and eco-friendly microwave assisted methodology.

Introduction

The exploitation of biomass to reduce our reliance upon fossil fuels is receiving growing attention within the context of the biorefinery, an agro/industrial facility whereby biomass feedstock is processed into fuels, power and chemicals with low emissions and wastes.[1] Biomass conversion to power and biofuels meets the energy demand and decrease overall costs, but requires integration with low-volume high-value chemicals and building blocks that have the potentiality to be transformed into useful compounds in order to increase the profitability of a biorefinery. Cellulose, a fibre found in all plant materials and structurally defined as a polysaccharide made of D-glucose units connected *via* β-1-4 glycosidic linkage (Scheme 1), is the most abundant biosynthesised organic substance on earth, and therefore represents a key biomass component to foster proficient utilisation of plant-derived resources. Cellulose and its repeating unit, glucose, can be transformed into hundreds of chemical compounds, some of them with growth potential as building blocks, by means of several processes, including aerobic and anaerobic fermentation, enzymatic reactions, chemical and thermochemical conversion.[2] Among the latter, pyrolysis is a one-step thermal degradation under non-oxidative conditions which leads to a liquid fraction (bio-oil) containing low molecular weight compounds, including polyfunctional dehydrated C_6 monomers (anhydromonosaccharides).[3]

Examples of pyrolytically formed chiral anhydromonosaccharides comprise the well known levoglucosan (LGA), levoglucosenone (LGO) and 1,4:3,6-dianhydro-α-D-glucopyranose (DGP), as well as the hydroxylactone **1** abbreviated here as LAC (Scheme 1). A peculiarity of these anhydrosugars

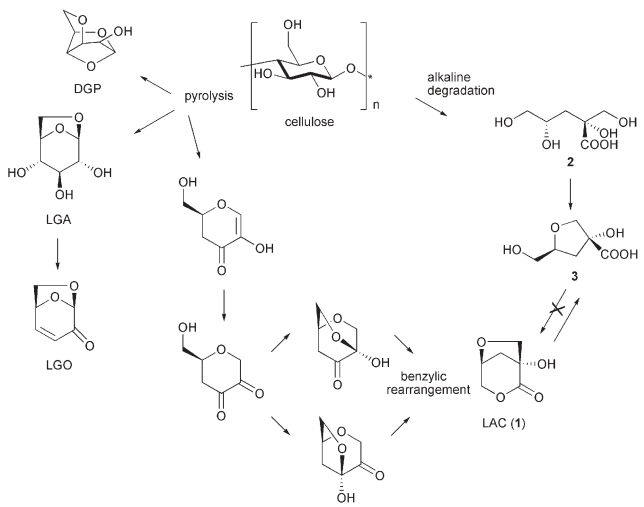

Scheme 1 Anhydrosugars from the pyrolysis of cellulose. Lewis acid catalysed formation of LAC (**1**) according to the mechanism proposed by Furneaux *et al.*[5] and alkaline degradation giving hydroxyacid **3** *via* β-D-isosaccharinic acid **2**.[6]

[a]*Laboratorio di Chimica, Centro Interdipartimentale di Ricerca in Scienze Ambientali (C.I.R.S.A), Università di Bologna, via S.Alberto 163, I-48100, Ravenna, Italy*
[b]*Laboratorio di Chimica Bioorganica, Dipartimento di Fisica, Università di Trento, via Sommarive 14, I-38050 Povo-Trento, Italy*

is that they retain the structural record of the original stereochemistry and thus exist in pure enantiomeric form, which accounts for their employment as chiral building blocks in organic synthesis. LGA and LGO are being and have been thoroughly investigated as chiral synthons and intermediates in organic synthesis,[4] whereas DGP is a minor product which has not appealed to this sort of study. LAC, bearing a tetrahydrofuran ring with two chiral centres, is an attractive structure as a potential building block due to the presence of a lactone unit easily convertible into versatile functional groups without affecting the stereocentres. To the best of our knowledge, it was never investigated after its first identification by Furneaux *et al.* as a product isolated in a one milligram amount from Lewis acid catalysed pyrolysis of cellulose.[5] The authors proposed its formation by a rearrangement of a cyclic hexose precursor obtained from cellulose degradation. Alternative pathways *via* cyclisation of the linear β-D-isosaccharinic acid **2**, which is a known product of alkaline treatment of cellulose, were unsuccessful in giving products with a hydrolactone skeleton, providing more frequently the hydroxyacid **3**, as revealed by GC-MS analysis.[6] It is noteworthy that the non-alkaline conditions required for the LAC isolation are in line with the reactivity of the lactone group which is known to give nucleophilic opening to the hydroxyl acid derivative.

The practical employment of building blocks produced by pyrolysis is limited by the fact that bio-oil is a very complex matrix in which target compounds may occur at relatively low concentrations. Pyrolysis of cellulose and cellulosic materials (*e.g.* wood) could be oriented towards bio-oils with different product composition when conducted in the presence of appropriate reactants and catalysts (reactive and catalytic pyrolysis), polar solvents, protic acids, resins and a series of catalysts.[3d,7] However, less attention has been given to the performance of more recent nanostructured materials, such as mesophases and nanopowders.[8] A previous analytical study on the effect of different catalysts on the pyrolytic behaviour of cellulose showed that the levels of LAC and LGO were significantly increased in the presence of nanopowder (NP) metal oxides based on Ti and Al.[9] In particular, the nanosized feature of aluminium titanate (AlTi) was considered a determinant factor for its activity, as powdered aluminium titanate proved ineffective.

We report now on the results from the preparative pyrolysis of cellulose in the presence of NP Ti and Al oxides to give bio-oils enriched with LAC in order to isolate this compound and to provide a detailed characterisation for its definitive structural attribution. Based on the potential to produce top value added chemicals from biomass, the present study was also aimed at exploring the potential role of LAC as a chiral building block to be used in organic synthesis.

Results and discussion

Pyrolytic production of hydroxylactone LAC from cellulose

Preliminary experiments were carried out by analytical pyrolysis, in order to optimise the proportion of NP metal oxide to be mixed with cellulose for preparative pyrolysis. To this purpose, cellulose was physically admixed with different amounts of nanopowder aluminium titanate (NP AlTi) and heated at 500 °C under nitrogen inside a commercial analytical pyrolyser. The yields of chiral anhydrosugars obtained using different NP AlTi/cellulose mass ratio are reported in Table 1. While the production of LGA was strongly reduced compared to neat cellulose, the levels of LGO and LAC increased noticeably by increasing the quantity of NP AlTi. The 30% NP AlTi/cellulose mass ratio was eventually selected for preparative pyrolysis experiments as a balance between high LGO and LAC production and low catalyst load.

Table 1 Analytical pyrolysis. Yields of chiral anhydrosugars from cellulose mixed with different amount of nanopowder (NP) aluminium titanate

NP AlTi/ cellulose ratio	LAC (%mass)	LGO (%mass)	DGP (%mass)	LGA (%mass)
0	1.5 ± 0.7	3.5 ± 0.8	3.0 ± 1	11 ± 3
0.1	3.5 ± 2	6.4 ± 0.2	0.7 ± 0.4	2.6 ± 2
0.3	5.9 ± 0.2	19 ± 5	1.6 ± 0.2	2.3 ± 0.4
0.7	6.6 ± 0.1	25 ± 3	1.4 ± 0.2	1.1 ± 0.3

The pyrolysis of cellulose at two different temperatures (350 °C and 500 °C) with a fixed bed reactor (Fig. 1) resulted in the production of a liquid material (bio-oil), the yields of which were not strongly modified by the addition of NP metal oxides (Table 2). Nevertheless, the distribution of the four main anhydromonosaccharides was significantly altered, as one can see from Fig. 2a–c where the GC-MS traces of the bio-oil obtained with and without NP AlTi are reported. Table 3 shows that at 350 °C all the investigated NP oxides led to an increase in the yields of the most dehydrated compounds LGO and LAC. The mixed oxide NP AlTi exhibited the largest activity, as the yields of LGO increased from 5.7% to 22%, and those of LAC from 0.4% to 8.6%, with respect to neat cellulose. While the yields of DGP remained fairly low with all the tested oxides, those of LGA were affected by the nature of the catalyst and were remarkably reduced with the addition of mixed oxides.

Beside their chemical composition, the nanosized features of the particles should play a crucial role for the activity of these

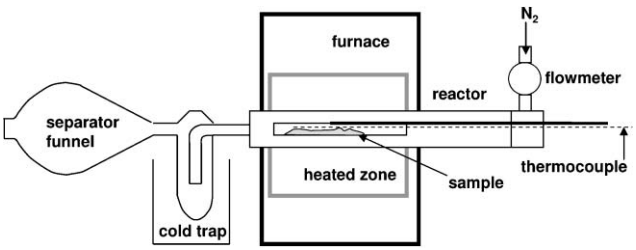

Fig. 1 Scheme of the bench pyrolysis reactor.

Table 2 Preparative pyrolysis. Yields of bio-oil from cellulose pyrolysed at 350 °C and 500 °C in the presence of 30% NP metal oxides/cellulose mass ratio (mean ± s.d., $n = 3$)

Catalyst	350 °C (% mass)	500 °C (% mass)
NP Al	51 ± 2	51 ± 5
NP AlTi	52 ± 1	59 ± 1
NP Ti	47 ± 6	49 ± 1
absent	46 ± 1	57 ± 1

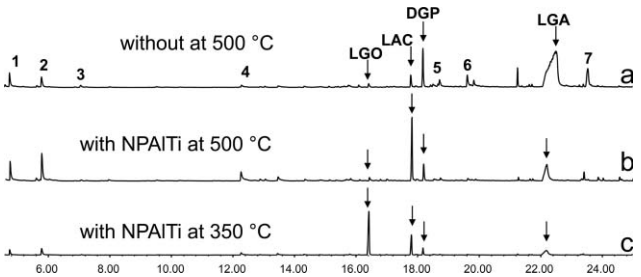

Fig. 2 GC-MS traces of bio-oil obtained from the pyrolysis of cellulose at 500 °C (a), and cellulose in the presence of 30% nanopowder aluminium titanate at 500 °C (b) and 350 °C (c). The arrows indicate the anhydrosugars investigated in this study. Peak identification and estimated yields of additional pyrolysis products (1), (2*H*)-furan-3-one (0.5%); (2), 2-furaldehyde (1.3%); (3), 2-furanmethanol (0.1%); (4), 5-methyl-2-furaldehyde (0.1%); (5), 5-hydroxymethyl-2-furaldehyde (0.8%); (6), 1,5-anhydro-4-deoxy-D-*glycero*-hex-1-en-3-ulose (ascopyrone P)(1.8%); (7), 1,6-anhydro-β-D-glucofuranose (2.5%).

Table 3 Yields of chiral anhydrosugars from preparative pyrolysis of cellulose at 350 °C in the presence of 30% NP metal oxides/cellulose mass ratio (mean ± s.d., $n = 3$). Comparison with the pyrolysis of neat cellulose and cellulose mixed with 30% coarse AlTi

Catalyst	LAC (%mass)	LGO (%mass)	DGP (%mass)	LGA (%mass)
NP Al	5.7 ± 2	8.0 ± 0.1	1.9 ± 0.2	12.1 ± 0.2
NP AlTi	8.6 ± 0.7	22 ± 2	1.1 ± 0.1	3.3 ± 0.1
NP Ti	1.4 ± 0.3	7.8 ± 2	1.7 ± 0.1	9.0 ± 4
coarse AlTi	0.32 ± 0.2	3.6 ± 0.6	2.3 ± 0.8	4.0 ± 2
absent	0.4 ± 0.2	5.7 ± 1.3	3.0 ± 0.9	9.7 ± 1

solids, as the coarse AlTi was unable to increase the yields of LAC and LGO compared to untreated cellulose (Table 3). This finding is in accordance with a previous investigation showing the remarkable difference between nanopowder and coarse AlTi in the production of anhydroglucoses by analytical pyrolysis.[9] Moreover, there is growing evidence of the enhancement in chemical reactivity exhibited by nanoparticle oxides in catalytic and reactive pyrolysis of organic materials.[10] The observed diversity of the investigated oxides in affecting the pyrolytic behaviour of cellulose was supported by the results of thermogravimetric analyses performed on the same samples subjected to pyrolysis. The weight loss maximum rate (DTG peak) measured at 354 °C for neat cellulose increased only slightly to 358 °C when cellulose was admixed with coarse AlTi, but decreased remarkably to 333 °C with NP AlTi. This large difference in the decomposition temperature gives further support to the importance of the nanosized characteristics of AlTi as a determining factor for the increased production of LAC. In agreement, less pronounced but still significant diminution of temperature was observed at 348 °C and 349 °C for NP Al and NP Ti, respectively.

The relatively high yields of LGO might be partly ascribed to the enhanced dehydration of cellulose chains in contact with the catalyst, similar to what was observed when cellulose was pyrolysed with a low quantity of Lewis acids (*e.g.* Fe^{3+}, Zn^{2+}).[11] In addition, the Lewis acidity of titanium compounds and its ability to coordinate glucopyranosides is well known.[12] The quantity of exposed Al(III) an Ti(IV) acidic centres in nanoparticles is expected to be considerably higher than in coarse materials explaining the enhanced reactivity of nanopowder oxides.

Table 4 Yields of chiral anhydrosugars from preparative pyrolysis of cellulose at 500 °C in the presence of 30% NP metal oxides/cellulose mass ratio (mean ± s.d., $n = 3$)

Catalyst	LAC (%mass)	LGO (%mass)	DGP (%mass)	LGA (%mass)
NP Al	3.7 ± 2	0.38 ± 0.1	1.4 ± 0.2	10 ± 2
NP AlTi	6.2 ± 0.5	0.77 ± 0.1	0.60 ± 0.01	2.2 ± 0.2
NP Ti	1.4 ± 0.1	0.35 ± 0.02	1.1 ± 0.1	9.3 ± 0.8
absent	1.2 ± 0.2	—	1.6 ± 0.1	14 ± 2.5

Increasing the pyrolysis temperature from 350 °C to 500 °C had a profound effect on the production of LGO, the yields of which decreased to less than 1%, whereas the effect on the other anhydrosugars was less pronounced (Table 4). The most remarkable consequence was that LAC became the predominant anhydromonosaccharide when pyrolysis was performed in the presence of NP AlTi, as shown in Fig. 2b. Therefore, these latter conditions (500 °C with NP AlTi) were selected as favorable for obtaining a bio-oil enriched in LAC suitable for its isolation by chromatography.

In order to investigate the catalytic role of NP AlTi, the persistence of its activity after repeated recycling was evaluated as follows. The solid left in the quartz boat after pyrolysis of the cellulose/NP AlTi mixture was calcined at 650 °C under air until the black char was completely eliminated (0.5 h). The resulting white solid was utilised for a successive pyrolysis run with cellulose at 500 °C and treated again as described above. Bio-oils resulting from four consecutive pyrolyses always contained LAC as the principal component, even though the corresponding yields decreased slightly from 6.2% (run I) to 5.6% (run II), 5.4% (run III) and 4.1% (run IV). These data indicate that the activity of NP AlTi was not strongly impaired by repeated thermal treatments in the presence of organic matter. This may partly be due to the high thermal shock resistance of aluminium titanate. Nevertheless, some structural modifications of the catalyst have occurred as supported by X-ray diffraction (XRD) patterns. The XRD pattern of NP AlTi after four catalytic cycles showed an enhancement in the peak intensity if compared to the pattern for the fresh catalyst, tentatively attributable to increasing of the particle size and the presence of additional signals probably due to the formation of separated TiO_2 and Al_2O_3 phases.

Structural elucidation of LAC and synthesis of LAC derivatives

For pure hydroxylactone **1** the composition $C_6H_8O_4$ was deduced by EI-MS high resolution experiment (Experimental). ^1H NMR data resulted in spectra superimposable to the reported ones,[5] but the structure elucidation is now supported by ^{13}C NMR spectrum, $^1H,^1H$-COSY and $^1H,^{13}C$-correlations, the latter both one bond (HSQC) and multiple bond (HMBC), providing the assignments reported in Table 5. In particular, significant nuclear Overhauser enhancement (NOE) effects were observed for H-8 in axial position at δ_H 2.18 ppm with the axial H-4 at δ 4.30 ppm and for H-8 in the equatorial position at δ_H 2.53 ppm both with H-5 at δ_H 4.54 ppm and H-7

Table 5 NMR spectral data for LAC (**1**) in $CDCl_3$

Atom	δ_H (ppm), J (Hz)	δ_C (ppm)[a]	HMBC correlation[b]
1	—	79.24	—
2	—	175.03	—
4	ax 4.30 dd, J_{gem}11.8, $J_{4ax,5}$ 1.7		C-2, C-8
	eq 4.45 dd, J_{gem}11.8, $J_{4eq,8eq}$ 1.5	75.35	C-2, C-8
5	4.54 brdd, $J_{5,8eq}$ 5.9, $J_{5,4ax}$ 1.7	74.39	
7	β 4.08 d, J_{gem}8.4		C-2, C-5, C-8
	α 3.75 d, J_{gem}8.4	74.01	C-2
8	ax 2.18 d, J_{gem}11.6		C-2, C-4
	eq 2.53 ddd, J_{gem}11.6, $J_{8eq,5}$ 5.9, $J_{8eq,4eq}$ 1.5	35.32	C-2, C-4

[a] Values from ^{13}C NMR spectrum and assignments from one bond heterocorrelation HSQC experiment. [b] Long range heterocorrelation of the indicated C-atom(s) with the proton listed in the row.

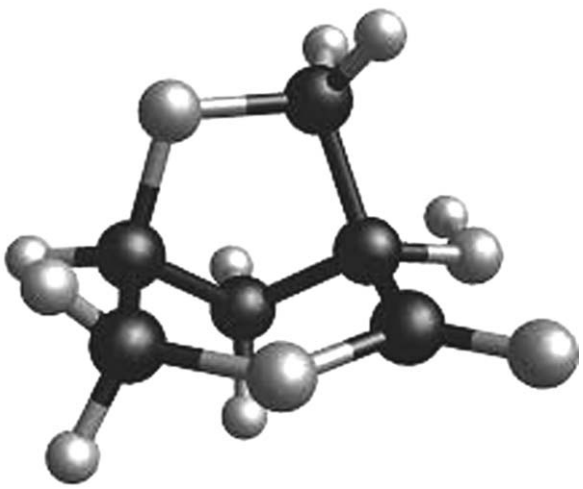

Fig. 3 Energy minimized conformation of LAC (**1**) from MM calculations.

at 3.75 ppm, resulting in agreement with their relative positions for the energy-minimized structure by molecular mechanics calculations reported in Fig. 3. According to the mechanism of formation proposed in Scheme 1, the stereochemistry of **1** arises from a retention of configuration at C-5, common to other pyrolytic products from degradation of cellulose,[5] and from the new chiral centre C-1 formed during the rearrangement and defined by the hemiketal bridge. No data of optical activity were given for **1**,[5] but the comparison was possible for the methyl ester derivative **4** (Scheme 2), which retains the absolute configuration and showed a value in agreement with the reported one.[5]

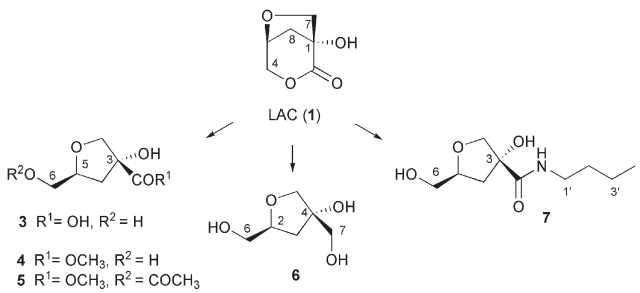

Scheme 2 Some examples of chiral molecules derived from hydroxylactone **1**.

Based on this first availability of hydroxylactone **1** from cellulose pyrolysis in a suitable amount, our following aim regarded the access to chiral compounds as materials for enantioselective synthesis. The production of compounds maintaining the original stereocentres by simple conversion of the functionalities of **1**, underlines its versatility as a building block. Some examples of the available derivatives are included in Scheme 2. Hydrolysis of **1** rapidly affords the known acid **3**,[5] bearing two differently reactive hydroxyl groups, where the primary one can be converted to a series of suitable derivatives (*e.g.* halides and amines). Similarly, alcoholysis of **1** furnishes hydroxyl esters here represented by the methyl ester **4**, where the primary alcohol is converted to the acetate group giving the compound **5**. The reduction of lactone ring in **1** by treatment with sodium borohydride in ethanol[13] gave the chiral triol **6**.[6a] Finally, **1** furnished the amide **7** by treatment with a suitable amine, *n*-butylamine as a choice, under a rapid and easy microwave assisted procedure, reported as an effective and environmentally benign alternative methodology to conventional heating.[14]

Conclusions

This study proves that pyrolysis coupled *in situ* with a nanopowder catalyst can be a valid tool in the green challenge of increasing the number of chemicals affordable from biomass components. When applied to the pyrolysis of cellulose, nanopowder titanium and aluminium oxides aided the production of dehydrated C_6 monomers with the potential both to replace strong inorganic acids used widely up until today (*e.g.* in the production of LGO) and to be recycled in their use quite effectively. The behaviour of nanopowder aluminium titanate resulted uniquely in promoting the formation of the hydroxylactone LAC and in favouring its isolation from the pyrolytic liquid. These conditions open the route to its application as a starting material for providing enantiopure compounds to be applied in chiral pool synthesis. As a preliminary application, LAC was easily converted into polyfunctional tetrahydrofurane derivatives bearing two chiral centres at C-2 and C-4, with the promise to replace monosaccharides as a building block for the many tetrahydrofurane structures found in natural and synthetic products.

Experimental

Material and apparatus

High purity microgranular cellulose and levoglucosan (LGA) were purchased from Fluka. Nanopowder aluminium oxide (NP Al, Al_2O_3, specified as average particle size 40–47 nm), titanium dioxide (NP Ti, TiO_2, <150 nm, mixture of anatase and rutile) and aluminium titanate (NP AlTi, $TiO_2{\cdot}Al_2O_3$, 30–60 nm) as well as powder aluminium titanate (coarse AlTi, particle size 10–100 μm by sieving) were purchased from Sigma–Aldrich.

The reagents and solvents were used in chemical reactions without purification. All evaporations were carried out at room temperature at reduced pressure. Molar yields are given

on reacted compounds. Microwave irradiation was achieved in a domestic microwave oven TdA Electronics MG717ADL at 540 W. TLC chromatography was carried out on *Merck Kieselgel 60 PF_{254}* and *Merck RP-18 F_{254}*. and flash-chromatography (FC) on Merck silica gel 60 (15–25 μm), or on reversed-phased Merck Lichroprep RP-18 (15–25 μm); preparative thin layer chromatography (TLC) was realized on 20 × 20 cm *Merck Kieselgel 60 F_{254}* 0.5 mm plates; HPLC purification for LAC was achieved on 25 × 1 cm columns packed with Merck LiChrospher RP-18 (7 μm) under UV monitoring at λ = 220 nm and solvent flux = 5 ml min^{-1}. NMR spectra were taken with an Avance 400 Bruker spectrometer; ^1H at 400 MHz and ^{13}C at 100 MHz in $CDCl_3$ (by previous treatment on basic alumina to avoid acidic traces), δ values in ppm in $CDCl_3$ relative to the solvent residual signals δ_H = 7.25 and δ_C = 77.00 ppm; *J* values in Hz. Structural assignments are from ^1H,^1H-COSY, heteronuclear single quantum correlation (HSQC), heteronuclear multiple bond correlation (HMBC) and 2D-nuclear Overhauser enhancement (NOESY) experiments. Electron-impact (EI) mass spectra (*m*/*z*; rel.%) and HR-EI data were taken with a Kratos-MS80 mass spectrometer with home-built computerized acquisition software; ESI-MS mass spectra were taken with a Bruker Esquire-LC spectrometer with an electrospray ion source used in positive ion mode by direct infusion of a methanolic solution of the sample. Molecular mechanics (MM) calculations were carried out by the computer program PCMODEL 7.0, Serena Software, Bloomington, Indiana which uses MM3 force field.

Analytical and preparative pyrolysis of cellulose

Off-line flash pyrolysis experiments were performed as detailed elsewhere.[9] Briefly, pyrolyses were perfomed at 500 °C for 60 seconds on a 5 mg cellulose/catalyst sample with a CDS 1000 pyroprobe equipped with a resistive heated platinum filament connected to a glass chamber under a nitrogen stream. Pyrolysis products were trapped onto a XAD-2 resin and eluted with acetonitrile (5 cm^3) prior to GC-MS analysis.

The configuration of the fixed bed reactor set up for preparative pyrolysis was similar to that described by Cozzani *et al.*[15] It consisted of a tubular quartz reactor (length: 650 mm, internal diameter: 37 mm) placed coanularly within a furnace refractory (Carbolite, Italy), equipped with a thermo-couple, connected to the nitrogen inlet by means of pressure valve and a flow meter and connected downstream to an ice trap and a separator funnel for trapping condensable compounds (Fig. 1). Sample mixture (3 g cellulose mixed with 30% by mass active solid) was uniformly placed onto a sliding quartz boat, the nitrogen flow was set at 1500 cm^3 min^{-1} and the oven was turned on. As soon as the temperature inside the reactor reached the established value, the sample was positioned into the central part of the oven for 5 minutes, then retrieved upstream in the colder part of the reactor. The bio-oil recovered in the cold trap and separator funnel was weighed and dissolved in acetonitrile. An aliquot of bio-oil solution was further diluted with acetonitrile and analysed by GC-MS for the quantitation of anhydrosugars. Yields (as % $w_{as}/w_{cellulose}$) were calculated from the amount of anhydrosugar (w_{as}) evolved from a known amount of cellulose ($w_{cellulose}$) subjected to pyrolysis. The quantitation of LGO, LAC, DGP was performed by external calibration using purified LGO. The concentration of LGA was determined after trimethylsilylation using *meso*-erythritol as internal standard.[9]

Purification and structural elucidation of LAC

Bio-oil (1700 mg) deriving from the pyrolysis at 500 °C of cellulose in the presence of 30% NP AlTi was fractionated by flash chromatography over silica gel using pentane–ethyl acetate at gradient elution. The first fraction (50 cm^3, 2/3 v/v) contained LGO, while the evaporated second fraction (50 cm^3 1/1 v/v) afforded a yellow oil containing LAC with 90% GC purity (200 mg, 6% by weight from cellulose). This sample was used for chemical reactions, while a pure sample for structural characterisation was obtained by preparative RP-18 HPLC purification using 1 : 9 acetonitrile–water as eluant (t_R 3.0 min).

(1*R*,5*S*)-1-hydroxy-3,6-dioxa-bicyclo[3.2.1]octan-2-one, 1

NMR data in Table 5; EI-MS (*m*/*z*, %) 144 (11, $M^{+\bullet}$), 126 (36, $M^{+\bullet}$-H_2O), 97(19), 69 (13), 43 (100); HR-EIMS: found 144.0425 ± 0.0030, calc. for $C_6H_8O_4$ 144.023; found 126.0319 ± 0.0030, calc. for $C_6H_6O_3$ 126.0317.

Synthesis and characterisation of LAC derivatives

(3*R*,5*S*)-Methyl 3-hydroxy-5-(hydroxymethyl)-tetrahydro-furan-3-carboxylate, 4. LAC (**1**, 50 mg, 0.34 mmol) was stirred for 2 h at r.t with anhydrous methanol containing 0.01 M acetyl chloride as HCl source.[16] The crude reaction mixture was concentrated and the resulting residue was subjected to chromatography on silica gel by elution with pentane–ethyl acetate 1 : 1 and then with ethyl acetate to give **4** as a yellowish oil (50 mg, 82%). A sample was purified by a preparative TLC on silica gel eluted with CH_2Cl_2/MeOH 9 : 1, to give pure compound for spectroscopic analysis.

4: $[\alpha]_D$ +8.9° (c 0.16 in $CHCl_3$) [lit.[5] +10°]; ^1H-and ^{13}C NMR, and HR-EIMS data resulted in agreement with the ones reported by Furneaux *et al.*[5] Significant HMBC correlations: δ_H 3.85 ppm (dd, H-2) with C-4; δ_H 4.23 (d, H-2) with C-4, C-5, COO; δ_H 2.06 (ddd, H-4) with C-3; δ_H 2.37 (dd, H-4) with C-6, COO; δ_H 3.86 (s, OCH_3) with C-3, COO.

(3*R*,5*S*)-Methyl 5-(acetoxymethyl)-3-hydroxy-tetrahydro-furan-3-carboxylate, 5. Methyl ester **4** (40 mg, 0.22 mmol) was dissolved into acetic anhydride (5 cm^3) and stirred at 60 °C for 8 h. After evaporation of the crude mixture, the residue was subjected to silica gel chromatography and eluted with dichloromethane followed by ethyl acetate. Evaporation of this last fraction gave pure acetate **5** (26 mg, 54%).

5: ^1HNMR (400 MHz, $CDCl_3$) δ_H 4.45 (1H, m, H-5), 4.27 (1H, dd, *J* 11.8, 3.4 Hz, 1H-6), 4.12 (1H, dd, *J* 11.8, 7.0 Hz, 1H-6), 4.21 (1H, d, *J* 9.6 Hz, 1H-2), 3.84 (1H, d, *J* 9.6 Hz, 1H-2), 3.63 (1H, br.s, OH), 2.14 (2H, m, 2H-2), 3.85 (3H, s, $COOCH_3$), 2.09 (3H, s, $OCOCH_3$); ^{13}C NMR (100 MHz, $CDCl_3$) δ_C 174.70 (s, *C*$OOCH_3$), 171.07 (s, CH_3*C*O), 80.83 (s, C-3), 78.26 (s, C-2), 77.14 (s, C-5), 64.80 (t, C-6), 53.15 (q, COO*C*H_3), 41.86 (t, C-4), 20.93 (q, *C*H_3CO); EI-MS (*m*/*z*, %)

219 (1), 218 (1, $M^{+\cdot}$), 145 (9), 140 (16), 127 (56), 59 (27), 43 (100); HR-EIMS: found 218.0786 ± 0.0030, calc. for $C_9H_{14}O_6$ 218.0790.

(2*S*,4*S*)-4-Hydroxy-tetrahydrofuran-2,4-dimethanol, 6. Sodium borohydride (5.3 mg, 0.14 mmol) was stirred in EtOH (0.5 cm^3) at room temperature for 10 min, then a solution of LAC (**1**, 6.5 mg, 0.045 mmol) in EtOH (0.5 cm^3) was added. The resulting solution was stirred for 2 h, following on TLC plate the disappearance of the starting material, adding then H_2O (2 cm^3) under stirring. The reaction mixture was evaporated and the residue subjected to flash chromatography on RP-18 phase, eluting with H_2O/MeOH 8:2, followed by MeOH, obtaining pure triol **6** by evaporation of fractions 3–5 (4.5 mg, 68%).

6: ^{1}HNMR (400 MHz, $CDCl_3$+ CD_3OD) δ_H 3.95 (1H, d, *J* 9.6 Hz, 1H-5), 3.78 (3H, m, 1H-4, 1H-6, 1H-7), 3.55 (2H, m, 1H-6, 1H-7), 2.05 and 1.80 (2H, two m, 2H-3); ESI (+) MS: *m*/*z* 171 (M + Na^+), 149 (M + H^+); EI-MS (*m*/*z*, %) 130 (1, $M^{+\cdot}$-H_2O), 112 (9), 94 (4), 80 (7); HR-EIMS: found 130.1412 ± 0.0050, calc. for $C_6H_{10}O_3$ 130.1448.

(3*R*,5*S*)-*N*-Butyl-3-hydroxy-5-(hydroxymethyl)-tetrahydrofuran-3-carboxamide, 7. LAC (**1**, 5.2 mg, 0.036 mmol) and an excess of *n*-butylamine (0.1 cm^3) were added in a closed glass vessel and the resulting mixture was MW irradiated for 10 min. The crude mixture was evaporated to give pure amide **7** (6.5 mg, 84%).

7: ^{1}HNMR (400 MHz, $CDCl_3$) δ_H 4.34 (1H, m, H-5), 4.07 (1H, d, *J* 9.6 Hz, 1H-2), 3.87 (1H, dd, *J* 11.6, 3.2 Hz, 1H-6), 3.71 (1H, d, *J* 9.6 Hz, 1H-2), 3.67 (1H, dd, *J* 11.6, 4.4 Hz, 1H-6), 3.35 (2H, m, 2H-1′), 2.37 (1H, dd, *J* 13.8, 8.9 Hz, 1H-4), 2.10 (1H, dd, *J* 13.8, 7.7 Hz, 1H-4), 1.55.(2H, quint, *J* 7.2 Hz, 2H-2′), 1.36 (2H, m, 2H.-3′), 0.93 (3H, t, *J* 7.2 Hz, H-4′); ^{13}C NMR (100 MHz, $CDCl_3$) δ_C 174.18 (s, CONH), 82.10 (s, C-3), 79.84 (s, C-5), 77.97 (s, C-2), 63.75 (t, C-6), 40.31 (t, C-4), 39.58 (t, C-1′), 32.03 (t, C-2′), 19.80 (t, C-3′), 13.8 (q, C-4′); EI-MS (*m*/*z*, %) 218 (4), 217 (4, $M^{+\cdot}$), 199 (4, $M^{+\cdot}$-H_2O), 168 (27), 132 (4), 100 (38), 85 (9), 57 (100); HR-EIMS: found 217.1313 ± 0.0030, calc. for $C_{10}H_{19}NO_4$ 217.1314.

Acknowledgements

Research supported by the University of Bologna, C.I.R.S.A. and Provincia di Ravenna. We thank Mr A. Sterni, University of Trento for high resolution EI-MS experiments and Dr G. Lesci and Dr B. Palazzo, University of Bologna, for DTG and XRD data acquisition and interpretation.

References

1 (*a*) B. Kamm, M. Kamm, P. R. Gruber and S. Kromus, Biorefinery systems. An Overview, in *Biorefineries. Industrial Processes and Products*, ed. B. Kamm, P. R. Gruber and M. Kamm, Wiley, VCH, Weinham, Germany, 2006, vol. I, ch. 1, pp.3–40; (*b*) J. H. Clark, V. Budarin, F. E. I. Deswart, J. J. E. Hardy, F. M. Kerton, A. J. Hunt, R. Luque, D. J. Macquarrie, K. Milkowski, A. Rodriguez, O. Samuel, S. J. Tavener, R. J. White and A. J. Wilson, *Green Chem.*, 2006, **8**, 853; (*c*) S. Fernando, S. Adhikari, C. Chandrapal and N. Murali, *Energy Fuels*, 2006, **20**, 1727; (*d*) V. V. Zverlov, O. Berezina, G. A. Velikodvorskaya and W. H. Schwarz, *Appl. Microbiol. Biotechnol.*, 2006, **71**, 587; (*e*) P. Gallezot, *Green Chem.*, 2007, **9**, 295.

2 (*a*) M. Bols, in *Carbohydrate building blocks*, J. Wiley & Sons, Inc., New York, 1996; (*b*) F. W. Lichtenthaler, A. Brust and E. Cuny, *Green Chem.*, 2001, **3**, 201; (*c*) *Top Added Values Chemicals from Biomass*, ed. T. Werpy and G. Petersen, U.S. Department of Energy, Pacific Northwest National Laboratory, National Renewable Energy Laboratory, DOE/GO-1002004-1992, august 2004, vol. I, available at www.osti.gov/bridge; (*d*) F. W. Lichtenthaler, The Key Sugars of Biomass: Availability, Present NonFood Uses and Potential Future Development Lines, in *Biorefineries. Industrial Processes and Products*, ed. B. Kamm, P. R. Gruber and M. Kamm, Wiley, VCH, Weinham, Germany, 2006, vol.II, ch. 1, pp.3–59; (*e*) B. Kamm, M. Kamm, M. Schmidt, I. Starke and E. Kleinpeter, *Chemosphere*, 2006, **62**, 97.

3 (*a*) A. V. Bridgwater, *Catal. Today*, 1996, **29**, 285; (*b*) J. Piskorz, P. Majerski, D. Radlein, A. Vladars-Usas and D. S. Scott, *J. Anal. Appl. Pyrolysis*, 2000, **56**, 145; (*c*) S. Czernick and A. V. Bridgewater, *Energy Fuels*, 2004, **18**, 590; (*d*) D. Mohan, C. U. Pittman and P. H. Steele, *Energy Fuels*, 2006, **20**, 848.

4 (*a*) Z. J. Witczak, *Levoglucosenone and Levoglucosans: Chemistry and Applications*, ed. Z. J.Witczak, ATL press, Mount Prospect, 1994; (*b*) M. S. Miftakhov, F. A. Vallev and I. N. Gaisina, *Russ. Chem. Rev.*, 1994, **63**, 869.

5 R. H. Furneaux, J. M. Mason and I. J. Miller, *J. Chem. Soc., Perkin Trans. 1*, 1988, 49.

6 (*a*) G. Petersson and O. Samuelson, *Acta Chem. Scand., Ser. B*, 1976, **30**, 27; (*b*) K. Niemela and E. Sjostrom, *Biomass*, 1986, **11**, 215; (*c*) A. Raimo, *Carbohydr. Res.*, 1985, **144**, 163.

7 (*a*) H. Kawamoto, M. Murayama and S. Saka, *J. Wood Sci.*, 2003, **49**, 469; (*b*) H. Kawamoto, W. Hatanaka and S. Sata, *J. Anal. Appl. Pyrolysis*, 2003, **70**, 303; (*c*) G. Dobele, T. Dizhbite, G. Rossinkaja, G. Telysheva, D. Meier, S. Radtke and O. Faix, *J. Anal. Appl. Pyrolysis*, 2003, **197**, 68; (*d*) P. Rutkowski and A. Kubacki, *Energy Conv. Manage.*, 2006, **47**, 716.

8 (*a*) J. Adam, M. Blazsò, E. Mészàros, M. Stocker, M. H. Nilsen, A. Bouzga, J. E. Hustad, M. Gronli and G. Oye, *Fuel*, 2005, **84**, 1494; (*b*) J. Adam, E. Antonakou, A. Lappas, M. Stocker, M. H. Nilsen, A. Bouzga, J. E. Hustad and G. Oye, *Microporous Mesoporous Mater.*, 2006, **96**, 93.

9 D. Fabbri, C. Torri and V. Bavarelli, *J. Anal. Appl. Pyrolysis*, 2007, **80**, 24.

10 (*a*) J. Aguado, D. P. Serrano and G. San Miguel, *J. Polym. Environ.*, 2007, **15**, 107; (*b*) A. Marcilla, A. Gòmez-Siurana and F. Valdés, *J. Anal. Appl. Pyrolysis*, 2007, **79**, 433; (*c*) D. Fabbri, F. Fabbri, G. Falini, V. Baravelli, C. Torri, H. Maskrot and Y. Leconte, Analysis of fatty acids in triglycerides by pyrolysis methylation with dimethyl carbonate. The activity of titanium MCM-41 and oxide nanopowders, submitted.

11 (*a*) G. Varhegyi, M. J. Antal, Jr., T. Szekely, F. Till and E. Jakab, *Energy Fuels*, 1988, **2**, 267; (*b*) C. W. Klampfl, G. Breuer, C. Schwarzinger and B. Köll, *Acta Chim. Slov.*, 2006, **53**, 437.

12 D. Küntzer, L. Jessen and J. Heck, *Chem. Commun.*, 2005, 5653.

13 V. Dalla, J. P. Catteau and P. Pale, *Tetrahedron Lett.*, 1999, **40**, 5193.

14 P. Lindrström, J. Tierney, B. Wathey and J. Westman, *Tetrahedron*, 2001, **57**, 9225–9283.

15 V. Cozzani, C. Nicolella, L. Petrarca, M. Rovatti and L. Tognotti, *Ind. Eng. Chem. Res.*, 1995, **34**, 2006.

16 (*a*) J. Bleton, P. Mejanelle and J. Sansoulet, *J. Chromatogr., A*, 1996, **720**, 27; (*b*) T. Doco, M. A. O'Neill and P. Pellerin, *Carbohydr. Polym.*, 2003, **46**, 249.

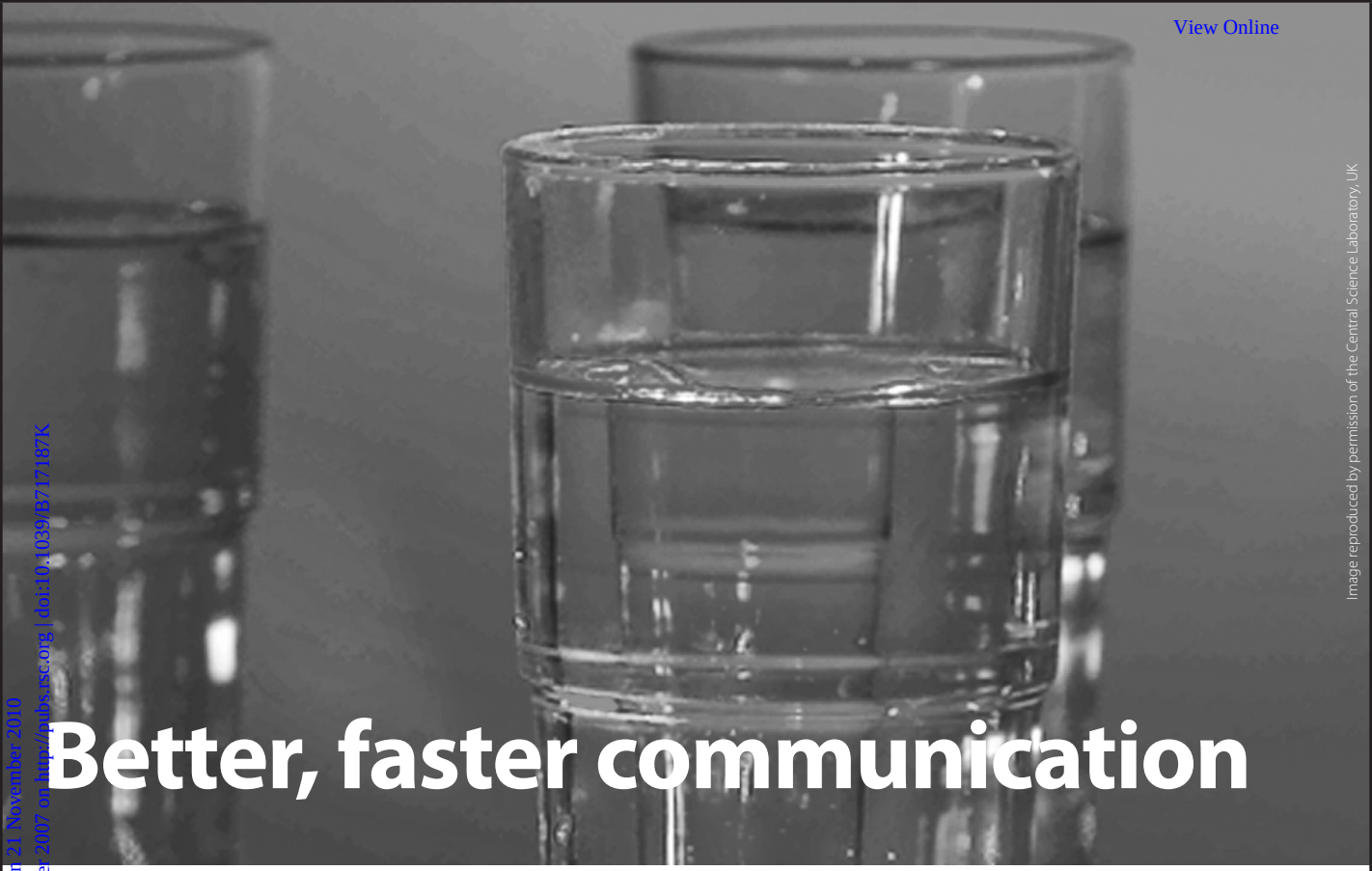

Better, faster communication

Look no further than the *Journal of Environmental Monitoring* for urgent publication of your cutting-edge research on all aspects of environmental science in the natural and anthropogenic environment.

Journal of Environmental Monitoring communications report high impact, preliminary results of current and immediate interest. Communications are fast-tracked through the publication process, given a high profile in the journal and widely promoted.

Featured on the cover is a recent communication on the rapid detection of contaminants in potable water.
Adrian J. Charlton *et al., J. Environ. Monit.,* 2006, **8**, 1106

Submit your communication today!

RSC Publishing

www.rsc.org/jem/communications

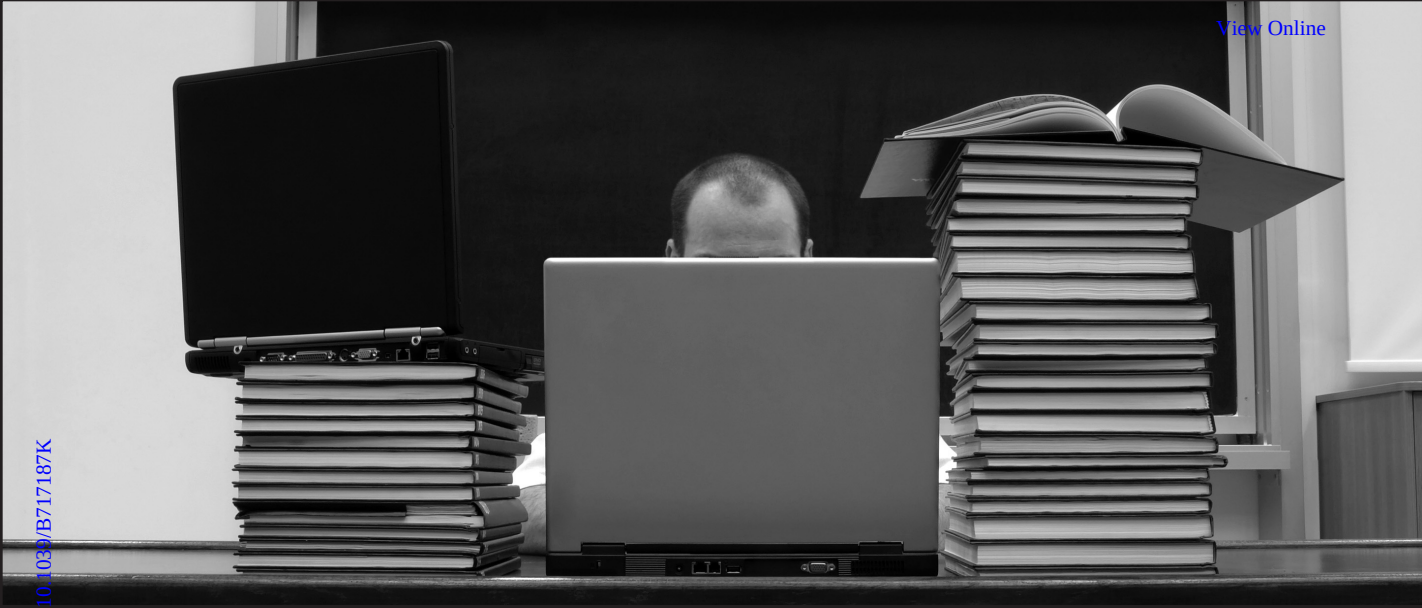

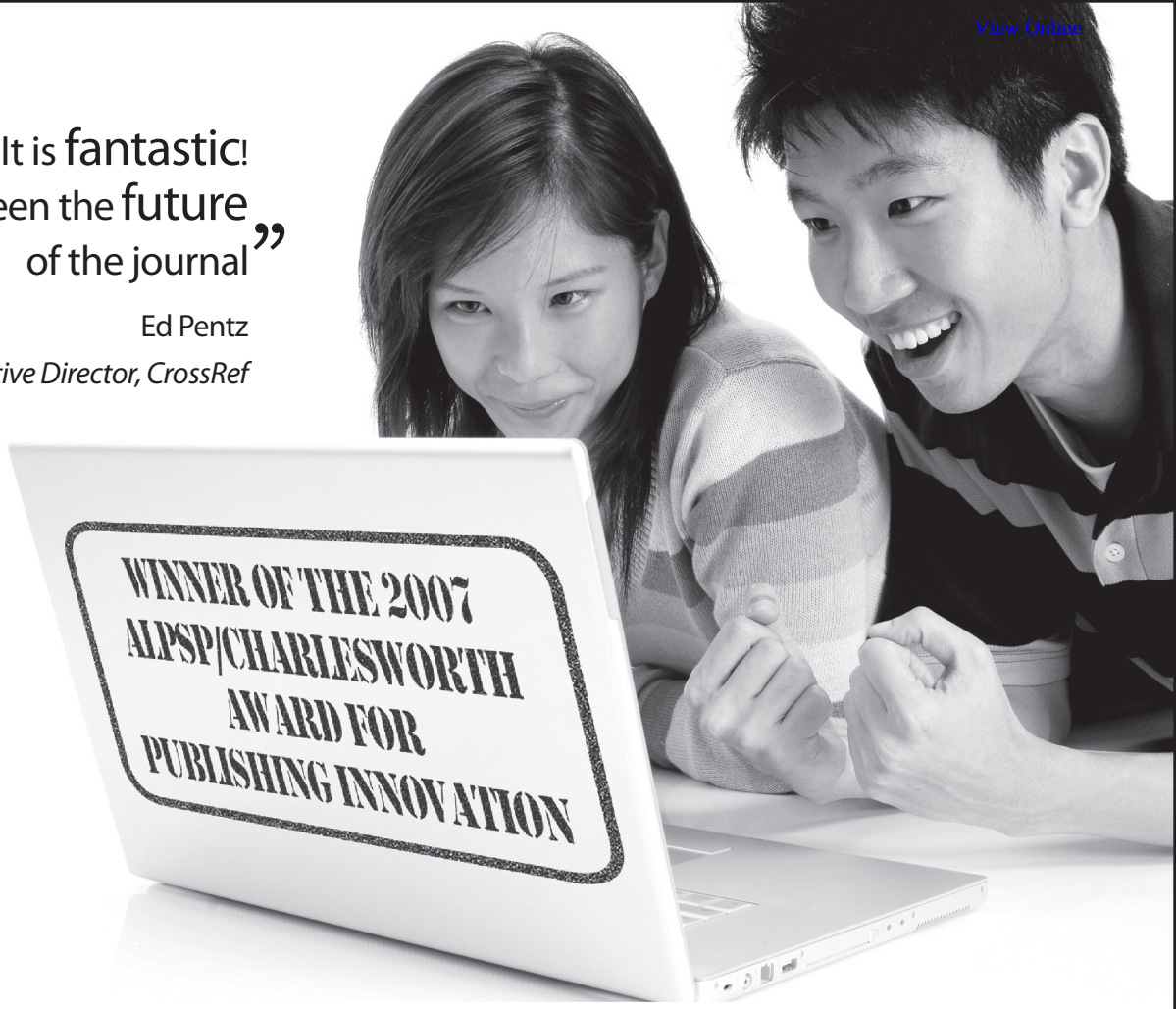

“It is fantastic! I've just seen the future of the journal”

Ed Pentz

Executive Director, CrossRef

Features include

IUPAC Gold Book terms linked

Hyperlinked compound information in text

Ontology terms linked to definitions and related papers

RSS feeds with ontology terms and compound structures

Benefits

Completely free service

At a glance HTML view with additional features accessed by toolbox

Downloadable compound structures

Printer friendly

Science comes alive with RSC Project Prospect

Scientists trawling through the thousands of research papers published every month must wish their computer could do the job for them. This could soon be a reality thanks to RSC Project Prospect, an initiative developed by RSC Publishing together with academic partners. Readers can click on named compounds and scientific concepts in an electronic journal article to download structures, understand topics, or link through to electronic databases. Powerful functionality instantly helps researchers to find, understand and share (bio)chemical knowledge with each other quicker than ever before. See the science in journal articles come alive: visit the RSC Project Prospect website for FAQs, examples, contact information and latest news.

RSC Publishing

www.projectprospect.org

Registered Charity Number 207890

Specialised searching

The graphical abstracting services at the RSC are an indispensable tool to help you search the literature. Focussing on specific areas of research they review key primary journals for novel and interesting chemistry.

requires specialised tools

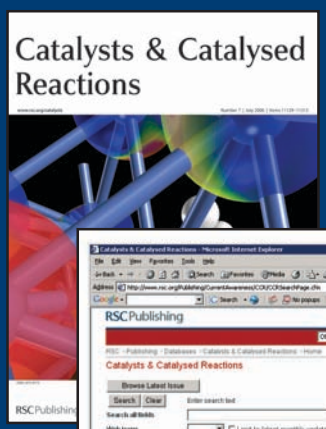

Catalysts and Catalysed Reactions covers all areas of catalysis research, with particular emphasis on chiral catalysts, polymerisation catalysts, enzymatic catalysts and clean catalytic methods.

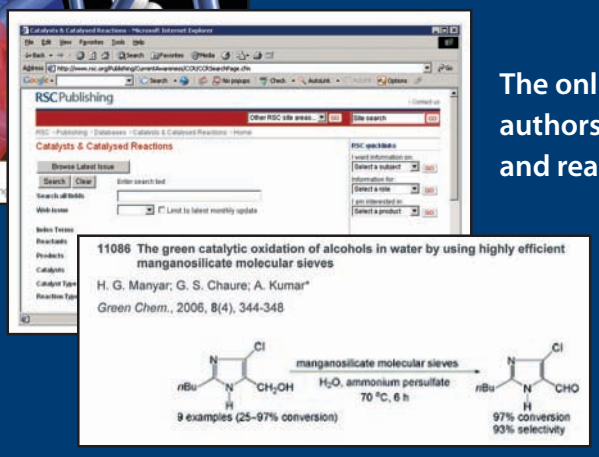

The online database has excellent functionality. Search by: authors, products, reactants and catalysts, catalyst type and reaction type.

With Catalysts and Catalysed Reactions you can find exactly what you need. Search results include diagrams of reaction schemes. Also available as a print bulletin.

For more information visit

RSC Publishing

www.rsc.org/databases

RSC eBook Collection

Access and download existing and new books from the RSC

- **Comprehensive:** covering all areas of the chemical sciences
- **Fully searchable:** advance search and filter options
- **Wide ranging:** from research level monograph to popular science book

See for yourself –

go online to search the collection and read selected chapters for free!